UNIVERSIDAD DE GRANADA

Instituto Andaluz de Geofísica

Complex Steps Finite Differences

with applications to seismic problems

DISSERTATION

for the degree of

Doctor of Earth Sciences

presented by

Rafael **ABREU**

on the recommendation of

PhD Daniel **STICH**

PhD José **MORALES**

Granada, Spain

December, 2013

Editor: Editorial de la Universidad de Granada
Autor: Rafael Abreu
D.L.: GR 1059-2014
ISBN: 978-84-9028-960-0

A complex number is no more absurd than a negative number.

John Wallis (1616-1703), English mathematician.

Copyright

Spanish Copyright

Spanish Copyright

El doctorando Rafael Abreu y los directores de la tesis Dr. Daniel Stich y Dr. José Morales Soto. Garantizamos, al firmar esta tesis doctoral, que el trabajo ha sido realizado por el doctorando bajo la dirección de los directores de la tesis y hasta donde nuestro conocimiento alcanza, en la realización del trabajo, se han respetado los derechos de otros autores a ser citados, cuando se han utilizado sus resultados o publicaciones.

En Granada, España a 15 de Noviembre de 2013.

Directores de la Tesis

Fdo.: _____

Dr. Daniel Stich

Fdo.: _____

Dr. José Morales Soto

Doctorando

Fdo.: _____

Msc. Rafael Abreu

v

Figure 1: Scanned image of the Spanish copyright.

Financial Support

This study was supported by the following research projects:

- Spanish National Project CGL2008-01830.
- Spanish National Project CGL2012-31472.
- Andalusian Project P09-RNM-5100.
- FPI Spanish National Fellowship BES-2009-025033.
- Project grant #195-2979.
- Project grant #195-2256.

Preface

This study represents an inquiry into developing a better and improved numerical method for solving differential equations in general and the wave propagation problem in particular. We developed a numerical technique by generalizing a previous one and we investigated its properties.

This work aims to make contributions to new knowledge of applications of new numerical techniques on one hand, and to make advances in the understanding of the Finite Differences method (FDM) in seismology and its generalizations to the use of imaginary numbers on the other hand.

This thesis is divided into seven hapters: Chapter 1 gives an introduction to the most common numerical methods in seismology, standing out its importance over analytical methods. Chapter 2 briefly explains the importance of complex numbers in sciences. Chapter 3 introduces the fundamentals of the Finite Differences Method (FDM) applied to the wave equation; from the most basic discretizations to the famous staggered grid. Chapter 4 generalizes the Complex Step method (CSM) to the use of complex numbers in a strict sense, allowing high order accurate results using compact stencils. Chapter 5 applies the CSM to the 1D, 2D and 3D acoustic wave equation in homogeneous medium, showing the methodology and feasibility of the use of imaginary numbers in numerical modeling, in this Chapter the authors named it the Complex Step Finite Differences Method (CSFDM). Chapter 6 examines stability and dispersion properties of the CSFDM applied to the 1D elastic wave equation in a heterogeneous medium. Finally in Chapter 7, a general conclusions analysis of this work is made and also the future direction of the introduced method is proposed.

Most of this work have been published in or submitted to peer-reviewed journals [1] [2] [3].

During the preparation of this work, the author also worked on a different topic [4] [5] which is not included in this monograph for the sake of uniformity.

[1] Rafael Abreu, Daniel Stich and José Morales. (2013). On the generalization of the complex step method. Journal of Computational and Applied Mathematics, 241(0):84 - 102.

[2] Rafael Abreu, Daniel Stich and José Morales. (2013). The Complex Step Finite Differences Method Applied to the Acoustic Wave Equation. Geophysical Journal International. Submitted.

[3] Rafael Abreu, Daniel Stich and José Morales. (2013). The Complex Step Finite Difference Method Applied to the 1D Elastic Wave Equation: stability and dispersion analysis. Geophysical Journal International. Submitted.

[4] Rafael Abreu, Jeroen Tromp, Daniel Stich and José Morales. (2013). Micro-continuum forward and adjoint equations and noise cross-correlation sensitivity kernels: Theory. Geophysical Journal International. To be submitted.

[5] Rafael Abreu, Jeroen Tromp, Hom-Nath Gharti, Daniel Stich and José Morales. (2013). Micro-continuum forward and adjoint equations and noise cross-correlation sensitivity kernels: Applications. Geophysical Journal International. To be submitted.

Acknowledgments

Mis más sinceros agradecimientos van para mis dos tutores: Dani y Pepe. Son dos personas a las cuales simplemente les debo mucho. Gracias por haber aceptado todas las situaciones por las cuales he pasado durante los últimos años y por haberme apoyado (con mucha empatía) en todo. Sobretodo gracias por haberme enseñado muchas más cosas que simplemente no se aprenden en un libro. He cambiado mucho para bien durante los últimos años y ciertamente mucho de ello se lo debo a uds. dos.

A mi pequeña familia Eliana, Elías y Cesar por tanto amor, y por supuesto a todos los que ellos traen consigo.

A la gente del Instituto Andaluz de Geofísica. Un lugar donde he conocido amigos y gente de buen corazón.

Many thanks to Mr. Jeroen Tromp for showing me the importance of physics.

Resumen Extendido

Este trabajo introduce una nueva técnica numérica para aproximar ecuaciones diferenciales, el cual es desarrollado y probado con el propósito de calcular la propagación de ondas en medios heterogéneos. Como primer paso se generaliza el Método del Paso Complejo para calcular primeras y segundas derivadas desarrollado por Squire and Trapp (1998) y se introducen nuevas formas de calcular aproximaciones de diferencias finitas, haciendo uso de variable compleja y/o pasos complejos para funciones analíticas y/o ecuaciones diferenciales.

Las aproximaciones más simples y básicas de diferencias finitas para la primera y segunda derivada son llamadas *aproximación hacia adelante* y *aproximación centrada*, las cuales viene dadas por las siguientes expresiones respectivamente

$$f'(x) = \frac{f(x+\Delta x) - f(x)}{\Delta x} + \mathcal{O}\left(\Delta x\right), \tag{1}$$

$$f''(x) = \frac{f(x+\Delta x) - 2f(x) + f(x-\Delta x)}{\Delta x^2} + \mathcal{O}\left(\Delta x^2\right), \tag{2}$$

donde Δx es un numero pequeño llamado *el paso diferencial* $(\Delta x \to 0)$ y el símbolo $\mathcal{O}$ se refiere al error de aproximación.

El MPC usa un numero imaginario puro $(\mathbf{i}^2 = -1)$ para calcular primeras y segundas derivadas de una función analítica haciendo uso de las siguientes expresiones respectivamente

$$f'(x) = \frac{\mathfrak{Im}(f(x+\mathbf{i}\Delta x))}{\Delta x} + \mathcal{O}\left(\Delta x^2\right), \tag{3}$$

$$f''(x) = \frac{2(f(x) - \mathfrak{Re}(f(x+\mathbf{i}\Delta x)))}{\Delta x^2} + \mathcal{O}\left(\Delta x^2\right), \tag{4}$$

donde los términos $\mathfrak{Im}$ y $\mathfrak{Re}$ son operadores que toman la parte imaginaria y real de una función respectivamente.

Las aproximaciones de pasos complejos (PC) poseen un gran número de ventajas en comparación con aproximaciones de Diferencias Finitas (DF) convencionales: inestabilidades numéricas relacionadas con errores de cancelación de la resta pueden ser evitados (note el termine de resta en el numerador de la Ec. 1 está ausente en la Ec. 3), mayor precisión en la aproximación (note que el error es de segundo orden en la Ec. 3 y de primer orden en la Ec. .1 teniendo ambos una sola perturbación Δx) y por otro lado, las derivadas de segundo orden pueden ser calculadas a un solo paso (Ec. 4).

Derivadas de segundo orden no pueden ser calculadas con el MPC usando la parte imaginaria de la función ($\mathfrak{Im}$) puesto que la unidad imaginaria desaparece después de la doble diferenciación. Es mostrado en este trabajo que cuando se introducen pasos complejos desde

un sentido estricto, es decir, tomando en cuenta las direcciones reales e imaginarias en la aproximación de PC 3, podemos escribir lo siguiente

$$f'(x) = \frac{\mathfrak{Im}(f(x+h+\mathbf{i}v))}{v} + \mathcal{O}\left(h, v^2\right), \tag{5}$$

donde $h, v \in \mathbb{R}$ y $h, v \to 0$, el MPC puede ser generalizado.

Aunque a primera vista, ésta aproximación de PC de primer orden (Ec. 5) es menos precisa que la original (Ec. 3), este tipo de paso diferencial permite calcular derivadas de segundo orden, lo cual no era posible con el MPC original.

Varias aproximaciones pueden ser encontradas, por ejemplo, la aproximación centrada para la primera y segunda derivada viene dadas respectivamente por las siguientes expresiones

$$f'(x) = \frac{\mathfrak{Im}(f(x+h+\mathbf{i}v)) + \mathfrak{Im}(f(x-h+\mathbf{i}v))}{2v} + \mathcal{O}\left(3h^2 - v^2\right), \tag{6}$$

$$f''(x) = \frac{\mathfrak{Im}(f(x+h+\mathbf{i}v)) - \mathfrak{Im}(f(x-h+\mathbf{i}v))}{2hv} + \mathcal{O}\left(h^2 - v^2\right), \tag{7}$$

donde el error de aproximación es de 4^{to} orden si $v = \sqrt{3}h$ y $h = v$ es respectivamente elegido.

Para cada expresión diferente encontrada, una apropiada combinación de términos y apropiada elección del tamaño del paso diferencial en las dirección real e imaginaria (h, v) debe ser hecha, llevando en varios casos a obtener precisión de 4^{to} orden, logrado de una forma simple y compacta para derivadas de primer orden y de orden superior.

Varios tipos de aproximaciones para calcular derivadas de primer, segundo, tercero y quinto orden son encontradas en este trabajo, donde la simplicidad de las ecuaciones en relación con aproximaciones de DF comunes se mantiene prácticamente igual, con todas las ventajas que conllevan los nuevos enfoques, tales como la no cancelación de términos en muchos casos.

Todas las nuevas aproximaciones fueron validadas teóricamente y verificadas numéricamente haciendo uso de en código numérico escrito en lenguaje Fortran90, usando el compilador gfortran con un formato de doble precisión para todas las variables, y a su vez usando la misma función analítica usada por Squire and Trapp (1998), y subsecuentemente por muchos otros autores, mostrando la superioridad de las nuevas aproximaciones sobre el MPC y el Método de Diferencias Finitas (MDF).

Luego de desarrollada y validada la nueva técnica numérica, nos enfocamos en la aplicación en el contexto geofísico y sismológico.

Debido al gran crecimiento de tecnologías computacionales, la simulación numérica de propagación de ondas ha estado en el centro de atención de sismólogos el las últimas cinco décadas. Por muchas razones, la teoría de propagación de ondas sísmicas en medios acústicos/elásticos heterogéneos es de gran importancia en el campo de la sismología. El desarrollo de tecnologías computacionales facilita la aplicación de más precisas, eficientes y complejas metodologías numéricas, ayudando al mejor entendimiento del planeta Tierra y sus procesos.

A pesar del gran incremento de poder de cómputo en los años recientes, las técnicas numéricas aún requieren una cantidad inmensa de almacenaje de datos para la simulación la propagación de ondas en medios realísticos y a gran escala. Por esta razón, la herramienta numérica debería ser simplificada tanto como sea posible, tratando de mantener la precisión y exactitud de las soluciones.

Este trabajo tiene como principal objetivo el desarrollo de una nueva, simple, eficiente y muy precisa herramienta numérica para la solución de ecuaciones diferenciales en general y la ecuación de onda en particular.

El problema de propagación de ondas unidimensional (1D) está gobernado por dos ecuaciones básicas: la ecuación de onda unidireccional y bidireccional dadas por las siguientes expresiones matemáticas respectivamente

$$\frac{\partial u}{\partial t} = c\frac{\partial u}{\partial x}, \tag{8}$$

$$\frac{\partial^2 u}{\partial t^2} = c^2\frac{\partial^2 u}{\partial x^2}, \tag{9}$$

donde $u = u(x,t)$ es el campo de desplazamiento y $c = c(x)$ es la velocidad del medio.

En el contexto de problemas sismológicos, las dos ecuaciones anteriores son usadas con diferentes propósitos. Mientras la ecuación de onda de primer orden (Ec. 8) ha sido ampliamente usada en el diseño de condiciones de borde no absorbentes (ej. Clayton and Engquist (1980)) y migración geofísica (ej. Claerbout (1986), Tappert (1977)). La ecuación de onda de segundo orden (Ec. 9) ha sido usada para propiamente resolver el problema de propagación de onda. Esto es debido a la naturaleza intrínseca de los operadores de DF para las derivadas de primero y segundo orden.

Las aproximaciones más básicas de FD para la primera y segunda derivada son dadas por la Ec. 1 y Ec. 2 respectivamente. Las aproximaciones mas simples de DF para las ecuaciones de onda de primero y segundo orden usando las Ecs. 1 - 2 son respectivamente dadas por las siguientes expresiones

$$u_x^{t+\Delta t} = \mathrm{S}\, u_{x+\Delta x}^t + \left(1-\mathrm{S}\right) u_x^t + \mathcal{O}\left(\Delta t, \Delta x\right), \tag{10}$$

$$u_x^{t+\Delta t} = \mathrm{S}^2\left(u_{x+\Delta x}^t + u_{x+\Delta x}^t\right) + 2\left(1-\mathrm{S}^2\right) u_x^t + \mathcal{O}\left(\Delta t^2, \Delta x^2\right), \tag{11}$$

donde $\mathrm{S} = c\frac{\Delta t}{\Delta x}$ es llamado el *número de Courant* y/o *factor de estabilidad*. Comúnmente el número de Courant S es también representado por el símbolo λ.

La principal diferencia entre las discretizaciones 10 y 11 es que la primera propaga la ecuación en una sola dirección (izquierda) mientras que la segunda en dos direcciones (izquierda y derecha).

De igual manera que en el caso de DF, el uso de números complejos es muy inusual en análisis numérico. Este trabajo extiende el MDF y muestra como aplicar los esquemas desarrollados para calcular primera y segunda derivadas para resolver el problema de propagación de ondas.

Basados en el trabajo de Abreu et al. (2013b), se introdujo y dio nombre al Método del Paso Complejo con Diferencias Finitas (MPCDF) como generalización del bien ya conocido MDF.

El MPCDF es simplemente la aplicación de aproximaciones basadas en pasos complejos encontradas en Abreu et al. (2013b) para derivadas de primero y segundo orden de la ecuación de ondas. Por ejemplo, podemos escribir aproximaciones de pasos complejos con diferencias finitas (PCDF) para la ecuación de onda de primer orden usando las aproximaciones 5 and 6 como sigue a continuación

$$\mathfrak{Im}\left(u_{x+\mathbf{i}\Delta x}^{t+\Delta t+\mathbf{i}\Delta t}\right) = \mathrm{S}\,\mathfrak{Im}\left(u_{x+\Delta x+\mathbf{i}\Delta x}^{t+\mathbf{i}\Delta t}\right) + \mathcal{O}\left(\Delta t, \Delta x\right), \tag{12}$$

$$\mathfrak{Im}\left(u_{x+\mathbf{i}\sqrt{3}\Delta x}^{t+\Delta t+\mathbf{i}\sqrt{3}\Delta t}\right)+\mathfrak{Im}\left(u_{x+\mathbf{i}\sqrt{3}\Delta x}^{t-\Delta t+\mathbf{i}\sqrt{3}\Delta t}\right)$$
$$=\mathrm{S}\left[\mathfrak{Im}\left(u_{x+\Delta x+\mathbf{i}\sqrt{3}\Delta x}^{t+\mathbf{i}\sqrt{3}\Delta t}\right)+\mathfrak{Im}\left(u_{x-\Delta x+\mathbf{i}\sqrt{3}\Delta x}^{t+\mathbf{i}\sqrt{3}\Delta t}\right)\right]+\mathcal{O}\left(\Delta t^4,\Delta x^4\right). \tag{13}$$

También podemos construir una discretización para la ecuación de onda de segundo orden (Ec. 9) usando la aproximación 7 como sigue a continuación

$$\mathfrak{Im}\left(u_{x+\mathbf{i}\Delta x}^{t+\Delta t+\mathbf{i}\Delta t}\right)=\mathrm{S}^2\left[\mathfrak{Im}\left(u_{x+\Delta x+\mathbf{i}\Delta x}^{t+\mathbf{i}\Delta t}\right)-\mathfrak{Im}\left(u_{x-\Delta x+\mathbf{i}\Delta x}^{t+\mathbf{i}\Delta t}\right)\right]$$
$$+\mathfrak{Im}\left(u_{x+\mathbf{i}\Delta x}^{t-\Delta t+\mathbf{i}\Delta t}\right)+\mathcal{O}\left(\Delta t^4,\Delta x^4\right). \tag{14}$$

Se investigan propiedades de propagación de la onda tales como estabilidad y dispersión de las aproximaciones de PCDF introducidas para las soluciones de las ecuaciones de onda unidireccional y bidireccional (ej. Ecs. 13-14) y se comparan con esquemas de DF clásicos.

No existe un método numérico perfectamente preciso cuando nos encontramos en presencia de heterogeneidad del medio (diferentes propiedades del medio en cada dirección) ya que todos sufren de diferentes factores los cuales lo permiten que reproduzcan la solución real (exacta) del problema. Uno de los análisis más comunes que ayudan a la comprensión de la naturaleza de la discretización numérica, el cual nos permitirá decidir si el método puede o no ser usado bajo ciertas condiciones, es el análisis de dispersión.

La base del análisis de dispersión en una onda plana de la forma siguiente

$$u(x,t)=\mathrm{A}e^{\mathbf{i}(kx+\omega t)}, \tag{15}$$

donde ω es la frecuencia de la onda, k es el número de onda y A es la amplitud.

Usualmente k y ω son variables dependientes. La relación entre ω y k es comúnmente llamada la relación de dispersión.

En este trabajo se calculan propiedades de estabilidad y dispersión para los más comunes esquemas de DF de la ecuación de onda de segundo orden en una forma estandarizada y unificada. Se comparan los operadores de PCDF introducidos para la ecuación de onda unidireccional con los esquemas de DF.

El MPCDF puede ser entendido como una técnica que complementa el MDF convencional. Puesto que el método numérico introducido está basado en una generalización de DF, su implementación es simple. Se compararon las ventajas del MPCDF sobre el MDF en relación a la imposición de diferentes tipos de condiciones iniciales y se muestra su mayor precisión bajo el mismo costo computacional y dispersión numérica.

Ventajas del MPCDF introducido es la separación entre velocidades y gradientes como condiciones iniciales del problema de propagación de ondas. El método introducido ofrece una nueva forma de intercambiar dispersión por disipación (y al revés) en ecuaciones diferenciales. A pesar de que el método propuesto no presenta ningún aporte significativo en presencia de medios heterogéneos sobre los populares esquemas de DF, estos también pueden ser usados para la resolución del problema de la ecuación de onda.

Finalmente hemos encontrado una relación directa en el modelado de la ecuación de onda de segundo orden (Ec. 9) haciendo uso de el MDF y el ecuación de onda de primer orden (Ec. 8) haciendo uso del MPCDF en medios 1D, 2D y 3D.

Extended Abstract

This work introduces a new numerical approach to approximate differential equations (DE) that is developed and tested with the purpose of computing wave propagation in heterogeneous media. It generalizes the Complex Step Method (CSM) for computing first and second derivatives introduced by Squire and Trapp (1998) and introduces a new way of computing Finite Difference (FD) approximations, making use of complex variables or complex steps for analytic functions and/or differential equations.

The most basic and simple FD approximations for computing first and second order derivatives are called the *forward* and *centered* approximations, given by the following expressions respectively

$$f'(x) = \frac{f(x + \Delta x) - f(x)}{\Delta x} + \mathcal{O}\left(\Delta x\right), \tag{16}$$

$$f''(x) = \frac{f(x + \Delta x) - 2f(x) + f(x - \Delta x)}{\Delta x^2} + \mathcal{O}\left(\Delta x^2\right), \tag{17}$$

where Δx is a small number called the *differential step* $(\Delta x \to 0)$ and the term $\mathcal{O}$ refers to the approximation error.

The CSM uses a pure imaginary number $(\mathbf{i}^2 = -1)$ for computing the first and second order derivatives of an analytic function by the following equations respectively

$$f'(x) = \frac{\mathfrak{Im}(f(x + \mathbf{i}\Delta x))}{\Delta x} + \mathcal{O}\left(\Delta x^2\right), \tag{18}$$

$$f''(x) = \frac{2(f(x) - \mathfrak{Re}(f(x + \mathbf{i}\Delta x)))}{\Delta x^2} + \mathcal{O}\left(\Delta x^2\right), \tag{19}$$

where the terms $\mathfrak{Im}$ and $\mathfrak{Re}$ are operators that takes the imaginary and real part respectively of the function .

Complex Steps (CS) approximations have a number of advantages compared to traditional FD approximations: numerical instabilities related to subtraction cancellation errors can be avoided (note the subtraction term in the numerator in Eq. 16 is absent in Eq. 18), higher order accuracy (note the error is second order in Eq. 18 and first order in Eq.16 with both having a single perturbation) and second order derivatives can be calculated with a single step (Eq. 19).

Second order derivatives can not be computed with the CSM using the imaginary part of the function ($\mathfrak{Im}$) because the imaginary unit disappears after double differentiation.

It is shown in this work when introducing complex steps in a strict sense, i.e., taking into account both real and imaginary directions in the CS approximation 18, we can write the following

$$f'(x) = \frac{\mathfrak{Im}(f(x+h+\mathbf{i}v))}{v} + \mathcal{O}\left(h, v^2\right), \tag{20}$$

where $h, v \in \mathbb{R}$ and $h, v \to 0$, the CSM can be generalized.

Although at a first look, this generalized CS first order approximation (Eq. 20) is less accurate than the original one (Eq. 18), this kind of differential steps allow computations of second order derivatives, not possible using the original CSM.

Many different approximations can be found, for instance, the centered approximation for the first and second order derivatives are respectively given by the expressions

$$f'(x) = \frac{\mathfrak{Im}(f(x+h+\mathbf{i}v)) + \mathfrak{Im}(f(x-h+\mathbf{i}v))}{2v} + \mathcal{O}\left(3h^2 - v^2\right), \tag{21}$$

$$f''(x) = \frac{\mathfrak{Im}(f(x+h+\mathbf{i}v)) - \mathfrak{Im}(f(x-h+\mathbf{i}v))}{2hv} + \mathcal{O}\left(h^2 - v^2\right), \tag{22}$$

where the approximation error is 4^{th} order if $v = \sqrt{3}h$ and $h = v$ is respectively chosen.

For each different kind of approximation found, an appropriate combination of terms and appropriate choice of the step size in real and imaginary direction (h, v) has to be done, leading in many cases to a 4^{th} order accuracy, achieved in a very simple and compact stencils for first and higher order derivatives.

Many different kind of approximations for computing first, second, third and fifth derivatives are found in this work, where the simplicity of the equations in relation to the ordinary FD approximations remains almost the same, with all the advantages that brings all the new approaches, like non-cancellation of terms in many cases.

All the new approximations were validated theoretically and verified numerically by a numerical code written in Fortran90 language, using the GNU Fortran compiler gfortran with standard double precision format for all variables, and using the same analytical test function used by Squire and Trapp (1998), and subsequently by many other authors, showing the superiority of the new approximations on each simulation over the ordinary CSM and Finite Differences method (FDM).

After developing and validating the numerical tool, we focused on the application in the geophysical-seismological context.

Due to the large increase in computational technologies, the numerical simulation of the wave propagation problem has been at the center of attention of seismologists in the last five decades. For many reasons, the theory of seismic wave propagation in heterogeneous acoustic/elastic media is very important in the seismological field. The development of computer technologies facilitates the application of more accurate, efficient and complex numerical methodologies, helping to better understanding of the Earth and its processes.

Despite the rapid increase of computing power in recent years, numerical methods still requires a huge amount of memory for simulating wave propagation for realistic heterogeneity. For this reason, the numerical tool should be simplified as much as possible, maintaining the precision and accuracy of the solutions.

This work aims at the development of a new simple, efficient and very accurate numerical technique for solving partial differential equations in general, and the wave propagation problem in particular.

The 1D wave propagation problem is governed by two basic equations: the one-way and the two-way wave equations given by the following mathematical expressions respectively

$$\frac{\partial u}{\partial t} = c\frac{\partial u}{\partial x}, \tag{23}$$

$$\frac{\partial^2 u}{\partial t^2} = c^2\frac{\partial^2 u}{\partial x^2}, \tag{24}$$

where $u = u(x,t)$ is the displacement field and $c = c(x)$ is the velocity of the medium.

In the context of seismological problems, the previous two equations are used with very different purposes. While the first order wave equation (Eq. 23) has been widely used in the design of non reflecting (absorbing) boundary conditions (e.g. Clayton and Engquist (1980)) and geophysical imaging/migration (e.g. Claerbout (1986), Tappert (1977)). The second order wave equation (Eq. 24) has been used in order to properly solve the wave propagation problem. This is due to the intrinsic nature of the FD operator for the first and second order derivatives.

The most basic FD approximations for the first and second order derivatives are given by Eq. 16 and Eq. 17 respectively. The simplest FD approximations for the first and second order wave equations using Eqs. 16 - 17 are respectively given by the following expressions

$$u_x^{t+\Delta t} = \mathrm{S}\, u_{x+\Delta x}^t + \left(1-\mathrm{S}\right) u_x^t + \mathcal{O}\left(\Delta t, \Delta x\right), \tag{25}$$

$$u_x^{t+\Delta t} = \mathrm{S}^2\left(u_{x+\Delta x}^t + u_{x+\Delta x}^t\right) + 2\left(1-\mathrm{S}^2\right) u_x^t + \mathcal{O}\left(\Delta t^2, \Delta x^2\right), \tag{26}$$

where $\mathrm{S} = c\frac{\Delta t}{\Delta x}$ is called the *Courant number* and/or the *stability factor*. Commonly the Courant number S is also represented by λ symbol.

The main difference between FD scheme 25 and FD scheme 26 is the first one propagates the wave in a single direction (left) while the second one in two directions (left and right).

Like in the FD case, the use of complex numbers is very rare in numerical analysis. This work extends the FDM and shows how to apply the developed schemes for computing first and second order derivatives in order to solve the wave propagation problem.

Based on the work by Abreu et al. (2013b), we introduced and named the Complex Step Finite Differences method (CSFDM) as a generalization of the well known Finite Differences method.

The CSFDM is simply the application of the complex-step based approximation found in Abreu et al. (2013b) to first and second order derivatives of the wave equation. For instance, we can write CSFD discretizations for the one-way wave equation using approximations 20 and 21 as follows

$$\mathfrak{Im}\left(u_{x+\mathbf{i}\Delta x}^{t+\Delta t+\mathbf{i}\Delta t}\right) = \mathrm{S}\,\mathfrak{Im}\left(u_{x+\Delta x+\mathbf{i}\Delta x}^{t+\mathbf{i}\Delta t}\right) + \mathcal{O}\left(\Delta t, \Delta x\right), \tag{27}$$

$$\begin{aligned}\mathfrak{Im}\left(u_{x+\mathbf{i}\sqrt{3}\Delta x}^{t+\Delta t+\mathbf{i}\sqrt{3}\Delta t}\right) + \mathfrak{Im}\left(u_{x+\mathbf{i}\sqrt{3}\Delta x}^{t-\Delta t+\mathbf{i}\sqrt{3}\Delta t}\right) \\ = \mathrm{S}\left[\mathfrak{Im}\left(u_{x+\Delta x+\mathbf{i}\sqrt{3}\Delta x}^{t+\mathbf{i}\sqrt{3}\Delta t}\right) + \mathfrak{Im}\left(u_{x-\Delta x+\mathbf{i}\sqrt{3}\Delta x}^{t+\mathbf{i}\sqrt{3}\Delta t}\right)\right] + \mathcal{O}\left(\Delta t^4, \Delta x^4\right).\end{aligned} \tag{28}$$

Also a discretization for the second order wave equation (Eq. 24) using approximation 22 is given by

$$\mathfrak{Im}\left(u_{x+\mathbf{i}\Delta x}^{t+\Delta t+\mathbf{i}\Delta t}\right) = \mathrm{S}^2\left[\mathfrak{Im}\left(u_{x+\Delta x+\mathbf{i}\Delta x}^{t+\mathbf{i}\Delta t}\right) - \mathfrak{Im}\left(u_{x-\Delta x+\mathbf{i}\Delta x}^{t+\mathbf{i}\Delta t}\right)\right] + \mathfrak{Im}\left(u_{x+\mathbf{i}\Delta x}^{t-\Delta t+\mathbf{i}\Delta t}\right) + \mathcal{O}\left(\Delta t^4, \Delta x^4\right). \tag{29}$$

We investigated properties of propagation, stability and dispersion of Complex Step Finite Differences (CSFD) based approximations to the one-way and two-way wave equations (e.g. Eqs. 28-29) and compared it to the classical FD schemes.

There does not exist a perfectly accurate numerical method in presence of a general heterogeneous media (different velocity values at different grid locations), but all numerical methods suffer from different factors which do not allow them to reproduce the real (analytical) solution of the problem. One of the most common basis to understand the nature of a numerical discretization, which will allow us to decide whether or not the method can be used under certain conditions, is the stability and dispersion analysis.

The basis of the stability and dispersion analysis is a plane wave of the form

$$u(x,t) = \mathrm{A}e^{\mathbf{i}(kx+\omega t)}, \tag{30}$$

where ω is the frequency of the wave, k is the wave number and A is the amplitude.

Usually k and ω are dependent variables. The relation between ω and k is commonly called the dispersion relation.

We computed stability and dispersion properties of the most common second order FD schemes for the wave equation in a standard and unified way. We have introduced CSFD difference operators for the first order wave equation and compared to the FD schemes.

The introduced CSFDM can be seen as numerical technique that complements the conventional FDM. Because the introduced numerical method is based on a generalization of the standard FDM, its implementation is rather simple and straightforward. We compared advantages of the CSFDM over the FDM related to imposing different kinds of initial conditions and showing its higher order accuracy under the same computational cost and numerical dispersion.

Advantages related to the introduced CSFDM is the separation between gradients and velocities as initial conditions of the wave propagation problem. The introduced method (CSFDM) offers a new way of translate dispersion by dissipation and the other way around in differential equations. Although the proposed CSFD schemes does not bring any contribution in presence of heterogeneous media over the popular FD schemes, they can also be applied to solve the wave propagation problem.

We have found a direct relationship between modeling the second order wave equation (Eq. 24) by FDM and the first order wave equation (Eq. 23) by CSFDM in 1D, 2D and 3D media. We also develop and present the numerical methodology in order to apply the introduced CSFDM.

Contents

Chapter 1

Introduction

Seismology is a complex field in science which uses physics, geology, mathematics and more recently numerical analysis techniques in order to make advances. Usually a seismologist pursuits matching theoretical and/or computational results with experimental seismograms of a determined region.

In the most basic fashion, we will try to explain why numerical methods are so important nowadays:

Theoretical physicists describe our world naming physical variables like displacement, time, forces, etc. and relating them by using mathematical relations which are functionals like derivatives, integrals, transformations, etc. of the named variables.

From the mathematical point of view, a theoretical physicist deduces a functional relation of different variables, which is supposed to describe a physical phenomenon. The exact solution of this proposed functional is called the analytical solution. By finding this analytical solution, for the general case or under certain conditions, physicist try to predict the behavior of the physical system in study. The deduced functional relation and its solution will have to reproduce the physical phenomenon in study, otherwise, it is said the theoretical model does not match the reality of our world.

The main problem arises when the proposed functional, which often describes a complex physical phenomenon, has an analytical solution which is extremely hard to find, sometimes impossible for the mathematical tools we have nowadays. The fact that we can not find the analytical solution of the functional does not mean the model is incorrect.

It is here were computers take so much importance. With the use of computers, scientist are now often able to find the approximate solutions of the functional relations which describe a realistic physical problem, avoiding the need of finding the analytical solution. This task of finding numerical solutions really simplifies the problem and allow scientist to make faster and high impact progress in all different fields of science.

In the specific case of seismology, scientist are mainly interested in having knowledge of two ambits: Earthquake sources and Earth structure. Those have to be reconstructed from recordings of ground motion (seismograms), usually following an earthquake, although studies of Earth structure may be based on different seismic sources such as ambient noise or man-made explosions. The relationship between source, Earth structure and ground motion can be described as a linear filter, where perturbations from a seismic source are modified by a number of propagation effects before being recorded at a seismic station. This point of view is called the *forward problem*, leading to a prediction of ground motion for a given source and given Earth structure.

A more realistic and challenging case is the *inverse problem*, that usually does not have a unique solution. It arises when scientists have information on ground motion (seismograms) and want to infer the corresponding Earth structure, the corresponding source characteristics,

or both. The most common case is that one of this two unknowns (source or structure) is inferred under certain assumptions about the other unknown (structure or source).

Both forward and inverse problems depend mathematically on the solution of the forward problem, making the solution of the forward problem of great importance in seismology. The solution of the forward problem or computation of synthetic seismograms is necessary for the determination of Earth structure and earthquake source parameters. There are many papers and a number of textbooks in the literature addressing this kind of problems. They find analytical solutions for specific configurations of each problem. Usually these configurations are simplifications of the physical model. Commonly as the problem gets more realistic, the analytical solution becomes extremely complex from the mathematical point of view.

The most simple analytical solution for a synthetic seismogram, emanated from a point source in a 1D medium consisting of two homogeneous half spaces, was found by Lamb (1904). In the analytical solution, the spherical wave emanating from a point source is expressed as a superposition of plane waves (the Weyl integral) and then as a superposition of cylindrical waves (the Sommerfeld integral). In the interaction of the spherical wave with a plane boundary between two different half spaces, the resulting wave systems can be naturally divided into three mayor types: (i) waves that are directly reflected from or transmited through the boundary, (ii) waves that travel from source to receiver via a path involving refraction along the boundary at body wave speed (head waves), (iii) and waves of Rayleigh or Stoneley type, with amplitude decaying exponentially with distance from the interface, Aki and Richards (2009). Although, seismologists investigated and solved more elaborate versions of the Lamb's problem over the next several decades, very little progress was made in developing any method to calculate analytical seismograms for a more realistic Earth model, Clarke (1989).

Nevertheless, there are several widely used techniques for computing synthetic seismograms of the Earth in a pseudo-analytical way. They all have in common that strong assumptions about wave propagation or model geometry are involved. In particular many of those techniques assume 1D Earth models which means a strong simplifications of Earth structure (horizontal and homogeneous layers).

In order to avoid clutter, it is important to recall what a 1D (one dimensional) model in a 3D (three dimensional) space is: imagine we are on the surface of the Earth (Fig. 1.1) and we are able to dig a hole as deep as we want. In a 1D model on a 3D space, while digging, we are always going to find the same discontinuities at the same depth, that is, it won't matter our location over the Earth's surface, we will find the same discontinuities at the same depth. Fig. 1.1 illustrates a simplistic 1D model of the Earth.

Following Clarke (1989), the most popular methods for computing pseudo-analytical seismograms for layered media are: The *Frequency-Slowness domain*, *Reflectivity method*, *Generalized Ray Theory*, *Full wave Theory*, the *WKBJ method* and *Normal Mode Summation*. Such analytical techniques usually involve the Fourier and/or Hankel transform of the equation of motion and integrations in slowness or wavenumber domains that have to be evaluated numerically, which is why they are often described as pseudo-analytical.

Commonly the expressions for the synthetic seismograms in heterogeneous media are quite complicated, although the analytical solution may be based on significant simplifications and/or being given for a specific type of wave, only (P,S or surface wave). Nevertheless, the fact that pseudo-analytical synthetic seismograms can be computed with reasonable effort and precision for laterally heterogeneous media solves the theoretical problem, as long as 1D Earth models appear to be sufficient to describe propagation effects for our purposes.

Pseudo-analytical synthetic seismograms can also be computed for laterally varying media by the *Geometric Ray Theory*, *Gaussian Beams*, *Maslov Theory* and *Normal Mode Method*. Seismic Ray Theory (SRT) is one of the most popular of these techniques.

Ray Theory (RT) is based on a high-frequency approximation of the elastic equations of

Figure 1.1: 1D (one dimensional) model of the 3D (three dimensional) Earth. Figure by Halldin (2013).

motion. The great significance of the Seismic Ray Method (SRM) is it universally, effectiveness, conceptual clarity, and its ability to investigate various seismic high frequency body waves independently of other waves in structurally complex media, Cerveny (2011). SRM is also known as the Ray Series Method (RSM), the Asymptotic Ray Theory (ART) or Geometric Ray Theory (GRT).

In case of global Earth models, 1D simplifications have been made for a long time. A giant step was done with the first 1D (radially anisotropic) tomographic global Earth model developed by Dziewonski and Anderson (1981) (see Fig. 1.2), which stayed as the predominant global model for at least two decades. 1D Earth models have allowed for great progress in science mainly because they provide a very reasonable approximation to true Earth structure, that is dominated by the vertical differentiation of materials with different density (and wave speed) in the gravity field of the Earth. However, when second order properties need to be taken into account, we have to face the unpleasant truth that the Earth is not strictly 1D.

Actually, the Earth presents different properties in composition, temperature, density, elastic parameters and anelastic properties in every direction of the three dimensional space. In addition, some of those parameters may be anisotropic. We can blame this heterogeneity on thermodynamics. It is the outcome of the dynamic evolution of the Earth, where mantle convection and plate tectonics are working against the equilibrium case of lateral homogeneity. The Earth has been revealed to be laterally heterogeneous everywhere, from the crust and the mantle to the core, with scales from the size of rocks to the size of continents, Wu (1989). The comparison of 1D models obtained from local and regional data in different parts of the world gives clues on important lateral heterogeneity, such as the different characteristics of oceanic and continental crust.

A widely used technique known as seismic tomography provides a systematic way of explaining the important deviations between observed and theoretical travel times of seismic

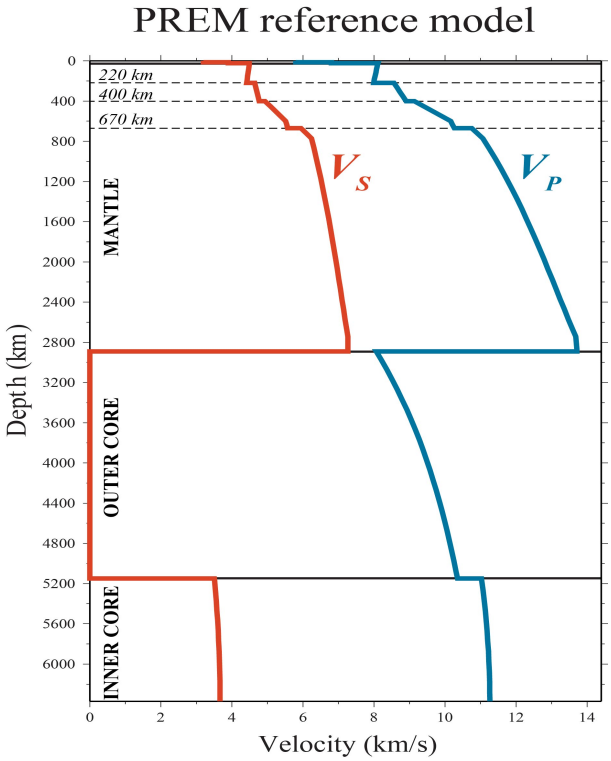

Figure 1.2: Preliminary Reference Earth Model (PREM) developed by Dziewonski and Anderson (1981). Figure by Thorne et al. (2013).

waves with respect to 1D reference models. Classical tomography techniques try to find perturbations in wave speed that can be later superimposed on 1D models. The development history of seismic tomography techniques is vast and extensive. Many important works has been published since 1971, P. Bois at the French Institute of Petroleum was the first to suggest the tomographic method in order to locate the causes of delays in seismic waves between two bore-holes, Nolet (2011). Considering the forward problem, seismic Ray theory has been the most popular technique in tomography (e.g. van der Hilst and Spakman (1989), Spakman et al. (1993), Fig. 1.3 by Bezada et al. (2010)). For decades, the lateral variation of physical properties within the different layers of the Earth was inferred by tomographic studies to be relatively small $(< 10\%)$, Montagner (2011).

However, recent studies that explore better data coverage and involve more advanced methodology give a completely different picture: Heterogeneity of several 10% is present in the Earths' crust (e.g. Tape et al. (2010)). This can be considered a surprising result given the expectation of Scientists used to tomography images with anomalies of a few $\%$, and a relevant development for the purpose of this study in several ways. First, the use of 1D models appears much less justified than a couple of years ago. Second, the case history of tomography has shown the intertwinning of physical assumptions (small variations of wave speed, approximate solution to wave propagation) and results that apparently confirmed these assumptions. The lesson is that simplified Earth models and simplified theory should be treated with caution in seismology.

This situation does not mean, of course, that average Earth models and pseudo-analytical methods have to be banned from seismology. For many purposes, 1D models or ray theory remain an appropriate framework, like for example in the inversion of earthquake slip maps from teleseismic body waves. Even in the more complicate case of regional surface wave propagation, suitable 1D models may be used to predict waveforms with reasonable accuracy,

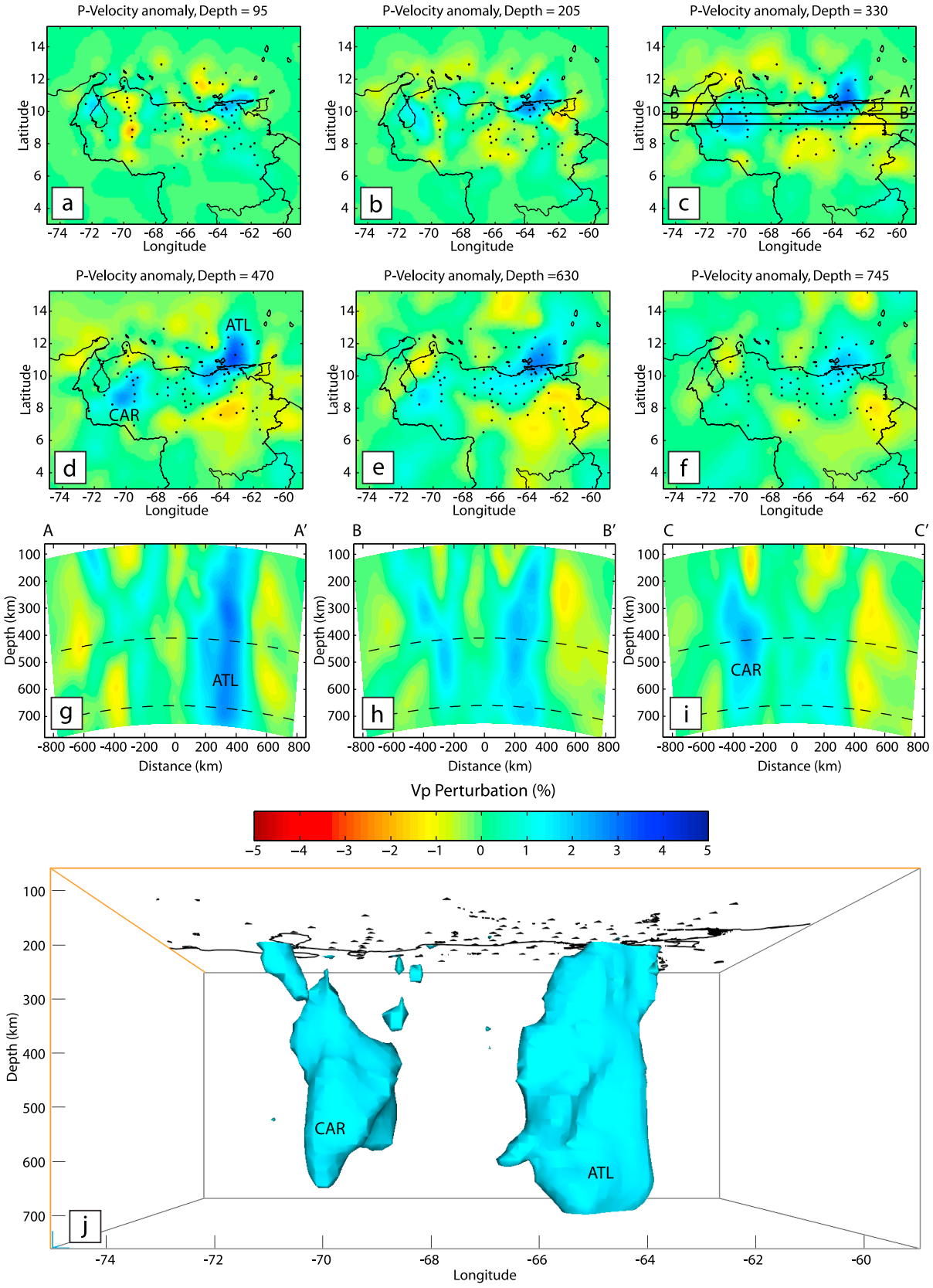

Figure 6

Figure 1.3: P wave velocity anomalies from finite-frequency P wave tomography. In the east, we image the subducting Atlantic slab, while in the west, we image a steeply dipping slab that we interpret as a subducted fragment of the southernmost Caribbean plate. Figure by Bezada et al. (2010).

underlying regional lithospheric models are described by *Stich et al.* [2003]. We compute fundamental fault Green's function with a reflection matrix algorithm [*Randall et al.*,

for faulting mechanism and source depth [e.g., *Ammon et al.*, 1998; *Mancilla et al.*, 2002]. We select the recordings that show less complicated waveforms in their respective azimuth range, hereby excluding the waveforms that are

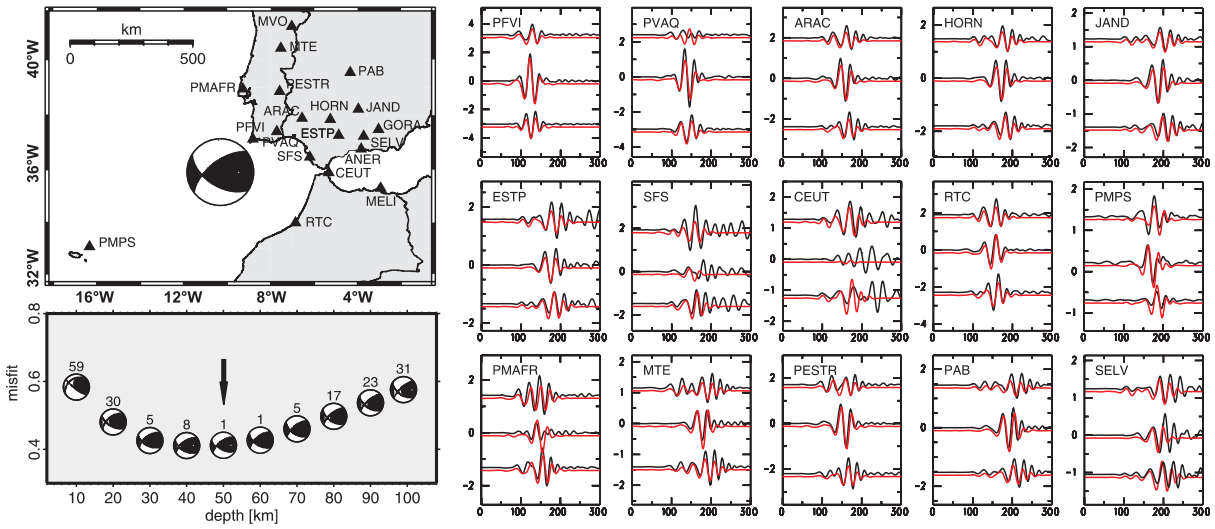

Figure 2. Moment tensor inversion results. We show a map with station distribution and the best solution, fits between observed (black) and predicted (red) intermediate-period waveforms at selected stations (radial, transverse and vertical components from top to bottom, units in [s; 10^{-4}m]), as well as the depth-dependence of L2-misfit, source mechanism and CLVD component (numbers above beach balls, in [%]).

Figure 1.4: Moment tensor inversion results. We show a map with station distribution and the best solution, fits between observed (black) and predicted (red) intermediate-period wave-forms at selected stations (radial, transverse and vertical components from top to bottom, units in [s; 10^{-4}m]), as well as the depth-dependence of L2-misfit, source mechanism and CLVD component (numbers above beach balls, in [%]).

see Fig. 1.4. In many cases, routine seismology applications based on average 1D models or smoothly varying models produced reliable and consistent data inventories over decades, such as hypocenter or moment tensor catalogues (e.g. CMT catalogue, Dziewonski...) that should be continued in the same way to assure the homogeneity of the catalogue. In general, due to our incomplete knowledge of the Earth, any 3D models will contain inaccuracies just as their 1D counterparts, and introduce errors and artifacts in seismological methods. In this sense, an advantage of 1D models is that many of these artifacts are well-known. An advantage of 3D models is that the artifacts should be overall less important due to a better approximation to the true Earth.

If we accept that 3D models can lead to more accurate predictions in many cases, then we have to provide the tools to use 3D models in seismology. Considering realistic heterogeneity of the Earth represents a huge challenge from the theoretical point of view. As seen before, pseudo-analytical solution are not available for cases that are interested in full 3D heterogeneity and full solutions of the wavefield. The use of numerical techniques helps to circumvent these limitations.

Numerical methods are essentially methods that are build directly on the very basic equations (which describes the physical model) and do not involve any mathematical representation of specific boundary conditions to these equations, necessary to find analytical solutions for specific cases such like plane layered media. For a general 3D Earth, no analytical solutions to the elastodynamic wave equation can be given. On the other hand, a numerical solution will be conceptually independent of the degree of heterogeneity (homogeneous, 1D, 2D, 3D), as long as any heterogeneity is represented appropriately in the numerical Earth model.

Of course, not all is beautiful with numerical methods. There does not exist a perfect numerical technique and different numerical techniques may be suitable for different type of problems. In the following we give a very brief overview of the most commonly used numerical methods to simulate seismic wave propagation.

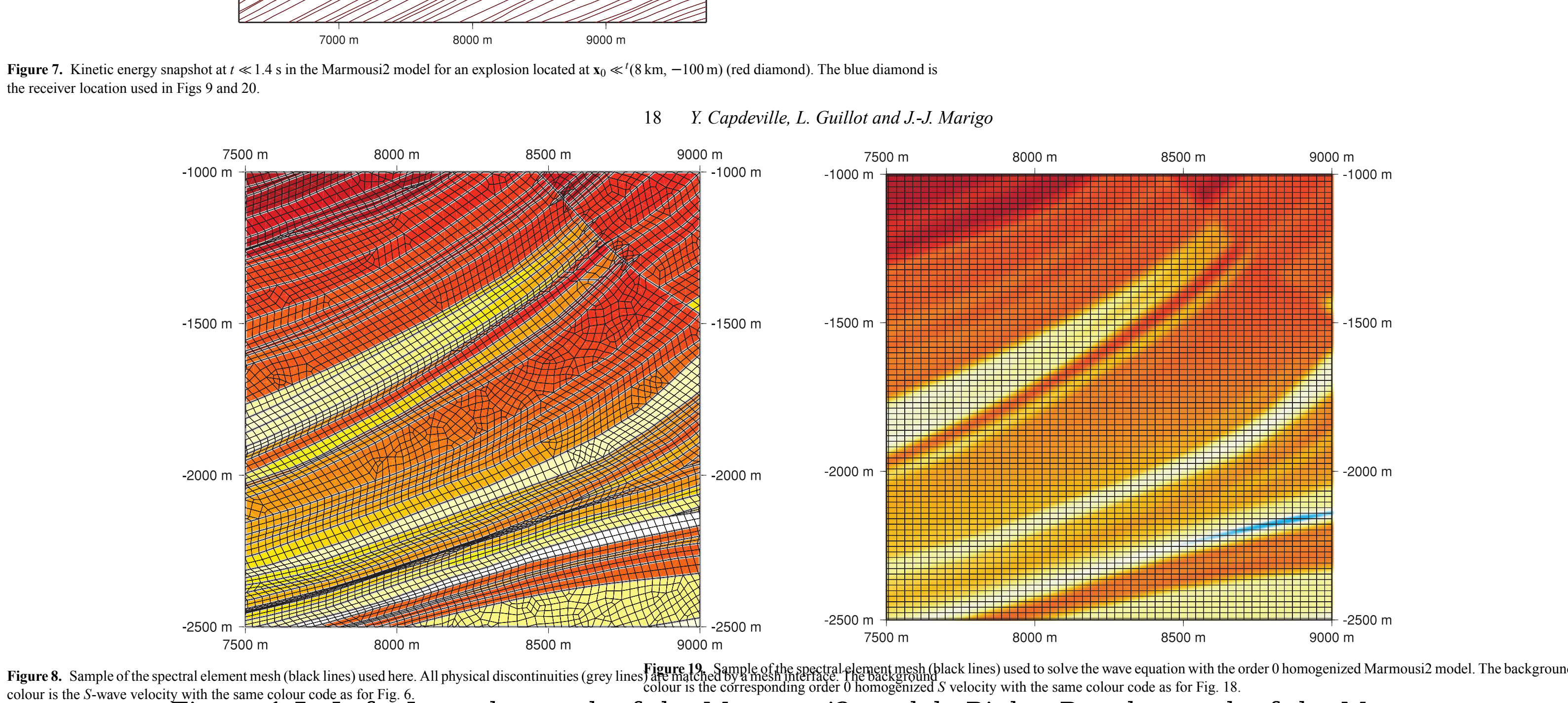

Figure 1.5: Left: Irregular mesh of the Marmousi2 model. Right: Regular mesh of the Marmousi2 model. The elements of both meshes are represented by black lines. The background color is the S-wave velocity values (varies from 0.5-3 km/s), which in the case of the regular mesh are homogenized. Note the difference between the regular and irregular mesh: in the irregular mesh all physical discontinuities are matched by a mesh interface while in the regular mesh are not. Figures by Capdeville et al. (2010).

The **Finite Differences [redacted]hod (FDM)** is one of the oldest, simplest and more powerful (in terms of computationa[redacted]ost) numerical techniques, but has its limitations. The main limitations are in general related to the restriction on regular grids (see Fig. 1.5), smooth heterogeneity of the model, and difficulties to impose free boundary conditions for the elastic wave equation.

FDM discretizes the strong form of the equations of motion by replacing partial derivatives by difference approximations using local values. FDM is typically designed to be accurate for low order polynomials, although the concept of derivative is a local property of the function, many high order finite difference (FD) schemes, commonly applied to heterogeneous media, invoke many function's values far away from the point of interest.

Perhaps the most popular FD scheme in seismology is the staggered grid introduced by Virieux (1984) and Virieux (1986) who used the idea of staggered grid implemented first in seismology by Madariaga (1976) who in turn applied the famous Yee scheme (Yee, 1966) for the elastic wave equations of motion.

The revolutionary idea of the staggered grid is based on the location of different variables (velocity and stress) at different spatial points or grid points and at different time levels. This brings down the elastodynamic wave equation to a system of first order differential equations that are easier to handle in many ways. The stability condition and the P-wave phase velocity dispersion curve do not depend on the Poisson's ratio, while the S-wave phase velocity dispersion curve behavior is rather insensitive to the Poisson's ratio, Virieux (1986). Also, the use of different time levels for velocity and stress allow to significantly reduce the computational cost of the simulations.

FD simulation techniques have been used in several fields of seismology, just to mention a few: simulations of seismic scattering (e.g. Frankel and Clayton (1986)), seismic wave propagation (e.g. Moczo et al. (2002), Moczo et al. (2004a), Aochi et al. (2013)), simulations in viscoelastic media (e.g. Kristek and Moczo (2003), Galis et al. (2008)), full waveform inversions (e.g. Fichtner et al. (2006), Abubakar et al. (2011)), rupture propagation (e.g. Virieux

and Madariaga (1982), Rojas et al. (2009)) and surface wave tomography using adjoint techniques (e.g. Peter et al. (2007)).

FDM schemes are conceptually closely related to the numerical technique presented in this study and will be discussed in detail in the next chapter.

More recent methods like the Pseudo-Spectral method (PSM) (e.g. Yan and Wang (2008), Sidler et al. (2013)), Finite Elements method (FEM) (e.g. Koketsu et al. (2004)), Spectral Elements method (SEM) (e.g. Komatitsch and Vilotte (1998) Komatitsch and Tromp (1999)), Discontinuous Galerking method (DGM) (e.g. Käser et al. (2008)), Boundary Element method (BEM) (e.g. Chaillat et al. (2008)), Finite Volume method (FVM) (e.g. Tadi (2004)) and Hamiltonian Particle method (HPM) (e.g. Takekawa et al. (2012)), among others, can be applied for more realistic configurations of the Earth structure (see Fig. 1.6).

The **Pseudo-Spectral Method (PSM)** can be seen as a liming case of increasing (spatial) order FD methods. PSM unlike FDM present exponential convergence rate for the space domain, that is, the space derivatives are calculated using orthogonal polynomials and the time discretization is simply given by a FD approximation. Orthogonal polynomials are used as basis of interpolation of the spatial field. The most common polynomials used are Fourier, Chebyshev and Legendre polynomials.

In case of use of Fourier polynomials (trigonometric functions), the Fast Fourier transform (FFT) is used to compute derivatives, that is, the space derivatives are calculated in the wavenumber domain by multiplication of the spectrum with $\mathbf{i}k$. Due the periodicity of the FFT, its use is justified when the physical problem in study is periodic in space. In case of non-periodic problems, Chebyshev or Legendre polynomials can be used. In this sense, PSM is a global approximation in space, which makes the method virtually free of dispersion and dissipation errors.

The orthogonal polynomials are either evaluated using matrix-matrix multiplications, FFT or convolutions. The optimum spectral convergence depends on the optimum choice of orthogonal polynomials (periodic or non-periodic case), optimum collocation points (meshing) and the global influence of the high-order polynomials over the whole domain.

The main difficulties with PSM is that any change of geometry or boundary conditions requires a considerable change in the method. Also difficulties are related to parallelizing the problems because global memory access is required for the computation of the Fourier and Chebyshev transforms (e.g. Igel (1999)). However, for the simulation of turbulence in relative simple domains are ideally suited (e.g. Hesthaven et al. (2007)).

The **Finite Element Method (FEM)** is a high-order accurate method and is suitable for complex geometries but is implicit in time and has a large amount of numerical dispersion. FEM belongs to the family of the so called *Methods of Weighted Residuals* (MWR). The first step of the MWR is to take the PDE in study and multiply it by a general weighting function. After this multiplication, integration by parts over each term of the PDE is performed in order to reduce second order derivatives to first order (in case there are), and to obtain an explicit expression for the boundaries of the PDE problem.

At this point we have an integral expression of the original PDE which, unlike FDM or PSM, includes explicit expressions for the boundaries of the problem. This integral expression, obtained after integration by parts, is called the *weak formulation* of the PDE. The *strong formulation* of the PDE is given before the integration by parts.

The next step of the MWR is to choose the nature of the so called *trial functions*. Trial functions are just approximations to our field variables (displacement, velocity, accelerations, etc.), that is, the method chooses a general mathematical expression with unknown coefficients (to be determined later), which is supposed to reproduce reliable values of the field variables. For instance, we can choose the trial function to be the equation of a straight line with two coefficients to be determined. This expression will give us approximate information of the field

...ab rollback are emergent consequences of slab descent in the upper ... the lower mantle couple into oceanic plates through narrow ...y of oceanic plates. Viscous dissipation within the bending lithosphere ... the total dissipation through the entire lithosphere and mantle.

...ociated plate ...ntrols on the ...olution of the ...o our under- ...n of tectonic ...thermal and ...nd ultimately ...Plate creation ...of heat from ...of plates may ...nce heat loss ..., despite the ...cs, there are ...rces resisting

...the 1- to 10- ...en largely by ...cted slabs (3) ...d-solid phase ...c lithosphere ...f the aseismic ...r mantle (5) ...of subducted ...of plate tec- ...ble negative ...he transition ...s are strong, ...ctly into the ...6). However, ...during initial ...nch, then the

dissipation within the narrow high-viscosity slab could limit plate velocity (*7*). Although the importance of plate margin and slab strength has been studied in two- and three-dimensional Car-

...fractions of Earth's surface (~15% globally) do not follow a rigid plate tectonic model but undergo deformation close to trenches and farther from plate margins (*16*). Some oceanic plates are deforming diffusively within their interiors, especially the Indo-Australian plates (*17*). The rich array of geodetic, topographic, gravitational, and seismic observations from local to regional scales constrains these deformations and could validate global

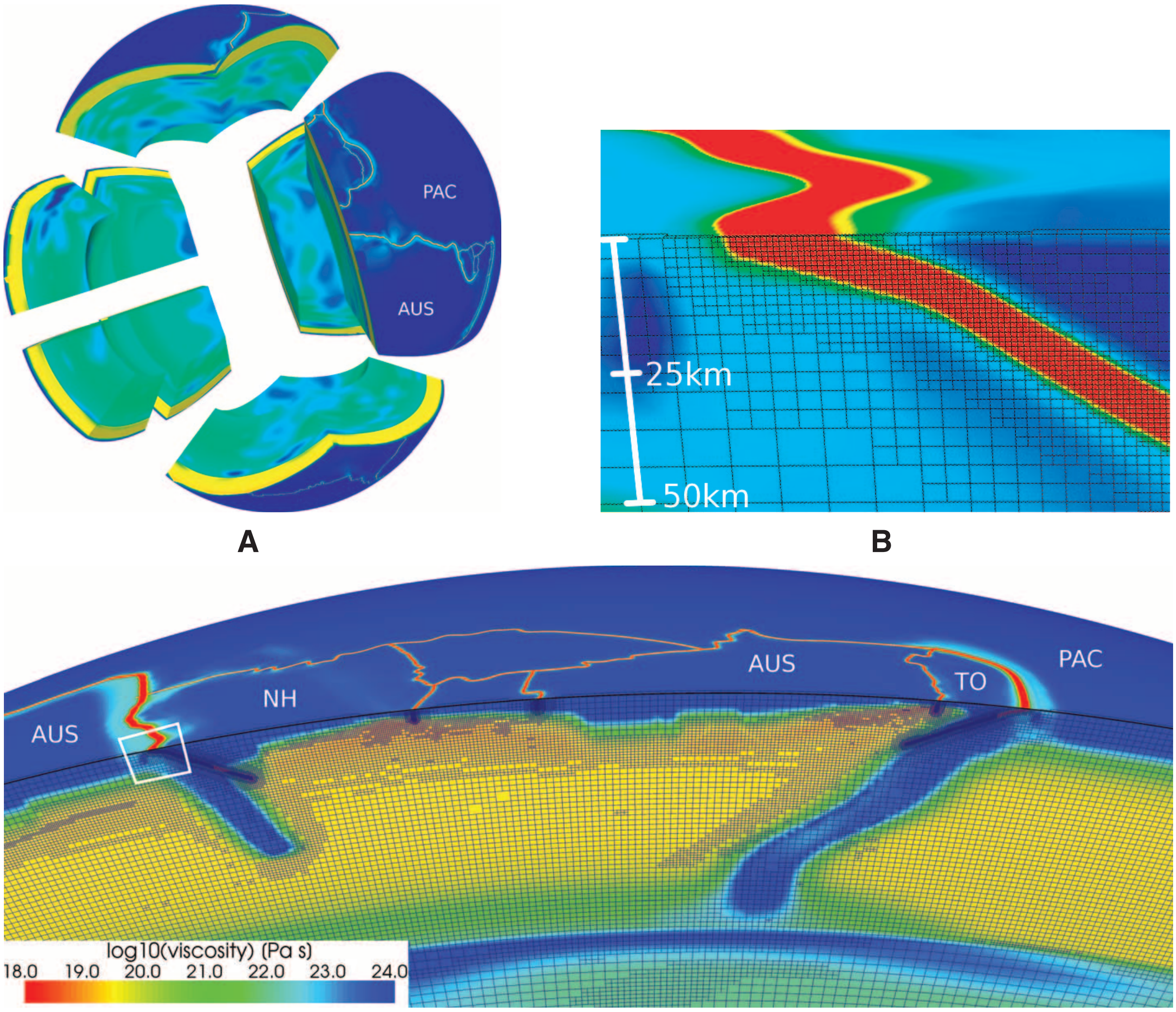

Fig. 1. (**A**) Splitting of Earth's mantle into 24 warped cubes. The effective viscosity field is shown; the narrow low-viscosity zones corresponding to plate boundaries are seen as red lines on Earth's surface. (**B**) Zoom into the hinge zone of the Australian plate [as indicated by the box in (**C**)] showing the adaptively refined mesh with a finest resolution of about 1 km. (C) Cross section showing the refinement that occurs both around plate boundaries and dynamically in response to the nonlinear viscosity, with plastic failure in the region from the New Hebrides to Tonga in the SW Pacific. Plates are labeled Australian, AUS; New Hebrides, NH; Tonga, TO; and Pacific, PAC.

Figure 1.6: (A) Splitting of Earth's mantle into 24 warped cubes. The effective viscosity field is shown; the narrow low-viscosity zones corresponding to plate boundaries are seen as red lines on Earth's surface. (B) Zoom into the hinge zone of the Australian plate [as indicated by the box in (C)] showing the adaptively refined mesh with a finest resolution of about 1 km. (C) Cross section showing the refinement that occurs both around plate boundaries and dynamically in response to the nonlinear viscosity, with plastic failure in the region from the New Hebrides to Tonga in the SW Pacific. Plates are labeled Australian, AUS; New Hebrides, NH; Tonga, TO; and Pacific, PAC. Figure by Stadler et al. (2010).

...d Sciences, The ...712, USA. [2]Seis- ...of Technology, ...of Geosciences, ...X 78713, USA. ...he University of ...ressed. E-mail: ...e Village, CA

variable of interest at certain spatial location and certain time level.

We emphasize the difference between the trial and the weighting functions: the trial function is the approximation to the field variable and the weighting functions is a function which multiplies the PDE.

It is at this point where different methods like FEM are born. FEM (like many others) chooses the weighting function to be the derivative of the trial function, that is, the method multiply the PDE by an interpolation function of the field variables. Commonly, FEM chooses the trial function to be a linear approximation. These kind of methods that uses the weighting function to be the derivative of the trial function are called *Galerkin methods*.

The chosen linear approximation of he field variables by the FEM requires that such approximation gives accurate results of the field variables over the whole domain. In other words, a linear approximation is performed over the entire domain. For this to work, the linear approximation has to be done several times, which in computational terms, is translated into a discretization of the spatial domain.

To illustrate this, imagine the seismic wave propagation over the Earth produced by an earthquake. We want to infer reliable information of the Earth movement (displacement, velocity and acceleration) at certain location on the surface. We know that the most simple shape of a general wave does not look like a straight line but rather like a high order polynomial. Still, we want to use a linear approximation in order to solve the PDE. The way to attack the problem is selecting the wavelength of interest (that we want to solve numerically) and then dividing that wavelength into several parts, each part in which a linear approximation of the waveform will be performed. This task of dividing the space domain into smaller parts where the linear approximations will be performed is called the meshing (see Fig. 1.6).

Due to the complex shape of waveforms, higher order approximations are found to have a much better efficiency towards numerical dispersion (e.g. Komatitsch et al. (2010)) than low order. For this reason, FEM is more often to be used as a technique for computing seismic responses of structures (e.g. Nour et al. (2003)) than for simulating seismic ground motion (e.g. Koketsu et al. (2004)).

We have seen, a linear approximation is preformed over the space domain. For the case of dynamic problems, which involves derivatives of the field variables respect to time, a FD discretization in time is performed in order to solve the problem to the time level of interest. In this sense, FEM can be seen as an hybrid technique which uses linear approximations if space and FD discretizations in time.

The **Spectral Element Method (SEM)** is considered to be a high order FEM and a continuous Galerkin technique. It was implemented first in fluid dynamics by Patera (1984) and later in seismology (e.g. Komatitsch and Vilotte (1998)). SEM is possibly the most popular method to simulate wave propagation in media with realistic heterogeneity nowadays. Like FEM, it is based on the weak form of the equations of motion. Unlike FEM, the fields (displacement, velocity, acceleration, etc.) are approximated by *Lagrange polynomials* which gives to the method spectral accuracy. In fact, in wave propagation simulations, a spatial sampling of approximately 5 points per wavelength is found to be accurate (from a mathematicians perspective) when working with a polynomial of eighth degree, Komatitsch and Vilotte (1998), and found to be accurate (from a seismologists pespective), when working with degree five polynomials (Komatitsch and Tromp (2002a), Komatitsch and Tromp (2002b)).

The use of Lagrange polynomials for approximating the solution in conjunction with GLL (Gauss-Lobatto-Legendre) points of integration produces a diagonal mass matrix, which makes the problem tractable from a point of view of computational cost. High order accuracy and reasonable computational requirements have made SEM the one of the most attractive numerical methods in seismology.

SEM (unlike many others methods) has been able to simulate the elastic wave propagation

over the entire Earth globe with considerable accuracy and modest computational requirements (e.g. Komatitsch and Tromp (2002a), Komatitsch and Tromp (2002b)). The method decomposes the entire globe intro irregular hexahedra. This kind of Earth mesh is called the cubed sphere (see Fig. 1.7). Different properties can be assigned over each element of the cubed sphere. In fact, each element should contain a single value of a certain property (for instance, Lamé elastic parameters), but in practice, the method allows to introduce small heterogeneities over each element. In case of strong discontinuities, the mesh must honor the interfaces, otherwise, the numerical model is an insufficient representation of the physical model. Therefor, recent efforts in global SEM include the appropriate translation of physical Earth models into equivalent numerical models to be used on regular SEM grids (e.g. Fichtner et al. (2010)), and sophisticated meshing techniques that approximate complex structures by hexahedral elements in local SEM (e.g. Tromp et al. (2010)).

SEM like FEM commonly uses FD discretizations in time in order to solve the PDE to the time level of interest. Unlike FEM, SEM can be easily designed to be explicit in time, which significantly reduces the computational cost. The flexibility of SEM allows the use of different time discretizations (explicit or implicit), which depending on physical requirements, allow to simulate seismic wave propagation with considerable time accuracy over long time periods. Clearly, the use of higher order accurate time discretizations leads to the increment in computational cost.

The **Discontinuous Galerkin Method (DGM)** is perhaps one of the most complete numerical methods. DGM is a Galerkin method just as FEM or SEM, with the difference that the interpolation functions are piecewise continuous. The basis functions are combinations of Jacobi-polynomials and form an orthogonal basis on triangles and tetrahedrons. Therefore, the mass matrix is always diagonal. These kind of functions are suitable for simple and flexible mesh design involving, for example, non/conforming tetrahedrons, and allowing to solve problems with highly complex geometries and heterogeneity, of course, with the cost of the increment in computational requirements. The method is also well-suited for parallelization due to its local character of interpolation.

In seismology, DGM has proven to be a reliable method for simulations of high-frequency wavefields over long propagation distances. It has been used in regional wave propagation in unstructured meshes (e.g. Wenk et al. (2013)), Pelties et al. (2012), Käser and Dumbser (2006), Dumbser et al. (2007b)), dynamic rupture simulations using unstructured grids (e.g. Pelties et al. (2012)), wavefield modeling in exploration seismology (e.g. Käser et al. (2010)), effective wave propagation in viscoelastic media (e.g. Käser et al. (2007)) and poroelastic media (e.g. de la Puente et al. (2008)).

The **Boundary Element Method (BEM)** uses the integral formulation of the PDE. Unlike Galerkin type's methods, BEM uses the boundary expression of the integral formulation to set numerical values, rather than values inside the spatial domain. In the 3D case, the surface of the spatial domain (boundaries) is discretized into elements where the approximation polynomials are used to find approximate solutions between the spatial points.

After imposing boundary values, the integral equation is used to compute numerically the solution of the PDE at any interior point of the spatial domain and at any time level. Because BEM is focused on imposing numerical values at the boundaries only, the method is well suited for Earth configurations with special boundary conditions like cracks and rupture propagation.

The advantage of BEM over SEM, FEM, DGM and FDM is that only the boundaries of the body need to be meshed, which in the case of SEM is a huge task. The disadvantage is, for many physical problems, the method can be very computational expensive. As an example, BEM has found widespread use in the sub-field of structural geology for solving problems of deformation and propagation of opening mode and sliding mode fractures, Cooke (2011).

The **Finite Volume Method (FVM)** like Galerkin type's methods, uses the integral form

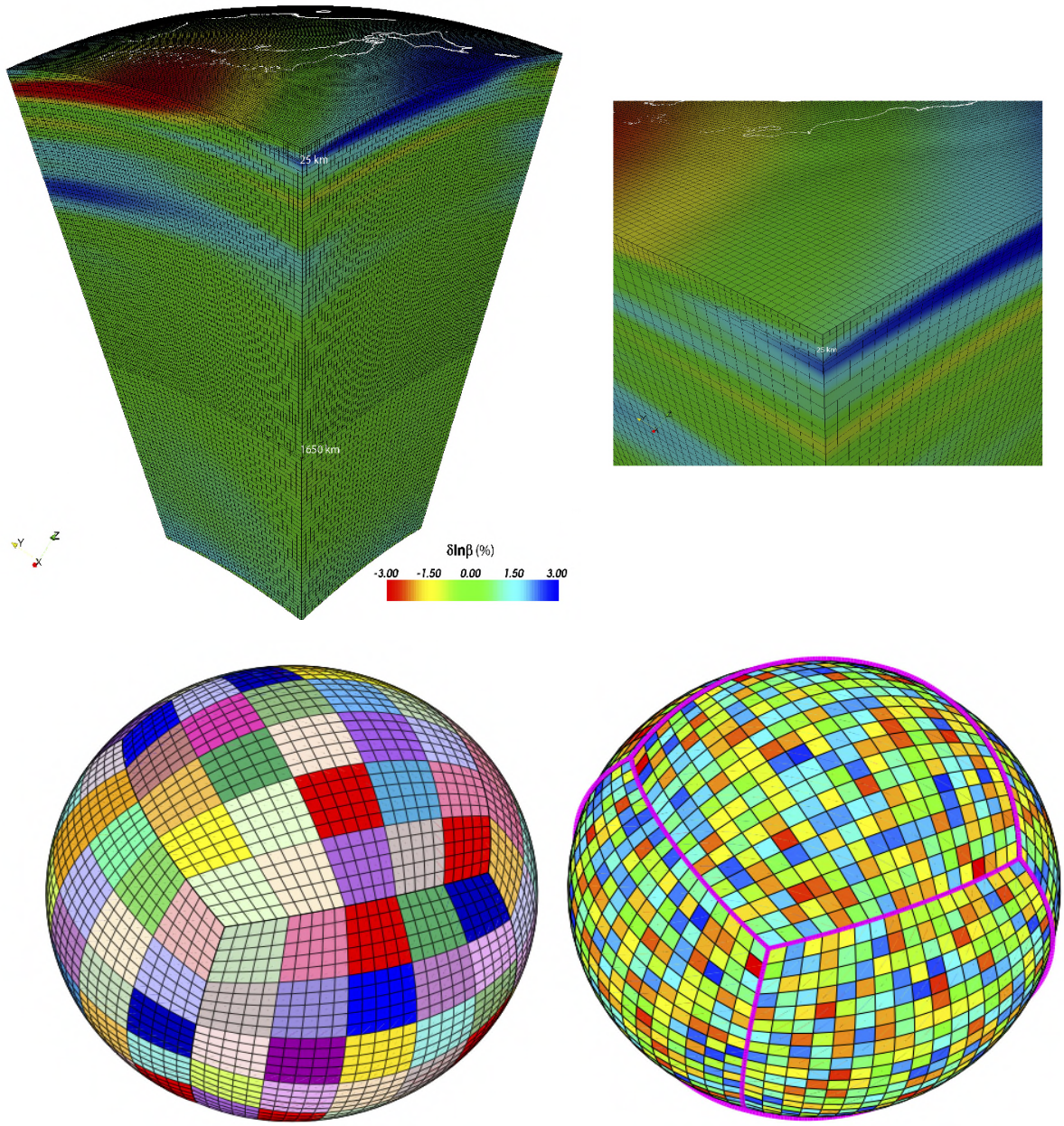

Figure 1.7: Figure on the upper left: S-wave velocity anomalies from the global tomographic model s20rts (Ritsema and Van Heijst, 2000) are superimposed on the mesh. For parallel computing purposes, the one-chunk SEM simulation is subdivided in terms of 64 slices. The center of the chunk is at (38.5°N, 137.5°E), and the lateral dimensions are 30° x 30°. Two doubling layers are indicated at a depth of 25 km (PREM Moho depth) and a depth of about 1650 km. Shows full view of 25 neighboring slices. Figure upper right: Close-up view of the upper mantle mesh. Note that the element size in the crust (top layer) is 13 km x 13 km, and that the size of the spectral elements is doubled in the upper mantle. The velocity variation is captured by NGLL = 5 grid points in each direction of the elements, Komatitsch and Tromp (2002a), Komatitsch and Tromp (2002b). Bottom: each of the 6 chunks that constitutes the cubed sphere is subdivided in terms of n^2 slices of elements, where $n \geq 1$ is a positive integer, for a total of $6 \times n^2$ slices (and therefore processors). The figure on the left shows a mesh that is divided in terms of $6 \times 52 = 150$ slices as indicated by the various colors. In this cartoon, each slice contains $5 \times 5 = 25$ spectral elements at the Earth's surface. The figure on the right shows a mesh that is divided over $6 \times 182 = 1944$ processors as indicated by the various colors. Regional simulations can be accommodated by using only 1, 2 or 3 chunks of the cubed sphere. One-chunk simulations may involve a mesh with lateral dimensions smaller than 90 degrees, thereby accommodating smaller-scale simulations. Figures by Komatitsch et al. (2013).

of the PDE. FVM first divides the spatial domain into discrete non-overlapping control volumes (CVs) or non-overlapping elements, which in contrast to FDM, FEM, SEM and DGM, defines the control volume boundaries, not the nodes. The usual approach is to assign the computational node to the center of each CV, however it is not a rule. The advantage of the first approach is that the nodal point represents the mean over the CV, which is translated into higher order accuracy. For control volumes that are adjacent to the domain boundaries the general discretised equation is modified to incorporate boundary conditions. Then, the method uses FD approximations to solve the derivatives inside the integral from of the PDE over each control volume. The volume and surface integrals are approximated using quadrature rules, thus the integration of the governing equation (or equations) over a control volume yields to a discretized equation at its nodal point (mesh points). Depending on the approximation used, the finite volume (FV) discretized equation may be the same obtained by the FDM. The most simplest approximation to the integral is the midpoint rule, where the integral is approximated as a product of the integrand at the center the cell-face and the are of the cell-face. The main advantage of the FVM over FDM is regarding the integral expression for the boundaries of the spatial domain, which in case of seismic wave propagation reduce the difficulty to impose free surface conditions (zero traction at the surface).Also, unlike FDM, discontinuities of the properties of the model are not a problem if the mesh is chosen to honor that discontinuities (e.g. Dumbser and Käser (2007)), also, unlike Galerkin type's methods, the method does not require a coordinate transformation to be applied to irregular meshes.

FVM has been able to simulate seismic wave propagation on unstructured meshes with high order accuracy (e.g. Dumbser et al. (2007a)). The method is sometimes called a *discontinuous finite element method* or *cell centered difference scheme*.

The commonly called **Meshfree Methods (MFM)** are another family of numerical methods. FDM, FEM, SEM, DGM and FVM are numerical methods which require a certain kind of discrete approximation of the space domain in order to solve the PDE, that is, they require the meshing process. The meshing process may not be an easy task and usually requires mathematical transformations that can be even more expensive than solving the PDE itself. Also, the process of creating a mesh for complex geometries many times requires a significant human effort. However, there are several numerical methods in the literature which do not require the discretization of the space domain (MFM).

MFM provide accurate and stable solutions for integral equations of PDE (weak or strong form) or for the PDE itself under all kinds of boundary conditions without using the concept of a connected mesh among distributed nodes. MFM modify the structure of mesh based methods like FDM and FEM to become more adaptive, versatile and robust. Advantages of MFM are related to efficient performance over large deformations, since the positions of the nodes can change with time.

In several applications it is more computational efficient to discretize the space domain by only a set of nodal points, or particles, without caring about constraints. This kind of methods are called **Particle Methods (PM)**. PM may or may not be meshfree. Following Shaofan and Wing-Kam (2002), PM can be classified based on physical principles, or computational formulations. According to the physical modeling, they may be deterministic or probabilistic models. According to computational modeling, they may be based on the strong or the weak form of the PDE.

Mesh Free Particle Methods (MFPM) can be seen as a generalization of FEM and a combination of MFM and PM. They are designed to be accurate and efficient because they discretize the continuum by a set of nodal points or particles without the mesh constrain, in other words, they adapt the changes of the topological structure of the space continuum. There are many version of MFPM, for instance Meshfree Finite Difference Method (MFFDM) (e.g. Liszka and Orkisz (1980)) and Smoothed Particle Hydrodynamics (SPH) (e.g. Gingold

and Monaghan (1977)). SPH as one of the oldest MFM is capable of successfully dealing with problems with free surface, deformable boundaries, moving interfaces as well as extremely large deformations. Its applications are very wide, from micro to macro scales and from truly discrete to discretized continuous systems.

A very popular and young family of MFPM are the so called *Meshfree Galerkin Methods* (MFGM). MFGM offers considerable advantages over the traditional FEM in crack growth simulation, because remeshing is avoided. Examples of MFGM are Element free Galerkin method (EFGM) (e.g. Belytschko et al. (1994)) and Moving Particle Finite Element Method (MPFEM) (e.g. Hao et al. (2002)).

MFPM has not been widely used in computational seismology, except for perhaps the **Hamiltonian Particle method** (HPM). HPM is a meshless simulation technique in which the space domain is approximated by discrete dynamics of a finite number of particles, Suzuki and Koshizuka (2008). In HPM particles are connected by virtual springs and interact with each other through both normal and shear forces at contact points. The particle motion is computed based on the deformation gradient tensor estimated at each particle position. The advantages of HPM are the simplicity and flexibility to create numerical models containing arbitrary topography shapes and the simplicity of its data structure, Takekawa et al. (2012). The method is also suitable for very heterogeneous models and non-linear problems.

As shown, the list of numerical methods to be applied in seismology is extensive nowadays, but certainly the method which requires the smallest amount of computational resources is still FDM. And although the family of numerical techniques is huge and there are many methods being born nowadays, only a few of them are applied in the seismology field.

It is important to emphasize that for general seismological problems there does not exist a best numerical method a priori, that would perform better than all others. The success of the numerical method depends on the kind of physical problem to be addressed, and it is up to the user of a numerical technique to choose the most suitable method for the physical problem to be solved. Of course, there are cases when several numerical techniques can be applied to the same problem; in that case, similar results can be obtained using different techniques, see Fig. 1.8 (e.g. Chaljub et al. (2010)). In that situation the selection of the numerical tool is based usually on our access to the numerical code and most importantly, the amount of computational resources we have.

Today it is a reality that numerical techniques allow for finding approximate solutions to very complex physical problems, however there are still many relevant problems that are beyond the reach of present computational resources. Like mentioned before, as the physical configuration of the problem becomes more and more realistic and/or the scale of the problem becomes larger, the computational requirements become bigger. For instance, seismic wave propagation on the entire Earth is a reality nowadays thanks to the use of the so called computer clusters. The computer cluster is a set of interconnected computers working as a unit. Like the Belgium national motto “unity makes strength”, scientist divide the numerical task into the number of computers components of the cluster. Interchanging information during the simulation, each computer of the cluster will solve a part of the problem, all of them helping together to solve the whole numerical task.

There are several ways that scientist divide the numerical task to solve. Usually the way to do it is by decomposing the domain in space and/or time. In the spatial domain decomposition, the domain is divided into smaller non-overlapping sub-domains. Each sub-domain is then assigned to a certain processor, trying to assign the same amount of information to each processor in order to gain efficiency by giving the same amount of work to each one. In time domain decomposition, several computers simultaneously perform work on the same sub-domain region for different time steps.

In seismology, the use of computer clusters has allowed the application of very complex

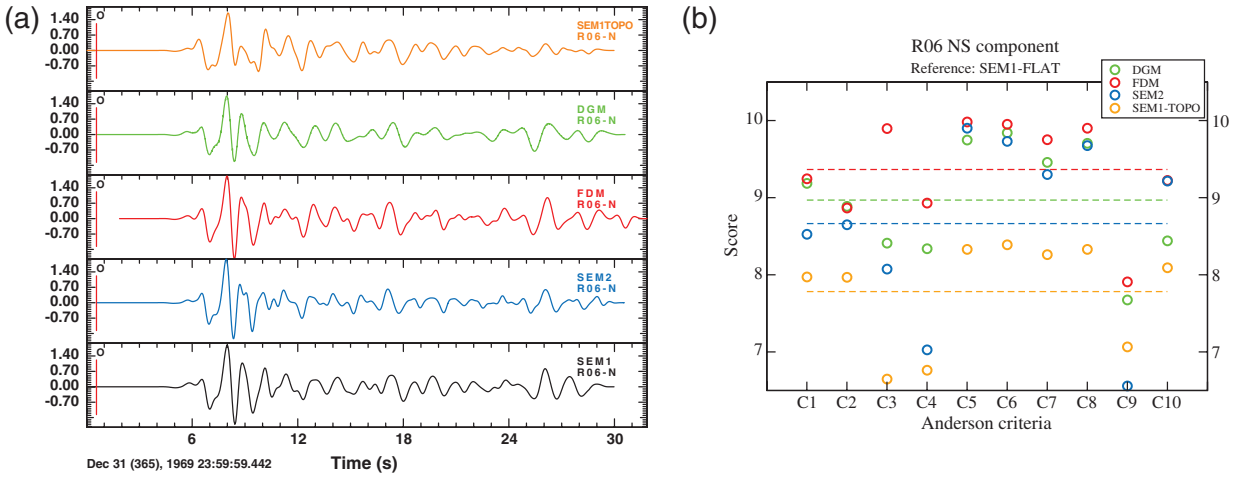

Figure 10. (a) Time series of the NS ground acceleration computed at receiver R06 by 4 different codes for the strong motion case S1-FLAT: DGM (green), FDM (red), SEM1 (black) and SEM2 (blue). The topmost trace (orange curve) was computed by the code SEM1 including surface topography (S1-TOPO). (b) Goodness-of-fit as measured by the 10 criteria proposed by Anderson (2004). The SEM1-FLAT prediction is used as reference in each case. The dashed lines indicate the levels of the global similarity scores for each prediction. Note that the fit between different predictions of the same simulation case (S1-FLAT) is better than the fit between predictions of different simulation cases (S1-TOPO and S1-FLAT) by the same code (SEM1).

Figure 1.8: Time series of the NS ground acceleration of the Grenoble Valley, France, computed at receiver R06 by 4 different codes for the strong motion case S1-FLAT: DGM (green), FDM (red), SEM1 (black) and SEM2 (blue). The topmost trace (orange curve) was computed by the code SEM1 including surface topography (S1-TOPO). (b) Goodness-of-fit as measured by the 10 criteria proposed by Anderson (2004). The SEM1-FLAT prediction is used as reference in each case. The dashed lines indicate the levels of the global similarity scores for each prediction. Note that the fit between different predictions of the same simulation case (S1-FLAT) is better than the fit between predictions of different simulation cases (S1-TOPO and S1-FLAT) by the same code (SEM1). Figure by Chaljub et al. (2010).

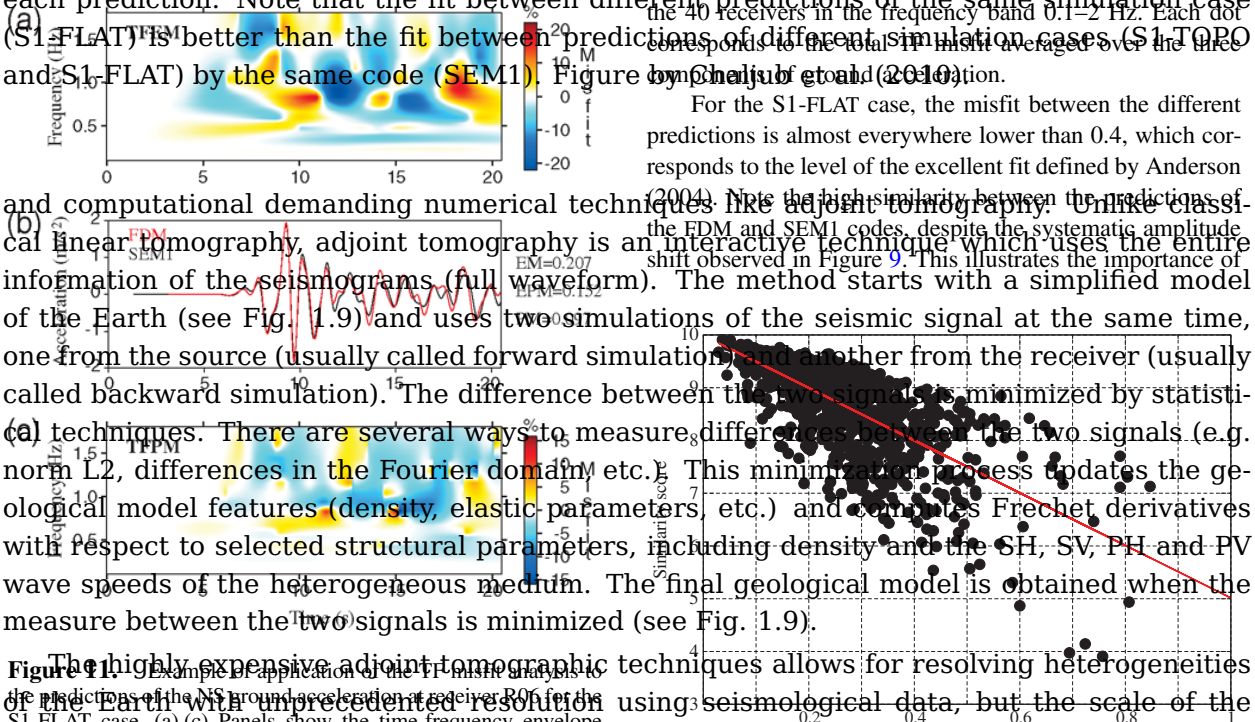

Figure 11. Example of application of the TF misfit analysis to the predictions of the NS ground acceleration at receiver R06 for the S1-FLAT case. (a),(c) Panels show the time-frequency envelope (TFEM) and phase (TFPM) misfits, respectively, taking the SEM1 prediction as a reference. (b) Time series of acceleration predicted by codes FDM (red) and SEM1 (black) are shown. Single-valued envelope (EM) and phase (PM) misfits are obtained by averaging the absolute values of TFEM and TFPM over time and frequency. The total TF misfit is obtained by averaging the envelope and phase misfits. (d) Comparison of results obtained with the TF misfit (M) plotted against those using the similarity score (S). Both measures have been applied to the 3 components of the 40 receivers for the benchmark cases S1-FLAT, S1-TOPO, and W1-FLAT. A global linear trend with a correlation coefficient of 0.96 is found.

Figure 13 shows the TF misfits between the different predictions of the S1-FLAT and W1-FLAT cases computed at the 40 receivers in the frequency band 0.1–2 Hz. Each dot corresponds to the total TF misfit averaged over the three components of ground acceleration.

For the S1-FLAT case, the misfit between the different predictions is almost everywhere lower than 0.4, which corresponds to the level of the excellent fit defined by Anderson (2004). Note the high similarity between the predictions of the FDM and SEM1 codes, despite the systematic amplitude shift observed in Figure 9. This illustrates the importance of

and computational demanding numerical techniques like adjoint tomography. Unlike classical linear tomography, adjoint tomography is an interactive technique which uses the entire information of the seismograms (full waveform). The method starts with a simplified model of the Earth (see Fig. 1.9) and uses two simulations of the seismic signal at the same time, one from the source (usually called forward simulation) and another from the receiver (usually called backward simulation). The difference between the two signals is minimized by statistical techniques. There are several ways to measure differences between the two signals (e.g. norm L2, differences in the Fourier domain etc.). This minimization process updates the geological model features (density, elastic parameters, etc.) and computes Frechet derivatives with respect to selected structural parameters, including density and the SH, SV, PH and PV wave speeds of the heterogeneous medium. The final geological model is obtained when the measure between the two signals is minimized (see Fig. 1.9).

The highly expensive adjoint tomographic techniques allows for resolving heterogeneities of the Earth with unprecedented resolution using seismological data, but the scale of the problem is still a challenge. Up to the present day, adjoint tomography techniques requires incredible amount of computer resources in order to be applied to the entire Earth, although simulations are being carried out by Jeroen Tromp's research group at Princeton University (e.g. Bozdag et al. (2013)), the process has been slow.

The use of adjoint tomografic techniques combined with SEM has proven to be a powerful tool for Earth imaging in general (e.g. Luo et al. (2013)). Adjoint tomography were tested using the Marmousi model by Luo (2013). The Marmousi model, created in 1988 by the Institut Français du Pétrole (IFP), consist on a profile through the North Quenguela in the Cuanza basin, Angola. Fig. 1.9 illustrates the process of the adjoint method: starting from a very simplified model, the method is able reproduce with high accuracy the target model.

Adjoint tomography combined with SEM has produced high resolutions images of the Eu-

Chapter 4. Seismic Inversion

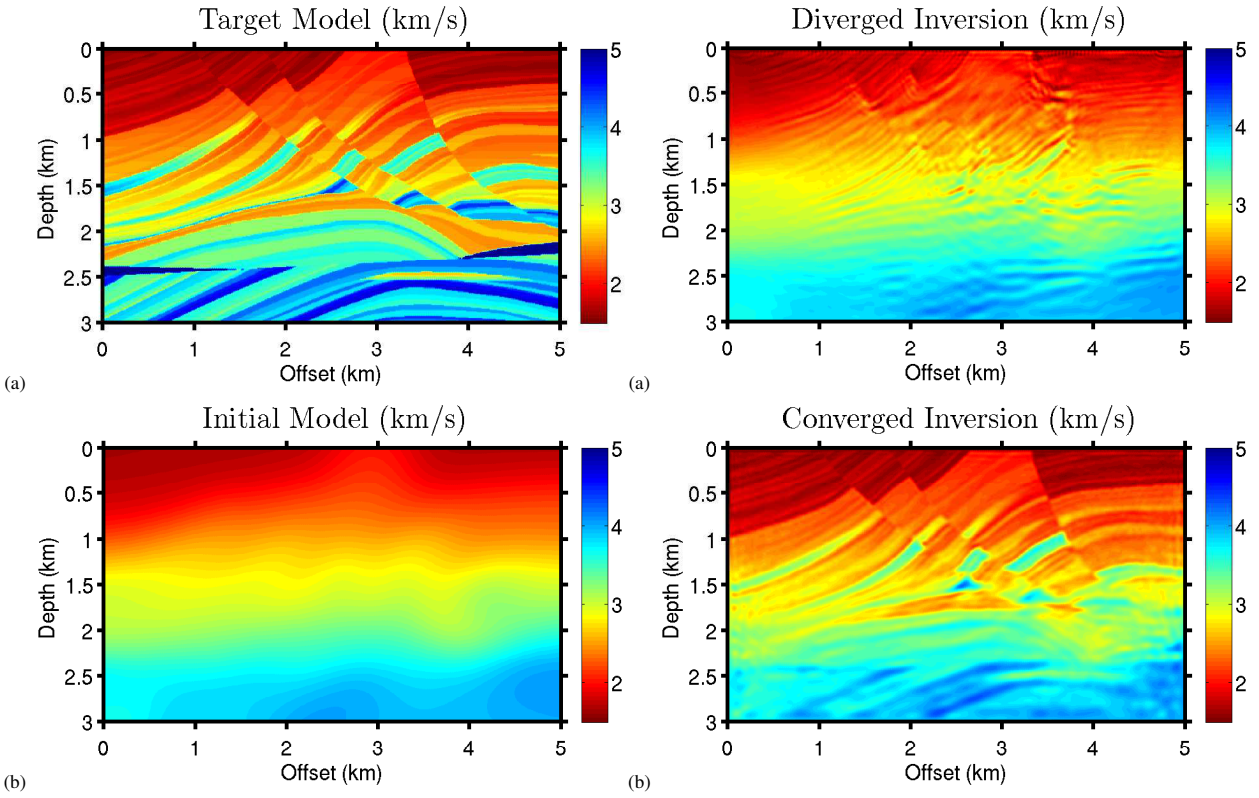

Figure 4.9: Inversion set-up of the Marmousi model. (a) Target model. (b) Initial model. Sources and receivers are deployed on the free surface.

Figure 4.10: Inversion results of the Marmousi model. (a) Inversion gets trapped in local minimum, if we blindly back-project the waveform differences. (b) Inversion succeeds when we start from long period dataset and early arrivals and gradually increase the frequency content and window length.

Figure 1.9: Inversion set-up and inversion results of the Marmousi model. Sources and receivers are deployed on the free surface. Figures by Luo (2013).

123

124

ropean upper mantle, which are consistent with previous studies but helping to constrain the details of both crustal and upper-mantle structure and revealing some hitherto unidentified structures (Zhu et al. (2012), Fichtner et al. (2013)), see Fig. 1.10.

The importance and power of numerical techniques and computer clusters is in constant growth nowadays. Ambitious projects showing the scope, feasibility and high impact in the society have been carried out by many researchers around the world. Particularly in seismology, astonishing projects like Tromp et al. (2010) (among many others) are currently in operation: They have developed a near real-time system for the simulation of global earthquakes. The developed near real-time system automatically calculates normal-mode synthetic seismograms (at periods of 8 sec. and longer) for the Preliminary Reference Earth Model, and spectral-element synthetic seismograms (at periods of 17 to 500 sec.) for 3-D mantle model S362ANI in combination with crustal model Crust2.0. The system also produces a number of earthquake animations (through Princeton's web page), as well as various record sections comparing simulated and observed seismograms.

For all the reasons presented here (and many more), numerical analysis is an area of huge importance and continuous growth is seismology. The huge family of numerical methods allow to study in detail many different configuration of the Earth. Due to their very wide range of applications (in seismology and practically the entire sciences), the use and development of new and improved numerical techniques should be an active area of research in many countries.

Scientist like Chin et al. (1984) refers: *our principal conclusion is that there exists no single method which can compute with efficiency and with uniform accuracy the response of an inhomogeneous elastic medium to an arbitrary source with a spectrum of frequencies. An efficient and accurate general software package must be a hybrid of many computational procedures.*

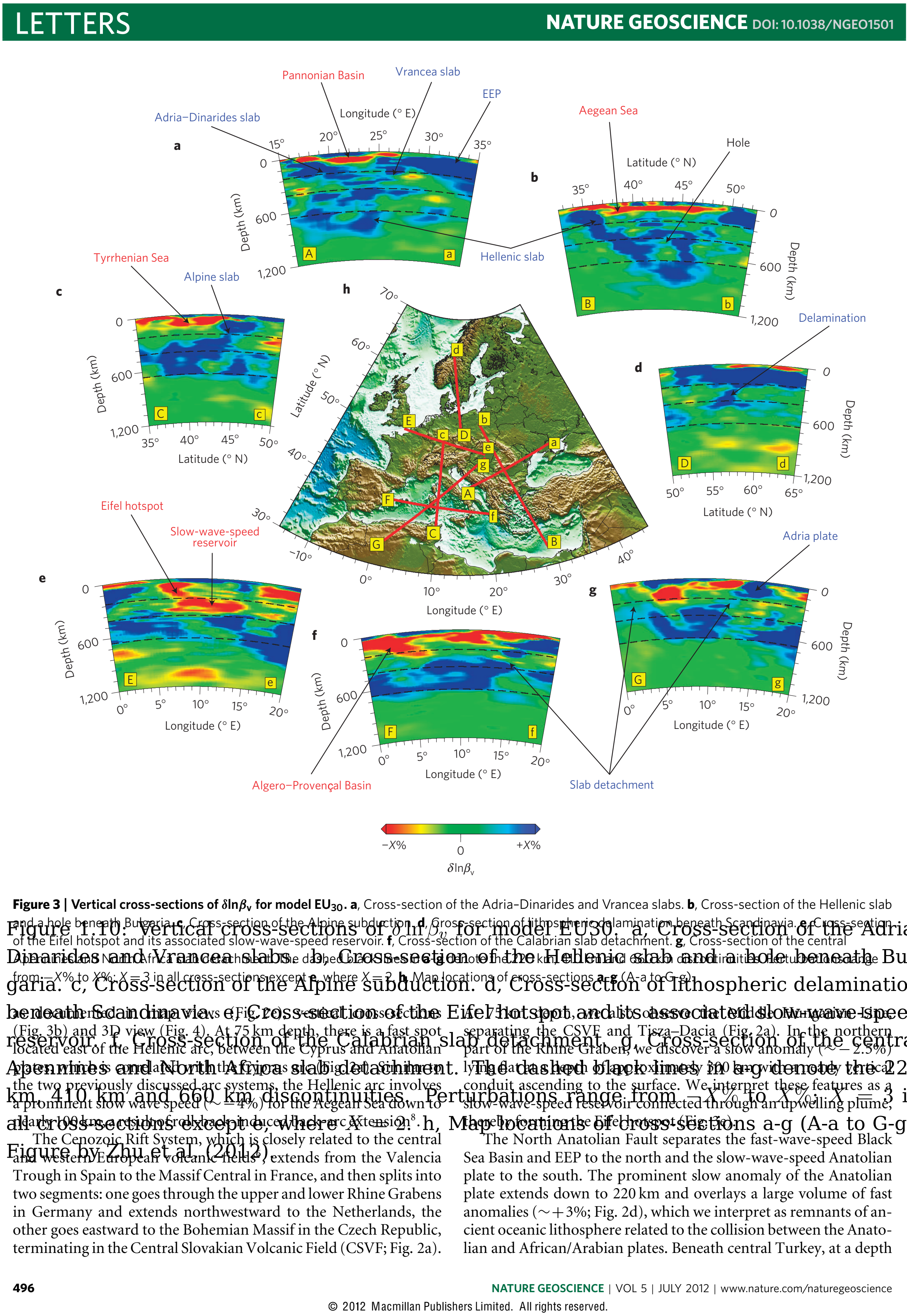

LETTERS NATURE GEOSCIENCE DOI: 10.1038/NGEO1501

Figure 3 | Vertical cross-sections of $\delta\ln\beta_v$ for model EU_{30}. **a**, Cross-section of the Adria–Dinarides and Vrancea slabs. **b**, Cross-section of the Hellenic slab and a hole beneath Bulgaria. **c**, Cross-section of the Alpine subduction. **d**, Cross-section of lithospheric delamination beneath Scandinavia. **e**, Cross-section of the Eifel hotspot and its associated slow-wave-speed reservoir. **f**, Cross-section of the Calabrian slab detachment. **g**, Cross-section of the central Apennines and North Africa slab detachment. The dashed black lines in **a–g** denote the 220 km, 410 km and 660 km discontinuities. Perturbations range from $-X\%$ to $X\%$; $X = 3$ in all cross-sections except **e**, where $X = 2$. **h**, Map locations of cross-sections **a–g** (A-a to G-g).

are documented in map views (Fig. 2e), vertical cross-sections (Fig. 3b) and 3D view (Fig. 4). At 75 km depth, there is a fast spot located east of the Hellenic arc, between the Cyprus and Anatolian plates, which is correlated with the Cyprus arc (Fig. 2a). Similar to the two previously discussed arc systems, the Hellenic arc involves a prominent slow wave speed ($\sim -4\%$) for the Aegean Sea down to nearly 100 km, a result of roll-back-induced back-arc extension[8].

The Cenozoic Rift System, which is closely related to the central and western European volcanic fields[6], extends from the Valencia Trough in Spain to the Massif Central in France, and then splits into two segments: one goes through the upper and lower Rhine Grabens in Germany and extends northwestward to the Netherlands, the other goes eastward to the Bohemian Massif in the Czech Republic, terminating in the Central Slovakian Volcanic Field (CSVF; Fig. 2a).

At 75 km depth, we also observe the Middle Hungarian Line, separating the CSVF and Tisza–Dacia (Fig. 2a). In the northern part of the Rhine Graben, we discover a slow anomaly ($\sim -2.5\%$) lying flat at a depth of approximately 300 km with a nearly vertical conduit ascending to the surface. We interpret these features as a slow-wave-speed reservoir connected through an upwelling plume, thereby forming the Eifel hotspot (Fig. 3e).

The North Anatolian Fault separates the fast-wave-speed Black Sea Basin and EEP to the north and the slow-wave-speed Anatolian plate to the south. The prominent slow anomaly of the Anatolian plate extends down to 220 km and overlays a large volume of fast anomalies ($\sim +3\%$; Fig. 2d), which we interpret as remnants of ancient oceanic lithosphere related to the collision between the Anatolian and African/Arabian plates. Beneath central Turkey, at a depth

496 NATURE GEOSCIENCE | VOL 5 | JULY 2012 | www.nature.com/naturegeoscience

© 2012 Macmillan Publishers Limited. All rights reserved.

Figure 1.10: Vertical cross-sections of $\delta \ln \beta_v$ for model EU30. a, Cross-section of the Adria-Dinarides and Vrancea slabs. b, Cross-section of the Hellenic slab and a hole beneath Bulgaria. c, Cross-section of the Alpine subduction. d, Cross-section of lithospheric delamination beneath Scandinavia. e, Cross-section of the Eifel hotspot and its associated slow-wave-speed reservoir. f, Cross-section of the Calabrian slab detachment. g, Cross-section of the central Apennines and North Africa slab detachment. The dashed black lines in a-g denote the 220 km, 410 km and 660 km discontinuities. Perturbations range from $-X\%$ to $X\%$; $X = 3$ in all cross-sections except e, where $X = 2$. h, Map locations of cross-sections a-g (A-a to G-g). Figure by Zhu et al. (2012).

Such a package is yet to be developed. Three decades later, the seismological community is a bit closer to that goal, there are available advanced, well-tested and well-documented codes that make use of modern, large-scale computational infrastructures and can be applied to a large range of problems in wave propagation. Especially the spectral element package Specfem (www.geodynamics.org/cig/software/specfem3d) has become the dominant code in the community. Bringing other numerical techniques to a level of completeness and user-friendliness comparable to the Specfem package is a long-term developing goal that requires considerable resources. Such an efforts would have to be justified by relevant advantages of the chosen numerical method, which prompts the need for further basic research in the field of computational seismology.

This thesis aims at contributing to this topic through the development of an improved computational tool for wave propagation, based on the combination of different numerical techniques.

Chapter 2

Some remarks on complex numbers in sciences

The use of complex numbers in sciences has been crucial in the development of the human civilization as we know it. Their use has been essential for the developing of new fundamental theories and the finding of its solutions. For example, the joint use of complex numbers and probability theory brought to live in the early XX century the theory of quantum mechanics that gave to the world a new tool for describing processes at atomic scale, allowing the development of numerous applications in engineering like transistors, microchips, lasers and many others. As another example we may cite elasticity, where the use of complex variable theory provides a very powerful tool for the solution of many problems. Such applications are most important for two-dimensional solutions. The technique is also useful for cases involving anisotropic and thermoelastic materials. Employing complex variable methods enables many problems to be solved that would be intractable by other schemes, Sadd (2005). To show the superiority of the method, the theory of elasticity requires the fulfillment of the differential equilibrium, the compatibility equations and the boundary conditions. By formulating the problem using stress functions, the differential equilibrium is fulfilled by definition, and one is left with the compatibility equations and the boundary conditions. However, by employing the method of complex potentials, compatibility is also inherently fulfilled. Hence, one is left with the boundary conditions only, Rand and Rovenski (2005).

Since the appearance of the imaginary unit ($\mathbf{i}^2 = -1$) for the first time in *Ars Magna* (1545) by the italian mathematician Girolamo Cardano (1501-1576), the square root of minus one was used as a mathematical tool rather than a physical entity. It was Carl Friedrich Gauss (1777-1855) a german mathematician and physicist who introduced the concept of *complex number* (a number formed by a real and imaginary components). He tried to give to the imaginary number a different concept from the taken before, where the imaginary number is non an impossible or useless entity but a different direction one just like $+1$ or -1.

Based on the concept of different directions for imaginary and real numbers, in 1843 the mathematician Sir William Rowan Hamilton described the quaternion algebra $\mathbb{H}$, as a more general framework of the complex numbers. The Quaternion algebra is a 4 dimensional space that uses three imaginary numbers and one real number as directions. Recent developments have favored the geometric approach (geometric algebra) leading to an algebra (space-time algebra) complexified by the algebra $\mathbb{H} \otimes \mathbb{H}$ where $\mathbb{H}$ is the quaternion algebra. The general theory of relativity is developed within the Clifford algebra $\mathbb{H} \otimes \mathbb{H}$ over $\mathbb{R}$. Furthermore the algebra $\mathbb{H} \otimes \mathbb{H}$ constitutes the framework of a relativistic multivector calculus, equipped with an associative exterior product and interior products generalizing the classical vector and scalar products, Girard (2007). This kind of calculus is a generalization of the classical vector calculus and allow to reproduce the relativity theory in a very easy way. Unlike the Clifford

algebra the vector calculus described over $\mathbb{R}$ does not allow for describing the relativity theory. For this reason, tensor calculus was introduced to describe more complex systems, but still the tensor calculus does not allow a double representation of the Lorentz group and thus seems incompatible with relativistic quantum mechanics. A third calculus is then introduced, the spinor calculus, to formulate relativistic quantum mechanics. The set of mathematical tools used in physics thus appears as a succession of more or less coherent formalisms. Is it possible to introduce more coherence and unity in this set? The answer seems to reside in the use of Clifford algebra, Girard (2007). For several reasons, the Clifford calculus seems to be the calculus of the future, allowing to deal with more complicated and more realistic theories.

Not only realistic theories are based on the use of complex numbers. Futuristic technologies like quantum computers are also possible (from the theoretical point of view) thanks to the use complex numbers. Quantum computing uses qubits (quantum bits) instead of bits as their basic unit of information. A qubit unlike the bit can represent 0, 1 or a superposition of both: Using bra-ket notation (Dirac notation) we can represent a qubit as a linear combination of $|0\rangle$ and $|1\rangle$, where the weights are probabilities amplitudes which can be given by complex values. This basic assumption of using linear combination of probabilistic complex values of the bits' basic units of information, allow to speculate (theoretically) that quantum computers are able to solve problems much more faster than conventional computers. Although the pros and cons that this kind of theories entails are still open problems.

To summarize, the use of complex numbers have a extreme importance to formulate general mathematical theories of a physical or pure theoretical problem and their use to compute the analytical solutions. However, a field of mathematics that remains yet to be deeply explored is the use of complex numbers in numerical modeling. In this work we do a step in this direction and explore the idea to use complex numbers for the solution of the wave propagation problem in heterogeneous media.

Chapter 3

Fundamentals of the Finite Differences Method

The study of integro-differential equations to model real or ideal problems is the most powerful tool to predict the behavior of any known system. The exact solution of the mathematical problem is called the analytical solution. Usually this analytical solution is extremely difficult to find for realistic problems, for this reason the numerical solution takes so much importance. As shown in chapter 1, the numerical solution gives an approximation to the analytical solution usually transforming the continuous domain into a discrete domain that can be later solved on a computer, e.g., Finite Differences method (FDM), Finite Elements method (FEM), Finite Volume method (FVM) and Spectral Elements method (SEM) among many others.

Given the importance of integro-differential equations, the concept of derivative is one of the most important concepts in science and engineering. It can be described from two equally valid points of view: the geometrical and the physical. From the geometrical point of view, the derivative can be seen as the tangent line to a function in a certain evaluation point. From the physical point of view, the derivative can be seen as a measure of the rate of change of the function in this point. Most fundamental laws in physics are expressed in differential equations involving the rate of change in space and/or time of some continuous and differentiable function, bringing about the need for resolving the derivative for the majority of modeling approaches. FDM specifically targets those derivatives.

The FDM is one of the most simple, intuitive and easy to implement numerical method. Its origins dates back to the times of Isaac Newton (1642-1727) and Gottfried Leibniz (1646-1716) who are recognized as the fathers of the differential calculus. In fact, the apparently modern, numerical notion of finite differences was the historical basis for developing the concept of derivative in mathematics. The FDM is based on the concept of the finite difference (FD) operator, hence its name: **Finite**, because transform a infinite dimensional problem (continuous problem) into a finite dimensional problem (discrete problem) and **Differences**, because computes derivatives using subtractions. The FDM approximates derivatives of an ordinary differential equation (ODE) and/or partial differential equation (PDE) by divided differences defined at the so called grid points (refereed as spatial discretization).

Despite the FDM is one of the oldest technique remains as one of the most powerful (in terms of computational cost) methods for solving differential equations nowadays. Despite its limitations, the FDM remains one of the most popular methods due to its relatively straightforward and intuitively understanding from a physical point of view.

3.1 Finite differences and the 1D one-way wave equation

The technique of differentiation was introduced independently by Isaac Newton (1642-1727) and Gottfried Leibniz (1646-1716). Formally the slope of the tangent line at a point X is the limit of the ratio of the change in the function to the change in the independent variable, as that change approaches 0, i.e.:

$$f'(x) = \lim_{\Delta x \to 0} \frac{f(x + \Delta x) - f(x)}{\Delta x}. \tag{3.1}$$

The quotient in 3.1 is referred to as the Newton quotient or the difference quotient. Another way of expressing the derivative of a function derives from its expansion in a Taylor series, introduced by Brook Taylor in 1715. The Taylor series expresses any analytic function by an infinite sum over its derivative terms:

$$f(x) = f(a) + \frac{f'(x)}{1!}(x-a) + \frac{f''(x)}{2!}(x-a)^2 + \frac{f'''(x)}{3!}(x-a)^3 + ... = \sum_{n=0}^{\infty} \frac{f^{(n)}(a)}{n!}(x-a)^n. \tag{3.2}$$

Hence, for an analytic function, differentiation is equivalent to evaluating terms of a Taylor series.

Taking $a = x + \Delta x$ in 3.2 and reordering we can obtain an expression for the first order derivative similar to 3.1:

$$f'(x) = \frac{f(x + \Delta x) - f(x)}{\Delta x} + \mathcal{O}\left(\Delta x\right). \tag{3.3}$$

An expression like 3.3 is called a Finite Difference (FD) approximation, in this case the first order forward approximation for the first derivative, where the differential step is taken in the positive direction. The symbol $\mathcal{O}$ expresses the error related to truncating the Taylor series in the second order derivative. FD approximations are still the most classic, simple and intuitive approach to approximate derivatives of a function, and are widely used in numerical schemes. Based on the Taylor series 3.2, many different approximations can be made, for example the backward approximation where we take the differential step in the negative direction (see Fig. 3.1):

$$f'(x) = \frac{f(x) - f(x - \Delta x)}{\Delta x} + \mathcal{O}\left(\Delta x\right), \tag{3.4}$$

or the centered FD approximation, where we take the differential step in both directions. i.e.,

$$f'(x) = \frac{f(x + \Delta x) - f(x - \Delta x)}{2\Delta x} + \mathcal{O}\left(\Delta x^2\right), \tag{3.5}$$

which is a second order approximation ($\mathcal{O}\left(\Delta x^2\right)$) by the price of using more information of the function than the forward approximation, i.e., we need information at two points different from ($x + \Delta x$ and $x - \Delta x$) from the evaluation point x.

The FDM allows for computing higher order derivatives based on the same principle. For example, if we want to compute the second order derivative, we can apply the centered derivative operator twice to find the following expression

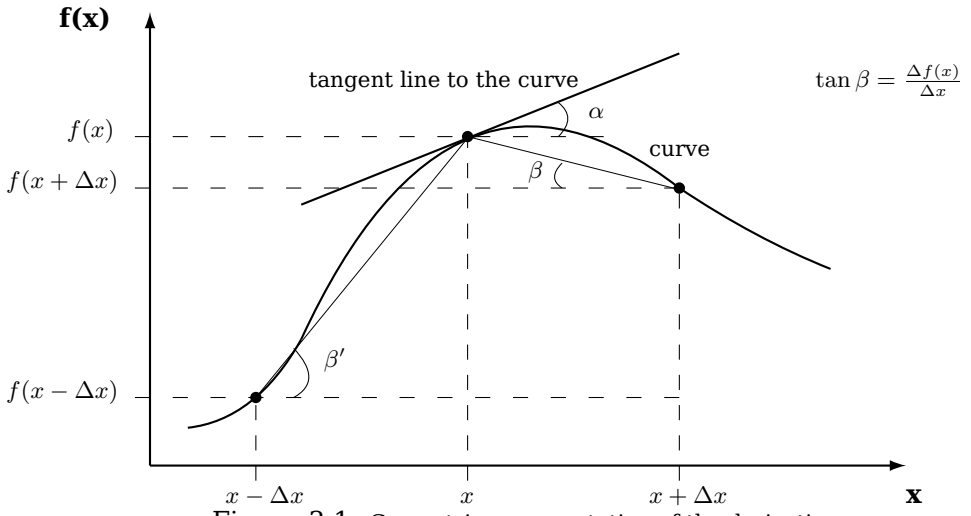

Figure 3.1: Geometric representation of the derivative.

$$f''(x) = \frac{f(x+\Delta x) - 2f(x) + f(x-\Delta x)}{\Delta x^2} + \mathcal{O}\left(\Delta x^2\right), \tag{3.6}$$

where the error $\mathcal{O}\left(\Delta x^2\right)$ is found by manipulating the Taylor series of $f(x+\Delta x)$ and $f(x-\Delta x)$.

The basic nature of the FD method becomes clear from the comparison between equations 3.1 and 3.3: on one hand we have the limit $\Delta x \to 0$ and on the other hand the truncation error, which indicates that only in the limit when Δx approaches zero the truncation error of the FD approximation will vanish. Usually the order of the error in FD approximations is related to the number of differential steps that we take, i.e., in 3.5 we take one step forward and one backward, that is two steps unlike in 3.3 and 3.4 which have a single step. Consequently, the accuracy of the centered approximation 3.5 is of second order, and the truncation error is smaller than in the forward and backward approximations.

Taking into account a second layer of surrounding grid points, fourth order accuracy can be achieved, of course at the price of increasing computational cost. Whatever the order of accuracy, all FD approximations involve a truncation error depending on the step size Δx, so we should choose Δx small to obtain accurate results.

Numerical analysis of the one dimensional (1D) first-order wave equation are one of the basis for most of the numerical methods that are implemented in realistic media (acoustic or elastic) in the geophysical field. The 1D first-order scalar wave equation, also called the 1D one-way wave equation, is given by the following mathematical expression:

$$\frac{\partial u}{\partial t} = c\,\frac{\partial u}{\partial x}, \tag{3.7}$$

where $u = u(x,t)$ is the displacement field, x is the space variable, t is the time variable and c the propagation velocity.

To solve the partial differential equation (PDE) 3.7 we need an initial condition of displacement. This initial condition can be given by the initial particle displacement $(u(x,0))$ imposed over the entire space domain (x), or over a single point (x_s) as a time dependent function $(u(x_s,t))$, usually referred as a point source. Equation 3.7 in conjunction with its initial condition of displacement is called *the initial value problem*.

The most basic FD approximation to the one-way wave equation can be made by substituting the forward approximation (Eq. 3.3) at both sides of the equation. After rearranging we can obtain the following expression,

$$u_x^{t+\Delta t} = \mathrm{S}\,u_{x+\Delta x}^{t} + \left(1-\mathrm{S}\right)u_x^t + \mathcal{O}\left(\Delta t, \Delta x\right), \tag{3.8}$$

where $\mathrm{S} = \frac{c\Delta t}{\Delta x}$ is called the *Courant number* and/or *stability factor*. The parameter Δx is refereed as the *grid size* and Δt as the *time step*. Eq. 3.8 is a well known stable and convergent FD discretization to the one-way wave propagation problem and is called the *upwind* discretization and it is first order accurate in time and space. Now, if we use the centered approximation (Eq. 3.5) at both sides of the one-way wave equation (Eq. 3.7), the following expression is obtained:

$$u_x^{t+\Delta t} = \mathrm{S}\,\left(u_{x+\Delta x}^{t} - u_{x-\Delta x}^{t}\right) + u_x^{t-\Delta t} + \mathcal{O}\left(\Delta t^2, \Delta x^2\right). \tag{3.9}$$

Equation 3.9 is the well known *Leapfrog* discretization to the one-way wave equation and it is second order accurate in time and space (see Strang (2007) for further details).

Expressions 3.8 and 3.9 can be respectively written in a general operator form as follows

$$\mathrm{val}\left(x, t+\Delta t\right) = \mathrm{S}\,\mathrm{val}\left(x+\Delta x, t\right) + \left(1-\mathrm{S}\right)\mathrm{val}\left(x, t\right), \tag{3.10}$$

$$\mathrm{val}\left(x, t+\Delta t\right) = \mathrm{S}\,\left[\mathrm{val}\left(x+\Delta x, t\right) - \mathrm{val}\left(x-\Delta x, t\right)\right] + \mathrm{val}\left(x, t-\Delta t\right), \tag{3.11}$$

where $\mathrm{val}\left(x, t\right)$ represents the numerical value of the displacement to be propagated.

Having a FD approximation to the wave equation is not enough, we are interested in knowing how the numerical solution can whether or not reproduce the exact (analytical) solution of the problem.

The analytical solution to the one-way wave equation with an initial condition of displacement over the entire domain $(u(x,0) = f(x))$ is given by the following mathematical expression,

$$u(x,t) = f(x+ct). \tag{3.12}$$

Note that solution 3.12 is just a shift to the left of the initial condition function $(f(x))$.

When the displacement movement is generated by a time dependent function (source), the one-way wave equation (Eq. 3.7) becomes,

$$\frac{\partial u}{\partial t} = c\,\frac{\partial u}{\partial x} + f(x_s, t), \tag{3.13}$$

where x_s is the application point of the source. The analytical solution to problem 3.13 is given by the following mathematical expression (see Strikwerda (2004) for further details),

$$u(x,t) = \int_0^t f(x - c(t-\tau), \tau)\,\mathrm{d}\tau. \tag{3.14}$$

3.2 Finite differences and the 1D two-way wave equation

The 1D second-order scalar wave equation, also called the 1D two-way wave equation, is given by the following mathematical expression:

$$\frac{\partial^2 u}{\partial t^2} = c^2\,\frac{\partial^2 u}{\partial x^2}. \tag{3.15}$$

Subject to initial conditions of displacement and speed,

$$u(x,0) = f(x) \quad \text{and} \quad \dot{u}(x,0) = g(x). \tag{3.16}$$

is called the initial value problem.

To illustrate how the FDM solves the initial value problem in the most simple way, let us the centered approximation for the second order derivative (Eq. 3.6) to discretize PDE 3.15 to obtain the following expression

$$u_x^{t+\Delta t} = \mathrm{S}^2 \left(u_{x+\Delta x}^t + u_{x-\Delta x}^t\right) + 2\left(1 - \mathrm{S}^2\right)\, u_x^t - u_x^{t-\Delta t} + \mathcal{O}\left(\Delta t^2, \Delta x^2\right). \tag{3.17}$$

Equation 3.17 is a well known convergent and stable FD discretization called the *Leapfrog* approximation for the second-order wave equation, Strang (2007).

To solve Eq. 3.15 by using FD discretization 3.17 we need two initial conditions; these initial conditions are given by the initial displacement of the particle $(u(x,0))$ and velocity $(\dot{u}(x,0))$ and/or in case of a point source, only displacements at each time step over a space location is required $(u(x_s,t))$.

Like in the one-way wave equation case, we can write discretization 3.17 in a general operator form as follows

$$\begin{aligned}\text{val}\left(x, t+\Delta t\right) = \mathrm{S}^2 \left[\text{val}\left(x+\Delta x, t\right) + \text{val}\left(x-\Delta x, t\right)\right] + 2\left(1-\mathrm{S}^2\right)\, \text{val}\left(x,t\right) \\ - \text{val}\left(x, t-\Delta t\right),\end{aligned} \tag{3.18}$$

where val $\left(x,t\right)$ represents the numerical value of the displacement referred in Eq. 3.17.

The general analytic solution for the second order wave equation was found by Jean le Rond d'Alembert (1717-1783), and is called the d'Alembert formula. The d'Alembert solution is based on the *Characteristic method* developed by Hamilton. Hamilton discovered that the wave equation can be solved by integrating it along special curves that he called characteristics. In the special case of the 1D scalar wave equation with constant velocity, these curves are exactly the straight lines given by $F(x+ct)$ and $G(x-ct)$, where F and G are $\mathbb{C}$ functions. Particularly when this function is applied to the second order scalar wave equation with initial displacement $f(x,0)$ and initial velocity $g(x,0)$ the formula becomes the d'Alembert solution,

$$u(x,t) = \frac{f(x+ct) + f(x-ct)}{2} + \frac{1}{2c} \int_{x-ct}^{x+ct} g(\zeta)\, \mathrm{d}\zeta. \tag{3.19}$$

In case of a point source $s(x_s,t)$ the solution becomes

$$u(x,t) = \frac{f(x+ct) + f(x-ct)}{2} + \frac{1}{2c} \int_{x-ct}^{x+ct} g(\zeta)\, \mathrm{d}\zeta + \frac{1}{2c} \int_0^t \int_{x-c(t-\xi)}^{x+c(t-\xi)} s(\eta,\xi)\, \mathrm{d}\eta\, \mathrm{d}\xi. \tag{3.20}$$

Simulations to the wave equation can be carried out using different FD discretizations and compared with the analytical solutions to determine whether or not reliable results are obtained. Not all of the FD discretizations that can be made by combining different approximations to the wave equation are useful. To determine whether a certain FD discretization can be applied to the problem we have to use concepts of convergence, consistency, stability, dispersion and dissipation of the numerical solution (see Chapters 5-6).

Discretization to the one-way wave equation $\left(\frac{\partial u}{\partial t} = c\frac{\partial u}{\partial x}\right)$	**Name**
forward approx. in time = forward approx. in space	Upwind
forward approx. in time = centered approx. in space	Forward Euler
backward approx. in time = centered approx. in space	Backward Euler
centered approx. in time = centered approx. in space	Leapfrog

Table 3.1: Most basic finite differences schemes to the first order wave equation.

3.3 Finite differences discretizations

The most basic FD discretizations to the one-way wave equation are made by combining forward, backward and centered FD approximations. All of this combinations are tested in order to determine whether they produce a reliable solution to the initial value problem.

Table 3.3 show the discretization made and its respective name. Forward and backward Euler are unconditional unstable but they can be modified to solve the problem efficiently (Lax-Friedrichs method) (see Thomas (1995)).

3.4 Second order 1D wave equation as a first-order coupled system of equations

The 1D acoustic second order equation can be written in a first-order system of two coupled equations by introducing the velocity as follows

$$\begin{aligned} \frac{1}{\kappa}\frac{\partial u}{\partial t} &= \frac{\partial v}{\partial x} + F(x,t), \\ \rho\frac{\partial v}{\partial t} &= \frac{\partial u}{\partial x}, \end{aligned} \tag{3.21}$$

where $v = v(x,t)$ is the velocity field, $\rho = \rho(x)$ is the density, $\kappa = \kappa(x)$ is the elastic parameter and $F(x,t) = \int_0^t f(x,\tau)\,\mathrm{d}\tau$.

The velocity c of sound wave propagation is given by

$$c = \sqrt{\frac{\kappa}{\rho}}. \tag{3.22}$$

In case of absence of sources the equations are subject to initial conditions of displacement and velocity

$$u(x,0) = f(x), \quad v(x,0) = g(x).$$

The Leapfrog method is the simplest second order accurate FD method which is a one step three time levels scheme.

Applying the centered FD discretization (Eq. 3.9) to Eqs. 3.21 we obtain the following,

$$\begin{aligned} \frac{1}{\kappa(x)}\frac{u_x^{t+\Delta t} - u_x^{t-\Delta t}}{2\Delta t} &= \frac{v_{x+\Delta x}^t - v_{x-\Delta x}^t}{2\Delta x} + F(x,t) + \mathcal{O}\left(\Delta t^2, \Delta x^2\right), \\ \rho(x)\frac{v_x^{t+\Delta t} - v_x^{t-\Delta t}}{2\Delta t} &= \frac{u_{x+\Delta x}^t - u_{x-\Delta x}^t}{2\Delta x} + \mathcal{O}\left(\Delta t^2, \Delta x^2\right). \end{aligned} \tag{3.23}$$

It is well known that the Leapfrog scheme for the first-order coupled equations (Eq. 3.23) is non-dissipative, stable, consistent and convergent discretization, which has a dispersion-dissipation relation given by the following expression (Moczo et al., 2004b)

$$\sin^2 \omega \Delta t = \frac{\kappa(x)}{\rho(x)} \left(\frac{\Delta t}{\Delta x} \right)^2 \sin^2 k \Delta x. \tag{3.24}$$

3.4.1 Staggered grid scheme

Nowadays, perhaps the most popular FD discretization in the seismological context is the so called *staggered grid* scheme often also called *interleaved Leapfrog*.

The staggered grid scheme is obtained by the use of the central difference approximation evaluated over smaller grid distances and time steps. We can write it in the following way,

$$\begin{aligned}
\frac{1}{\kappa(x)} \frac{u_x^{t+\frac{\Delta t}{2}} - u_x^{t-\frac{\Delta t}{2}}}{\Delta t} &= \frac{v^t_{x+\frac{\Delta x}{2}} - v^t_{x-\frac{\Delta x}{2}}}{\Delta x} + F(x,t) + \mathcal{O}\left(\Delta t^2, \Delta x^2\right), \\
\rho(x) \frac{v^{t+\Delta t}_{x+\frac{\Delta x}{2}} - v^t_{x+\frac{\Delta x}{2}}}{\Delta t} &= \frac{u^{t+\frac{\Delta t}{2}}_{x+\Delta x} - u_x^{t+\frac{\Delta t}{2}}}{\Delta x} + \mathcal{O}\left(\Delta t^2, \Delta x^2\right),
\end{aligned} \tag{3.25}$$

it also can be written in a equivalent form,

$$\begin{aligned}
\frac{1}{\kappa(x)} \frac{u_x^{t+\Delta t} - u_x^t}{\Delta t} &= \frac{v^{t+\frac{\Delta t}{2}}_{x+\frac{\Delta x}{2}} - v^{t+\frac{\Delta t}{2}}_{x-\frac{\Delta x}{2}}}{\Delta x} + F(x,t) + \mathcal{O}\left(\Delta t^2, \Delta x^2\right), \\
\rho(x) \frac{v^{t+\frac{\Delta t}{2}}_{x+\frac{\Delta x}{2}} - v^{t-\frac{\Delta t}{2}}_{x+\frac{\Delta x}{2}}}{\Delta t} &= \frac{u^t_{x+\Delta x} - u^t_x}{\Delta x} + \mathcal{O}\left(\Delta t^2, \Delta x^2\right).
\end{aligned} \tag{3.26}$$

By observing discretization 3.26 it is clearly appreciated that we evaluate one variable at regular space-time grid points while the second variable is evaluated at mid-space-time grid points. The differencing over twice smaller grid distances implies that the leading term of the approximation error is now four times smaller, Moczo et al. (2004b). Discretizations 3.25-3.26 should not be confused with a forward discretization in time-space for variable u, otherwise it is not trivial to understand where the second order approximation comes from.

The staggered grid discretization comes from just discretizing both equations with a centered approximation evaluated over a twice smaller time-space grid distances. After this, just relocate displacement variables to the next time-space mid point, i.e., replace $t = t + \frac{\Delta t}{2}$ and $x = x + \frac{\Delta x}{2}$ on the time derivative and the space derivative respectively. This change of variable keeps the second order error term of the centered discretization.

The most important features of the staggered grid are that we keep the properties of dispersion-dissipation of the Leapfrog approximation, that is, the dispersion-dissipation relation for the staggered grid discretization is the same of the centered discretization (Eq. 3.24), and on the other and, due to the evaluation of different time levels for both variables,the computational algorithm for propagating the wave can be written in a very simple form, allowing to reduce the computational cost.

3.5 Finite differences schemes in heterogeneous media

FDM is also useful in presence of heterogeneous media. The main difference with homogeneous schemes is that the velocity (or density and elastic constants) values are not evaluated

at the same grid point. In this sense we can write the staggered grid approximation in heterogeneous media as follows

$$\begin{aligned}
&\frac{1}{\kappa(x)}\frac{u_x^{t+\frac{\Delta t}{2}}-u_x^{t-\frac{\Delta t}{2}}}{\Delta t}=\frac{v^t_{x+\frac{\Delta x}{2}}-v^t_{x-\frac{\Delta x}{2}}}{\Delta x}+F(x,t)+\mathcal{O}\left(\Delta t^2,\Delta x^2\right),\\
&\rho\left(x+\frac{\Delta x}{2}\right)\frac{v^{t+\Delta t}_{x+\frac{\Delta x}{2}}-v^t_{x+\frac{\Delta x}{2}}}{\Delta t}=\frac{u^{t+\frac{\Delta t}{2}}_{x+\Delta x}-u_x^{t+\frac{\Delta t}{2}}}{\Delta x}+\mathcal{O}\left(\Delta t^2,\Delta x^2\right).
\end{aligned}\tag{3.27}$$

Commonly second order FD discretizations of the wave equation are not used in realistic (heterogeneous) simulations of wave propagation. Instead higher order FD approximations are included in space (or time) to get 4^{th} or 6^{th} order accuracy into the discretization.

For instance, the very widely used scheme in seismology is the staggered FD discretization with 2^{th} order of accuracy in time and 4^{th} order of accuracy in space. The FD discretization can be found by just introducing the FD fourth order approximation give by the following expression

$$f'(x)=\frac{1}{\Delta x}\left[\frac{9}{8}\left(f\left(x+\frac{\Delta x}{2}\right)-f\left(x-\frac{\Delta x}{2}\right)\right)-\frac{1}{24}\left(f\left(x+\frac{3\Delta x}{2}\right)-f\left(x-\frac{3\Delta x}{2}\right)\right)\right]+\mathcal{O}\left(\Delta x^4\right).\tag{3.28}$$

Inserting approximation 3.28 into the space discretization of the first order coupled wave equation (Eq. 3.21) we can get the FD24 staggered grid approximation

$$\begin{aligned}
&\frac{1}{\kappa(x-\frac{\Delta x}{2})}\frac{u_x^t-u_x^{t-\Delta t}}{\Delta t}=\frac{9}{8}\frac{v_x^{t-\frac{\Delta t}{2}}-v_{x-\Delta x}^{t-\frac{\Delta t}{2}}}{\Delta x}-\frac{1}{24}\frac{v_{x+\Delta x}^{t-\frac{\Delta t}{2}}-v_{x-2\Delta x}^{t-\frac{\Delta t}{2}}}{\Delta x}+F(x,t)+\mathcal{O}\left(\Delta t^2,\Delta x^4\right),\\
&\rho(x)\frac{v_x^{t+\frac{\Delta t}{2}}-v_x^{t-\frac{\Delta t}{2}}}{\Delta t}=\frac{9}{8}\frac{u^t_{x+\frac{\Delta x}{2}}-u^t_{x-\frac{\Delta x}{2}}}{\Delta x}-\frac{1}{24}\frac{u^t_{x+\frac{3\Delta x}{2}}-u^t_{x-\frac{3\Delta x}{2}}}{\Delta x}+\mathcal{O}\left(\Delta t^2,\Delta x^4\right).
\end{aligned}\tag{3.29}$$

Note, the price of getting more accuracy in space is given by including more spatial points into the dicretization.

Heterogeneous formulations (in 2D and 3D) for FD approximations using of the second order wave equation (Eq. 3.15) are also widely used in seismology (see Cohen (2001)). This kind of discretizations are well illustrated in Chapter 6 explaining the preferences of choosing certain discretization over another based on the dispersion analysis.

In case of 2D and 3D elastic problems, the FD concepts of the discretizations presented here do not change. Discretizations of the elastic wave equation in a 2D space are given by adding into Eq. 3.29 the y or z coordinate and replacing the displacement field $(u(x,t))$ by the second order stress tensor $(\boldsymbol{\sigma})$. In a fully 3D elastic space all the coordinates are used into the right hand side of Eq. 3.29 and also he displacement field is replaced by the stress tensor (see Fig. 3.2).

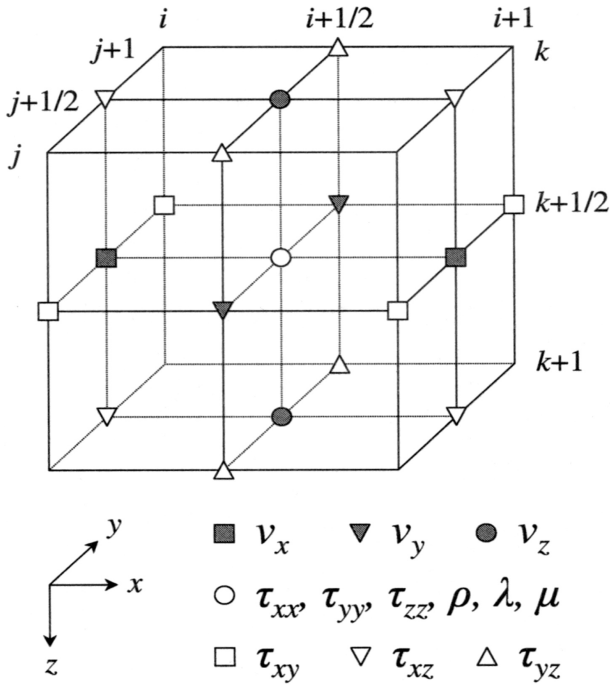

Figure 3.2: Regular staggered-grid system used in 3D velocity-stress FD method. $v(v_x, v_y, v_z)$ and $\tau(\tau_{xx}, \tau_{yy}, \tau_{zz}, \tau_{xy}, \tau_{xz}, \tau_{yz})$ denote the components of the particle velocity and stress tensor, respectively. ρ the density; λ and μ, Lame parameters. The indices i, j and k represent values of the spatial x, y and z coordinates, respectively. A left-handed coordinate system is used. Figure by Kang and Baag (2004).

Chapter 4

On the Generalization of the Complex Step Method

4.1 Introduction

As discussed in the previous Chapter, the FDM expresses the geometrical definition of gradients as the local slope of the original functions. As a consequence, working with FD approximations of derivatives of analytic functions involves computing small differential steps (Δx) to get close to Newton's and Leibnitzs' original definition (Eq. 3.1). However, evaluating arbitrarily small steps is not feasible on a computer. FD schemes, as the name suggests, involve some difference operator in the numerator, and this difference itself is an intrinsic problem. For a given step size Δx, and particularly for small steps, the differences of the values of our function at successive evaluation points may become small, leading to a loss of significant digits as we approach machine precision, and eventually a value zero for the numerator and the derivative when the computer fails to recognize the difference between the two numbers. This problem is known as subtractive cancellation or term cancellation. Since in numerical simulations we often have little hints on the actual shape of the functions involved, subtractive cancellation is not straightforward to control, which forces us into a conservative choice of step size at the expense of larger truncation errors. This contribution readdresses subtractive cancellation and other accuracy and stability issues in FD for the case that Δx is a complex number.

In this Chapter we generalize the well known Complex Step Method for computing derivatives by introducing a complex step in a strict sense. Exploring different combinations of terms, we derive 52 approximations for computing the first order derivatives and 43 for the second order derivatives. For an appropriate combination of terms and appropriate choice of the step size in the real and imaginary directions, fourth order accuracy can be achieved in a very simple and efficient scheme on a compact stencil. New different ways of computing second order derivatives in one single step are shown. Many of the first order derivative approximations avoid the problem of subtractive cancellation inherent to the classic finite difference approximations for real valued steps, and the superior accuracy and stability of the generalized complex step approximations are demonstrated for an analytic test function.

4.2 The Complex Step Method

Most naturally, derivatives of real functions are evaluated using real numbers, but the less intuitive idea of using an imaginary number in real functions differentiation has been shown capable of overcoming the term cancellation inherent to the ordinary FD method, as well as reducing the associated approximation error. The use of complex variables in numerical

differentiation was introduced by Lyness and Moler (1967), describing a method for computing the derivatives of any analytic function. The base of these methods is Cauchy's theorem which relates the n^{th} derivative $f^n(0)$ of an analytic function $f(z)$ at $z = 0$ to the value of a closed integral, the contour C enclosing the origin once and remaining within a domain of analyticity of $f(z)$, Lyness (1968).

Later Fornberg (1981) presented a FORTRAN algorithm for computing derivatives of real analytic functions evaluated in complex values. After that, the use of complex variables in numerical differentiation apparently fell into oblivion until it reappeared in the scientific literature when Squire and Trapp (1998) presented the formally called Complex Step Method (CS). Squire and Trapp (1998) use a purely imaginary number $\mathbf{i}$ ($\mathbf{i}^2 = -1$) for computing the first and second derivatives of real functions, and their CS should be called the imaginary step method more properly.

One of the limitations of the CS method is that only the first order derivative is accessible using the imaginary part of the function, while second derivatives are proportional to $\mathbf{i}^2$ and have to be evaluated by taking the real part of the function. These limitations were overcome by the generalization of the method by using the complex representation of the Taylor series by Lai and Crassidis (2008) and additional sample points in the complex plane and using Fast Fourier Transform (FFT) by Bagley (2006), allowing to compute high order derivative approximations with high accuracy. Major extensions of the method were made by Cerviño and Bewley (2003) with an application to pseudospectral simulation codes which uses the FFT. Optimization problems involving dynamical systems modeled as nonlinear differential equations were carried out by Kim et al. (2005) and Kim et al. (2006), where the method is applied to two robust performance analysis problems. Several new CS approximations based on orthogonal complex numbers coupled with Richardson extrapolations were presented by Lai et al. (2005) and successfully applied to a second order Kalman filter. Sensitivity analysis using the CS method was carried out by Veer N. (1999), Martins et al. (2000), Burg and Newman (2003), Anderson et al. (2001), Martins et al. (2003), Burg and Newman (2003), DePauw and Vanrolleghem (2005), Gao and He (2005), Wang and Apte (2006), Voorhees et al. (2009), Jin et al. (2010) and Voorhees et al. (2011). Recently the CS method has been applied as a tool for computing Fréchet derivatives of a matrix function by Al-Mohy and Higham (2010) showing its superiority over finite differences. Inverse problems in structural mechanics by Dennis et al. (2011). In the field of geophysics it was Abokhodair (2007) and Abokhodair (2009) who extended the CS method using central differencing in the complex plane; he referred to the new method as semiautomatic differentiation (SD) and applied it for computing accurate approximation of gradients, Jacobians and Hessians as well as 2D and 3D partial and cross-partial spatial derivatives in the geophysical inversion and the geophysical source imaging processes.

The CS method can be very easily derived from the Taylor series expansion of $f(x + \mathbf{i}\Delta x)$, i.e.,

$$f(x + \mathbf{i}\Delta x) = f(x) + \mathbf{i}\Delta x f'(x) + \frac{(\mathbf{i}\Delta x)^2}{2!} f''(x) + \frac{(\mathbf{i}\Delta x)^3}{3!} f'''(x) + ... = \sum_{n=0}^{\infty} \frac{(\mathbf{i}\Delta x)^n}{n!} f^n(x). \tag{4.1}$$

Taking the imaginary part on both sides and reordering we obtain the CS expression for the first derivative found by Squire and Trapp (1998),

$$f'(x) = \frac{\mathfrak{Im}(f(x + \mathbf{i}\Delta x))}{\Delta x} + \mathcal{O}\left(\Delta x^2\right). \tag{4.2}$$

Note that, $\mathfrak{Im}(f(x)) = 0$ because x is set to be a real number.

The second order term in the Taylor series expansion of $f(x+\mathbf{i}\Delta x)$ appears with a factor of $\mathbf{i}^2$, meaning it is a real quantity. An expression for the second order derivative can be found by taking the real part of 4.1 and reordering,

$$f''(x) = \frac{2(f(x) - \mathfrak{Re}(f(x+\mathbf{i}\Delta x)))}{\Delta x^2} + \mathcal{O}\left(\Delta x^2\right). \tag{4.3}$$

Using the Taylor series expansion of $f(x-\mathbf{i}\Delta x)$, it can be verified that

$$\mathfrak{Re}(f(x+\mathbf{i}\Delta x)) = \mathfrak{Re}(f(x-\mathbf{i}\Delta x)) \quad \text{and} \quad \mathfrak{Im}(f(x+\mathbf{i}\Delta x)) = -\mathfrak{Im}(f(x-\mathbf{i}\Delta x)). \tag{4.4}$$

Therefore, Eqs. 4.2 and 4.3 can be respectively written as

$$f'(x) = -\frac{\mathfrak{Im}(f(x-\mathbf{i}\Delta x))}{\Delta x} + \mathcal{O}\left(\Delta x^2\right), \tag{4.5}$$

$$f''(x) = \frac{2(f(x) - \mathfrak{Re}(f(x-\mathbf{i}\Delta x)))}{\Delta x^2} + \mathcal{O}\left(\Delta x^2\right). \tag{4.6}$$

Eqs. 4.2 and 4.3 are the most basic equations that can be found using 4.1. The numerical advantages of the CS method are noticeable: Eq. 4.2 actually shows a single term in the numerator rather than a difference, and hereby circumvents the instability related to term cancellation inherent to all classic real valued FD approximations besides being more accurate. Eqs. 4.3 and 4.6 allows to compute an approximation to the second derivative in a single step that can not be achieved by any FD approximation.

Generalizations to high order derivatives made by Bagley (2006) and Lai and Crassidis (2008) were done by converting the Taylor series into a Fourier series (Taylor expansion of $f(x+\Delta x\, e^{\mathbf{i}\theta})$), i.e.,

$$f(x+\Delta x\, e^{\mathbf{i}\theta}) = f(x) + \Delta x e^{\mathbf{i}\theta} f'(x) + \frac{\Delta x^2}{2!} e^{2\mathbf{i}\theta} f''(x) + ... = \sum_{n=0}^{\infty} \frac{(\Delta x)^n}{n!} e^{n\mathbf{i}\theta} f^n(x). \tag{4.7}$$

In the expression 4.7 the imaginary step does not vanish with even powers of the Taylor series which allows to compute high order derivatives by combining different Δx steps values and using the real or imaginary part without the limitations of the ordinary CS method. The main limitation of this formulation is that the real and imaginary steps are set to be orthogonal ($e^{\mathbf{i}\theta} = \cos\theta + \mathbf{i}\sin\theta$) depending on a parameter θ, in other words we can not choose the relation between real and imaginary step sizes which brings many advantages as discussed below.

4.3 Generalization of the Complex Step Method

In this work a very simple and straightforward generalization of all the previous variants of the CS method is done. Interpreting the concept of the CS method in a more strict sense, we introduce both real and imaginary differential steps together. Based on a function $f(x+h+\mathbf{i}v)$, the corresponding Taylor series expansion is

$$f(x+h+\mathbf{i}v) = f(x) + (h+\mathbf{i}v) f'(x) + \frac{(h+\mathbf{i}v)^2}{2!} f''(x) + ... = \sum_{n=0}^{\infty} \frac{(h+\mathbf{i}v)^n}{n!} f^n(x), \tag{4.8}$$

where h and v are real numbers related to the real and imaginary differential steps.

We explore the range of possibilities arising from the Taylor series expansion of $f(x+h+\mathbf{i}v)$, $f(x-h+\mathbf{i}v)$, $f(x-h-\mathbf{i}v)$ and $f(x+h-\mathbf{i}v)$, taking their real and imaginary parts, as well as the Taylor expansions of $f(x+h)$ and $f(x-h)$. Note that unlike in the Taylor expansion for the CS method 4.1, for the generalized CS the imaginary unit remains alive in the even terms of the Taylor series 4.8, which allow us to extend the CS method to second order derivatives using the imaginary part of the function in a very easy way. We want to emphasize that beyond the possibilities considered here, many more different expressions for the first and second order derivative approximations can be derived, for example using the terms $f(x+2h+2\mathbf{i}v)$ and $f(x+h+\mathbf{i}v)$ to find an expression for the second order derivative. However, our intention is to find expressions as close as possible to the evaluation point x that enable designing a generalized complex step finite difference scheme on a compact stencil. Here, only one layer of differential complex steps of magnitude h and v in positive and negative, real and imaginary directions is considered.

In the following subsections we present a complete list of different kinds of approximations for the first and second order derivatives on a compact stencil. After this exercise, we will test the numerical performance of each approximation and discuss their behavior.

4.3.1 First Order Derivatives using the imaginary part

The first approximation that can be found by using 4.8 is

$$f'(x) = \frac{\mathfrak{Im}(f(x+h+\mathbf{i}v))}{v} + \mathcal{O}\left(h, v^2\right). \tag{4.9}$$

Note that the approximation error is expressed with a coma; this means the truncation error related to the real and the imaginary step that are not in the same term of the Taylor series. It is easy to see that letting $h = 0$, the Eq. 4.2 and the CS expression for the first derivative 4.9 are equivalent.

$$f'(x) = \frac{\mathfrak{Im}(f(x-h+\mathbf{i}v))}{v} + \mathcal{O}\left(h, v^2\right). \tag{4.10}$$

$$f'(x) = -\frac{\mathfrak{Im}(f(x-h-\mathbf{i}v))}{v} + \mathcal{O}\left(h, v^2\right). \tag{4.11}$$

$$f'(x) = -\frac{\mathfrak{Im}(f(x+h-\mathbf{i}v))}{v} + \mathcal{O}\left(h, v^2\right). \tag{4.12}$$

$$f'(x) = \frac{\mathfrak{Im}(f(x+h+\mathbf{i}v)) - \mathfrak{Im}(f(x+h-\mathbf{i}v))}{2v} + \mathcal{O}\left(hv\right). \tag{4.13}$$

$$f'(x) = \frac{\mathfrak{Im}(f(x-h+\mathbf{i}v)) - \mathfrak{Im}(f(x-h-\mathbf{i}v))}{2v} + \mathcal{O}\left(hv\right). \tag{4.14}$$

$$f'(x) = \frac{\mathfrak{Im}(f(x+h+\mathbf{i}v)) + \mathfrak{Im}(f(x-h+\mathbf{i}v))}{2v} + \mathcal{O}\left(3h^2 - v^2\right). \tag{4.15}$$

$$f'(x) = \frac{\mathfrak{Im}(f(x+h+\mathbf{i}v)) - \mathfrak{Im}(f(x-h-\mathbf{i}v))}{2v} + \mathcal{O}\left(3h^2 - v^2\right). \tag{4.16}$$

Eq. 4.16 was suggested by Lai et. al Lai et al. (2005), considering $h = v = \frac{\sqrt{2}}{2}$.

$$f'(x) = \frac{\mathfrak{Im}(f(x-h+\mathbf{i}v)) - \mathfrak{Im}(f(x+h-\mathbf{i}v))}{2v} + \mathcal{O}\left(3h^2 - v^2\right). \tag{4.17}$$

$$f'(x) = -\frac{\mathfrak{Im}(f(x-h-\mathbf{i}v)) + \mathfrak{Im}(f(x+h-\mathbf{i}v))}{2v} + \mathcal{O}\left(3h^2 - v^2\right). \tag{4.18}$$

$$f'(x) = \frac{\mathfrak{Im}(f(x+h+\mathbf{i}v)) + \mathfrak{Im}(f(x-h+\mathbf{i}v)) - \mathfrak{Im}(f(x+h-\mathbf{i}v)) - \mathfrak{Im}(f(x-h-\mathbf{i}v))}{4v} + \mathcal{O}\left(3h^2 - v^2\right). \tag{4.19}$$

Note that for the particular choice $v = \sqrt{3}h$ in Eqs. 4.15, 4.16, 4.17, 4.18 and 4.19, the truncation error becomes $\mathcal{O}\left(h^4\right)$. Also note that many expressions are equivalent by applying $\mathfrak{Im} f(x \pm h + \mathbf{i}v)) = -\mathfrak{Im}(f(x \pm h - \mathbf{i}v))$.

Now, by using $f(x+h)$ and $f(x-h)$ in conjunction with the imaginary parts we can obtain the following.

$$f'(x) = \frac{\mathfrak{Im}(f(x+h+\mathbf{i}v)) + f(x+h) - f(x)}{h+v} + \mathcal{O}\left(\frac{hv + \frac{h^2}{2}}{h+v}\right). \tag{4.20}$$

$$f'(x) = \frac{\mathfrak{Im}(f(x+h+\mathbf{i}v)) - f(x-h) + f(x)}{h+v} + \mathcal{O}\left(\frac{hv - \frac{h^2}{2}}{h+v}\right). \tag{4.21}$$

$$f'(x) = \frac{\mathfrak{Im}(f(x-h+\mathbf{i}v)) + f(x+h) - f(x)}{h+v} + \mathcal{O}\left(\frac{\frac{h^2}{2} - hv}{h+v}\right). \tag{4.22}$$

$$f'(x) = \frac{\mathfrak{Im}(f(x-h+\mathbf{i}v)) - f(x-h) + f(x)}{h+v} + \mathcal{O}\left(\frac{hv + \frac{h^2}{2}}{h+v}\right). \tag{4.23}$$

$$f'(x) = \frac{f(x+h) - f(x) - \mathfrak{Im}(f(x-h-\mathbf{i}v))}{h+v} + \mathcal{O}\left(\frac{\frac{h^2}{2} - hv}{h+v}\right). \tag{4.24}$$

$$f'(x) = \frac{f(x) - f(x-h) - \mathfrak{Im}(f(x-h-\mathbf{i}v))}{h+v} + \mathcal{O}\left(\frac{hv + \frac{h^2}{2}}{h+v}\right). \tag{4.25}$$

$$f'(x) = \frac{f(x+h) - f(x) - \mathfrak{Im}(f(x+h-\mathbf{i}v))}{h+v} + \mathcal{O}\left(\frac{hv + \frac{h^2}{2}}{h+v}\right). \tag{4.26}$$

$$f'(x) = \frac{f(x) - f(x-h) - \mathfrak{Im}(f(x+h-\mathbf{i}v))}{h+v} + \mathcal{O}\left(\frac{hv - \frac{h^2}{2}}{h+v}\right). \tag{4.27}$$

If we set $h = 2v$ in Eqs. 4.21, 4.22, 4.24 and 4.27 the truncation error becomes $\mathcal{O}\left(v^2\right)$.

$$f'(x) = \frac{\mathfrak{Im}(f(x+h+\mathbf{i}v)) + \mathfrak{Im}(f(x-h+\mathbf{i}v)) + f(x+h) - f(x-h)}{2h+2v} + \mathcal{O}\left(\frac{2h^3+3h^2v-v^3}{2h+2v}\right). \tag{4.28}$$

$$f'(x) = \frac{\mathfrak{Im}(f(x+h+\mathbf{i}v)) - \mathfrak{Im}(f(x-h-\mathbf{i}v)) + f(x+h) - f(x-h)}{2h+2v} + \mathcal{O}\left(\frac{2h^3+3h^2v-v^3}{2h+2v}\right). \tag{4.29}$$

$$f'(x) = \frac{\mathfrak{Im}(f(x+h+\mathbf{i}v)) - \mathfrak{Im}(f(x+h-\mathbf{i}v)) + f(x+h) - f(x-h)}{2h+2v} + \mathcal{O}\left(\frac{2h^3+3h^2v-v^3}{2h+2v}\right). \tag{4.30}$$

$$f'(x) = \frac{\mathfrak{Im}(f(x-h+\mathbf{i}v)) - \mathfrak{Im}(f(x-h-\mathbf{i}v)) + f(x+h) - f(x-h)}{2h+2v} + \mathcal{O}\left(\frac{2h^3+3h^2v-v^3}{2h+2v}\right). \tag{4.31}$$

$$f'(x) = \frac{f(x+h) - f(x-h) - \mathfrak{Im}(f(x-h-\mathbf{i}v)) - \mathfrak{Im}(f(x+h-\mathbf{i}v))}{2h+2v} + \mathcal{O}\left(\frac{2h^3+3h^2v-v^3}{2h+2v}\right). \tag{4.32}$$

$$\begin{aligned} f'(x) = & \frac{\mathfrak{Im}(f(x+h+\mathbf{i}v)) + \mathfrak{Im}(f(x-h+\mathbf{i}v)) - \mathfrak{Im}(f(x-h-\mathbf{i}v))}{2h+4v} \\ & + \frac{f(x+h) - f(x-h) - \mathfrak{Im}(f(x+h-\mathbf{i}v))}{2h+4v} + \mathcal{O}\left(\frac{2h^3+3h^2v-v^3}{2h+4v}\right). \end{aligned} \tag{4.33}$$

Making the expression $2h^3 + 3h^2v - v^3 = 0$, by selecting the right values of h and v, the truncation error for Eqs. 4.28 - 4.33 becomes $\mathcal{O}\left(\frac{2h^5+5h^4v-10h^2v^3+v^5}{2h+2v}\right)$.

If we consider $h = 0$ in the imaginary part only we can obtain several approximations with similar structure of equations 4.20 - 4.27 but only reaching to first order of accuracy without having the chance of choosing values of h and v. The following approximation can reach to higher order accuracy:

$$f'(x) = \frac{\mathfrak{Im}(f(x+\mathbf{i}v)) - \mathfrak{Im}(f(x-\mathbf{i}v)) + f(x+h) - f(x-h)}{2h+2v} + \mathcal{O}\left(\frac{h^3-v^3}{2h+2v}\right). \tag{4.34}$$

Setting $h = v$ the truncation error for Eq. 4.34 becomes $\mathcal{O}\left(h^4\right)$.

4.3.2 Second Order Derivatives using the imaginary part

$$f''(x) = \frac{\mathfrak{Im}(f(x+h+\mathbf{i}v)) - \mathfrak{Im}(f(x-h+\mathbf{i}v))}{2hv} + \mathcal{O}\left(h^2 - v^2\right). \tag{4.35}$$

Eq. 4.35 has been suggested by several authors: Abokhodair Abokhodair (2007),Abokhodair (2009), recommends choosing $h \ll v$, Cao Cao (2008) with $h = v = \sqrt{\epsilon}$, where ϵ is the machine accuracy. Lai et. al Lai and Crassidis (2008) obtain a similar approximation by considering orthogonal complex steps.

$$f''(x) = \frac{\mathfrak{Im}(f(x+h+\mathbf{i}v)) + \mathfrak{Im}(f(x-h-\mathbf{i}v))}{2hv} + \mathcal{O}\left(h^2 - v^2\right). \tag{4.36}$$

Eq. 4.36 has been suggested by Lai et. al Lai et al. (2005), considering $h = v = \frac{\sqrt{2}}{2}$.

$$f''(x) = -\frac{\mathfrak{Im}(f(x-h+\mathbf{i}v)) + \mathfrak{Im}(f(x+h-\mathbf{i}v))}{2hv} + \mathcal{O}\left(h^2 - v^2\right). \tag{4.37}$$

$$f''(x) = \frac{\mathfrak{Im}(f(x-h-\mathbf{i}v)) - \mathfrak{Im}(f(x+h-\mathbf{i}v))}{2hv} + \mathcal{O}\left(h^2 - v^2\right). \tag{4.38}$$

$$f''(x) = \frac{\mathfrak{Im}(f(x+h+\mathbf{i}v)) - \mathfrak{Im}(f(x-h+\mathbf{i}v)) + \mathfrak{Im}(f(x-h-\mathbf{i}v)) - \mathfrak{Im}(f(x+h-\mathbf{i}v))}{4hv} + \mathcal{O}\left(h^2 - v^2\right). \tag{4.39}$$

If we set $v = h$ in Eqs. 4.35 - 4.39 the truncation error becomes $\mathcal{O}\left(h^4\right)$.

Now using $f(x+h)$ and $f(x-h)$ we can obtain (from the approximations 4.40 - 4.47 we have to assume that $h = v$) the following.

$$f''(x) = \frac{2(\mathfrak{Im}(f(x+h+\mathbf{i}h)) - f(x+h) + f(x))}{h^2} + \mathcal{O}\left(h\right). \tag{4.40}$$

$$f''(x) = \frac{2(\mathfrak{Im}(f(x+h+\mathbf{i}h)) + f(x-h) - f(x))}{3h^2} + \mathcal{O}\left(h\right). \tag{4.41}$$

$$f''(x) = \frac{2(f(x+h) - \mathfrak{Im}(f(x-h+\mathbf{i}h)) - f(x))}{3h^2} + \mathcal{O}\left(h\right). \tag{4.42}$$

$$f''(x) = \frac{2(f(x) - \mathfrak{Im}(f(x-h+\mathbf{i}h)) - f(x-h))}{h^2} + \mathcal{O}\left(h\right). \tag{4.43}$$

$$f''(x) = \frac{2(\mathfrak{Im}(f(x-h-\mathbf{i}h)) + f(x+h) - f(x))}{3h^2} + \mathcal{O}\left(h\right). \tag{4.44}$$

$$f''(x) = \frac{2(\mathfrak{Im}(f(x-h-\mathbf{i}h)) + f(x) - f(x-h))}{h^2} + \mathcal{O}\left(h\right). \tag{4.45}$$

$$f''(x) = \frac{2(f(x) - \mathfrak{Im}(f(x+h-\mathbf{i}h)) - f(x+h))}{h^2} + \mathcal{O}\left(h\right). \tag{4.46}$$

$$f''(x) = \frac{2(f(x-h) - \mathfrak{Im}(f(x+h-\mathbf{i}h)) - f(x))}{3h^2} + \mathcal{O}\left(h\right). \tag{4.47}$$

$$f''(x) = \frac{\mathfrak{Im}(f(x+h+\mathbf{i}v)) - \mathfrak{Im}(f(x-h+\mathbf{i}v)) + f(x+h) + f(x-h) - 2f(x)}{h^2+2hv} + \mathcal{O}\left(\frac{h^4+4h^3v-4hv^3}{h^2+2hv}\right). \tag{4.48}$$

$$f''(x) = \frac{\mathfrak{Im}(f(x+h+\mathbf{i}v)) + \mathfrak{Im}(f(x-h-\mathbf{i}v)) + f(x+h) + f(x-h) - 2f(x)}{h^2+2hv} + \mathcal{O}\left(\frac{h^4+4h^3v-4hv^3}{h^2+2hv}\right). \tag{4.49}$$

$$f''(x) = \frac{\mathfrak{Im}(f(x-h-\mathbf{i}v)) - \mathfrak{Im}(f(x+h-\mathbf{i}v)) + f(x+h) + f(x-h) - 2f(x)}{h^2+2hv} + \mathcal{O}\left(\frac{h^4+4h^3v-4hv^3}{h^2+2hv}\right). \tag{4.50}$$

$$f''(x) = \frac{\mathfrak{Im}(f(x+h+\mathbf{i}v)) + \mathfrak{Im}(f(x-h-\mathbf{i}v)) - \mathfrak{Im}(f(x-h+\mathbf{i}v))}{h^2+4hv} + \frac{f(x+h) + f(x-h) - 2f(x) - \mathfrak{Im}(f(x+h-\mathbf{i}v))}{h^2+4hv} + \mathcal{O}\left(\frac{h^4+4h^3v-4hv^3}{h^2+2hv}\right). \tag{4.51}$$

Making the expression $h^4 + 4h^3v - 4hv^3 = 0$, by selecting the right values of h and v, the truncation error for Eqs. 4.48 - 4.51 becomes $\mathcal{O}\left(\frac{2h^6+6h^5v-20h^3v^3+6hv^5}{h^2+2hv}\right)$.

4.3.3 First Order Derivatives using the real part

$$f'(x) = \frac{\mathfrak{Re}(f(x+h+\mathbf{i}v)) - f(x)}{h} + \mathcal{O}\left(\frac{h^2-v^2}{h}\right). \tag{4.52}$$

$$f'(x) = \frac{f(x) - \mathfrak{Re}(f(x-h+\mathbf{i}v))}{h} + \mathcal{O}\left(\frac{h^2-v^2}{h}\right). \tag{4.53}$$

$$f'(x) = \frac{f(x) - \mathfrak{Re}(f(x-h-\mathbf{i}v))}{h} + \mathcal{O}\left(\frac{h^2-v^2}{h}\right). \tag{4.54}$$

$$f'(x) = \frac{\mathfrak{Re}(f(x+h-\mathbf{i}v)) - f(x)}{h} + \mathcal{O}\left(\frac{h^2-v^2}{h}\right). \tag{4.55}$$

If we set $h = v$ in Eqs. 4.52 - 4.55, the truncation error becomes $\mathcal{O}\left(h^2\right)$.

$$f'(x) = \frac{\mathfrak{Re}(f(x+h+\mathbf{i}v)) - \mathfrak{Re}(f(x-h+\mathbf{i}v))}{2h} + \mathcal{O}\left(h^2 - 3v^2\right). \tag{4.56}$$

Eq. 4.56 has been suggested by Abokhodair Abokhodair (2007),Abokhodair (2009).

$$f'(x) = \frac{\mathfrak{Re}(f(x+h+\mathbf{i}v)) - \mathfrak{Re}(f(x-h-\mathbf{i}v))}{2h} + \mathcal{O}\left(h^2 - 3v^2\right). \tag{4.57}$$

$$f'(x) = \frac{\mathfrak{Re}(f(x+h-\mathbf{i}v)) - \mathfrak{Re}(f(x-h+\mathbf{i}v))}{2h} + \mathcal{O}\left(h^2 - 3v^2\right). \tag{4.58}$$

$$f'(x) = \frac{\mathfrak{Re}(f(x+h-\mathbf{i}v)) - \mathfrak{Re}(f(x-h-\mathbf{i}v))}{2h} + \mathcal{O}\left(h^2 - 3v^2\right). \tag{4.59}$$

$$f'(x) = \frac{\mathfrak{Re}(f(x+h+\mathbf{i}v)) - \mathfrak{Re}(f(x-h+\mathbf{i}v)) + \mathfrak{Re}(f(x+h-\mathbf{i}v)) - \mathfrak{Re}(f(x-h-\mathbf{i}v))}{4h} + \mathcal{O}\left(h^2 - 3v^2\right). \tag{4.60}$$

If we set $h = \sqrt{3}v$ in Eqs. 4.56 - 4.60, the truncation error becomes $\mathcal{O}\left(v^4\right)$.

$$f'(x) = \frac{\mathfrak{Re}(f(x+h+\mathbf{i}v)) + \mathfrak{Re}(f(x+h-\mathbf{i}v)) - 2f(x)}{2h} + \mathcal{O}\left(\frac{h^2 - v^2}{h}\right). \tag{4.61}$$

$$f'(x) = \frac{2f(x) - \mathfrak{Re}(f(x-h-\mathbf{i}v)) - \mathfrak{Re}(f(x-h+\mathbf{i}v))}{2h} + \mathcal{O}\left(\frac{h^2 - v^2}{h}\right). \tag{4.62}$$

If we set $h = v$ in Eqs. 4.61 and 4.62 the truncation error becomes $\mathcal{O}\left(h^2\right)$.
Note that many expressions are equivalent by applying $\mathfrak{Re}(f(x+h\pm\mathbf{i}v)) = -\mathfrak{Re}(f(x-h\pm\mathbf{i}v))$.
Now using $f(x+h)$ and $f(x-h)$ we can obtain the following

$$f'(x) = \frac{\mathfrak{Re}(f(x+h+\mathbf{i}v)) + f(x+h) - 2f(x)}{2h} + \mathcal{O}\left(h, v\right). \tag{4.63}$$

$$f'(x) = \frac{\mathfrak{Re}(f(x+h+\mathbf{i}v)) - f(x-h)}{2h} + \mathcal{O}\left(h, v\right). \tag{4.64}$$

$$f'(x) = \frac{f(x+h) - \mathfrak{Re}(f(x-h+\mathbf{i}v))}{2h} + \mathcal{O}\left(h, v\right). \tag{4.65}$$

$$f'(x) = \frac{2f(x) - \mathfrak{Re}(f(x-h+\mathbf{i}v)) - f(x-h)}{2h} + \mathcal{O}\left(h, v\right). \tag{4.66}$$

$$f'(x) = \frac{f(x+h) - \mathfrak{Re}(f(x-h-\mathbf{i}v))}{2h} + \mathcal{O}\left(h, v\right). \tag{4.67}$$

$$f'(x) = \frac{2f(x) - \mathfrak{Re}(f(x-h-\mathbf{i}v)) - f(x-h)}{2h} + \mathcal{O}\left(h, v\right). \tag{4.68}$$

$$f'(x) = \frac{\mathfrak{Re}(f(x+h-\mathbf{i}v)) + f(x+h) - 2f(x)}{2h} + \mathcal{O}\left(h, v\right). \tag{4.69}$$

$$f'(x) = \frac{\mathfrak{Re}(f(x+h-\mathbf{i}v)) - f(x-h)}{2h} + \mathcal{O}\left(h, v\right). \tag{4.70}$$

$$f'(x) = \frac{\mathfrak{Re}(f(x+h+\mathbf{i}v)) - \mathfrak{Re}(f(x-h+\mathbf{i}v)) + f(x+h) - f(x-h)}{4h} + \mathcal{O}\left(2h^2 - 3v^2\right). \tag{4.71}$$

$$f'(x) = \frac{\mathfrak{Re}(f(x+h+\mathbf{i}v)) - \mathfrak{Re}(f(x-h-\mathbf{i}v)) + f(x+h) - f(x-h)}{4h} + \mathcal{O}\left(2h^2 - 3v^2\right). \tag{4.72}$$

$$f'(x) = \frac{\mathfrak{Re}(f(x+h-\mathbf{i}v)) - \mathfrak{Re}(f(x-h+\mathbf{i}v)) + f(x+h) - f(x-h)}{4h} + \mathcal{O}\left(2h^2 - 3v^2\right). \tag{4.73}$$

$$f'(x) = \frac{\mathfrak{Re}(f(x+h-\mathbf{i}v)) - \mathfrak{Re}(f(x-h-\mathbf{i}v)) + f(x+h) - f(x-h)}{4h} + \mathcal{O}\left(2h^2 - 3v^2\right). \tag{4.74}$$

$$\begin{aligned} f'(x) = {} & \frac{\mathfrak{Re}(f(x+h+\mathbf{i}v)) - \mathfrak{Re}(f(x-h+\mathbf{i}v)) - \mathfrak{Re}(f(x-h-\mathbf{i}v))}{6h} \\ & + \frac{\mathfrak{Re}(f(x+h-\mathbf{i}v)) + f(x+h) - f(x-h)}{6h} + \mathcal{O}\left(h^2 - 2v^2\right). \end{aligned} \tag{4.75}$$

If we set $2h^2 = 3v^2$ in Eqs. 4.71 - 4.74 and letting $h^2 = 2v^2$ in Eq. 4.75, the truncation error becomes $\mathcal{O}\left(h^4\right)$.

$$f'(x) = \frac{\mathfrak{Re}(f(x+h+\mathbf{i}v)) + \mathfrak{Re}(f(x+h-\mathbf{i}v)) + f(x+h) - f(x-h) - 2f(x)}{4h} + \mathcal{O}\left(\frac{h^2 - v^2}{h}\right). \tag{4.76}$$

$$f'(x) = \frac{2f(x) - \mathfrak{Re}(f(x-h+\mathbf{i}v)) - \mathfrak{Re}(f(x-h-\mathbf{i}v)) + f(x+h) - f(x-h)}{4h} + \mathcal{O}\left(\frac{h^2 - v^2}{h}\right). \tag{4.77}$$

If we set $v = h$ in Eqs. 4.76 and 4.77, the truncation error becomes $\mathcal{O}\left(h^2\right)$.

4.3.4 Second Order Derivatives using the real part

$$f''(x) = \frac{\mathfrak{Re}(f(x+h+\mathbf{i}v)) + \mathfrak{Re}(f(x-h+\mathbf{i}v)) - 2f(x)}{(h^2-v^2)} + \mathcal{O}\left(\frac{h^4 - 6h^2v^2 + v^4}{h^2-v^2}\right). \tag{4.78}$$

$$f''(x) = \frac{\mathfrak{Re}(f(x+h-\mathbf{i}v)) + \mathfrak{Re}(f(x-h-\mathbf{i}v)) - 2f(x)}{(h^2-v^2)} + \mathcal{O}\left(\frac{h^4 - 6h^2v^2 + v^4}{h^2-v^2}\right). \tag{4.79}$$

$$f''(x) = \frac{\mathfrak{Re}(f(x+h+\mathbf{i}v)) + \mathfrak{Re}(f(x-h-\mathbf{i}v)) - 2f(x)}{(h^2-v^2)} + \mathcal{O}\left(\frac{h^4 - 6h^2v^2 + v^4}{h^2-v^2}\right). \tag{4.80}$$

$$f''(x) = \frac{\mathfrak{Re}(f(x+h-\mathbf{i}v)) + \mathfrak{Re}(f(x-h+\mathbf{i}v)) - 2f(x)}{(h^2-v^2)} + \mathcal{O}\left(\frac{h^4 - 6h^2v^2 + v^4}{h^2-v^2}\right). \tag{4.81}$$

$$f''(x) = \frac{\mathfrak{Re}(f(x+h+\mathbf{i}v)) + \mathfrak{Re}(f(x-h+\mathbf{i}v)) + \mathfrak{Re}(f(x+h-\mathbf{i}v)) + \mathfrak{Re}(f(x-h-\mathbf{i}v)) - 4f(x)}{2(h^2-v^2)} + \mathcal{O}\left(\frac{h^4 - 6h^2v^2 + v^4}{h^2-v^2}\right). \tag{4.82}$$

Making the expression $h^4 - 6h^2v^2 + v^4 = 0$, by selecting the right values of h and v, the truncation error for Eqs. 4.78 - 4.82 becomes $\mathcal{O}\left(\frac{h^6 - 15h^4v^2 + 15h^2v^4 - v^6}{h^2-v^2}\right)$.

Now using $f(x+h)$ and $f(x-h)$ we can obtain the following

$$f''(x) = \frac{2(f(x+h) - \mathfrak{Re}(f(x+h+\mathbf{i}v)))}{v^2} + \mathcal{O}\left(h, v^2\right). \tag{4.83}$$

$$f''(x) = \frac{\mathfrak{Re}(f(x+h+\mathbf{i}v)) + f(x-h) - 2f(x)}{h^2 - \frac{v^2}{2}} + \mathcal{O}\left(\frac{v^2 h}{h^2 - \frac{v^2}{2}}\right). \tag{4.84}$$

$$f''(x) = \frac{\mathfrak{Re}(f(x-h+\mathbf{i}v)) + f(x+h) - 2f(x)}{h^2 - \frac{v^2}{2}} + \mathcal{O}\left(\frac{v^2 h}{h^2 - \frac{v^2}{2}}\right). \tag{4.85}$$

$$f''(x) = \frac{2(f(x-h) - \mathfrak{Re}(f(x-h+\mathbf{i}v)))}{v^2} + \mathcal{O}\left(h, v^2\right). \tag{4.86}$$

$$f''(x) = \frac{\mathfrak{Re}(f(x-h-\mathbf{i}v)) + f(x+h) - 2f(x)}{h^2 - \frac{v^2}{2}} + \mathcal{O}\left(\frac{v^2 h}{h^2 - \frac{v^2}{2}}\right). \tag{4.87}$$

$$f''(x) = \frac{2(f(x-h) - \mathfrak{Re}(f(x-h-\mathbf{i}v)))}{v^2} + \mathcal{O}\left(h, v^2\right). \tag{4.88}$$

$$f''(x) = \frac{2(f(x+h) - \mathfrak{Re}(f(x+h-\mathbf{i}v)))}{v^2} + \mathcal{O}\left(h, v^2\right). \tag{4.89}$$

$$f''(x) = \frac{\mathfrak{Re}(f(x+h-\mathbf{i}v)) + f(x-h) - 2f(x)}{h^2 - \frac{v^2}{2}} + \mathcal{O}\left(\frac{v^2 h}{h^2 - \frac{v^2}{2}}\right). \tag{4.90}$$

$$f''(x) = \frac{f(x+h) + f(x-h) - \mathfrak{Re}(f(x+h+\mathbf{i}v)) - \mathfrak{Re}(f(x-h+\mathbf{i}v))}{v^2} + \mathcal{O}\left(v^2 - 6h^2\right). \tag{4.91}$$

$$f''(x) = \frac{f(x+h) + f(x-h) - \mathfrak{Re}(f(x+h+\mathbf{i}v)) - \mathfrak{Re}(f(x-h-\mathbf{i}v))}{v^2} + \mathcal{O}\left(v^2 - 6h^2\right). \tag{4.92}$$

$$f''(x) = \frac{f(x+h) + f(x-h) - \mathfrak{Re}(f(x+h-\mathbf{i}v)) - \mathfrak{Re}(f(x-h+\mathbf{i}v))}{v^2} + \mathcal{O}\left(v^2 - 6h^2\right). \tag{4.93}$$

$$f''(x) = \frac{f(x+h) + f(x-h) - \mathfrak{Re}(f(x+h-\mathbf{i}v)) - \mathfrak{Re}(f(x-h-\mathbf{i}v))}{v^2} + \mathcal{O}\left(v^2 - 6h^2\right). \tag{4.94}$$

$$\begin{aligned} f''(x) = &\frac{2f(x+h) + 2f(x-h) - \mathfrak{Re}(f(x+h+\mathbf{i}v)) - \mathfrak{Re}(f(x-h+\mathbf{i}v))}{2v^2} \\ &- \frac{\mathfrak{Re}(f(x-h-\mathbf{i}v)) + \mathfrak{Re}(f(x+h-\mathbf{i}v))}{2v^2} + \mathcal{O}\left(v^2 - 6h^2\right). \end{aligned} \tag{4.95}$$

If we set $v^2 = 6h^2$ in Eqs. 4.91 - 4.95, the truncation error becomes $\mathcal{O}\left(h^4\right)$.

$$\begin{aligned} f''(x) = &\frac{\mathfrak{Re}(f(x+h+\mathbf{i}v)) + \mathfrak{Re}(f(x-h+\mathbf{i}v)) + f(x+h) + f(x-h) - 4f(x)}{2h^2 - v^2} \\ &+ \mathcal{O}\left(\frac{2h^4 - 6h^2v^2 + v^4}{2h^2 - v^2}\right). \end{aligned} \tag{4.96}$$

$$\begin{aligned} f''(x) = &\frac{\mathfrak{Re}(f(x+h+\mathbf{i}v)) + \mathfrak{Re}(f(x-h-\mathbf{i}v)) + f(x+h) + f(x-h) - 4f(x)}{2h^2 - v^2} \\ &+ \mathcal{O}\left(\frac{2h^4 - 6h^2v^2 + v^4}{2h^2 - v^2}\right). \end{aligned} \tag{4.97}$$

$$\begin{aligned} f''(x) = &\frac{\mathfrak{Re}(f(x+h-\mathbf{i}v)) + \mathfrak{Re}(f(x-h+\mathbf{i}v)) + f(x+h) + f(x-h) - 4f(x)}{2h^2 - v^2} \\ &+ \mathcal{O}\left(\frac{2h^4 - 6h^2v^2 + v^4}{2h^2 - v^2}\right). \end{aligned} \tag{4.98}$$

$$\begin{aligned} f''(x) = &\frac{\mathfrak{Re}(f(x+h-\mathbf{i}v)) + \mathfrak{Re}(f(x-h-\mathbf{i}v)) + f(x+h) + f(x-h) - 4f(x)}{2h^2 - v^2} \\ &+ \mathcal{O}\left(\frac{2h^4 - 6h^2v^2 + v^4}{2h^2 - v^2}\right). \end{aligned} \tag{4.99}$$

$$\begin{aligned} f''(x) = &\frac{\mathfrak{Re}(f(x+h+\mathbf{i}v)) + \mathfrak{Re}(f(x-h+\mathbf{i}v)) + \mathfrak{Re}(f(x-h-\mathbf{i}v))}{3h^2 - 2v^2} \\ &+ \frac{\mathfrak{Re}(f(x+h-\mathbf{i}v)) + f(x+h) + f(x-h) - 6f(x)}{3h^2 - 2v^2} + \mathcal{O}\left(\frac{3h^4 - 12h^2v^2 + 2v^4}{3h^2 - 2v^2}\right). \end{aligned} \tag{4.100}$$

Making the expressions $2h^4-6h^2v^2+v^4=0$ and $3h^4-12h^2v^2+2v^4=0$ by selecting the right values of h and v, the truncation error for Eqs. 4.96 - 4.99 becomes $\mathcal{O}\left(\frac{2h^6-15h^4v^2+15h^2v^4-v^6}{2h^2-v^2}\right)$ and $\mathcal{O}\left(\frac{2h^6-15h^4v^2+15h^2v^4-v^6}{3h^2-2v^2}\right)$ for Eq. 4.100.

If we consider $h=0$ in the real part only we can obtain the following approximations

$$f''(x)=\frac{\mathfrak{Re}(f(x+\mathbf{i}v))+\mathfrak{Re}(f(x-\mathbf{i}v))+f(x+h)+f(x-h)-4f(x)}{h^2-v^2}+\mathcal{O}\left(\frac{h^4+v^4}{h^2-v^2}\right). \tag{4.101}$$

$$f''(x)=\frac{f(x+h)+f(x-h)-\mathfrak{Re}(f(x+\mathbf{i}v))-\mathfrak{Re}(f(x-\mathbf{i}v))}{h^2+v^2}+\mathcal{O}\left(\frac{h^4-v^4}{h^2+v^2}\right). \tag{4.102}$$

Setting $v=h$ in Eq. 4.102, the truncation error becomes $\mathcal{O}\left(h^4\right)$.

$$f''(x)=\frac{f(x+h)+f(x-h)-f(x)-\mathfrak{Re}(f(x+\mathbf{i}v))}{h^2+\frac{v^2}{2}}+\mathcal{O}\left(\frac{2h^4-v^4}{h^2+\frac{v^2}{2}}\right). \tag{4.103}$$

Setting $\sqrt[4]{2}h=v$ in Eq. 4.103, the truncation error becomes $\mathcal{O}\left(v^4\right)$.

4.4 Numerical tests

The different kinds of approximations for the first and second order derivatives 4.9 - 4.102 show different truncation errors and - according to the structure of the numerator - either avoid subtractive cancellation, or not. Note that a formal summation in the numerator is not a sufficient criterion to decide this question, because the individual terms may have opposite sign. To validate Eqs. 4.9 - 4.102, we use an analytic test function that has become an established de-facto standard in numerical differentiation, used by Lyness and Sande (1971) and subsequently by many authors:

$$f(x)=\frac{e^x}{\sin^3(x)+\cos^3(x)}.$$

Consistent with previous work on complex variable differentiation, we evaluate the function at the test point $x=1.5$, which has the following values for the first and second derivatives: $f'(x)=3.622$ and $f''(x)=14.5683$.

Simulations have been carried out in Fortran90 language and the GNU Fortran compiler gfortran with standard double precision format for all variables.

Results are displayed systematically in tables where increment value h starts from $1e^{-1}$ decreasing geometrically to $1e^{-25}$, plotted in the left column of the tables. The v value is taken as $v=h$, unless a better, specific choice of v versus h was adopted to increase the order of the approximation error as indicated in the description of Eqs. 4.9 - 4.102 in the previous section. In the Tables, all errors are relative errors. The tested approximations are identified in the top row of the tables with the number of the respective equation.

h	Eq. 3.3	ERROR	Eq. 4.9	ERROR	Eq. 4.10	ERROR	Eq. 4.11	ERROR	Eq. 4.12	ERROR
0.1	4.4557	0.23016	5.2614	0.45262	2.35	0.35119	2.35	0.35119	5.2614	0.45262
0.01	3.6958	0.020374	3.7696	0.040744	3.4782	0.039698	3.4782	0.039698	3.7696	0.040744
0.001	3.6295	0.0020606	3.6366	0.0040276	3.6075	0.0040171	3.6075	0.0040171	3.6366	0.0040276
0.0001	3.6234	0.00036712	3.6235	0.00040236	3.6206	0.00040219	3.6206	0.00040219	3.6235	0.00040236
1e-05	3.627	0.0013782	3.6222	4.0236e-05	3.6219	4.0316e-05	3.6219	4.0316e-05	3.6222	4.0236e-05
1e-06	3.4542	0.046324	3.622	3.8184e-06	3.622	3.8532e-06	3.622	3.8532e-06	3.622	3.8184e-06
1e-07	4.3178	0.19209	3.622	4.7626e-07	3.622	4.8269e-07	3.622	4.8269e-07	3.622	4.7626e-07
1e-08	0	1	3.622	2.0979e-08	3.622	2.0979e-08	3.622	2.0979e-08	3.622	2.0979e-08
1e-09	0	1	3.622	4.3183e-08	3.622	4.3183e-08	3.622	4.3183e-08	3.622	4.3183e-08
1e-10	0	1	3.622	1.5497e-09	3.622	1.5497e-09	3.622	1.5497e-09	3.622	1.5497e-09
1e-11	0	1	3.622	1.8897e-08	3.622	1.8897e-08	3.622	1.8897e-08	3.622	1.8897e-08
1e-12	0	1	3.622	1.8897e-08	3.622	1.8897e-08	3.622	1.8897e-08	3.622	1.8897e-08
1e-13	0	1	3.622	3.2449e-08	3.622	3.2449e-08	3.622	3.2449e-08	3.622	3.2449e-08
1e-14	0	1	3.622	3.2449e-08	3.622	3.2449e-08	3.622	3.2449e-08	3.622	3.2449e-08
1e-15	0	1	3.622	1.1274e-08	3.622	1.1274e-08	3.622	1.1274e-08	3.622	1.1274e-08
1e-16	0	1	3.622	1.9612e-09	3.622	1.9612e-09	3.622	1.9612e-09	3.622	1.9612e-09
1e-17	0	1	3.622	3.1126e-08	3.622	3.1126e-08	3.622	3.1126e-08	3.622	3.1126e-08
1e-18	0	1	3.622	3.0913e-08	3.622	3.0913e-08	3.622	3.0913e-08	3.622	3.0913e-08
1e-19	0	1	3.622	1.7988e-08	3.622	1.7988e-08	3.622	1.7988e-08	3.622	1.7988e-08
1e-20	0	1	3.622	3.4144e-08	3.622	3.4144e-08	3.622	3.4144e-08	3.622	3.4144e-08
1e-21	0	1	3.622	4.6636e-08	3.622	4.6636e-08	3.622	4.6636e-08	3.622	4.6636e-08
1e-22	0	1	3.622	1.6473e-08	3.622	1.6473e-08	3.622	1.6473e-08	3.622	1.6473e-08
1e-23	0	1	3.622	1.5081e-08	3.622	1.5081e-08	3.622	1.5081e-08	3.622	1.5081e-08
1e-24	0	1	3.622	4.6403e-09	3.622	4.6403e-09	3.622	4.6403e-09	3.622	4.6403e-09
1e-25	0	1	3.622	4.6403e-09	3.622	4.6403e-09	3.622	4.6403e-09	3.622	4.6403e-09

Table 4.1: First order derivatives validation : $f(x) = \frac{e^x}{\sin^3(x)+\cos^3(x)}, \quad x = 1.5, \quad f'(x) = 3.622.$

h	Eq. 4.13	ERROR	Eq. 4.14	ERROR	Eq. 4.15	ERROR	Eq. 4.16	ERROR	Eq. 4.17	ERROR
0.1	5.2614	0.45262	2.35	0.35119	3.6006	0.0059312	3.6006	0.0059312	3.6006	0.0059312
0.01	3.7696	0.040744	3.4782	0.039698	3.622	6.3492e-07	3.622	6.3492e-07	3.622	6.3492e-07
0.001	3.6366	0.0040276	3.6075	0.0040171	3.622	2.4113e-08	3.622	2.4113e-08	3.622	2.4113e-08
0.0001	3.6235	0.00040236	3.6206	0.00040219	3.622	2.5651e-08	3.622	2.5651e-08	3.622	2.5651e-08
1e-05	3.6222	4.0236e-05	3.6219	4.0316e-05	3.622	1.638e-08	3.622	1.638e-08	3.622	1.638e-08
1e-06	3.622	3.8184e-06	3.622	3.8532e-06	3.622	1.6383e-08	3.622	1.6383e-08	3.622	1.6383e-08
1e-07	3.622	4.7626e-07	3.622	4.8269e-07	3.622	1.6382e-08	3.622	1.6382e-08	3.622	1.6382e-08
1e-08	3.622	2.0979e-08	3.622	2.0979e-08	3.622	3.6894e-08	3.622	3.6894e-08	3.622	3.6894e-08
1e-09	3.622	4.3183e-08	3.622	4.3183e-08	3.622	1.5653e-09	3.622	1.5653e-09	3.622	1.5653e-09
1e-10	3.622	1.5497e-09	3.622	1.5497e-09	3.622	3.3615e-08	3.622	3.3615e-08	3.622	3.3615e-08
1e-11	3.622	1.8897e-08	3.622	1.8897e-08	3.622	2.6478e-08	3.622	2.6478e-08	3.622	2.6478e-08
1e-12	3.622	1.8897e-08	3.622	1.8897e-08	3.622	1.3959e-08	3.622	1.3959e-08	3.622	1.3959e-08
1e-13	3.622	3.2449e-08	3.622	3.2449e-08	3.622	2.9608e-08	3.622	2.9608e-08	3.622	2.9608e-08
1e-14	3.622	3.2449e-08	3.622	3.2449e-08	3.622	4.8638e-08	3.622	4.8638e-08	3.622	4.8638e-08
1e-15	3.622	1.1274e-08	3.622	1.1274e-08	3.622	2.4186e-08	3.622	2.4186e-08	3.622	2.4186e-08
1e-16	3.622	1.9612e-09	3.622	1.9612e-09	3.622	6.3786e-09	3.622	6.3786e-09	3.622	6.3786e-09
1e-17	3.622	3.1126e-08	3.622	3.1126e-08	3.622	1.2724e-08	3.622	1.2724e-08	3.622	1.2724e-08
1e-18	3.622	3.0913e-08	3.622	3.0913e-08	3.622	1.2724e-08	3.622	1.2724e-08	3.622	1.2724e-08
1e-19	3.622	1.7988e-08	3.622	1.7988e-08	3.622	1.7124e-08	3.622	1.7124e-08	3.622	1.7124e-08
1e-20	3.622	3.4144e-08	3.622	3.4144e-08	3.622	3.5779e-08	3.622	3.5779e-08	3.622	3.5779e-08
1e-21	3.622	4.6636e-08	3.622	4.6636e-08	3.622	3.5779e-08	3.622	3.5779e-08	3.622	3.5779e-08
1e-22	3.622	1.6473e-08	3.622	1.6473e-08	3.622	3.5779e-08	3.622	3.5779e-08	3.622	3.5779e-08
1e-23	3.622	1.5081e-08	3.622	1.5081e-08	3.622	3.5779e-08	3.622	3.5779e-08	3.622	3.5779e-08
1e-24	3.622	4.6403e-09	3.622	4.6403e-09	3.622	1.3007e-08	3.622	1.3007e-08	3.622	1.3007e-08
1e-25	3.622	4.6403e-09	3.622	4.6403e-09	3.622	1.5459e-08	3.622	1.5459e-08	3.622	1.5459e-08

Table 4.2: First order derivatives validation : $f(x) = \frac{e^x}{\sin^3(x)+\cos^3(x)}, \quad x = 1.5, \quad f'(x) = 3.622.$

h	Eq. 4.18	ERROR	Eq. 4.19	ERROR	Eq. 4.20	ERROR	Eq. 4.21	ERROR	Eq. 4.22	ERROR
0.1	3.6006	0.0059312	3.6006	0.0059312	4.8586	0.34139	2.9807	0.17707	4.4557	0.23016
0.01	3.622	6.3492e-07	3.622	6.3492e-07	3.7327	0.030559	3.5501	0.019852	3.6958	0.020374
0.001	3.622	2.4113e-08	3.622	2.4113e-08	3.6331	0.0030441	3.6149	0.0019619	3.6295	0.0020606
0.0001	3.622	2.5651e-08	3.622	2.5651e-08	3.6234	0.00038474	3.6219	3.5223e-05	3.6234	0.00036712
1e-05	3.622	1.638e-08	3.622	1.638e-08	3.6246	0.00070921	3.6269	0.0013379	3.627	0.0013782
1e-06	3.622	1.6383e-08	3.622	1.6383e-08	3.5381	0.02316	3.4542	0.046328	3.4542	0.046324
1e-07	3.622	1.6382e-08	3.622	1.6382e-08	3.9699	0.096047	4.3178	0.19209	4.3178	0.19209
1e-08	3.622	3.6894e-08	3.622	3.6894e-08	1.811	0.5	0	1	0	1
1e-09	3.622	1.5653e-09	3.622	1.5653e-09	1.811	0.5	0	1	0	1
1e-10	3.622	3.3615e-08	3.622	3.3615e-08	1.811	0.5	0	1	0	1
1e-11	3.622	2.6478e-08	3.622	2.6478e-08	1.811	0.50001	0	1	0	1
1e-12	3.622	1.3959e-08	3.622	1.3959e-08	1.811	0.50001	0	1	0	1
1e-13	3.622	2.9608e-08	3.622	2.9608e-08	1.8119	0.49976	0	1	0	1
1e-14	3.622	4.8638e-08	3.622	4.8638e-08	1.8208	0.49731	0	1	0	1
1e-15	3.622	2.4186e-08	3.622	2.4186e-08	1.7764	0.50957	0	1	0	1
1e-16	3.622	6.3786e-09	3.622	6.3786e-09	0	1	0	1	0	1
1e-17	3.622	1.2724e-08	3.622	1.2724e-08	0	1	0	1	0	1
1e-18	3.622	1.2724e-08	3.622	1.2724e-08	0	1	0	1	0	1
1e-19	3.622	1.7124e-08	3.622	1.7124e-08	0	1	0	1	0	1
1e-20	3.622	3.5779e-08	3.622	3.5779e-08	0	1	0	1	0	1
1e-21	3.622	3.5779e-08	3.622	3.5779e-08	0	1	0	1	0	1
1e-22	3.622	3.5779e-08	3.622	3.5779e-08	0	1	0	1	0	1
1e-23	3.622	3.5779e-08	3.622	3.5779e-08	0	1	0	1	0	1
1e-24	3.622	1.3007e-08	3.622	1.3007e-08	0	1	0	1	0	1
1e-25	3.622	1.5459e-08	3.622	1.5459e-08	0	1	0	1	0	1

Table 4.3: First order derivatives validation : $f(x) = \frac{e^x}{\sin^3(x)+\cos^3(x)}, \quad x = 1.5, \quad f'(x) = 3.622.$

h	Eq. 4.23	ERROR	Eq. 4.24	ERROR	Eq. 4.25	ERROR	Eq. 4.26	ERROR	Eq. 4.27	ERROR
0.1	2.6653	0.26413	4.4557	0.23016	2.6653	0.26413	4.8586	0.34139	2.9807	0.17707
0.01	3.5142	0.029775	3.6958	0.020374	3.5142	0.029775	3.7327	0.030559	3.5501	0.019852
0.001	3.6112	0.0029895	3.6295	0.0020606	3.6112	0.0029895	3.6331	0.0030441	3.6149	0.0019619
0.0001	3.6212	0.00021871	3.6234	0.00036712	3.6212	0.00021871	3.6234	0.00038474	3.6219	3.5223e-05
1e-05	3.6244	0.00064877	3.627	0.0013782	3.6244	0.00064877	3.6246	0.00070921	3.6269	0.0013379
1e-06	3.5381	0.023166	3.4542	0.046324	3.5381	0.023166	3.5381	0.02316	3.4542	0.046328
1e-07	3.9699	0.096046	4.3178	0.19209	3.9699	0.096046	3.9699	0.096047	4.3178	0.19209
1e-08	1.811	0.5	0	1	1.811	0.5	1.811	0.5	0	1
1e-09	1.811	0.5	0	1	1.811	0.5	1.811	0.5	0	1
1e-10	1.811	0.5	0	1	1.811	0.5	1.811	0.5	0	1
1e-11	1.811	0.50001	0	1	1.811	0.5	1.811	0.5	0	1
1e-12	1.811	0.50001	0	1	1.811	0.5	1.811	0.5	0	1
1e-13	1.8119	0.49976	0	1	1.811	0.5	1.811	0.5	0	1
1e-14	1.8208	0.49731	0	1	1.811	0.5	1.811	0.5	0	1
1e-15	1.7764	0.50957	0	1	1.811	0.5	1.811	0.5	0	1
1e-16	0	1	0	1	1.811	0.5	1.811	0.5	0	1
1e-17	0	1	0	1	1.811	0.5	1.811	0.5	0	1
1e-18	0	1	0	1	1.811	0.5	1.811	0.5	0	1
1e-19	0	1	0	1	1.811	0.5	1.811	0.5	0	1
1e-20	0	1	0	1	1.811	0.5	1.811	0.5	0	1
1e-21	0	1	0	1	1.811	0.5	1.811	0.5	0	1
1e-22	0	1	0	1	1.811	0.5	1.811	0.5	0	1
1e-23	0	1	0	1	1.811	0.5	1.811	0.5	0	1
1e-24	0	1	0	1	1.811	0.5	1.811	0.5	0	1
1e-25	0	1	0	1	1.811	0.5	1.811	0.5	0	1

Table 4.4: First order derivatives validation : $f(x) = \frac{e^x}{\sin^3(x)+\cos^3(x)}, \quad x = 1.5, \quad f'(x) = 3.622.$

h	Eq. 4.28	ERROR	Eq. 4.29	ERROR	Eq. 4.30	ERROR	Eq. 4.31	ERROR	Eq. 4.32	ERROR
0.1	3.1888	0.11962	3.1888	0.11962	4.0931	0.13006	2.2844	0.36929	3.1888	0.11962
0.01	3.5953	0.007383	3.5953	0.007383	3.7191	0.026812	3.4714	0.041578	3.5953	0.007383
0.001	3.6207	0.00037869	3.6207	0.00037869	3.6342	0.0033481	3.6072	0.0041055	3.6207	0.00037869
0.0001	3.622	1.2671e-05	3.622	1.2671e-05	3.6234	0.00037533	3.6206	0.00040067	3.622	1.2671e-05
1e-05	3.6221	2.1946e-05	3.6221	2.1946e-05	3.6223	6.1545e-05	3.622	1.7653e-05	3.6221	2.1946e-05
1e-06	3.6207	0.00036481	3.6207	0.00036481	3.6207	0.000361	3.6207	0.00036862	3.6207	0.00036481
1e-07	3.6246	0.00070507	3.6246	0.00070507	3.6246	0.00070554	3.6246	0.00070459	3.6246	0.00070507
1e-08	3.6159	0.0017071	3.6159	0.0017071	3.6159	0.0017071	3.6159	0.0017071	3.6159	0.0017071
1e-09	3.6192	0.00079307	3.6192	0.00079307	3.6192	0.00079307	3.6192	0.00079307	3.6192	0.00079307
1e-10	3.6207	0.00036827	3.6207	0.00036827	3.6207	0.00036827	3.6207	0.00036827	3.6207	0.00036827
1e-11	3.6214	0.00017097	3.6214	0.00017097	3.6214	0.00017097	3.6214	0.00017097	3.6214	0.00017097
1e-12	3.6217	7.9363e-05	3.6217	7.9363e-05	3.6217	7.9363e-05	3.6217	7.9363e-05	3.6217	7.9364e-05
1e-13	3.6219	3.6845e-05	3.6219	3.6845e-05	3.6219	3.6845e-05	3.6219	3.6845e-05	3.6219	3.6839e-05
1e-14	3.622	1.7123e-05	3.622	1.7123e-05	3.622	1.7123e-05	3.622	1.7123e-05	3.622	1.7099e-05
1e-15	3.622	7.508e-06	3.622	7.508e-06	3.622	7.508e-06	3.622	7.508e-06	3.622	7.9369e-06
1e-16	3.622	5.8133e-06	3.622	5.8133e-06	3.622	5.8133e-06	3.622	5.8133e-06	3.622	3.684e-06
1e-17	3.622	4.4942e-06	3.622	4.4942e-06	3.622	4.4942e-06	3.622	4.4942e-06	3.622	1.71e-06
1e-18	3.622	4.2883e-06	3.622	4.2883e-06	3.622	4.2883e-06	3.622	4.2883e-06	3.622	7.937e-07
1e-19	3.6222	4.2699e-05	3.6222	4.2699e-05	3.6222	4.2699e-05	3.6222	4.2699e-05	3.622	3.684e-07
1e-20	3.6223	5.9974e-05	3.6223	5.9974e-05	3.6223	5.9974e-05	3.6223	5.9974e-05	3.622	1.71e-07
1e-21	3.6305	0.002332	3.6305	0.002332	3.6305	0.002332	3.6305	0.002332	3.622	7.937e-08
1e-22	3.5993	0.0062807	3.5993	0.0062807	3.5993	0.0062807	3.5993	0.0062807	3.622	3.684e-08
1e-23	3.7969	0.048281	3.7969	0.048281	3.7969	0.048281	3.7969	0.048281	3.622	1.71e-08
1e-24	3.5247	0.026862	3.5247	0.026862	3.5247	0.026862	3.5247	0.026862	3.622	7.937e-09
1e-25	0	1	0	1	0	1	0	1	3.622	3.684e-09

Table 4.5: First order derivatives validation : $f(x) = \frac{e^x}{\sin^3(x)+\cos^3(x)}, \quad x = 1.5, \quad f'(x) = 3.622.$

h	Eq. 4.33	ERROR	Eq. 4.34	ERROR
0.1	3.1148	0.14003	3.6234	0.00038916
0.01	3.5932	0.0079692	3.622	4.6438e-07
0.001	3.6206	0.00039493	3.6221	2.3374e-05
0.0001	3.622	1.5898e-05	3.6223	8.2979e-05
1e-05	3.6221	1.0623e-05	3.6245	0.00067899
1e-06	3.6214	0.00018315	3.5381	0.023163
1e-07	3.6233	0.00035318	3.9699	0.096046
1e-08	3.6189	0.00085426	1.811	0.5
1e-09	3.6206	0.00039669	1.811	0.5
1e-10	3.6214	0.00018417	1.811	0.5
1e-11	3.6217	8.5492e-05	1.811	0.5
1e-12	3.6219	3.9683e-05	1.811	0.50001
1e-13	3.622	1.8426e-05	1.8119	0.49976
1e-14	3.622	8.5729e-06	1.8208	0.49731
1e-15	3.622	4.0261e-06	1.7764	0.50957
1e-16	3.622	1.7128e-06	2.2204	0.38696
1e-17	3.622	3.6392e-06	0	1
1e-18	3.622	3.8914e-06	0	1
1e-19	3.6222	4.2884e-05	0	1
1e-20	3.6223	6.006e-05	0	1
1e-21	3.6305	0.0023321	0	1
1e-22	3.5993	0.0062807	0	1
1e-23	3.7969	0.048281	0	1
1e-24	3.5247	0.026862	0	1
1e-25	0	1	0	1

Table 4.6: First order derivatives validation : $f(x) = \frac{e^x}{\sin^3(x)+\cos^3(x)}, \quad x = 1.5, \quad f'(x) = 3.622.$

h	Eq. 3.6	ERROR	Eq. 4.35	ERROR	Eq. 4.36	ERROR	Eq. 4.37	ERROR	Eq. 4.38	ERROR
0.1	14.75	0.012476	14.5571	0.00076655	14.5571	0.00076655	14.5571	0.00076655	14.5571	0.00076655
0.01	14.57	0.00012088	14.5683	1.083e-06	14.5683	1.083e-06	14.5683	1.083e-06	14.5683	1.083e-06
0.001	14.5697	9.4661e-05	14.569	4.6748e-05	14.569	4.6748e-05	14.569	4.6748e-05	14.569	4.6748e-05
0.0001	14.5731	0.0003319	14.5707	0.00016596	14.5707	0.00016596	14.5707	0.00016596	14.5707	0.00016596
1e-05	14.6079	0.0027185	14.5881	0.001358	14.5881	0.001358	14.5881	0.001358	14.5881	0.001358
1e-06	13.2498	0.090501	13.8934	0.046326	13.8934	0.046326	13.8934	0.046326	13.8934	0.046326
1e-07	20.8722	0.43271	17.3667	0.19209	17.3667	0.19209	17.3667	0.19209	17.3667	0.19209
1e-08	0	1	0	1	0	1	0	1	0	1
:	:	:	:	:	:	:	:	:	:	:
1e-25	0	1	0	1	0	1	0	1	0	1

Table 4.7: Second order derivatives validation : $f(x) = \frac{e^x}{\sin^3(x)+\cos^3(x)}, \quad x = 1.5, \quad f''(x) = 14.5683$.

h	Eq. 4.39	ERROR	Eq. 4.40	ERROR	Eq. 4.41	ERROR
0.1	14.5571	0.00076655	16.1149	0.10616	15.205	0.043704
0.01	14.5683	1.083e-06	14.7565	0.012918	14.6322	0.0043865
0.001	14.569	4.6748e-05	14.249	0.021913	14.4628	0.0072414
0.0001	14.5707	0.00016596	2.5529	0.82477	10.5664	0.2747
1e-05	14.5881	0.001358	-969.2175	67.5293	-313.3339	22.5079
1e-06	13.8934	0.046326	335600.8846	23035.4042	111875.7948	7678.4077
1e-07	17.3667	0.19209	-13915323.5895	955180.3014	-4638427.2817	318393.1453
1e-08	0	1	724406717.4498	49724915.408	241468905.8166	16574971.136
1e-09	0	1	7244066463.9557	497249114.3072	2414688821.3186	165749704.1024
1e-10	0	1	72440717930.2603	4972494810.0663	24146905976.7534	1657498269.3554
1e-11	0	1	724398297518.6703	49724338443.9144	241466099172.8901	16574779480.6381
1e-12	0	1	7243982975186.702	497243384448.1436	2414660991728.901	165747794815.3812
1e-13	0	1	72475356887596.23	4974872507484.301	24158452295865.41	1658290835827.434
1e-14	0	1	728306282448883.6	49992591374238.53	242768760816294.6	16664197124745.51
1e-15	0	1	7105427145842768	487732598773067.7	2368475715280922	162577532924355.2
1e-16	0	1	0	1	0	1
:	:	:	:	:	:	:
1e-25	0	1	0	1	0	1

Table 4.8: Second order derivatives validation : $f(x) = \frac{e^x}{\sin^3(x)+\cos^3(x)}, \quad x = 1.5, \quad f''(x) = 14.5683$.

h	Eq. 4.42	ERROR	Eq. 4.43	ERROR	Eq. 4.44	ERROR
0.1	14.0379	0.036409	12.6135	0.13418	14.0379	0.036409
0.01	14.5055	0.0043074	14.3765	0.013164	14.5055	0.0043074
0.001	14.6756	0.0073668	14.8875	0.021911	14.6756	0.0073668
0.0001	18.5766	0.27514	26.5837	0.82477	18.5766	0.27514
1e-05	342.5233	22.5116	998.354	67.5293	342.5233	22.5116
1e-06	-111848.4365	7678.5298	-335571.8092	23035.4084	-111848.4365	7678.5298
1e-07	4638464.3483	318393.6897	13915351.3006	955180.2035	4638464.3483	318393.6897
1e-08	-241468905.8166	16574973.136	-724406717.4498	49724917.408	-241468905.8166	16574973.136
1e-09	-2414688821.3186	165749706.1024	-7244066463.9557	497249116.3072	-2414688821.3186	165749706.1024
1e-10	-24146905976.7534	1657498271.3554	-72440717930.2603	4972494812.0663	-24146905976.7534	1657498271.3554
1e-11	-241466099172.8901	16574779482.6381	-724398297518.6703	49724338445.9144	-241466099172.8901	16574779482.6381
1e-12	-2414660991728.901	165747794817.3812	-7243982975186.702	497243384450.1436	-2414660991728.901	165747794817.3812
1e-13	-24158452295865.41	1658290835829.433	-72475356887596.23	4974872507486.301	-24158452295865.41	1658290835829.433
1e-14	-242768760816294.6	16664197124747.51	-728306282448883.6	49992591374240.54	-242768760816294.6	16664197124747.51
1e-15	-2368475715280922	162577532924357.2	-7105427145842768	487732598773069.8	-2368475715280922	162577532924357.2
1e-16	0	1	0	1	0	1
:	:	:	:	:	:	:
1e-25	0	1	0	1	0	1

Table 4.9: Second order derivatives validation : $f(x) = \frac{e^x}{\sin^3(x)+\cos^3(x)}, \quad x = 1.5, \quad f''(x) = 14.5683$.

h	Eq. 4.45	ERROR	Eq. 4.46	ERROR	Eq. 4.47	ERROR
0.1	12.6135	0.13418	16.1149	0.10616	15.205	0.043704
0.01	14.3765	0.013164	14.7565	0.012918	14.6322	0.0043865
0.001	14.8875	0.021911	14.249	0.021913	14.4628	0.0072414
0.0001	26.5837	0.82477	2.5529	0.82477	10.5664	0.2747
1e-05	998.354	67.5293	-969.2175	67.5293	-313.3339	22.5079
1e-06	-335571.8092	23035.4084	335600.8846	23035.4042	111875.7948	7678.4077
1e-07	13915351.3006	955180.2035	-13915323.5895	955180.3014	-4638427.2817	318393.1453
1e-08	-724406717.4498	49724917.408	724406717.4498	49724915.408	241468905.8166	16574971.136
1e-09	-7244066463.9557	497249116.3072	7244066463.9557	497249114.3072	2414688821.3186	165749704.1024
1e-10	-72440717930.2603	4972494812.0663	72440717930.2603	4972494810.0663	24146905976.7534	1657498269.3554
1e-11	-724398297518.6703	49724338445.9144	724398297518.6703	49724338443.9144	241466099172.8901	16574779480.6381
1e-12	-7243982975186.702	497243384450.1436	7243982975186.702	497243384448.1436	2414660991728.901	165747794815.3812
1e-13	-72475356887596.23	4974872507486.301	72475356887596.23	4974872507484.301	24158452295865.41	1658290835827.434
1e-14	-728306282448883.6	49992591374240.54	728306282448883.6	49992591374238.53	242768760816294.6	16664197124745.51
1e-15	-7105427145842768	487732598773069.8	7105427145842768	487732598773067.7	2368475715280922	162577532924355.2
1e-16	0	1	0	1	0	1
:	:	:	:	:	:	:
1e-25	0	1	0	1	0	1

Table 4.10: Second order derivatives validation : $f(x) = \frac{e^x}{\sin^3(x)+\cos^3(x)}, \quad x = 1.5, \quad f''(x) = 14.5683.$

h	Eq. 4.48	ERROR	Eq. 4.49	ERROR	Eq. 4.50	ERROR	Eq. 4.51	ERROR
0.1	14.5602	0.0005573	14.5602	0.0005573	14.5602	0.0005573	14.5252	0.0029581
0.01	14.5683	1.3272e-06	14.5683	1.3272e-06	14.5683	1.3272e-06	14.5679	2.3839e-05
0.001	14.5692	6.1249e-05	14.5692	6.1249e-05	14.5692	6.1249e-05	14.5691	5.5095e-05
0.0001	14.5715	0.00021756	14.5715	0.00021756	14.5715	0.00021756	14.5711	0.00019649
1e-05	14.5942	0.0017811	14.5942	0.0017811	14.5942	0.0017811	14.5917	0.0016086
1e-06	13.6933	0.060063	13.6933	0.060063	13.6933	0.060063	13.7746	0.054478
1e-07	18.4581	0.26701	18.4581	0.26701	18.4581	0.26701	17.9971	0.23536
1e-08	0	1	0	1	0	1	0	1
:	:	:	:	:	:	:	:	:
1e-25	0	1	0	1	0	1	0	1

Table 4.11: Second order derivatives validation : $f(x) = \frac{e^x}{\sin^3(x)+\cos^3(x)}, \quad x = 1.5, \quad f''(x) = 14.5683.$

h	Eq. 3.3	ERROR	Eq. 4.52	ERROR	Eq. 4.53	ERROR	Eq. 4.54	ERROR	Eq. 4.55	ERROR
0.1	4.4557	0.23016	3.3913	0.063692	3.4628	0.043954	3.4628	0.043954	3.3913	0.063692
0.01	3.6958	0.020374	3.6201	0.00053409	3.6202	0.00051425	3.6202	0.00051425	3.6201	0.00053409
0.001	3.6295	0.0020606	3.6222	4.1663e-05	3.6222	4.1307e-05	3.6222	4.1307e-05	3.6222	4.1663e-05
0.0001	3.6234	0.00036712	3.6226	0.00016594	3.6226	0.00016581	3.6226	0.00016581	3.6226	0.00016594
1e-05	3.627	0.0013782	3.627	0.0013581	3.627	0.001358	3.627	0.001358	3.627	0.0013581
1e-06	3.4542	0.046324	3.4542	0.046326	3.4542	0.046326	3.4542	0.046326	3.4542	0.046326
1e-07	4.3178	0.19209	4.3178	0.19209	4.3178	0.19209	4.3178	0.19209	4.3178	0.19209
1e-08	0	1	0	1	0	1	0	1	0	1
:	:	:	:	:	:	:	:	:	:	:
1e-25	0	1	0	1	0	1	0	1	0	1

Table 4.12: First order derivatives validation : $f(x) = \frac{e^x}{\sin^3(x)+\cos^3(x)}, \quad x = 1.5, \quad f'(x) = 3.622.$

h	Eq. 4.56	ERROR	Eq. 4.57	ERROR	Eq. 4.58	ERROR	Eq. 4.59	ERROR	Eq. 4.60	ERROR
0.1	3.5984	0.0065157	3.5984	0.0065157	3.5984	0.0065157	3.5984	0.0065157	3.5984	0.0065157
0.01	3.622	2.9289e-07	3.622	2.9289e-07	3.622	2.9289e-07	3.622	2.9289e-07	3.622	2.9289e-07
0.001	3.6219	3.4084e-05	3.6219	3.4084e-05	3.6219	3.4084e-05	3.6219	3.4084e-05	3.6219	3.4084e-05
0.0001	3.6222	3.4742e-05	3.6222	3.4742e-05	3.6222	3.4742e-05	3.6222	3.4742e-05	3.6222	3.4742e-05
1e-05	3.6147	0.00203	3.6147	0.00203	3.6147	0.00203	3.6147	0.00203	3.6147	0.00203
1e-06	3.7393	0.032383	3.7393	0.032383	3.7393	0.032383	3.7393	0.032383	3.7393	0.032383
1e-07	2.4929	0.31174	2.4929	0.31174	2.4929	0.31174	2.4929	0.31174	2.4929	0.31174
1e-08	0	1	0	1	0	1	0	1	0	1
:	:	:	:	:	:	:	:	:	:	:
1e-25	0	1	0	1	0	1	0	1	0	1

Table 4.13: First order derivatives validation : $f(x) = \frac{e^x}{\sin^3(x)+\cos^3(x)}, \quad x = 1.5, \quad f'(x) = 3.622.$

h	Eq. 4.61	ERROR	Eq. 4.62	ERROR	Eq. 4.63	ERROR	Eq. 4.64	ERROR	Eq. 4.65	ERROR
0.1	3.3913	0.063692	3.4628	0.043954	3.9235	0.083235	3.186	0.12038	3.9593	0.093104
0.01	3.6201	0.00053409	3.6202	0.00051425	3.658	0.0099198	3.5851	0.010193	3.658	0.0099297
0.001	3.6222	4.1663e-05	3.6222	4.1307e-05	3.6258	0.0010511	3.6186	0.00096013	3.6258	0.0010509
0.0001	3.6226	0.00016594	3.6226	0.00016581	3.623	0.00026653	3.6223	6.5358e-05	3.623	0.00026646
1e-05	3.627	0.0013581	3.627	0.001358	3.627	0.0013681	3.6269	0.001348	3.627	0.0013681
1e-06	3.4542	0.046326	3.4542	0.046326	3.4542	0.046325	3.4542	0.046327	3.4542	0.046325
1e-07	4.3178	0.19209	4.3178	0.19209	4.3178	0.19209	4.3178	0.19209	4.3178	0.19209
1e-08	0	1	0	1	0	1	0	1	0	1
:	:	:	:	:	:	:	:	:	:	:
1e-25	0	1	0	1	0	1	0	1	0	1

Table 4.14: First order derivatives validation : $f(x) = \frac{e^x}{\sin^3(x)+\cos^3(x)}, \quad x = 1.5, \quad f'(x) = 3.622.$

h	Eq. 4.66	ERROR	Eq. 4.67	ERROR	Eq. 4.68	ERROR	Eq. 4.69	ERROR	Eq. 4.70	ERROR
0.1	3.2218	0.11051	3.9593	0.093104	3.2218	0.11051	3.9235	0.083235	3.186	0.12038
0.01	3.5851	0.010183	3.658	0.0099297	3.5851	0.010183	3.658	0.0099198	3.5851	0.010193
0.001	3.6186	0.00096031	3.6258	0.0010509	3.6186	0.00096031	3.6258	0.0010511	3.6186	0.00096013
0.0001	3.6223	6.5291e-05	3.623	0.00026646	3.6223	6.5291e-05	3.623	0.00026653	3.6223	6.5358e-05
1e-05	3.6269	0.0013479	3.627	0.0013681	3.6269	0.0013479	3.627	0.0013681	3.6269	0.001348
1e-06	3.4542	0.046327	3.4542	0.046325	3.4542	0.046327	3.4542	0.046325	3.4542	0.046327
1e-07	4.3178	0.19209	4.3178	0.19209	4.3178	0.19209	4.3178	0.19209	4.3178	0.19209
1e-08	0	1	0	1	0	1	0	1	0	1
:	:	:	:	:	:	:	:	:	:	:
1e-25	0	1	0	1	0	1	0	1	0	1

Table 4.15: First order derivatives validation : $f(x) = \frac{e^x}{\sin^3(x)+\cos^3(x)}, \quad x = 1.5, \quad f'(x) = 3.622.$

h	Eq. 4.71	ERROR	Eq. 4.72	ERROR	Eq. 4.73	ERROR	Eq. 4.74	ERROR	Eq. 4.75	ERROR
0.1	3.5726	0.013638	3.5726	0.013638	3.5726	0.013638	3.5726	0.013638	3.6135	0.0023583
0.01	3.6216	0.00013179	3.6216	0.00013179	3.6216	0.00013179	3.6216	0.00013179	3.622	1.1862e-06
0.001	3.6222	4.5408e-05	3.6222	4.5408e-05	3.6222	4.5408e-05	3.6222	4.5408e-05	3.6219	2.387e-05
0.0001	3.6226	0.00016591	3.6226	0.00016591	3.6226	0.00016591	3.6226	0.00016591	3.621	0.00027675
1e-05	3.627	0.001358	3.627	0.001358	3.627	0.001358	3.627	0.001358	3.6332	0.003095
1e-06	3.4542	0.046326	3.4542	0.046326	3.4542	0.046326	3.4542	0.046326	3.6638	0.011524
1e-07	4.3178	0.19209	4.3178	0.19209	4.3178	0.19209	4.3178	0.19209	3.0531	0.15706
1e-08	0	1	0	1	0	1	0	1	0	1
:	:	:	:	:	:	:	:	:	:	:
1e-25	0	1	0	1	0	1	0	1	0	1

Table 4.16: First order derivatives validation : $f(x) = \frac{e^x}{\sin^3(x)+\cos^3(x)}, \quad x = 1.5, \quad f'(x) = 3.622.$

h	Eq. 4.76	ERROR	Eq. 4.77	ERROR
0.1	3.5548	0.018573	3.5905	0.0087038
0.01	3.6215	0.00013675	3.6216	0.00012683
0.001	3.6222	4.5497e-05	3.6222	4.5319e-05
0.0001	3.6226	0.00016594	3.6226	0.00016588
1e-05	3.627	0.001358	3.627	0.001358
1e-06	3.4542	0.046326	3.4542	0.046326
1e-07	4.3178	0.19209	4.3178	0.19209
1e-08	0	1	0	1
:	:	:	:	:
1e-25	0	1	0	1

Table 4.17: First order derivatives validation : $f(x) = \frac{e^x}{\sin^3(x)+\cos^3(x)}, \quad x = 1.5, \quad f'(x) = 3.622.$

h	Eq. 4.78	ERROR	Eq. 4.79	ERROR	Eq. 4.80	ERROR	Eq. 4.81	ERROR	Eq. 4.82	ERROR
0.1	14.6682	0.0068618	14.6682	0.0068618	14.6682	0.0068618	14.6682	0.0068618	14.6682	0.0068618
0.01	14.571	0.00018444	14.571	0.00018444	14.571	0.00018444	14.571	0.00018444	14.571	0.00018444
0.001	14.5682	6.6845e-06	14.5682	6.6845e-06	14.5682	6.6845e-06	14.5682	6.6845e-06	14.5682	6.6845e-06
0.0001	14.5651	0.00021571	14.5651	0.00021571	14.5651	0.00021571	14.5651	0.00021571	14.5651	0.00021571
1e-05	14.5349	0.0022889	14.5349	0.0022889	14.5349	0.0022889	14.5349	0.0022889	14.5349	0.0022889
1e-06	13.9362	0.043387	13.9362	0.043387	13.9362	0.043387	13.9362	0.043387	13.9362	0.043387
1e-07	11.1013	0.23798	11.1013	0.23798	11.1013	0.23798	11.1013	0.23798	11.1013	0.23798
1e-08	0	1	0	1	0	1	0	1	0	1
:	:	:	:	:	:	:	:	:	:	:
1e-25	0	1	0	1	0	1	0	1	0	1

Table 4.18: Second order derivatives validation : $f(x) = \frac{e^x}{\sin^3(x)+\cos^3(x)}, \quad x = 1.5, \quad f''(x) = 14.5683$.

h	Eq. 4.83	ERROR	Eq. 4.84	ERROR	Eq. 4.85	ERROR	Eq. 4.86	ERROR	Eq. 4.87	ERROR
0.1	21.2869	0.46118	8.2131	0.43623	19.8571	0.36304	9.643	0.33809	19.8571	0.36304
0.01	15.1457	0.039636	13.9944	0.039394	15.1313	0.03865	14.0087	0.038408	15.1313	0.03865
0.001	14.6252	0.0039077	14.5141	0.0037183	14.6278	0.0040846	14.5115	0.0038953	14.6278	0.0040846
0.0001	14.574	0.00039031	14.5723	0.00027347	14.5836	0.0010539	14.5626	0.00039008	14.5836	0.0010539
1e-05	14.5688	3.8385e-05	14.6469	0.0053973	14.6481	0.0054754	14.5677	3.8433e-05	14.6481	0.0054754
1e-06	14.5697	9.5694e-05	11.93	0.1811	11.93	0.1811	14.5715	0.00021763	11.93	0.1811
1e-07	14.7438	0.012045	27.0006	0.85338	27.0006	0.85338	14.9214	0.024238	27.0006	0.85338
1e-08	0	1	0	1	0	1	0	1	0	1
:	:	:	:	:	:	:	:	:	:	:
1e-25	0	1	0	1	0	1	0	1	0	1

Table 4.19: Second order derivatives validation : $f(x) = \frac{e^x}{\sin^3(x)+\cos^3(x)}, \quad x = 1.5, \quad f''(x) = 14.5683$.

h	Eq. 4.88	ERROR	Eq. 4.89	ERROR	Eq. 4.90	ERROR	Eq. 4.91	ERROR	Eq. 4.92	ERROR
0.1	9.643	0.33809	21.2869	0.46118	8.2131	0.43623	14.3921	0.012091	14.3921	0.012091
0.01	14.0087	0.038408	15.1457	0.039636	13.9944	0.039394	14.5665	0.00012286	14.5665	0.00012286
0.001	14.5115	0.0038953	14.6252	0.0039077	14.5141	0.0037183	14.5683	1.1627e-06	14.5683	1.1627e-06
0.0001	14.5626	0.00039008	14.574	0.00039031	14.5723	0.00027347	14.5683	3.7228e-08	14.5683	3.7228e-08
1e-05	14.5677	3.8433e-05	14.5688	3.8385e-05	14.6469	0.0053973	14.5683	1.8053e-06	14.5683	1.8053e-06
1e-06	14.5715	0.00021763	14.5697	9.5694e-05	11.93	0.1811	14.5697	9.5694e-05	14.5697	9.5694e-05
1e-07	14.9214	0.024238	14.7438	0.012045	27.0006	0.85338	14.9214	0.024238	14.9214	0.024238
1e-08	0	1	0	1	0	1	0	1	0	1
:	:	:	:	:	:	:	:	:	:	:
1e-25	0	1	0	1	0	1	0	1	0	1

Table 4.20: Second order derivatives validation : $f(x) = \frac{e^x}{\sin^3(x)+\cos^3(x)}, \quad x = 1.5, \quad f''(x) = 14.5683$.

h	Eq. 4.93	ERROR	Eq. 4.94	ERROR	Eq. 4.95	ERROR	Eq. 4.96	ERROR	Eq. 4.97	ERROR
0.1	14.3921	0.012091	14.3921	0.012091	14.3921	0.012091	-15.8045	2.0849	-15.8045	2.0849
0.01	14.5665	0.00012286	14.5665	0.00012286	14.5665	0.00012286	14.6081	0.0027324	14.6081	0.0027324
0.001	14.5683	1.1627e-06	14.5683	1.1627e-06	14.5683	1.1628e-06	14.5685	1.6162e-05	14.5685	1.6162e-05
0.0001	14.5683	3.7228e-08	14.5683	3.7228e-08	14.5683	3.1132e-08	14.5688	3.8029e-05	14.5688	3.8029e-05
1e-05	14.5683	1.8053e-06	14.5683	1.8053e-06	14.5683	1.1956e-06	14.5617	0.00045142	14.5617	0.00045142
1e-06	14.5697	9.5694e-05	14.5697	9.5694e-05	14.5697	9.5694e-05	14.7763	0.01428	14.7763	0.01428
1e-07	14.9214	0.024238	14.9214	0.024238	14.9214	0.024238	13.3766	0.081803	13.3766	0.081803
1e-08	0	1	0	1	0	1	0	1	0	1
:	:	:	:	:	:	:	:	:	:	:
1e-25	0	1	0	1	0	1	0	1	0	1

Table 4.21: Second order derivatives validation : $f(x) = \frac{e^x}{\sin^3(x)+\cos^3(x)}, \quad x = 1.5, \quad f''(x) = 14.5683$.

h	Eq. 4.98	ERROR	Eq. 4.99	ERROR	Eq. 4.100	ERROR
0.1	-15.8045	2.0849	-15.8045	2.0849	-12.0536	1.8274
0.01	14.6081	0.0027324	14.6081	0.0027324	14.7732	0.014067
0.001	14.5685	1.6162e-05	14.5685	1.6162e-05	14.5702	0.00012924
0.0001	14.5688	3.8029e-05	14.5688	3.8029e-05	14.5672	7.452e-05
1e-05	14.5617	0.00045142	14.5617	0.00045142	14.5607	0.0005212
1e-06	14.7763	0.01428	14.7763	0.01428	14.4635	0.0071902
1e-07	13.3766	0.081803	13.3766	0.081803	14.4642	0.0071443
1e-08	0	1	0	1	18.1843	0.24821
1e-09	0	1	0	1	10.2736	0.2948
1e-10	0	1	0	1	1027.36	69.5203
1e-11	0	1	0	1	102736.0013	7051.0316
1e-12	0	1	0	1	10273600.7974	705202.2077
1e-13	0	1	0	1	1027360121.3562	70520322.6315
1e-14	0	1	0	1	102736009534.4629	7052032183.6007
1e-15	0	1	0	1	10273600628301.27	705203196140.3755
1e-16	0	1	0	1	1027360103473255	70520322403972.8
1e-17	0	1	0	1	102736005266934576	7052031891667850
1e-18	0	1	0	1	10273601161742327808	705203232757976704
1e-19	0	1	0	1	1027359957412026384384	70520312378000539648
1e-20	0	1	0	1	10273600814449968755072	705203208919043171942 4
1e-21	0	1	0	1	1027360019428508752360 2432	705203166349522364268544
1e-22	0	1	0	1	1027359941907906443532566528	705203113137626657283112 96
1e-23	0	1	0	1	1027360135709428856366647 21408	705203246167377282572956 4672
1e-24	0	1	0	1	1027360044864958275791221 2668416	705203183809676878772613 152768
1e-25	0	1	0	1	1027359969161242251367171 137470464	705203131844933031941797 91224832

Table 4.22: Second order derivatives validation : $f(x) = \frac{e^x}{\sin^3(x)+\cos^3(x)}, \quad x = 1.5, \quad f''(x) = 14.5683.$

h	Eq. 4.101	ERROR	Eq. 4.102	ERROR	Eq. 4.103	ERROR
0.1	15.6447	0.073888	14.5711	0.00019212	14.5703	0.00013494
0.01	14.5784	0.00069372	14.5683	9.8687e-07	14.5684	8.1679e-06
0.001	14.5679	2.7435e-05	14.569	4.6749e-05	14.5684	8.2108e-06
0.0001	14.5747	0.00044255	14.5707	0.00016597	14.5587	0.00065595
1e-05	14.6211	0.0036236	14.5881	0.0013601	14.6801	0.0076742
1e-06	15.0872	0.035619	13.9098	0.045202	14.4406	0.0087621
1e-07	22.7374	0.56074	17.9412	0.23152	23.5453	0.6162
1e-08	0	1	0	1	0	1
:	:	:	:	:	:	:
1e-25	0	1	0	1	0	1

Table 4.23: Second order derivatives validation : $f(x) = \frac{e^x}{\sin^3(x)+\cos^3(x)}, \quad x = 1.5, \quad f''(x) = 14.5683.$

4.5 Discussion

As expected from the different structure and formal accuracy of different CS approximations, the corresponding numerical simulations for our test function show very different behaviors. Following, we summarize and compare the Tables derived in the previous section. We divide the discussion into first order and second order derivatives on the one hand, and approximations based on the imaginary or real part of the function on the other hand.

Numerical approximations for the first derivative based on the imaginary part of the function (Eqs. 4.9 - 4.34) and the classic first order forward FD approximation are shown in Tables 4.1 - 4.6. The forward FD approximation and the equations which use one real step only (Eqs. 4.20 - 4.27) eventually collapse due to term cancellation. A different behavior can be seen for the group of ten equations 4.9 to 4.19, which do not collapse. For the group of equations 4.28 to 4.33, where numerical accuracy decreases for step sizes ($h < 1e^{-18}$) and full collapse occurs finally at ($h = 1e^{-25}$) (except Eq. 4.32), we have to recall that this instability in detail depends on the format of the variable and the particular compiler and compiler options, meaning that the collapse may be pushed to smaller values of h, and meaning that we can chose a conservatively large but still very small step size to perform stable and accurate simulations using

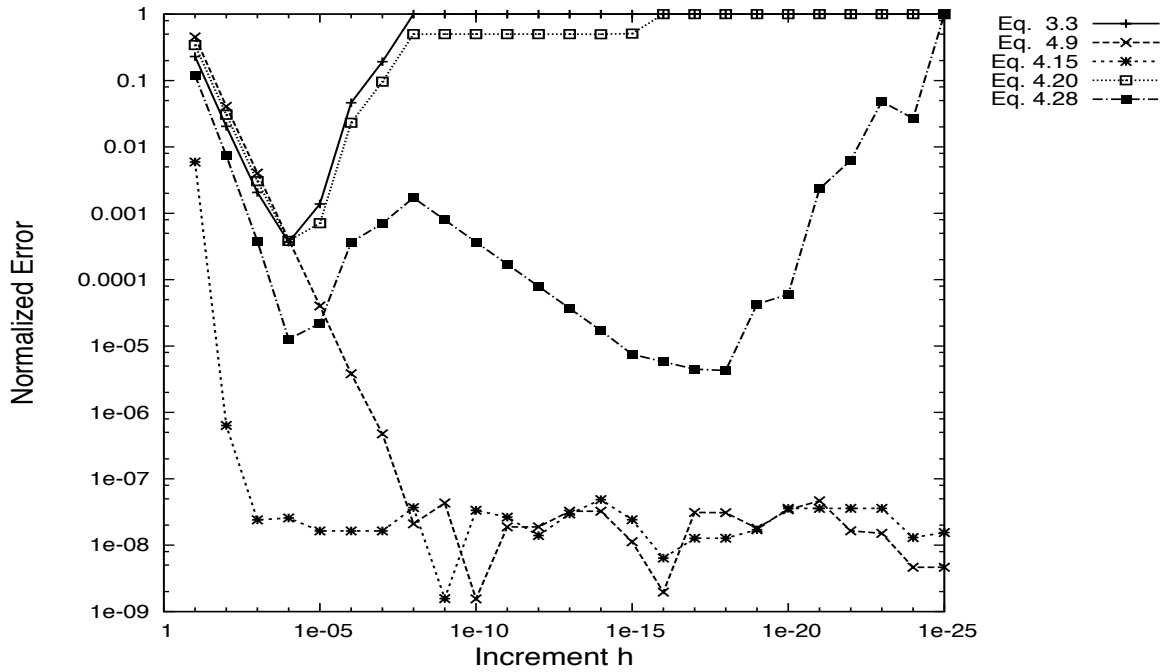

Figure 4.1: Comparison of stability, accuracy and convergence for an ordinary first order forward FD approximation and representative first order CS derivatives using the imaginary part (corresponding equations in legend).

these approximations. For the different first derivatives based on the imaginary part, we can further appreciate that the accuracy of different numerical simulations is consistent with the formal accuracy of the corresponding approximations. For the groups of equations 4.9 - 4.19 and 4.28 - 4.33 with the same order of accuracy (using a smart choice of $h - v$ for the second group), convergence is faster in the first group.

Tables 4.12 - 4.17 show numerical validations for the first order derivative using the real part (Eqs. 4.52 - 4.77). Although we can reach fourth order accuracy in this group, all the real part based approximations collapse. This indicates a clear preference for imaginary part based approximations for the first derivative.

Figure 4.1 summarizes stability, accuracy and convergence for representative imaginary part based first order derivative approximations. Therefore, we classify non cancelling approximations into three groups considering their degree of accuracy: the first one related to equations 4.9 - 4.14 (with error of $\mathcal{O}(h, v^2)$), the second one related to equations 4.15 - 4.19 (with error of $\mathcal{O}(3h^2 - v^2)$) and the third one related to Eqs. 4.20 - 4.27 (with error of $\mathcal{O}((h^2/2 + hv)/(h + v))$). A further group is related to collapsing approximations. This group is plotted for comparison, and not further subdivided because of a lack of relevance compared to non cancelling approximations; however we have shown previously that group of equations 4.28 - 4.33 still may be suitable for accurate numerical schemes. The first equation of each group is shown in Figure 4.1. One interesting feature is that the group of equations 4.15 - 4.19 and Eqs. 4.28 - 4.33 have the same order of accuracy (fourth) but not the same rate of convergence, being convergence faster in Eqs. 4.15 - 4.19. The classical first order forward FD approximation is given for comparison in Figure 4.1, showing the better performance of generalized CS schemes, and a very clear superiority of those particular approximations that avoid term cancellation.

Second order derivative validations using the imaginary part and the centered FD approximation correspond to Tables 4.7 - 4.11. All of the approximations collapse at some point,

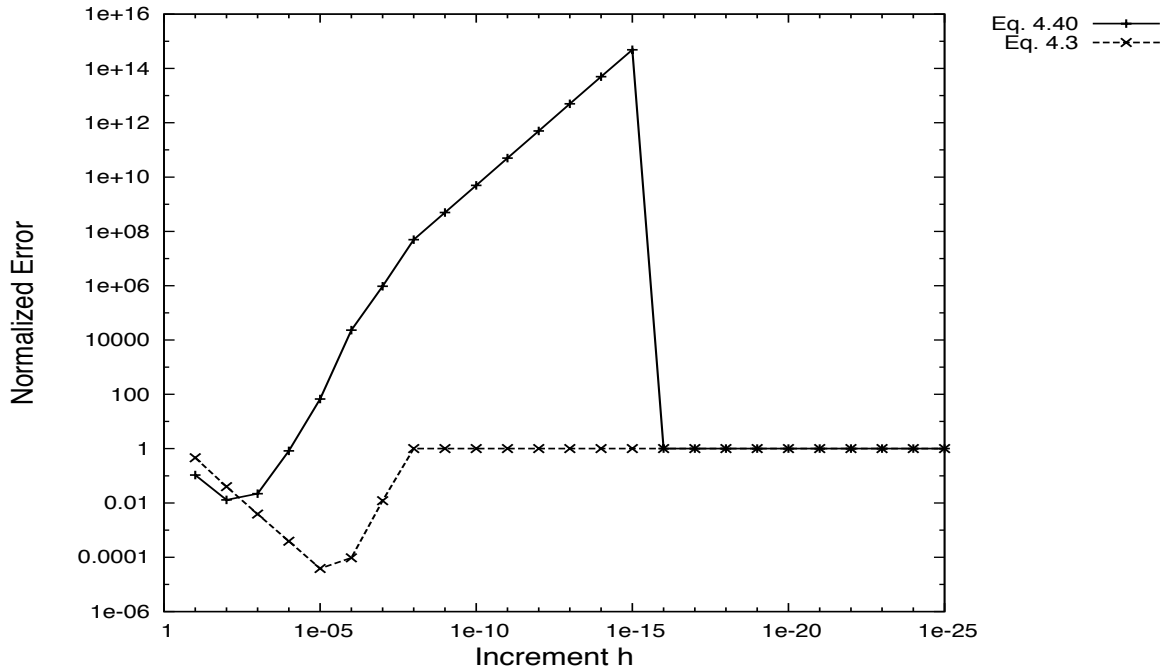

Figure 4.2: Comparison of stability, accuracy and convergence for the one step approximation for the second order derivative using the real and the imaginary part (corresponding equations in legend).

different from the non cancelling first order derivative approximations. All approximations reach the minimum error at $h = 1e^{-2}$. This behavior may appear surprising because many approximations like 4.36 do not contain negative terms and should avoid subtractive cancellation at first sight. However, they collapse because we are adding terms with different signs, i.e., the imaginary steps are opposite in signs in all of the second order approximations unlike in the first order approximations. The same sign in the imaginary step for the terms of the numerator guaranties non cancelling schemes for the first order derivative, but not for the second order. Despite serious instabilities, equations 4.40, 4.43, 4.45 and 4.46 have the advantage to compute second order derivatives in a single real step, in other words, they use the minimum amount of information of the analytic function for computing second derivatives, which can not be achieved with any ordinary FD approximation. The group of equations 4.35 to 4.39 and 4.48 to 4.51, despite having different error expressions, have the same order of accuracy for appropriate choice of real and imaginary step sizes (h and v) and show very similar results. The group of equations 4.40 - 4.47 shows drastic numerical instabilities. These instabilities are easily explained due to the cancellation between the terms $f(x \pm h)$ and $f(x)$ at some point. When these terms cancel, the only remaining term in the numerator of the expressions is $\mathfrak{Im}(f(x \pm h \pm \mathbf{i}v))$ which is proportional to h and not to h^2, so when $h \to 0 \Rightarrow \mathfrak{Im}(f(x \pm h \pm \mathbf{i}v))/h^2 \to \infty$.

Tables 4.18 - 4.23 show numerical validations for the second order derivative using the real part (Eqs. 4.78 - 4.103). All the approximations collapse at some point just like the imaginary part based approximations. However, the one step approximations given by the equations 4.83, 4.86, 4.88 and 4.89 show much higher stability compared to the imaginary part based one step, and achieve small relative errors of power $1e^{-5}$, which can be appreciated in Figure 4.2. Eq. 4.100 shows particularly unstable results. This instability can be easily explained by the remaining term $2f(x)$ which is proportional to h or v but not $3h^2 - 2v^2$, so when: $h, v \to 0 \Rightarrow f(x)/(3h^2 - 2v^2) \to \infty$, which produces the numerical instability similar

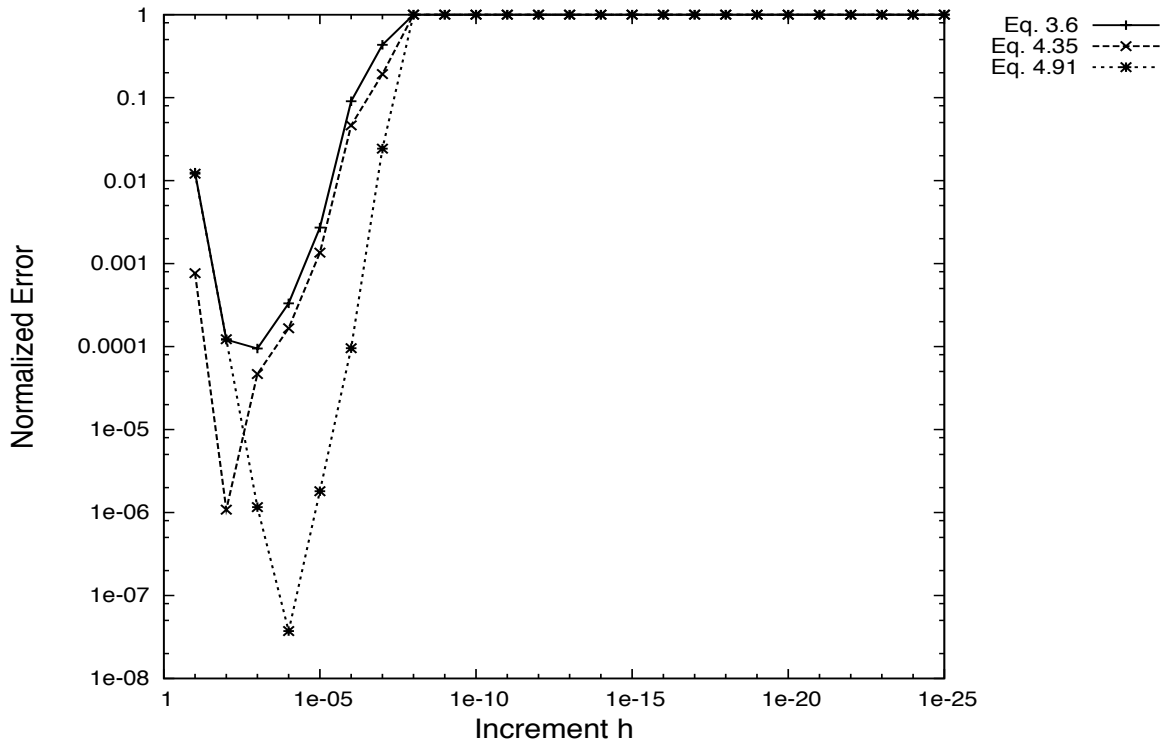

Figure 4.3: Comparison of stability, accuracy and convergence for an ordinary second order centered FD approximation and representative second order CS derivative using the real and the imaginary part (corresponding equations in legend).

to the case explained before. Summarizing, while the imaginary part based approximations are more stable for first order derivatives because they do not collapse, the real part based approximations are more stable for second order derivatives, which can be appreciated in Figure 4.3.

Chapter 5

The Complex Step Finite Differences Method Applied to the Acoustic Wave Equation

5.1 Introduction

In this Chapter we extend the concept of the Finite Differences method (FDM) for solving differential equations by using the generalization of the Complex Step (CS) method introduced in Chapter 4. We recall that the generalization involves introducing the complex step in a strict sense, which leads to many different possible approximations for the first and second order derivatives of any complex valued analytic function using its real and imaginary parts. Many of these approximations helps to avoid term cancellation inherent to classic finite differences (FD) approximations, as well as provide new ways of computing second order derivatives in a single step and reaching fourth accuracy in compact three levels stencil.

Here, we integrate the results of Chapter 4 with classic FD and introduce the Complex Step Finite Differences method (CSFDM) as a generalization of the well known FDM for solving the 1D, 2D and 3D acoustic wave equation in a homogeneous medium. We also present the numerical methodology in order to apply the new CSFDM. We illustrate the accuracy and stability of the introduced method by solving the acoustic wave propagation problem in one, two and three dimensions within a homogeneous medium. In Section 5.2 we formally introduce the Complex Step Finite Differences method (CSFDM) applied to the one dimensional first order acoustic wave equation. In Section 5.5 we apply the CSFDM to the 2D and 3D first order acoustic wave equation. Appendix A.1 we apply the CSFDM to the second order one dimensional acoustic wave equation, Appendix A.2 we apply the CSFDM to the second order two dimensional acoustic wave equation and Appendix B we show further applications of the CSFDM related to the translation between dispersion and dissipation in differential equations.

5.2 The 1D first order wave equation and the Complex Step Finite Differences method

The Complex Step method (CSM) was initially discovered by Squire and Trapp (1998); the method uses a purely imaginary number $\mathbf{i}$ ($\mathbf{i}^2 = -1$) for computing the first and second derivatives of real functions.

Recalling Chapter 4, the CSM can be easily derived from the Taylor series expansion of $f(x + \mathbf{i}\Delta x)$ (Eq. 4.1). The generalization made by Abreu et al. (2013b) consisted in taking a complex step in a strict sense, i.e., $h + \mathbf{i}v$, where h and v are differential steps ($h, v \in \mathbb{R}$ and

$h, v \to 0$).

To illustrate how the CS method can efficiently solve the one-way wave propagation problem and formally introduce the Complex Step Finite Differences method (CSFDM), we will apply different approximations based only in the imaginary part of the function found by Abreu et al. (2013b) to the one-way wave equation in a homogeneous medium.

We rewrite the approximations listed in Abreu et al. (2013b) (Chapter 4) and used in the present Chapter, by omitting all the equivalent expressions by considering $\mathfrak{Im} f(x \pm h + \mathbf{i}v)) = -\mathfrak{Im}(f(x \pm h - \mathbf{i}v))$.

$$f'(x) = \frac{\mathfrak{Im}(f(x + h + \mathbf{i}v))}{v} - hf''(x) + \mathcal{O}\left(h^2 - v^2\right). \tag{5.1}$$

$$f'(x) = \frac{\mathfrak{Im}(f(x + h + \mathbf{i}v)) + \mathfrak{Im}(f(x - h + \mathbf{i}v))}{2v} - \left(\frac{3h^2 - v^2}{6}\right) f'''(x) + \mathcal{O}\left(5h^4 - 10h^2v^2 + v^4\right), \tag{5.2}$$

where "$\mathfrak{Im}$" refers to the imaginary part of the function. Note that, $\mathfrak{Im}(f(x)) = 0$ because x is set to be a real number.

Note that if we set $v = \sqrt{3}h$ in Eq. 5.2, the approximation error becomes $\mathcal{O}\left(h^4\right)$. Equation 5.2 is able to compute fourth order accurate values of a first order derivative by requiring only three levels of information of the function ($x + h + \mathbf{i}v$, $x - h + \mathbf{i}v$ and $x + \mathbf{i}v$).

Each first derivative approximation (Eqs. 5.1 - 5.2) can be applied and/or combined in order to solve the first value problem.

In order to solve the one-way wave propagation problem, Eqs. 5.1 - 5.2 can be written including the initial and/or center point to include more information of the function into the discretization. Following this, we can write Eqs. 5.1 - 5.2 and a second order approximation for the third order derivative respectively

$$f'(x) = \frac{\mathfrak{Im}(f(x + h + \mathbf{i}v)) + \mathfrak{Im}(f(x + \mathbf{i}v))}{2v} + \mathcal{O}\left(h, v^2\right). \tag{5.3}$$

$$f''(x) = \frac{\mathfrak{Im}(f(x + h + \mathbf{i}v)) - \mathfrak{Im}(f(x + \mathbf{i}v))}{hv} + \mathcal{O}\left(h, v^2\right). \tag{5.4}$$

$$f'(x) = \frac{\mathfrak{Im}(f(x + h + \mathbf{i}v)) + \mathfrak{Im}(f(x + \mathbf{i}v)) + \mathfrak{Im}(f(x - h + \mathbf{i}v))}{3v} - \left(\frac{2h^2 - v^2}{6}\right) f'''(x) + \mathcal{O}\left(10h^4 - 20h^2v^2 + 3v^4\right). \tag{5.5}$$

$$f'''(x) = \frac{\mathfrak{Im}(f(x + h + \mathbf{i}v)) - 2\,\mathfrak{Im}(f(x + \mathbf{i}v)) + \mathfrak{Im}(f(x - h + \mathbf{i}v))}{h^2v} + \mathcal{O}\left(h^2 - 2v^2\right). \tag{5.6}$$

Note that the CSFD expression for the third order derivative (Eq. 5.6) is just a simple three levels scheme. We use this fact to approximate a more general and accurate expression for the first derivative given by the following

$$f'(x) = \left(\frac{1}{2v} - \frac{3h^2 - v^2}{6h^2v}\right)\left(\mathfrak{Im}(f(x + h + \mathbf{i}v)) + \mathfrak{Im}(f(x - h + \mathbf{i}v))\right) + \left(\frac{3h^2 - v^2}{3h^2v}\right)\mathfrak{Im}(f(x + \mathbf{i}v)) + \mathcal{O}\left(357h^4 - 713h^2v^2 + 70v^4\right). \tag{5.7}$$

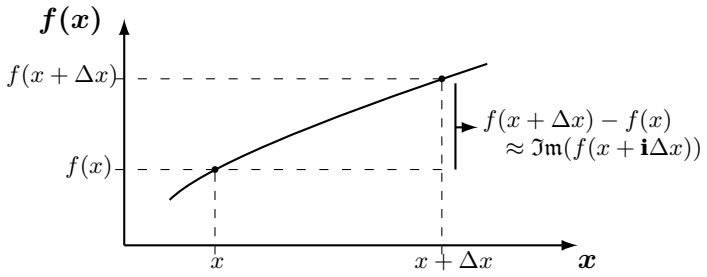

Figure 5.1: Geometric representation of the Complex Step.

$$f'(x) = \left(\frac{1}{3v} - \frac{2h^2 - v^2}{6h^2 v}\right)\left(\mathfrak{Im}(f(x + h + \mathbf{i}v)) + \mathfrak{Im}(f(x - h + \mathbf{i}v))\right) + \left(\frac{1}{3v} + \frac{2h^2 - v^2}{3h^2 v}\right)\mathfrak{Im}(f(x + \mathbf{i}v)) + \mathcal{O}\left(238h^4 - 475h^2v^2 + 70v^4\right). \tag{5.8}$$

Note that in Eqs. 5.7 - 5.8 we can choose the weights of each term $\mathfrak{Im}(f(x + h + \mathbf{i}v))$, $\mathfrak{Im}(f(x - h + \mathbf{i}v))$ and $\mathfrak{Im}(f(x + \mathbf{i}v))$ and the approximation will remain 4^{th} order accurate. If we choose $357h^4 - 713h^2v^2 + 70v^4 = 0$ and/or $238h^4 - 475h^2v^2 + 70v^4 = 0$ in Eqs. 5.7 - 5.8 respectively, the error becomes $\mathcal{O}\left(h^6\right)$.

In order to have a physical interpretation of how the CSFDM can effectively solve the wave propagation problem, we give a geometrical interpretation to the imaginary part of the imaginary perturbation. Figure 5.1 shows that the imaginary perturbation can be represented as an increment in the vertical axis. This approximation is just made by equating Eq. 3.8 and Eq. 4.2.

5.2.1 Discretizations

The most basic FD discretizations to the one-way wave equation are made by combining forward, backward and centered FD approximations (see Table 3.3). In this study we followed a similar strategy: we combine different CS discretizations to the first order wave equation and below we perform its respective convergence, stability and dispersion analysis. We only considered explicit schemes in this study.

In the next Sections we focused our attention in discretizations made using Eqs. 5.1 - 5.5 at both sides of the one-way wave equation and with and without including the initial/center point. We name our introduced discretizations Complex Step Finite Differences (CSFD) approximations to the one-way wave equation. Following we present a list of the mentioned discretizations (with and without including the initial/center point):

$$\mathfrak{Im}\left(u_{x+\mathbf{i}\Delta x}^{t+\Delta t+\mathbf{i}\Delta t}\right) = \mathrm{S}\,\mathfrak{Im}\left(u_{x+\Delta x+\mathbf{i}\Delta x}^{t+\mathbf{i}\Delta t}\right) + \mathcal{O}\left(\Delta t, \Delta x\right). \tag{5.9}$$

$$\mathfrak{Im}\left(u_{x+\mathbf{i}\sqrt{3}\Delta x}^{t+\Delta t+\mathbf{i}\sqrt{3}\Delta t}\right) + \mathfrak{Im}\left(u_{x+\mathbf{i}\sqrt{3}\Delta x}^{t-\Delta t+\mathbf{i}\sqrt{3}\Delta t}\right) = \mathrm{S}\left[\mathfrak{Im}\left(u_{x+\Delta x+\mathbf{i}\sqrt{3}\Delta x}^{t+\mathbf{i}\sqrt{3}\Delta t}\right) + \mathfrak{Im}\left(u_{x-\Delta x+\mathbf{i}\sqrt{3}\Delta x}^{t+\mathbf{i}\sqrt{3}\Delta t}\right)\right] + \mathcal{O}\left(\Delta t^4, \Delta x^4\right). \tag{5.10}$$

$$\mathfrak{Im}\left(u_{x+\mathbf{i}\Delta x}^{t+\Delta t+\mathbf{i}\Delta t}\right) = \mathrm{S}\,\mathfrak{Im}\left(u_{x+\Delta x+\mathbf{i}\Delta x}^{t+\mathbf{i}\Delta t}\right) + (\mathrm{S}-1)\,\mathfrak{Im}\left(u_{x+\mathbf{i}\Delta x}^{t+\mathbf{i}\Delta t}\right) + \mathcal{O}\left(\Delta t, \Delta x\right). \tag{5.11}$$

$$\begin{aligned}
&\mathfrak{Im}\left(u_{x+\mathbf{i}\sqrt{2}\Delta x}^{t+\Delta t+\mathbf{i}\sqrt{2}\Delta t}\right)+\mathfrak{Im}\left(u_{x+\mathbf{i}\sqrt{2}\Delta x}^{t-\Delta t+\mathbf{i}\sqrt{2}\Delta t}\right)\\
&\quad=\mathrm{S}\left[\mathfrak{Im}\left(u_{x+\Delta x+\mathbf{i}\sqrt{2}\Delta x}^{t+\mathbf{i}\sqrt{2}\Delta t}\right)+\mathfrak{Im}\left(u_{x-\Delta x+\mathbf{i}\sqrt{2}\Delta x}^{t+\mathbf{i}\sqrt{2}\Delta t}\right)\right]+(\mathrm{S}-1)\,\mathfrak{Im}\left(u_{x+\mathbf{i}\sqrt{2}\Delta x}^{t+\mathbf{i}\sqrt{2}\Delta t}\right)+\mathcal{O}\left(\Delta t^4,\Delta x^4\right).
\end{aligned}\tag{5.12}$$

Also by choosing the correct values of h and v we can write the following general approximation

$$\begin{aligned}
&\mathrm{A}\,\mathfrak{Im}\left(u_{x+\mathbf{i}v_x}^{t+\Delta t+\mathbf{i}v_t}\right)+\mathrm{A}\,\mathfrak{Im}\left(u_{x+\mathbf{i}v_x}^{t-\Delta t+\mathbf{i}v_t}\right)\\
&\quad=c\left[\mathrm{C}\,\mathfrak{Im}\left(u_{x+\Delta x+\mathbf{i}v_x}^{t+\mathbf{i}v_t}\right)+\mathrm{D}\,\mathfrak{Im}\left(u_{x+\mathbf{i}v_x}^{t+\mathbf{i}v_t}\right)+\mathrm{C}\,\mathfrak{Im}\left(u_{x-\Delta x+\mathbf{i}v_x}^{t+\mathbf{i}v_t}\right)\right]-\mathrm{B}\mathfrak{Im}\left(u_{x+\mathbf{i}v_x}^{t+\mathbf{i}v_t}\right)+\mathcal{O}\left(\Delta t^4,\Delta x^4\right),
\end{aligned}\tag{5.13}$$

where v_t and v_x refers to the imaginary differential perturbation and the weights $\mathrm{A},\mathrm{B},\mathrm{C},\mathrm{D}$ are easily selected by choosing the correct values by using Eq. 5.7 and/or Eq. 5.8.

Note that Eq. 5.9 and Eq. 5.11 are special cases of Eq. 5.10 and Eq. 5.13 respectively. Also note that Eq. 5.13 can be written respectively in a general operator form as follows

$$\begin{aligned}
\mathrm{val}\left(x,t+\Delta t\right)=c\frac{\mathrm{C}}{\mathrm{A}}\left[\mathrm{val}\left(x+\Delta x,t\right)+\mathrm{val}\left(x-\Delta x,t\right)\right]+\frac{c\mathrm{D}-\mathrm{B}}{\mathrm{A}}\mathrm{val}\left(x,t\right)\\
-\mathrm{val}\left(x,t-\Delta t\right),
\end{aligned}\tag{5.14}$$

where $\mathrm{val}\left(x,t\right)$ represents the values of $\mathfrak{Im}\left(u_{x+\mathbf{i}v_x}^{t+\mathbf{i}v_t}\right)$ to be propagated.

Note that Equations 3.18 and 5.14 are quite similar. If fact, Eq. 3.18 is a specific case of Eq. 5.14 when $c\frac{\mathrm{C}}{\mathrm{A}}=\mathrm{S}^2$ and $\frac{c\mathrm{D}-\mathrm{B}}{\mathrm{A}}=2\left(1-\mathrm{S}^2\right)$. Both discretizations produce the same operational computation with the distinction in the Courant number only.

5.2.2 Convergence, consistence and stability analysis

Based on the need to obtain reliable results in our approximate numerical solutions, we have to make a choice between which FD discretization to use in order to solve the initial value problem. To this end we use concepts of stability, consistency and convergence of the method. It is extremely important for a user of FD techniques to understand precisely what kind of type of convergence their scheme has, what kind of assumptions are made to get this convergence and how this convergence affects their accuracy, Thomas (1995). The main goal of a FD discretization of a PDE is to reproduce a convergent, consistent and stable numerical solution of the problem. Consistency of any FD discretization to the wave equation is already fulfilled by the Taylor series definition. The Lax Equivalence Theorem states the relation between convergence, consistence and stability in the following way: *a consistent and stable FD scheme converges with the rate equal to its order or accuracy*, i.e., we only need to prove that the FD scheme is consistent and stable in order to prove its convergence. In this study we are not interested in proving the Lax Equivalence Theorem, the interested reader can refers to any book of PDE's with FD approximations or directly in Lax and Richtmyer (1956).

Courant-Friedrichs-Lewy stability condition

For stability analysis of FD discretizations, the Courant-Friedrichs-Lewy condition (CFL) is a necessary but not sufficient condition of convergence, Strang (2007). The CFL condition is given by

$$\frac{c\Delta t}{\Delta x} = \mathrm{S} < \mathrm{C}, \tag{5.15}$$

where S is the Courant number and/or stability factor and C is a particular constant which depends on the PDE equation to be solved and the FD scheme to be used in the discretization.

Von Neumann stability condition

The Von Neumann stability condition is a necessary but not sufficient condition of convergence. Von Neumann stability analysis consider a complex exponential at the initial time, i.e., $u(x,0) = e^{\mathbf{i}kx}$, as the most general initial displacement of the problem. Any periodic function can be expressed in terms of this solution. We have seen in previous sections that the analytical solution to the one-way wave equation can be understood as a translation of the initial displacement. Assuming constant velocity and no boundaries at every time t, the solution will remain a multiple of the initial displacement $(e^{\mathbf{i}kx})$, i.e., $u(x,t) = \mathrm{G}\, e^{\mathbf{i}kx}$, where the term G is called the *growth factor* or *amplification factor*, and will depend on the frequency ω and time t, i.e., $u(x,t) = \mathrm{G}(\omega,t)e^{\mathbf{i}kx}$. In other words, we separate time and space variables in the general solution.

The main idea of the Neumann stability condition is to keep the magnitude of the growth factor less than or equal than one in order to maintain the solution within bounds when $t \to \infty$, i.e., the Von Neumann stability condition will be given by

$$\|\mathrm{G}\| \leq 1. \tag{5.16}$$

Since all discretizations are consistent (Taylor series definition), we apply Von Neumann stability analysis to each combination in order to determine whether an approximation is convergent (by Lax Equivalence Theorem). After this analysis we can determine its corresponding Courant-Friedrichs-Lewy condition.

To illustrate this procedure, substitute $u = \mathrm{G}(\omega,t)e^{\mathbf{i}kx}$ into discretization 5.9,

$$\mathfrak{Im}(\mathrm{G}^{t+\Delta t+\mathbf{i}\Delta t}e^{\mathbf{i}k(x+i\Delta x)}) = \mathrm{S}\,\mathfrak{Im}(\mathrm{G}^{t+\mathbf{i}\Delta t}e^{\mathbf{i}k(x+\mathbf{i}\Delta x+\Delta x)}), \tag{5.17}$$

solving,

$$\mathfrak{Im}(\mathrm{G}^{t+\mathbf{i}\Delta t}e^{\mathbf{i}k(x+\mathbf{i}\Delta x)}(\mathrm{G}^{\Delta t} - \mathrm{S}e^{\mathbf{i}k\Delta x})) = 0,$$

for the sake of simplicity we write $t = 0$ and $\Delta t = 1$,

$$\mathfrak{Im}(\mathrm{G}^{\mathbf{i}}e^{\mathbf{i}k(x+\mathbf{i}\Delta x)}(\mathrm{G} - \mathrm{S}e^{\mathbf{i}k\Delta x})) = 0,$$

we can write to ensure Von Neumann stability condition independent of kx,

$$\begin{aligned}\mathfrak{Im}(\mathrm{G} - \mathrm{S}e^{\mathbf{i}k\Delta x}) &= 0,\\ \mathfrak{Re}(\mathrm{G} - \mathrm{S}e^{\mathbf{i}k\Delta x}) &= 0.\end{aligned} \tag{5.18}$$

We conclude that discretization 5.9 is stable for $\mathrm{S} \leq 1$, i.e., $\|\mathrm{G}\| \leq 1 \quad \text{if} \quad \mathrm{S} \leq 1$.

Following the same procedure applied before, we can find the respective stability condition for discretization 5.11,

$$\mathrm{G} + 1 = \mathrm{S}(e^{\mathbf{i}k\Delta x} + 1). \tag{5.19}$$

which leads to $\|\mathrm{G}\| = |\mathrm{S} - 1| + |\mathrm{S}e^{\mathbf{i}k\Delta x}| \leq 1 \quad \text{if} \quad \mathrm{S} \leq 1$.

Von Neumann stability analysis of discretizations 5.10 and 5.12 leads to the following expressions respectively,

$$\mathrm{G}^2 - 2\mathrm{S}\cos k\Delta x + 1 = 0. \tag{5.20}$$

$$\mathrm{G}^2 - 2\left(\mathrm{S}\cos k\Delta x + \mathrm{S}/2 - 1/2\right)\mathrm{G} + 1 = 0. \tag{5.21}$$

Equations 5.20 - 5.21 are stable for $\mathrm{S} \leq 1$, i.e., $\|\mathrm{G}\| \leq 1 \quad \text{if} \quad \mathrm{S} \leq 1$.

Note for the particular case if $k\Delta x = 2\pi$, both roots are equal to one, i.e., $G_{1,2} = 1$, which warranties the convergence of the scheme.

Von Neumann stability analysis of the general expression (Eq. 5.13) leads to the following

$$\mathrm{G}^2 - 2\left(\frac{c\mathrm{C}}{\mathrm{A}}\cos k\Delta x + \frac{c\mathrm{D} - \mathrm{B}}{2\mathrm{A}}\right)\mathrm{G} + 1 = 0, \tag{5.22}$$

which Courant number will depend on the constants $\mathrm{A}, \mathrm{B}, \mathrm{C}$ and D.

5.2.3 Dispersion-dissipation analysis

In order analyze the behavior of stable discretizations to the wave equation, we have to introduce concepts of dispersion and dissipation. Dispersion and dissipation are concepts related to the analytic and numerical solutions of partial differential equations. Thomas (1995) defines "*dissipation* of solutions of partial differential equations is when the Fourier modes do not grow with time and at least one mode decays, and *dispersion* of solution of partial differential equations is when Fourier modes of different wave lengths (or wave numbers) propagate at different speed".

The properties of a PDE can be described by means of its effects on a single wave (plane wave) or Fourier mode in space and time given by the following mathematical expression (Inan and Marshall (2004))

$$u(x,t) = \mathrm{A}e^{\mathbf{i}(kx+\omega t)}, \tag{5.23}$$

where ω is the frequency of the wave and k is the wave number, related to wavelength, $\mathbf{i}$ is the imaginary unit ($\mathbf{i}^2 = -1$) and A is the amplitude. Usually k and ω are dependent variables. The relation written as $\omega = \omega(k)$ is called as the dispersion-dissipation relation.

In order to facilitate the dispersion-dissipation analysis lets consider the dispersion-dissipation relationship as a complex number in the following way $\omega = \alpha + \mathbf{i}\gamma$. By substituting the relation into the discrete plane wave solution given by the following expression

$$u(x,t) = A\, e^{\mathbf{i}(kn\Delta x + \omega m\Delta t)}, \tag{5.24}$$

where $x = n\Delta x$ and $t = m\Delta t$, with n, m as positive integers, we obtain the following

$$u(x,t) = A\, e^{-\gamma m\Delta t} e^{\mathbf{i}k(n\Delta x - (-\frac{\alpha}{k})m\Delta t)}. \tag{5.25}$$

Analyzing expression 5.25 and taking into account possible values of its real and imaginary parameters (α and γ), can be inferred what will happen with the solution (see Thomas (1995) for further details).

Parameter α:

- If $\alpha = 0$ there is no wave propagation.
- If $\alpha \neq 0$ there will be wave propagation with speed -$\frac{\alpha}{k}$.
- If -$\frac{\alpha}{k}$ is a non trivial function of $\omega(k)$, the scheme will be dispersive.

Parameter γ:

- If $\gamma < 0$ the solution to the scheme will grow without bounds.
- If $\gamma > 0$ the solution the scheme is dissipative.
- If $\gamma = 0$ the scheme will be non dissipative.

Commonly odd order derivative FD approximations are related to dispersion properties while FD approximations of even order derivatives to dissipation properties of the solution. This is illustrated in Appendix B.

To illustrate how to obtain dispersion-dissipation relations, we substitute the plane wave solution (Eq. 5.24) into discretization 5.9 and the following expression is obtained

$$e^{\mathbf{i}\omega\Delta t} = \mathrm{S}\, e^{\mathbf{i}k\Delta x}.$$

We can appreciate that the scheme is non-dissipative and dispersive. If we include the initial point $\left(u^{t+\mathbf{i}\Delta t}_{x+\mathbf{i}\Delta x}\right)$ into the approximation we obtain Eq. 5.11. Substituting the plane wave solution we get the following

$$e^{\mathbf{i}\omega\Delta t} = \mathrm{S}\, e^{\mathbf{i}k\Delta x} + (\mathrm{S} - 1). \tag{5.26}$$

Substituting the plane wave solution into discretizations 5.10 - 5.12 we get the following dispersion relation respectively,

$$\cos\omega\Delta t = \mathrm{S}\, \cos k\Delta x. \tag{5.27}$$

$$\cos\omega\Delta t = \mathrm{S}\, \cos k\Delta x + \frac{1}{2}\left(\mathrm{S} - 1\right). \tag{5.28}$$

for the general expression we have

$$\cos\omega\Delta t = \frac{c\mathrm{C}}{\mathrm{A}} \cos k\Delta x + \frac{c\mathrm{D} - \mathrm{B}}{2\mathrm{A}}. \tag{5.29}$$

Clearly the schemes are non-dissipative and dispersive.

If $\frac{c\mathrm{D}-\mathrm{B}}{2\mathrm{A}} = 2$ and $\frac{c\mathrm{C}}{\mathrm{A}} = \mathrm{S}^3$, we can write the following equation

$$\sin^2 \frac{\omega\Delta t}{2} = \mathrm{S}^3 \sin^2 \frac{k\Delta x}{2}, \tag{5.30}$$

which correspond to a discretization made using Eq. 5.6 in time and space, i.e., a discretization to a third order wave equation.

Equation 5.30 is the dispersion-dissipation relation of the Leapfrog scheme for the second order wave equation, with the difference only in the power of the Courant number, i.e., third order (S^3) in Eq. 5.30 and squared (S^2) for the conventional FD Leapfrog of the second order wave equation. It is important to recall that the CSFD Leapfrog discretization 5.12 is symmetric, this mean that the solution is non-dissipative; on the other hand it is fourth order accurate in time and space for a homogeneous and regular grid.

5.3 Comparison between first and second order 1D wave equations by using CSFD and FD methods

Recall the general FD expression for the second order wave equation (Eq. 3.18)

$$\begin{aligned}\text{val}\left(x,t+\Delta t\right) = \mathrm{S}^2\left[\text{val}\left(x+\Delta x,t\right)+\text{val}\left(x-\Delta x,t\right)\right]+2\left(1-\mathrm{S}^2\right)\text{val}\left(x,t\right)\\ -\text{val}\left(x,t-\Delta t\right),\end{aligned}$$

and the CSFD expression (Eq. 5.10) for the first order wave equation written in a general operator form as follows

$$\text{val}\left(x,t+\Delta t\right) = \mathrm{S}\left[\text{val}\left(x+\Delta x,t\right)+\text{val}\left(x-\Delta x,t\right)\right]-\text{val}\left(x,t-\Delta t\right). \tag{5.31}$$

Both expressions are equivalent for $\mathrm{S}=1$, that is, there is an equivalence for the maximum Courant number in both expressions, reproducing same results by solving the second-order wave equation with FDM and by solving the first-order wave equation with CSFDM.

5.4 Numerical examples: 1D one-way wave equation simulations

Numerical examples are presented using an initial function $f(x,0)$ and/or a point source $f(x_s,t)$ as conditions of initial movement in a homogeneous media only. One of the main advantage of the CSFDM over FDM is the order of accuracy at a single step and a two steps: we can obtain second order of accuracy at at single step, i.e., using two levels of information in time and in space, and fourth order of accuracy at two steps, i.e., using only three levels of information in time and in space. Another advantage is related to the methodology applied to impose initial conditions as it is shown in the next Section.

5.4.1 Numerical methodology

The numerical methodology presented here for using CSFD approximations to the wave equation is rather different from all previous known FD analysis. As mentioned before it is well known that there are several FD discretizations to the wave equation which solves the problem in a efficient way, for instance, Upwind, Leapfrog, Lax-Wendroff, Lax-Friedrichs, MacCormack and Beam-Warming among many others. In the most basic way, all of this methods use a *displacement* condition as an input to propagate the wave. These displacements are given as an initial displacement ($f(x,0)$) or a time dependent source ($f(x_s,t)$). All of this different methods are just simply *difference operators* (Eqs. 3.11 and 3.18) which solve the wave propagation problem in a convergent, consistent and stable way.

In CSFDM, in order to propagate the imaginary part of the imaginary perturbation (in time and/or space) of the displacement, we have to construct the initial condition equivalent

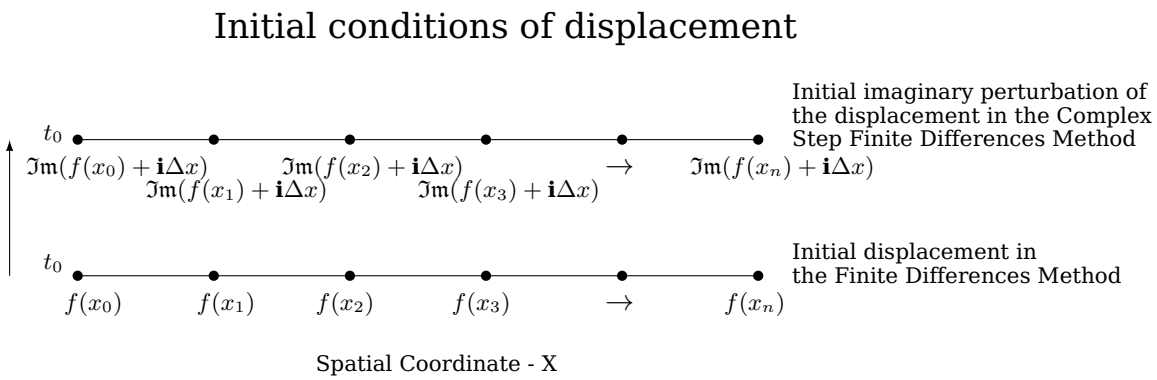

Figure 5.2: Initial conditions of displacement given in the conventional Finite Differences Method and the Complex Step Finite Differences Method: A replacement of the displacement $f(x,t_0)$ at initial time t_0 given in the Finite Differences Method by its respective imaginary part of the imaginary perturbation $\Im\mathfrak{m}(f(x+\mathbf{i}\Delta x,t_0))$ is made in the Complex Step Finite Differences method as an initial step of the process.

to those given. In case of initial displacement $(u(x,0))$, we just have to build its respective imaginary part of the imaginary perturbation $(\Im\mathfrak{m}(u(x+\mathbf{i}\Delta x,0)))$ at each corresponding grid point (see Fig. 5.2). In case of a point source, we have a time dependent function evaluated at certain spatial grid point $(u(x_s,t))$, we have to build its respective imaginary part of the imaginary perturbation $(\Im\mathfrak{m}(u(x_s,t+\mathbf{i}\Delta t)))$ at each time step.

It is important to recall that we are not doing any change of domain from the real space ($\mathbb{R}$) to the complex space ($\mathbb{C}$). Grid points remains the same, the only change that we apply is the numerical value to be propagated by using the selected *difference operator*. Based on this, it is clear why we are able to obtain with CSFD discretizations to the one-wave wave equation similar properties to FD discretizations.

The numerical methodology for using *higher order CSFD* discretizations is slightly different from *second order*. In order to get higher order accurate solutions we have build the imaginary grid of the of the imaginary perturbation, i.e., $\Im\mathfrak{m}(u(x+\mathbf{i}v_x,0))$ and/or $\Im\mathfrak{m}(u(x_s,t+\mathbf{i}v_t))$, where v_x and/or v_t are the correct values that produces the higher order accuracy into the discretization (e.g. Eqs. 5.2 and 5.7).

Because the three time levels of some CSFD approximations, like the FD Leapfrog method, we approximate the fist time step by a two time levels approximation when only an initial displacement condition is imposed.

A basic feature of the FD technique applied to the one-way wave equation is to compute/propagate displacements at each time step and to be able to compute velocities and/or accelerations by using those displacement values. Unlike FD, the main feature of the CSFD technique presented here is to compute/propagate the imaginary part of the imaginary perturbation of the displacement and to be able to compute displacement, gradient, velocity and/or acceleration values at each time step.

Figures 5.3 and 5.4 illustrate the one-way wave movement process of the imaginary part of different displacement conditions (initial displacement and/or time dependent source) given in the CSFDM.

To illustrate the one-way wave movement process, we have seen that Eqs. 5.9 - 5.12 can be written in a general operator way, i.e., as an operator that takes values from one time level and gives explicitly the next time level of values. Discretization 5.10 is just an operator

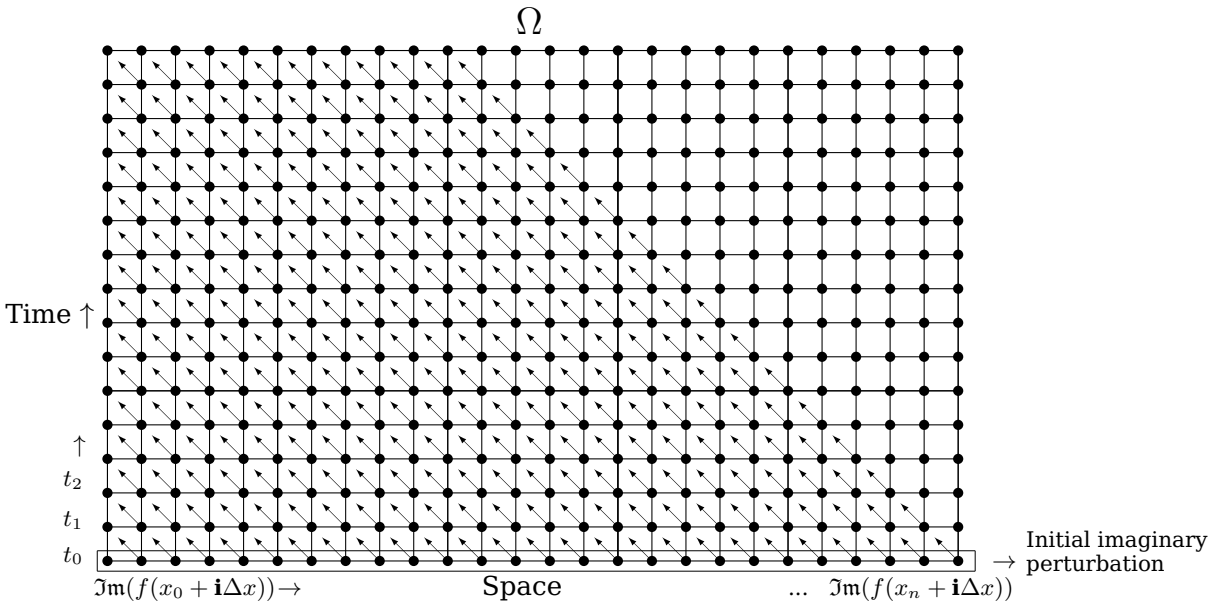

Figure 5.3: One-way wave simulation process: Propagation of the imaginary part of the imaginary perturbation in space in case of initial displacement given.

that propagates values (i.e. the imaginary part of the perturbation) following an approximate solution structure to the solution of one-way wave equation by the FD upwind method (Eq. 3.10). Figures 5.3 and 5.4 illustrate how operator 3.10 propagate values in case of initial condition over the entire space domain and by a point source respectively.

Initial condition: plane wave

For the first example consider the following initial displacement,

$$u(x,0) = \sin \pi x, \quad \text{for} \quad 0 \leq x \leq 3\pi. \tag{5.32}$$

The analytical displacement solution to the initial value problem is obtained by applying by the d'Alembert general formula (Eq. 3.19),

$$u(x,t) = \cos{(\pi x + \pi ct)}, \quad \text{for} \quad 0 \leq x \leq 3\pi \quad \text{and} \quad t > 0, \tag{5.33}$$

with analytical velocity

$$\dot{u}(x,t) = -\pi c \sin{(\pi x + \pi ct)}, \quad \text{for} \quad 0 \leq x \leq 3\pi \quad \text{and} \quad t > 0. \tag{5.34}$$

For numerical computations we use a regular grid: Total grid length 3π km. Number of space discretizations 1000 ($\Delta x = 0.0094$ km) , number of time discretizations 500 ($\Delta t = 0.0065$ seconds) and wave speed equal to 1.450 km/s (Courant number equal to one ($\mathrm{S} = 1$)).

Figure 5.5 show results (snapshot of time step equal to 250) using upwind discretization and second order CSFD (Eq. 5.11). As mentioned in previous sections the methodology here presented to compare results between FD and CSFD is simple: with FD we use Eq. 5.32 as a initial movement, with CSFD we have to construct initial conditions similar to those given. The idea is to compute for each

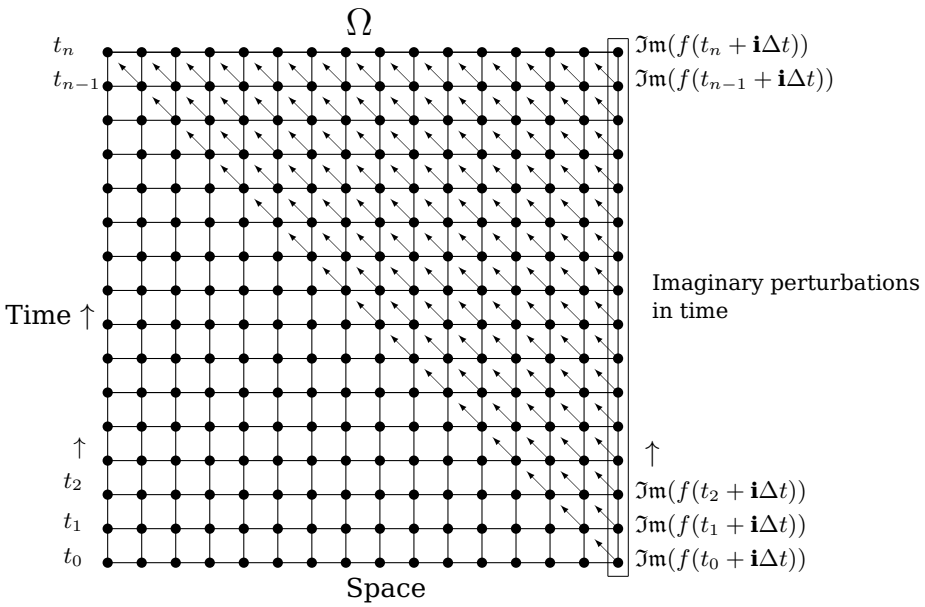

Figure 5.4: One-way wave simulation process: Propagation of the imaginary part of the imaginary perturbation in time in case of a point source.

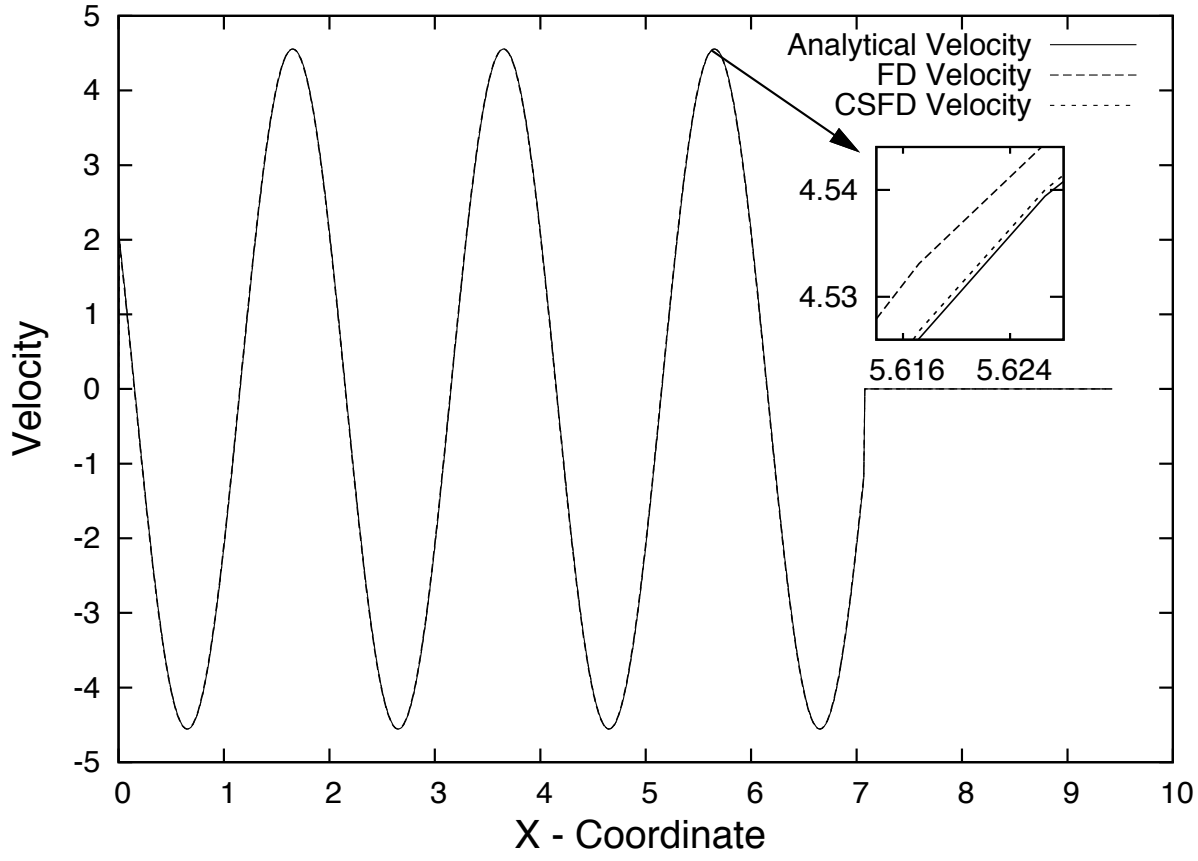

Figure 5.5: Comparison of velocity calculations using forward finite differences (FD) approximation (Eq. 3.8) and its respective analogous complex step finite differences (CSFD) approximation (Eq. 4.2) in one-way wave simulation process with initial condition: $f(x, 0) = \sin \pi x$. It can be appreciated how the CSFDM reproduces second order numerical values and the conventional FD only first order by using two time levels velocity approximation.

$$u(x + n\Delta x, 0) \quad \text{with} \quad n = 0, ..., N, \tag{5.35}$$

compute its corresponding imaginary part of imaginary perturbation

$$\mathfrak{Im}(u(x + n\Delta x + n\mathbf{i}\Delta x, 0)) \quad \text{with} \quad n = 0, ..., N, \tag{5.36}$$

as an initial step of the process. After that, discretization 5.11 can be used to propagate the wave to the time of interest. At this point we compute velocity values using two time levels for the FD case (first order approximation) and one time level for the CSFD case (second order approximation).

Note that CSFDM mainly differs of FDM in setting initial conditions: Because we make an imaginary perturbation in space with Eq. 5.36, by dividing by Δx we get displacement gradients at each time step. Boundary conditions will be related to displacement gradients values. In order to get velocity values we have to use the first order wave equation (Eq. 3.7).

We compare velocity values instead of displacement values (see Fig. 5.5). The reason of this is because we emphasize the fact that in order to compute velocity values using FDM we need to use two time levels which is first order accurate and by using one time level we get second order of accuracy in the CSFD case. Displacement values can be computed by the following expressions

$$u_x^{t+\Delta t} = u_x^t + \mathfrak{Im}\left(u_x^{t+\mathbf{i}\Delta t}\right) + \mathcal{O}\left(\Delta t^2\right), \tag{5.37}$$

using the initial displacement u_x^t and at each time level that the imaginary part of the displacement is computed, we can obtain $u_x^{t+n\Delta t}$. Or using

$$u_x^{t+\Delta t} = u_x^{t-\Delta t} + 2\,\mathfrak{Im}\left(u_x^{t+\mathbf{i}\Delta t}\right) + \mathcal{O}\left(\Delta t^3\right). \tag{5.38}$$

Note that Eqs. 5.37 - 5.38 are simple numerical integration expressions to compute displacements.

Continuing, as a second example we just use a slightly more complicated initial condition:

$$u(x, 0) = 3\sin 2\pi x + 6\cos 3\pi x, \quad \text{for} \quad 0 \leq x \leq 3\pi. \tag{5.39}$$

The analytical solution to the initial value problem is

$$u(x, t) = 3\sin\left(2\pi x + 2\pi ct\right) + 6\cos\left(3\pi x + 3\pi ct\right), \quad \text{for} \quad 0 \leq x \leq 3\pi \quad \text{and} \quad t > 0, \tag{5.40}$$

with analytical velocity

$$\dot{u}(x, t) = 6\pi c\cos\left(2\pi x + 2\pi ct\right) - 18\pi c\sin\left(3\pi x + 3\pi ct\right), \quad \text{for} \quad 0 \leq x \leq 3\pi \quad \text{and} \quad t > 0. \tag{5.41}$$

Figure 5.6 shows how CSFD reproduces the same results as FD using one time level only instead of three (FD velocity values are computed using centered approximation). It is here where lies one of the advantages of the CSFDM over the FDM; we can obtain same order of accuracy with less time levels for a homogeneous regular grid.

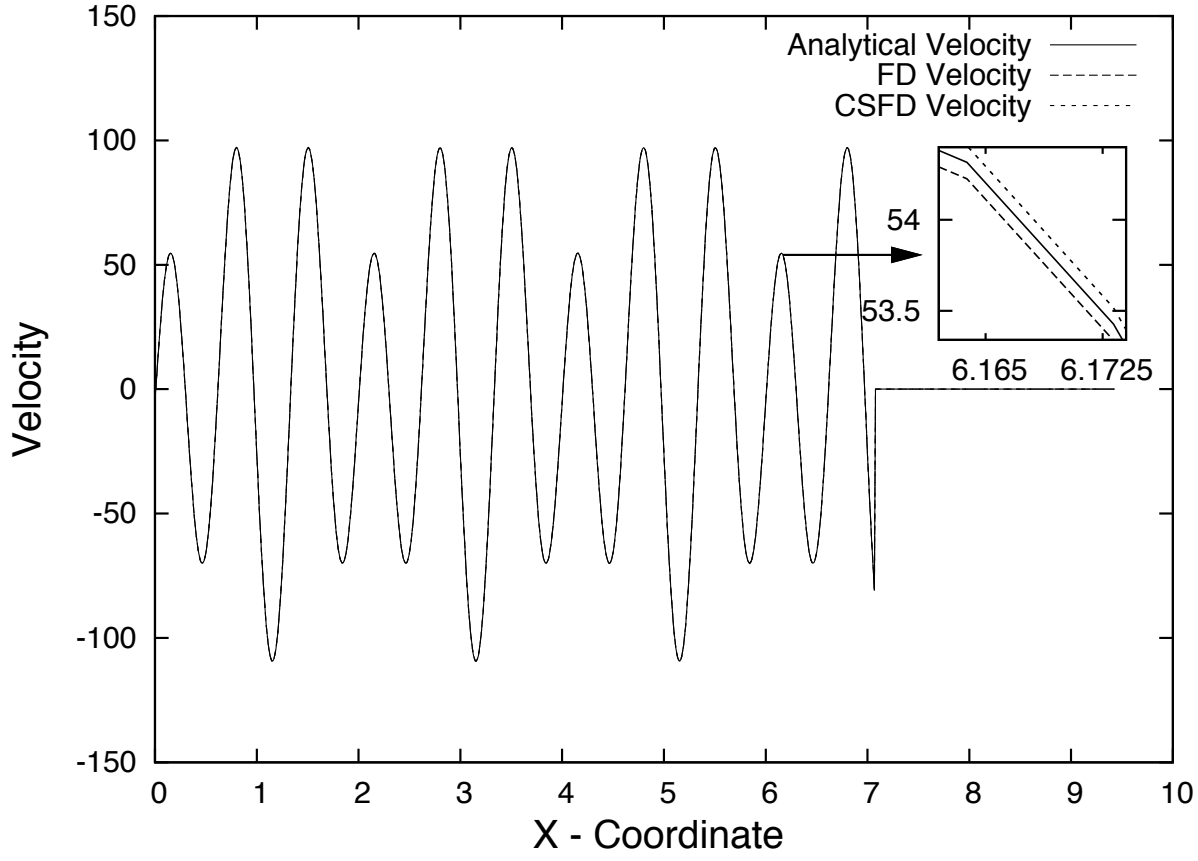

Figure 5.6: Comparison of velocity calculations using centered finite differences (FD) approximation (Eq. 3.9) and its respective analogous complex step finite differences (CSFD) approximation (Eq. 4.2) in one-way wave simulation process with initial condition: $f(x,0) = 3\sin 2\pi x + 6\cos 3\pi x$. It can be appreciated how the CSFDM reproduces second order numerical values by using two time levels approximation like the conventional FD by using three time levels velocity approximation.

Initial condition: source (time dependent function)

In previous Sections we have seen that we can use the CSFDM to propagate an initial displacement perturbation along the entire space domain to the time of interest. In this Section we show that we can also use the CSFDM to place an input source (time dependent function) on a single point to efficiently solve the source wave propagation problem.

The methodology for a single point source is similar to the previous case: with FDM, the input data for a single point source are displacements at a certain spatial location over a certain time lapse, i.e., $u(x_s, t)$, where x_s is the source location. In the CSFDM case, the idea is to compute for a certain time dependent function $f(x_s, t)$, its corresponding imaginary perturbation in time $\mathfrak{Im}(f(x_s, t + \mathbf{i}\Delta t))$, as an initial step of the process and later propagate the wave by using any CSFD discretization just like initial displacement case.

Note that the FD time-space grid does not change by using CSFDM. This mean we make an imaginary perturbation in time, and dividing by Δt we get approximate velocity values at each time step. The location of the source is the same initial location due to our FD grid has not changed. Boundary conditions will be related to velocities (imaginary perturbations of displacement in time). In order to get displacement gradients values we can apply the first order wave equation (Eq. 3.7).

To illustrate this, we use a Ricker source

$$f(x_s, t) = (1 - 2f_0^2(t - t_0)^2)\exp(-f_0^2(t - t_0)^2), \tag{5.42}$$

where f_0 is the dominant frequency and set to be in our example as $f_0 = 1/(40\Delta t)$, t_0 is the time delay (convenient to express it as multiple of $1/f_0$) and set to be $t_0 = 4/f_0$. We use the same domain used in the initial displacement example.

Figure 5.7 shows results using one-way propagation scheme. We can appreciate how CSFDM reproduces same velocity result as the FDM, i.e., FD velocity values are computed using the centered approximation (Eq. 3.9) and CSFD velocity values using one time level approximation (Eq. 4.2).

Figure 5.8 shows results using FD Leapfrog discretization (Eq. 3.9) and its analogous CSFD Leapfrog approximation (Eq. 5.12). We can appreciate how CSFD reproduces the solution in both directions without the parasitic root implicit in the Leapfrog Method to the one-way wave equation and at the same time computes fourth order accurate velocity values by using only three levels of information (regular and homogeneous grid). As many books in the literature refers, the Leapfrog method for the one-way wave equation has two solutions, one corresponding to the wave solution traveling in one direction and another one corresponding to the parasitic solution traveling in the opposite direction, usually called the parasitic mode (more information about the parasitic wave in the first order Leapfrog Method see Strang (2007)). This mode induces rapid oscillation in time. We have seen that the difference operator 5.31 propagates values by following the approximate structure solution to the second order wave equation given by the ordinary FDM (Eq. 3.18), that is why should be not surprising the absence of parasitic modes in the CSFD solution.

Figure 5.10 shows results of the simulation of the second order wave equation compared with the first order wave equation. As expected, both results are the same for the maximum Courant number ($\mathrm{S} = 1$), which allows to numerically describe two-way wave propagation with a first order differential equation.

5.5 Higher dimensional acoustic wave equation

In order to introduce the CSFDM in a more realistic way used in the geophysical and many other fields, in this section we adopt a more general expression for the acoustic wave equation

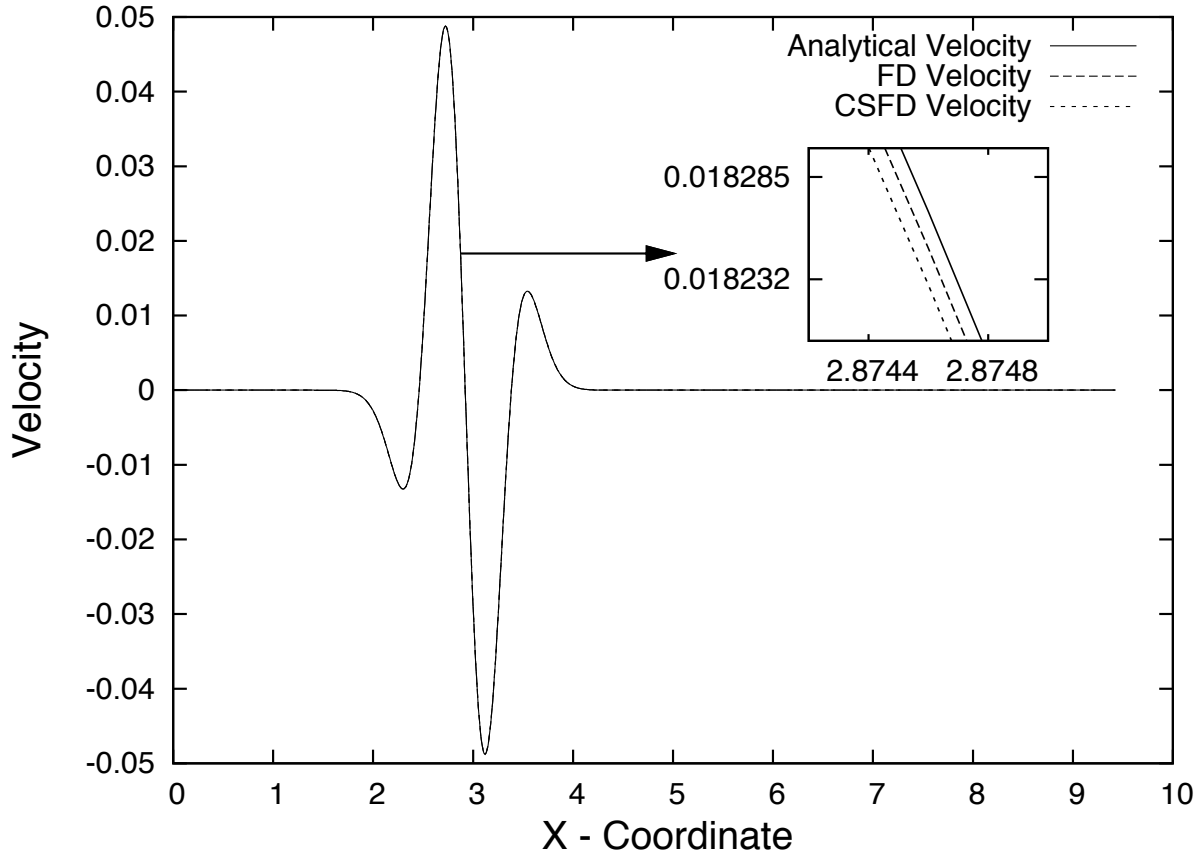

Figure 5.7: Comparison of velocity calculations using centered finite differences (FD) approximation (Eq. 3.9) and its respective analogous complex step finite differences (CSFD) approximation (Eq. 4.2) in one-way wave simulation process with a Ricker source. It can be appreciated how the CSFDM reproduces second order numerical values by using two time levels approximation like the conventional FD by using three time levels velocity approximation.

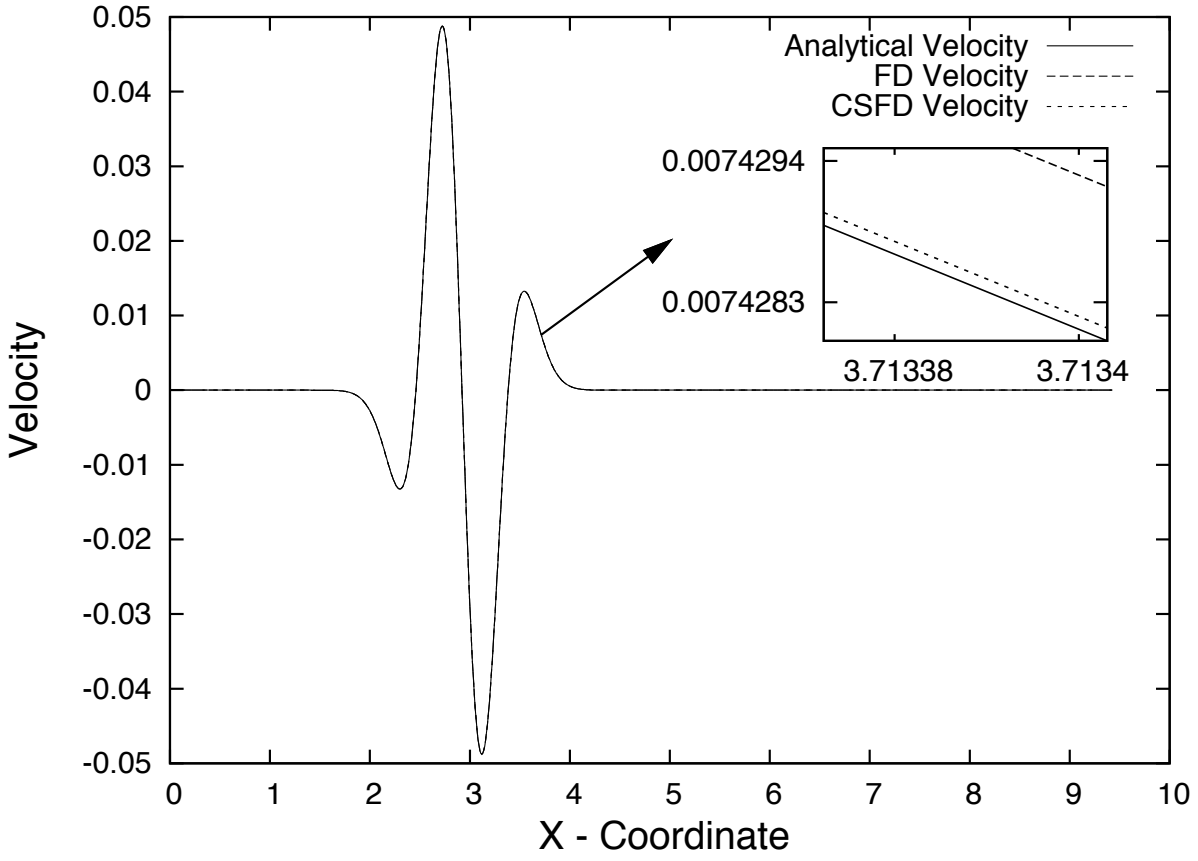

Figure 5.8: Comparison of velocity calculations using centered finite differences (FD) approximation (Eq. 3.9) and a fourth order complex step finite differences (CSFD) approximation (Eq. 5.2) in one-way wave simulation process with a Ricker source. It can be appreciated how the CSFDM reproduces fourth order numerical values by using three time levels approximation unlike the conventional FD by using three time levels velocity approximation.

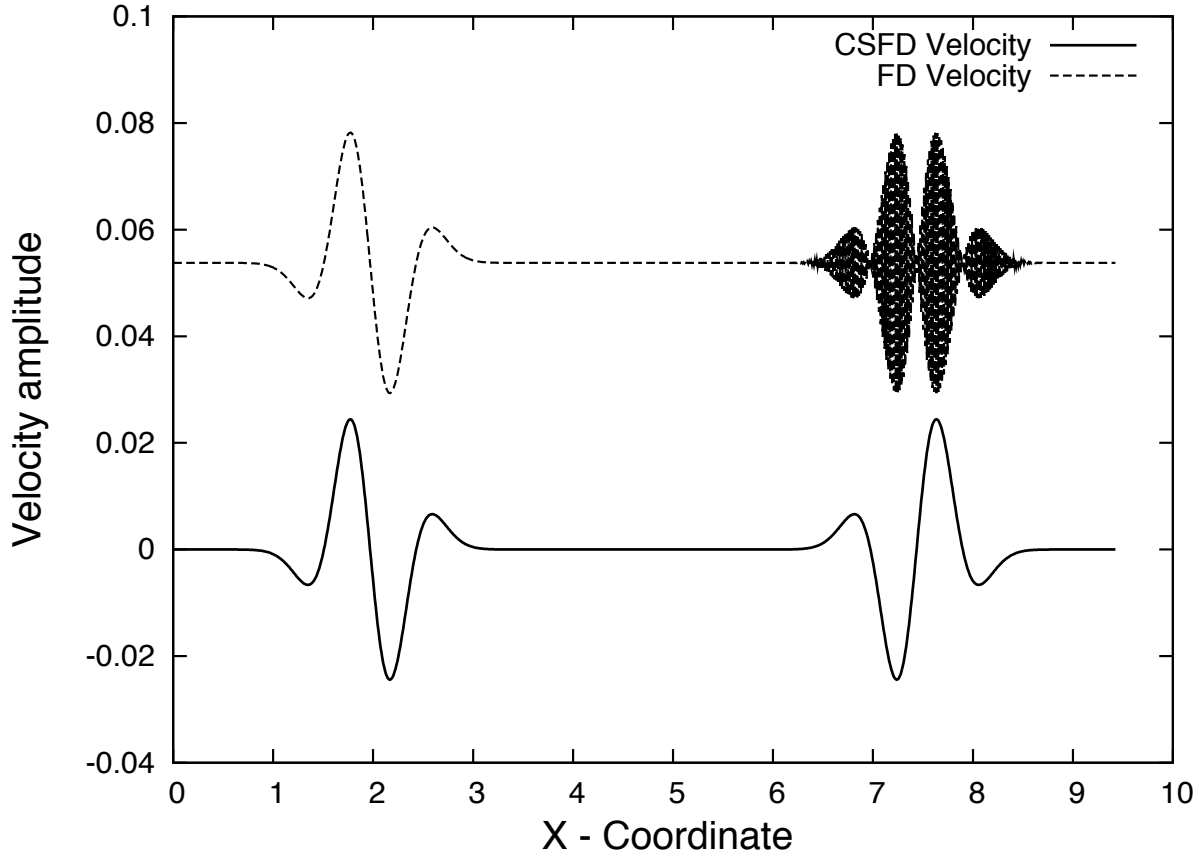

Figure 5.9: Comparison of velocity calculations using centered finite differences (FD) approximation (Eq. 3.9) and a fourth order complex step finite differences (CSFD) approximation (Eq. 5.2) in one-way wave simulation process with a Ricker source. It can be appreciated how the CSFDM propagates the wave in two directions without the presence of a parasitic root unlike the conventional FD Leapfrog Method. FD velocity values are displaced in the vertical axis in order to make a better comparison of both methods.

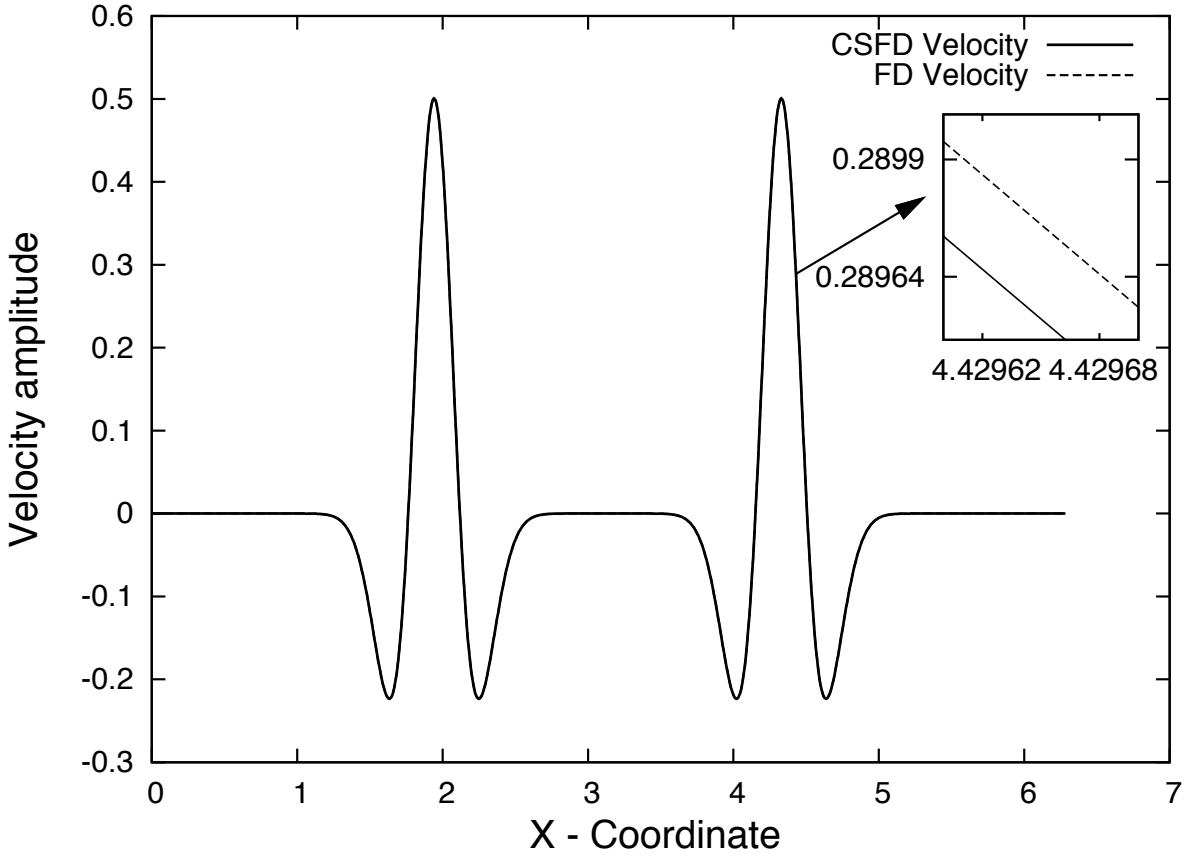

Figure 5.10: Comparison of velocity calculations using the second order wave equation solved with FDM (Eq. 3.17) and the first order wave equation solved with CSFDM (Eq. 5.12) in a homogeneous medium. It can be appreciated how the CSFDM propagates the wave in two directions giving the same result of the conventional FDM.

than the 1D case presented in previous Sections.

The acoustic wave equation in a 1D, 2D or 3D medium describes a longitudinal movement, i.e., the direction of the particle motion is the same of the direction of propagation. Gases and liquids are states of the matter that, except for viscous stresses, do not respond to shear strain. The restoring force responsible for wave propagation phenomena is due to a pressure change (normal stress) in the body.

The multidimensional second order (two-way) acoustic wave equation is given by the following expression (Cohen, 2001),

$$\frac{1}{\kappa(\mathbf{x})}\frac{\partial^2 \mathrm{P}}{\partial t^2}(\mathbf{x},t) - \nabla\cdot\left(\frac{1}{\rho(\mathbf{x})}\nabla \mathrm{P}(\mathbf{x},t)\right) = f(\mathbf{x},t), \tag{5.43}$$

where P is the pressure, the operator $\nabla = \left(\partial/\partial x_1, ..., \partial/\partial x_d\right)^T$, ρ is the density and κ is the bulk modulus, both strictly positive functions of position the vector $\mathbf{x}$.

The velocity c of sound wave propagation is given by

$$c(\mathbf{x}) = \sqrt{\frac{\kappa(\mathbf{x})}{\rho(\mathbf{x})}}. \tag{5.44}$$

In the absence of sources we must need to have initial conditions of displacement and velocity

$$\mathrm{P}(\mathbf{x},0) = \mathrm{P}_0(\mathbf{x}), \quad \frac{\partial \mathrm{P}}{\partial t}(\mathbf{x},0) = \mathrm{P}_1(\mathbf{x}).$$

The first order multidimensional wave equation or one-way acoustic wave equation in a "n" dimensional space is given by the following expression

$$\frac{1}{\sqrt{\kappa(\mathbf{x})}}\frac{\partial \mathrm{P}}{\partial t}(\mathbf{x},t) - \nabla\cdot\left(\frac{1}{\sqrt{\rho(\mathbf{x})}}\mathrm{P}(\mathbf{x},t)\right) = f(\mathbf{x},t), \tag{5.45}$$

In the absence of sources, with initial conditions of displacement

$$\mathrm{P}(\mathbf{x},0) = \mathrm{P}_0(\mathbf{x}).$$

Equation 5.45 has not been widely used in numerical simulations of the wave propagation problem in a 2D and/or 3D medium by the FDM, due to intrinsic limitations of the method to propagate the wave in all directions. However, this limitations of unidirectional propagation by the FD approximation to Eq. 5.45 in higher dimensions has been widely used in the design of non reflecting (absorbing) boundary conditions (e.g. Clayton and Engquist (1980)). On the other hand, paraxial approximations to the 2D and 3D one-way wave equation has been widely used in geophysical imaging/migration (e.g. Claerbout (1986), Tappert (1977)). Exact one-way wave equations in a 2D medium, has been used in the context of the Fourier domain, where the factorization of the wave equation is easily made (e.g. Angus et al. (2004)).

Commonly, first order hyperbolic systems of coupled PDE are used to solve the wave propagation problem (e.g. Virieux (1986), Moczo et al. (2004b)). That is not the case of Eq. 5.45, which is a higher dimensional non-coupled PDE. We illustrate the limitations of the FDM to solve the 2D one-way wave equation in all directions in the next Section.

5.5.1 2D first order acoustic wave equation

The first order acoustic wave equation in a homogeneous two dimensional space is given by the following mathematical expression

$$\frac{\partial \mathrm{P}}{\partial t} = \sqrt{\frac{\kappa}{\rho}} \left(\frac{\partial \mathrm{P}}{\partial x} + \frac{\partial \mathrm{P}}{\partial z} \right) + f, \tag{5.46}$$

where $\mathrm{P} = \mathrm{P}(x, z, t)$.

The most common FD discretization is made by using the centered approximation to the first derivative at both sides of Eq. 5.46, which leads to the following expression

$$\mathrm{P}^{t+\Delta t}_{x,z} = \Delta t \sqrt{\frac{\kappa}{\rho}} \left(\frac{\mathrm{P}^{t}_{x+\Delta x,z} - \mathrm{P}^{t}_{x-\Delta x,z}}{\Delta x} + \frac{\mathrm{P}^{t}_{x,z+\Delta z} - \mathrm{P}^{t}_{x,z-\Delta z}}{\Delta z} \right) + \mathrm{P}^{t-\Delta t}_{x,z} + \mathcal{O}\left(\Delta t^2, \Delta x^2, \Delta z^2\right). \tag{5.47}$$

The CSFD discretization to Eq. 5.46 in homogeneous media is given by the following expression

$$\begin{aligned}
&\mathfrak{Im}\left(\mathrm{P}^{t+\Delta t+\mathbf{i}\sqrt{3}\Delta t}_{x+\mathbf{i}\sqrt{3}\Delta x,z+\mathbf{i}\sqrt{3}\Delta z}\right) \\
&\quad = \Delta t \sqrt{\frac{\kappa}{\rho}} \left[\frac{\mathfrak{Im}\left(\mathrm{P}^{t+\mathbf{i}\sqrt{3}\Delta t}_{x+\Delta x+\mathbf{i}\sqrt{3}\Delta x,z+\mathbf{i}\sqrt{3}\Delta z}\right) + \mathfrak{Im}\left(\mathrm{P}^{t+\mathbf{i}\sqrt{3}\Delta t}_{x-\Delta x+\mathbf{i}\sqrt{3}\Delta x,z+\mathbf{i}\sqrt{3}\Delta z}\right)}{\Delta x} \right] \\
&\quad + \Delta t \sqrt{\frac{\kappa}{\rho}} \left[\frac{\mathfrak{Im}\left(\mathrm{P}^{t+\mathbf{i}\sqrt{3}\Delta t}_{x+\mathbf{i}\sqrt{3}\Delta x,z+\Delta z+\mathbf{i}\sqrt{3}\Delta z}\right) + \mathfrak{Im}\left(\mathrm{P}^{t+\mathbf{i}\sqrt{3}\Delta t}_{x+\mathbf{i}\sqrt{3}\Delta x,z-\Delta z+\mathbf{i}\sqrt{3}\Delta z}\right)}{\Delta z} \right] \\
&\quad - \mathfrak{Im}\left(\mathrm{P}^{t-\Delta t+\mathbf{i}\sqrt{3}\Delta t}_{x+\mathbf{i}\sqrt{3}\Delta x,z+\mathbf{i}\sqrt{3}\Delta z}\right) + \mathcal{O}\left(\Delta t^4, \Delta x^4, \Delta z^4\right).
\end{aligned} \tag{5.48}$$

Convergence, consistence and stability analysis

We apply Lax Equivalence Theorem and Von Neumann stability analysis to determine whether an approximation is convergent and stable. Substituting $\mathrm{P} = \mathrm{G}(\omega, t) e^{\mathbf{i}k(x+z)}$ into discretizations 5.47 and 5.48 and setting $\Delta x = \Delta z$ and $\mathrm{S} = \frac{\Delta t}{\Delta x}\sqrt{\frac{\kappa}{\rho}}$, we get the following expression for discretization 5.47

$$\mathrm{G}^2 - 4\mathbf{i}\mathrm{S}\sin k\Delta x\,\mathrm{G} - 1 = 0, \tag{5.49}$$

with solutions

$$\mathrm{G} = 2\mathbf{i}\mathrm{S}\sin k\Delta x \pm \sqrt{1 - 4\mathrm{S}^2 \sin^2 k\Delta x}, \tag{5.50}$$

if we call $\sin r = 2\mathrm{S}\sin k\Delta x$ we can write

$$\mathrm{G} = \mathbf{i}\sin r \pm \cos r,$$

which is

$$\mathrm{G}_1 = e^{\mathbf{i}\arcsin\left(2\mathrm{S}\sin k\Delta x\right)}, \tag{5.51}$$

$$\mathrm{G}_2 = -e^{-\mathbf{i}\arcsin\left(2\mathrm{S}\sin k\Delta x\right)}. \tag{5.52}$$

G_1 and G_2 are exactly on the unit circle. With $\|\mathrm{G}\| = 1$ there is no room to move, (Strang, 2007).

Note the particular case when $k\Delta x = \pi$, both solutions are different, i.e., the correct root is $\mathrm{G}_1 = 1$ and the other strange root is $\mathrm{G}_2 = -1$, which is related to the rapid oscillations in time of the parasitic mode (see Strikwerda (2004) for further details).

For Eq. 5.48 we get the following

$$\mathrm{G}^2 - 2\left(\mathrm{S}\cos k\Delta x\right)\mathrm{G} + 1 = 0, \tag{5.53}$$

with solutions

$$\mathrm{G} = \left(\mathrm{S}\cos k\Delta x\right) \pm \sqrt{\mathrm{S}^2\cos^2 k\Delta x - 1}. \tag{5.54}$$

Note the particular case when $k\Delta x = 2\pi$, both solutions are equal. This ensures the absence of numerical noise (parasitic waves) for certain wavelengths.

For both schemes to ensure $\|\mathrm{G}\| \leq 1$ we get $\mathrm{S} \leq 1/2$.

In previous Sections we have seen the equivalence of modeling the second order wave equation by FDM and the first order wave equation by CSFDM. This can be also appreciated in the 2D case. The only difference is now the Courant number stability conditions which is $\mathrm{S} \leq 1/2$ for the one-way wave equation and $\mathrm{S} \leq 1/\sqrt{2}$ for the two-way wave equation (see Appendix A.2). This mean we get the same results for the maximum Courant number of both schemes but over a different time scale, as long as the time dependent source is the same in both schemes.

Dispersion and dissipation analysis

Introducing the plane wave solution into discretizations 5.47 and 5.48 and setting $\Delta x = \Delta z$ and $\mathrm{S} = \frac{\Delta t}{\Delta x}\sqrt{\frac{\kappa}{\rho}}$ we get respectively

$$\sin\omega\Delta t = 2\mathrm{S}\sin k\Delta x, \tag{5.55}$$

$$\cos\omega\Delta t = 2\mathrm{S}\cos k\Delta x. \tag{5.56}$$

Clearly the schemes are dispersive and non-dissipative.

Numerical example

In order to illustrate the FD and CSFD disretizations to the one-way wave equation in a two dimensional space, we present numerical simulations of a point Ricker source in a homogeneous medium: length in the x direction $L_x = 2\pi$ km, length in the z direction $L_z = L_x$, number of space discretizations $nx = 200$ and $nz = nx$ ($\Delta x = \Delta z = 0.0314$ km), number of time steps $nt = 200$, wave speed $c = 1.45$ km/s, Courant number $\mathrm{S} = 0.5$, time step $\Delta t = \mathrm{S}\Delta x$. The Ricker source (Eq. 5.42) with parameters: dominant frequency $f0 = 1/(10\Delta t)$ and time delay $t0 = 4/f0$.

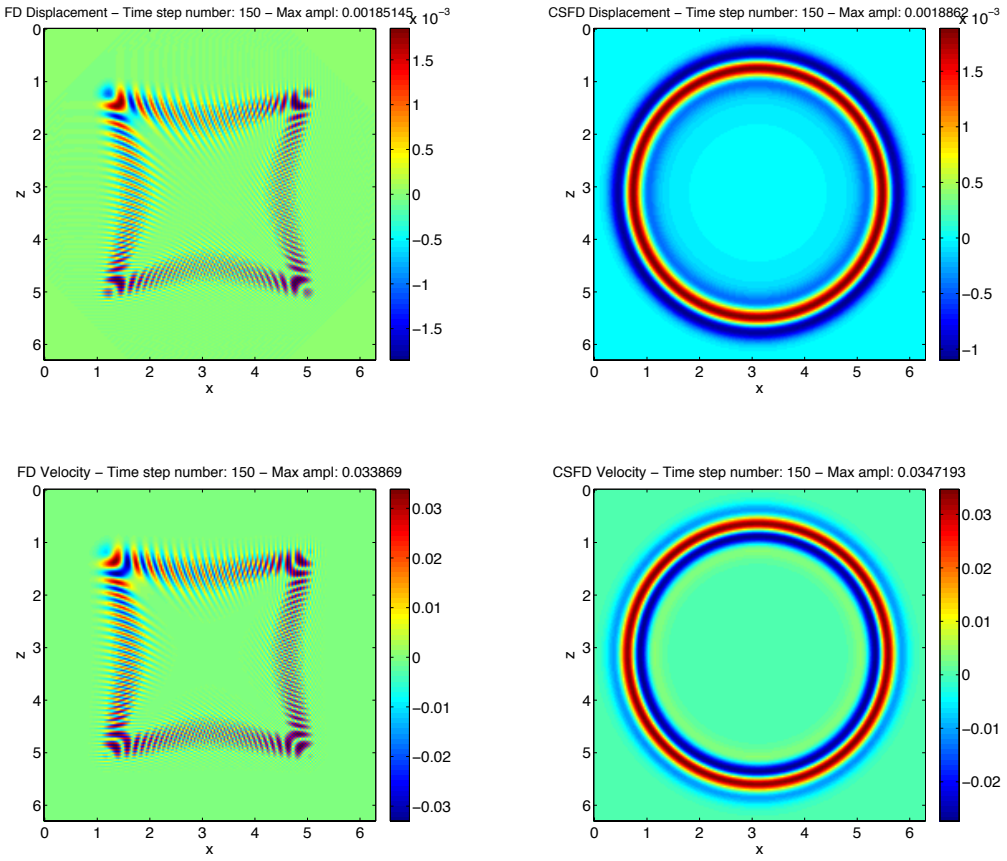

Figure 5.11: One-way two dimensional acoustic wave equation snapshot simulation with Finite Differences and Complex Step Finite Differences. We can appreciate how the FDM only propagate the wave in an angle of 45, 135, 225 and 315 degrees only unlike the CSFDM that correctly propagates the wave.

It is well know that the FD upwind scheme in a two dimensional media propagates wave in 45, 135, 225 and 315 degrees only. This fact is appreciated in Fig. 5.11, where the wave propagates in a direction of 45, 135, 225 and 315 degrees only and the rest of the space is filled by parasitic modes. Fig. 5.12 show seismogram comparisons of displacement and velocity with a receiver located in an angle of 45 degrees. It can be appreciated how both solutions fit. Fig. 5.13 show seismograms comparison of the CSFDM with the analytical solution, as expected with the maximum Courant number of 0.5 the method reproduces the analytical solution.

The superiority of the Leapfrog for the second order wave equation (discretization 5.48 in homogeneous media) over the Leapfrog for the first order wave equation (discretization 5.47) is regarding the presence of high order oscillations that does not affect the convergence of the second order Leapfrog and it does for the first order Leapfrog. This is due to the extra initial data in the discretization that restricts the amplitude of high frequencies that are growing linearly (see Strikwerda (2004) page 195 for further details).

5.5.2 3D first order acoustic wave equation

In order have a physical interpretation of the 3D first order wave equation, we first derive the equation of equilibrium in a infinitesimal medium due to an acoustic source perturbation:

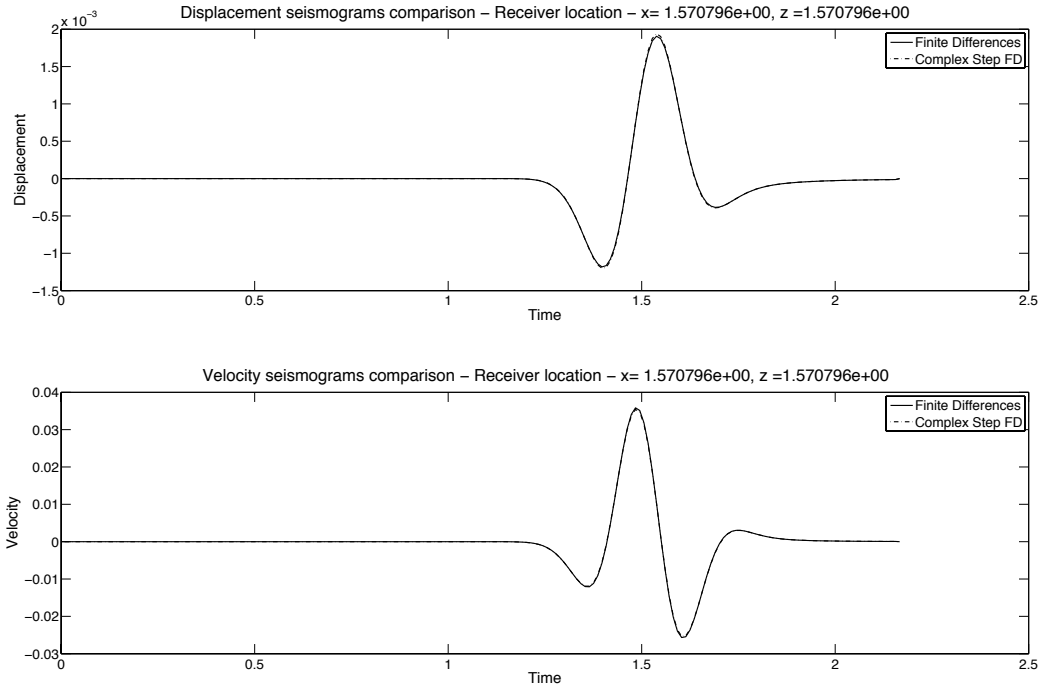

Figure 5.12: Finite Differences and Complex Step Finite Differences one-way two dimensional acoustic wave equation simulation seismograms comparison at a receiver located at 45 degrees.

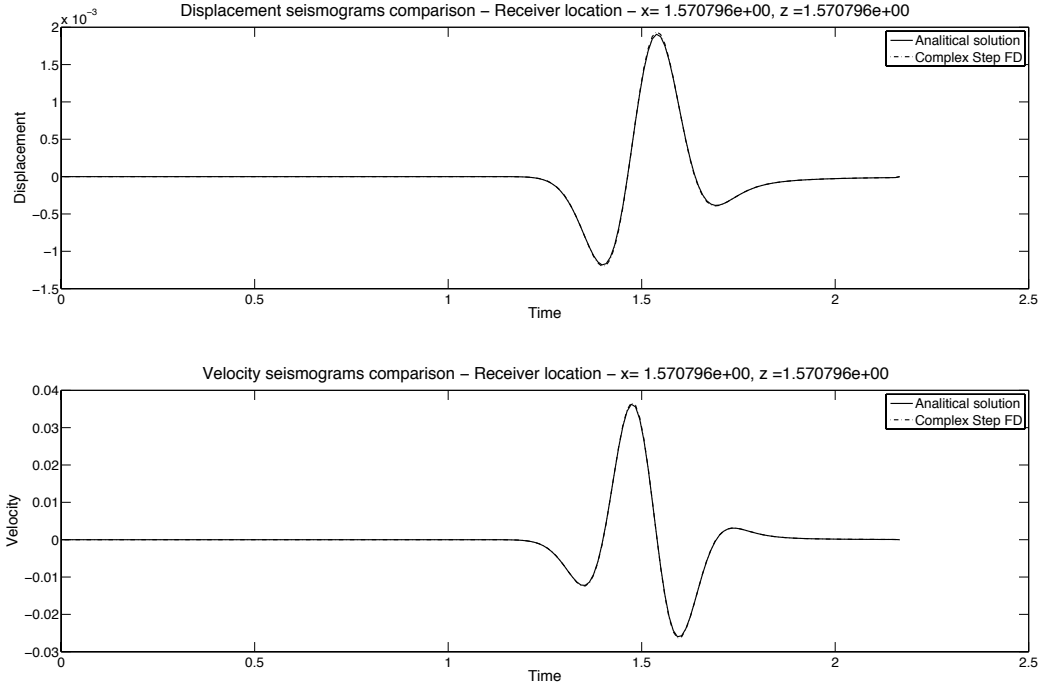

Figure 5.13: Complex Step Finite Differences one-way two dimensional acoustic wave equation simulation seismograms comparison with the analytical solution.

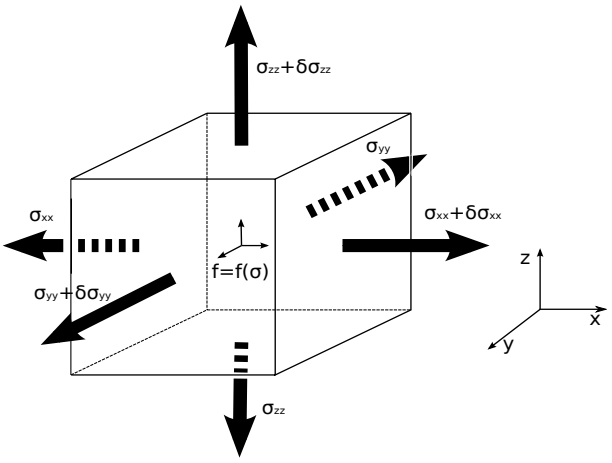

Figure 5.14: Three dimensional infinitesimal medium subject to a pressure force.

Consider the 3D medium given in Fig. 5.14. As mentioned before the acoustic movement is only affected by normal stress or pressure $(\mathrm{P} = \mathrm{P}(\sigma_{xx}, \sigma_{yy}, \sigma_{zz})) = \mathrm{P}(\mathrm{P}_x, \mathrm{P}_y, \mathrm{P}_z))$. The total amount of energy accumulation due to the acoustic source is given by

$$\begin{aligned}&\left(\sigma_{xx} + \delta\sigma_{xx} - \sigma_{xx}\right)\delta y\delta z + \left(\sigma_{yy} + \delta\sigma_{yy} - \sigma_{yy}\right)\delta x\delta z + \left(\sigma_{zz} + \delta\sigma_{zz} - \sigma_{zz}\right)\delta x\delta y \\ &+ f(\sigma_{xx}, \sigma_{yy}, \sigma_{zz})\delta x\delta y\delta z. \end{aligned} \tag{5.57}$$

In case of total equilibrium we get

$$\begin{aligned}&\left(\sigma_{xx} + \delta\sigma_{xx} - \sigma_{xx}\right)\delta y\delta z + \left(\sigma_{yy} + \delta\sigma_{yy} - \sigma_{yy}\right)\delta x\delta z + \left(\sigma_{zz} + \delta\sigma_{zz} - \sigma_{zz}\right)\delta x\delta y \\ &+ f(\sigma_{xx}, \sigma_{yy}, \sigma_{zz})\delta x\delta y\delta z = 0, \end{aligned} \tag{5.58}$$

dividing by $\delta x\delta y\delta z$ and taking the limit when $\delta x, \delta y, \delta z \to 0$ we get the equation of acoustic equilibrium

$$\frac{\partial\sigma_{xx}}{\partial x} + \frac{\partial\sigma_{yy}}{\partial y} + \frac{\partial\sigma_{zz}}{\partial z} + f(\sigma_{xx}, \sigma_{yy}, \sigma_{zz}) = 0. \tag{5.59}$$

In case of non-equilibrium the total amount of energy accumulation must be equal to the total flow of energy inside the body, i.e.,

$$\begin{aligned}&\left(\sigma_{xx} + \delta\sigma_{xx} - \sigma_{xx}\right)\delta y\delta z + \left(\sigma_{yy} + \delta\sigma_{yy} - \sigma_{yy}\right)\delta x\delta z + \left(\sigma_{zz} + \delta\sigma_{zz} - \sigma_{zz}\right)\delta x\delta y \\ &+ f(\sigma_{xx}, \sigma_{yy}, \sigma_{zz})\delta x\delta y\delta z = \sqrt{\frac{\rho}{\kappa}}\frac{\partial\sigma}{\partial t}\delta x\delta y\delta z, \end{aligned} \tag{5.60}$$

dividing by $\delta x\delta y\delta z$ and taking the limit when $\delta x, \delta y, \delta z \to 0$ we get the first order acoustic wave equation in a homogeneous three dimensional space

$$\frac{\partial\sigma}{\partial t} = \sqrt{\frac{\kappa}{\rho}}\left(\frac{\partial\sigma_{xx}}{\partial x} + \frac{\partial\sigma_{yy}}{\partial y} + \frac{\partial\sigma_{zz}}{\partial z}\right) + f, \tag{5.61}$$

by calling pressure $\mathrm{P} = \mathrm{P}(\sigma_{xx}, \sigma_{yy}, \sigma_{zz})$ we can write

$$\frac{\partial \mathrm{P}}{\partial t} = \sqrt{\frac{\kappa}{\rho}} \left(\frac{\partial \mathrm{P}}{\partial x} + \frac{\partial \mathrm{P}}{\partial y} + \frac{\partial \mathrm{P}}{\partial z} \right) + f, \tag{5.62}$$

with $\mathrm{P} = \mathrm{P}(x, y, z, t)$.

The CSFD discretization to Eq. 5.62 in homogeneous media is given by the following expression

$$\begin{aligned}
&\mathfrak{Im}\left(\mathrm{P}^{t+\Delta t+\mathbf{i}\sqrt{3}\Delta t}_{x+\mathbf{i}\sqrt{3}\Delta x,y+\mathbf{i}\sqrt{3}\Delta y,z+\mathbf{i}\sqrt{3}\Delta z}\right) \\
&= \Delta t\sqrt{\frac{\kappa}{\rho}}\left[\frac{\mathfrak{Im}\left(\mathrm{P}^{t+\mathbf{i}\sqrt{3}\Delta t}_{x+\Delta x+\mathbf{i}\sqrt{3}\Delta x,y+\mathbf{i}\sqrt{3}\Delta y,z+\mathbf{i}\sqrt{3}\Delta z}\right)+\mathfrak{Im}\left(\mathrm{P}^{t+\mathbf{i}\sqrt{3}\Delta t}_{x-\Delta x+\mathbf{i}\sqrt{3}\Delta x,y+\mathbf{i}\sqrt{3}\Delta y,z+\mathbf{i}\sqrt{3}\Delta z}\right)}{\Delta x}\right] \\
&+ \Delta t\sqrt{\frac{\kappa}{\rho}}\left[\frac{\mathfrak{Im}\left(\mathrm{P}^{t+\mathbf{i}\sqrt{3}\Delta t}_{x+\mathbf{i}\sqrt{3}\Delta x,y+\Delta y+\mathbf{i}\sqrt{3}\Delta y,z+\mathbf{i}\sqrt{3}\Delta z}\right)+\mathfrak{Im}\left(\mathrm{P}^{t+\mathbf{i}\sqrt{3}\Delta t}_{x+\mathbf{i}\sqrt{3}\Delta x,y-\Delta y+\mathbf{i}\sqrt{3}\Delta y,z+\mathbf{i}\sqrt{3}\Delta z}\right)}{\Delta y}\right] \\
&+ \Delta t\sqrt{\frac{\kappa}{\rho}}\left[\frac{\mathfrak{Im}\left(\mathrm{P}^{t+\mathbf{i}\sqrt{3}\Delta t}_{x+\mathbf{i}\sqrt{3}\Delta x,y+\mathbf{i}\sqrt{3}\Delta y,z+\Delta z+\mathbf{i}\sqrt{3}\Delta z}\right)+\mathfrak{Im}\left(\mathrm{P}^{t+\mathbf{i}\sqrt{3}\Delta t}_{x+\mathbf{i}\sqrt{3}\Delta x,y+\mathbf{i}\sqrt{3}\Delta y,z-\Delta z+\mathbf{i}\sqrt{3}\Delta z}\right)}{\Delta z}\right] \\
&- \mathfrak{Im}\left(\mathrm{P}^{t-\Delta t+\mathbf{i}\sqrt{3}\Delta t}_{x+\mathbf{i}\sqrt{3}\Delta x,y+\mathbf{i}\sqrt{3}\Delta y,z+\mathbf{i}\sqrt{3}\Delta z}\right) + \mathcal{O}\left(\Delta t^4, \Delta x^4, \Delta y^4, \Delta z^4\right).
\end{aligned} \tag{5.63}$$

Convergence, consistence and stability analysis

Substituting $\mathrm{P} = \mathrm{G}(\omega, t)e^{\mathbf{i}k(x+y+z)}$ into discretization 5.63 and by setting $\Delta x = \Delta y = \Delta z$ and $\mathrm{S} = \frac{\Delta t}{\Delta x}\sqrt{\frac{\kappa}{\rho}}$ we get

$$\mathrm{G}^2 - 2\left(3\mathrm{S}\cos k\Delta x\right)\mathrm{G} + 1 = 0. \tag{5.64}$$

For $\|\mathrm{G}\| \leq 1$ we get $\mathrm{S} \leq 1/3$.

Like the 2D case, the only difference modeling the second order wave equation by FDM and the first order wave equation by CSFDM is the Courant number stability condition which is $\mathrm{S} \leq 1/\sqrt{3}$ and $\mathrm{S} \leq 1/3$ respectively, which means we get the same results for the maximum Courant number of both schemes but over a different time scale, of course as long as the time dependent source is the same in both schemes.

Dispersion-dissipation analysis

Introducing the plane wave solution into discretization 5.63 and assuming $\Delta x = \Delta y = \Delta z$ we get

$$\cos\omega\Delta t = 3\mathrm{S}\cos k\Delta x. \tag{5.65}$$

Clearly the scheme is dispersive and non-dissipative.

Numerical example

In order to illustrate the CSFD disretization to the one-way wave equation in a three dimensional space, we present numerical simulations of a point Ricker source in a homogeneous medium: length in the x direction $L_x = 2\pi$ km, length in the y and z direction $L_z = L_y = L_x$, number of space discretizations $nx = 50$ and $nz = ny = nx$ ($\Delta x = \Delta y = \Delta z = 0.0314$ km),

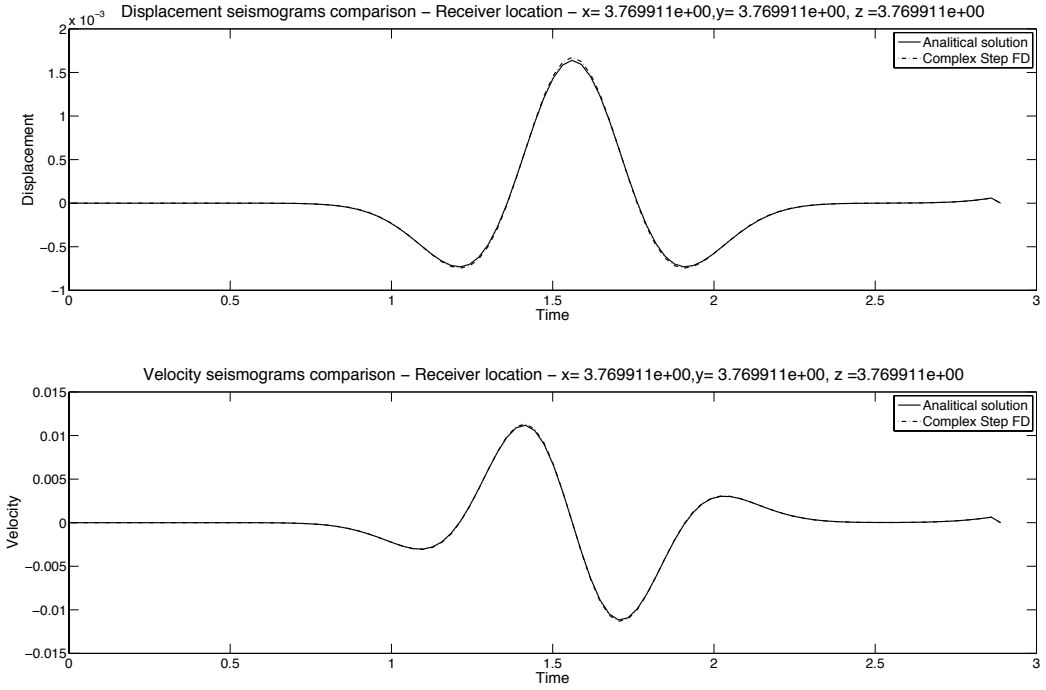

Figure 5.15: Complex Step Finite Differences one-way three dimensional acoustic wave equation simulation seismograms comparison with the analytical solution.

number of time steps $nt = 100$, wave speed $c = 1.45\,\text{km/s}$, Courant number $\text{S} = 1/3$, time step $\Delta t = \text{S}\Delta x$. The Ricker source (Eq. 5.42) with parameters: dominant frequency $f0 = 1/(10\Delta t)$ and time delay $t0 = 4/f0$.

Figure 5.15 shows comparison of CSFD seismograms results. As expected by using the maximum Courant number of $1/3$, the CSFDM reproduces the analytical solutions.

Chapter 6

The Complex Step Finite Differences Method Applied to the 1D Elastic Wave Equation: stability and dispersion analysis

6.1 Introduction

In this Chapter we investigate stability and dispersion properties of higher order finite differences (FD) and complexs Step finite differences (CSFD) approximations to the one dimensional acoustic/elastic wave equation. We compare stability and dispersion properties of the introduced CSFD schemes for the first order wave equation with the conventional FD approximations for the second order wave equation.

This Chapter first introduces (Section 6.2) the 1D Finite Differences Method (FDM) for the second order wave equation and the most common higher order schemes. In Section 6.3 the 1D Complex Steps Finite Differences Method (CSFDM) is introduced for solving the first order wave equation in two directions. In Section 6.4 a complete stability and dispersion analysis of the FD and CSFD schemes is done. In Section 6.5 explains the direct connection between FDM and CSFDM.

6.2 Higher order finite differences approximations to the 1D elastic wave equation

The study of 1D numerical partial differential problems correspond the basis of every 3D numerical method design. We need first to analyze properties of the 1D problem in order to establish the scope and application range of the numerical technique for 3D problems. After having determined advantages and disadvantages, that is, having knowledge where the numerical tool will reproduce reliable results, we can design the numerical experiment.

The mathematical expression for the 1D elastic wave equation is the same for the 1D acoustic wave equation with the only difference in the velocity propagation term. Recalling Chapter 3, the 1D acoustic/elastic wave equation in a homogeneous medium is given by Eq. 3.15, subject to initial conditions of displacement and speed is called the *initial value problem*.

In an elastic medium we can find different types of 1D waves, e.g., P, SV and SH waves. All of this waves belong to the same mathematical expression (Eq. 3.15), with the difference in the velocity expressions:

$$c = \sqrt{\frac{\lambda + 2\mu}{\rho}} \quad \text{for a P wave,} \tag{6.1}$$

$$c = \sqrt{\frac{\mu}{\rho}} \quad \text{for a SV and SH waves,} \tag{6.2}$$

where λ and μ are Lame elastic parameters and ρ is the density.

Generalization of Eq. 3.15 to non constant coefficients, i.e., taking into account variations of speed (heterogeneous media), is given by the following expression

$$\frac{\partial^2 u}{\partial t^2} = \nabla \cdot \left(c(x)^2 \, \nabla u \right), \tag{6.3}$$

where the operator ∇ is the gradient and $\nabla\cdot$ is the divergence. Note the velocity is non longer constant and this change is taken into account by the divergence operator.

Equation 3.15 and/or Eq. 6.3 are called two-way wave equations: this mean they are *differential operator* that propagates a wave in two directions (positive and negative directions).

If we rearrange and factorize Eq. 3.15 we can write the following

$$\frac{\partial^2 u}{\partial t^2} - c^2 \frac{\partial^2 u}{\partial x^2} = \left(\frac{\partial^2}{\partial t^2} - c^2 \frac{\partial^2}{\partial x^2} \right) u = \left[\left(\frac{\partial}{\partial t} - c \frac{\partial}{\partial x} \right) \left(\frac{\partial}{\partial t} + c \frac{\partial}{\partial x} \right) \right] u = 0. \tag{6.4}$$

The two differential operators in which the two-way wave equation (Eq. 3.15) can be decomposed are called one-way wave differential operators. Following this, we can write the one-way wave equation by the following expression

$$\frac{\partial u}{\partial t} = c \, \nabla \cdot u. \tag{6.5}$$

The one-way wave equation (Eq. 6.5) is also called the first order wave equation and propagates the wave in one direction only (positive or negative). The first order and second order wave equations are the basis of numerical experiments design in computational wave propagation in seismology.

6.2.1 Higher order Finite Differences discretizations

The FDM is nowadays a powerful method in computational seismology. Its simplicity and low computational cost despite its intrinsic limitations allow perform numerical experiments in the most highest levels. In this Section we show the most common FD approximations to the second order wave equation.

The most basic FD approximation to the second derivative is given by Eq. 3.6. High order FD approximations to the second and fourth order derivatives are given by

$$\begin{aligned} f''(x) = & \frac{4}{3} \frac{f(x + \Delta x) - 2f(x) + f(x - \Delta x)}{\Delta x^2} \\ & - \frac{1}{3} \frac{f(x + 2\Delta x) - 2f(x) + f(x - 2\Delta x)}{4\Delta x^2} + \mathcal{O}\left(\Delta x^4\right). \end{aligned} \tag{6.6}$$

$$f^{iv}(x) = \frac{f(x + 2\Delta x) - 4f(x + \Delta x) + 6f(x) - 4f(x - \Delta x) + f(x - 2\Delta x)}{\Delta x^4} + \mathcal{O}\left(\Delta x^4\right). \tag{6.7}$$

In order to avoid clutter in our study, lets introduce the following differential operators

$$\Delta_x^+ f(x) = f(x + \Delta x) - f(x), \tag{6.8}$$

$$\Delta_x^- f(x) = f(x) - f(x - \Delta x), \tag{6.9}$$

$$\square_x^{1/2} f(x) = f\left(x + \frac{\Delta x}{2}\right) - f\left(x - \frac{\Delta x}{2}\right). \tag{6.10}$$

In general we can write $\square$ operator as

$$\square_x^n f(x) = f\left(x + n\Delta x\right) - f\left(x - n\Delta x\right). \tag{6.11}$$

We can construct the second order derivative FD approximation (Eq. 3.6) as a convolution of two first order operators, that is

$$D_x^2 = \frac{\Delta_x^+}{\Delta x} \circ \frac{\Delta_x^-}{\Delta x} = \frac{\square_x^{1/2}}{\Delta x} \circ \frac{\square_x^{1/2}}{\Delta x}, \tag{6.12}$$

where

$$D_x^2 = \frac{f(x + \Delta x) - 2f(x) + f(x - \Delta x)}{\Delta x^2}. \tag{6.13}$$

Also, the fourth order approximation for the second derivative (Eq. 6.6) can be written as

$$D_x^{2^{4^{th}}} = \frac{4}{3}\left(\frac{\Delta_x^+}{\Delta x} \circ \frac{\Delta_x^-}{\Delta x}\right) - \frac{1}{12}\left(\frac{\square_x}{\Delta x} \circ \frac{\square_x}{\Delta x}\right) = \frac{4}{3}\left(\frac{\square_x^{1/2}}{\Delta x} \circ \frac{\square_x^{1/2}}{\Delta x}\right) - \frac{1}{12}\left(\frac{\square_x}{\Delta x} \circ \frac{\square_x}{\Delta x}\right), \tag{6.14}$$

where

$$D_x^{2^{4^{th}}} = \frac{4}{3}\frac{f(x + \Delta x) - 2f(x) + f(x - \Delta x)}{\Delta x^2} - \frac{1}{3}\frac{f(x + 2\Delta x) - 2f(x) + f(x - 2\Delta x)}{4\Delta x^2}. \tag{6.15}$$

In the same way, we can construct the fourth order derivative FD approximation (Eq. 6.7) by

$$D_x^4 = D_x^2 \circ D_x^2 = -4\left(\frac{\Delta_x^+}{\Delta x^2} \circ \frac{\Delta_x^-}{\Delta x^2}\right) + \frac{\square_x}{\Delta x^2} \circ \frac{\square_x}{\Delta x^2} = -4\left(\frac{\square_x^{1/2}}{\Delta x^2} \circ \frac{\square_x^{1/2}}{\Delta x^2}\right) + \frac{\square_x}{\Delta x^2} \circ \frac{\square_x}{\Delta x^2}, \tag{6.16}$$

where

$$D_x^4 = \frac{f(x + 2\Delta x) - 4f(x + \Delta x) + 6f(x) - 4f(x - \Delta x) + f(x - 2\Delta x)}{\Delta x^4}. \tag{6.17}$$

As we will see in the next Section, in general, the operator formulation of FD approximations is more convenient to express high order FD discretizations to the wave equation.

Finite Differences discretizations in homogeneous media (constant coefficients)

The simplest FD discretization to the second order wave equation in homogeneous medium (constant velocity, Eq. 3.15) is given by applying approximation 3.6 at both sides of the equation

$$\frac{u_x^{t+\Delta t} - 2u_x^t + u_x^{t-\Delta t}}{\Delta t^2} = c^2 \frac{u_{x+\Delta x}^t - 2u_x^t + u_{x-\Delta x}^t}{\Delta x^2} + \mathcal{O}\left(\Delta t^2, \Delta x^2\right). \tag{6.18}$$

If we do consider higher order derivatives in the Taylor's approximation of Eq. 3.6 we can write discretization 6.18 as follows

$$\frac{u_x^{t+\Delta t} - 2u_x^t + u_x^{t-\Delta t}}{\Delta t^2} - \frac{\Delta t^2}{12}\frac{\partial^4 u}{\partial t^4} = c^2 \frac{u_{x+\Delta x}^t - 2u_x^t + u_{x-\Delta x}^t}{\Delta x^2} - c^4 \frac{\Delta x^2}{12}\frac{\partial^4 u}{\partial x^4} + \mathcal{O}\left(\Delta t^4, \Delta x^4\right). \tag{6.19}$$

A popular discretization is seismology is given by considering a fourth order accurate approximation in space. Although this introduces numerical dispersion into the solution, it can handle smooth heterogeneous media in acceptable way unlike discretization 6.18. The second order accurate in time and fourth order accurate in space discretization is given by the following expression

$$\begin{aligned}\frac{u_x^{t+\Delta t} - 2u_x^t + u_x^{t-\Delta t}}{\Delta t^2} &= \frac{4}{3}c^2 \frac{u_{x+\Delta x}^t - 2u_x^t + u_{x-\Delta x}^t}{\Delta x^2} \\ &- \frac{1}{3}c^2 \frac{u_{x+2\Delta x}^t - 2u_x^t + u_{x-2\Delta x}^t}{4\Delta x^2} + \mathcal{O}\left(\Delta t^2, \Delta x^4\right).\end{aligned} \tag{6.20}$$

Commonly, seismologist are not interested in discretizing the fourth order derivative in time in Eq. 6.19 because it leads to more computational time consuming algorithms, so one way to introduce more accurate time discretizations, is to express the time derivative as a spatial derivative by considering higher order approximations in space. The modified equation approach, introduced by Dablain (1986), consist in expressing time derivatives as space derivatives by considering the continuity of the wave equation as follows

$$\frac{\partial^4 u}{\partial t^4} = \frac{\partial^2}{\partial t^2}\left(\frac{\partial^2 u}{\partial t^2}\right) = \frac{\partial^2}{\partial t^2}\left(c^2 \frac{\partial^2 u}{\partial x^2}\right) = c^2 \frac{\partial^2}{\partial x^2}\left(\frac{\partial^2 u}{\partial t^2}\right) = c^4 \frac{\partial^4 u}{\partial x^4}. \tag{6.21}$$

Based on Eq. 6.21 and using Eqs. 6.19-6.20 we can write a discretization fourth order accurate in space and time as follows

$$\begin{aligned}\frac{u_x^{t+\Delta t} - 2u_x^t + u_x^{t-\Delta t}}{\Delta t^2} &= \frac{4}{3}c^2 \frac{u_{x+\Delta x}^t - 2u_x^t + u_{x-\Delta x}^t}{\Delta x^2} \\ &- \frac{1}{3}c^2 \frac{u_{x+2\Delta x}^t - 2u_x^t + u_{x-2\Delta x}^t}{4\Delta x^2} + c^4 \frac{\Delta t^2}{12}\frac{\partial^4 u}{\partial x^4} + \mathcal{O}\left(\Delta t^4, \Delta x^4\right).\end{aligned} \tag{6.22}$$

finally, using approximation 6.7 we get

$$\begin{aligned}\frac{u_x^{t+\Delta t} - 2u_x^t + u_x^{t-\Delta t}}{\Delta t^2} &= \frac{4}{3}c^2 \frac{u_{x+\Delta x}^t - 2u_x^t + u_{x-\Delta x}^t}{\Delta x^2} - \frac{1}{3}c^2 \frac{u_{x+2\Delta x}^t - 2u_x^t + u_{x-2\Delta x}^t}{4\Delta x^2} \\ &+ c^4 \frac{\Delta t^2}{12} \frac{u_{x+2\Delta x}^t - 4u_{x+\Delta x}^t + 6u_x^t - 4u_{x-\Delta x}^t + u_{x-2\Delta x}^t}{\Delta x^4} + \mathcal{O}\left(\Delta t^4, \Delta x^4\right).\end{aligned} \tag{6.23}$$

Equations 6.18, 6.20 and 6.23 are the most common basis for FD simulations of wave propagation in seismology by using the second order wave equation. Another popular scheme is called the staggered grid. This staggered grid schemes decompose the second order wave equation into a coupled system of first order differential equations. In this study we only make analyses of non-coupled PDE's.

Equations 6.18, 6.20 and 6.23 can also be written in a general compact operator form respectively as follows

$$D_t^2 u = c^2 D_x^2 u + \mathcal{O}\left(\Delta t^2, \Delta x^2\right), \tag{6.24}$$

$$D_t^2 u = c^2 D_x^{2^{4^{th}}} u + \mathcal{O}\left(\Delta t^2, \Delta x^4\right), \tag{6.25}$$

$$D_t^2 u = c^2 D_x^{2^{4^{th}}} u + c^4 \frac{\Delta t}{12} D^4 u + \mathcal{O}\left(\Delta t^4, \Delta x^4\right). \tag{6.26}$$

Finite Differences discretization in heterogeneous media (non constant coefficients)

In the case of heterogeneous media, the wave equation is given by expression 6.3. In practical applications is convenient to express the wave speed in terms of the density and the elastic parameter. For instance, we can write the expression for a P wave as follows

$$\rho(x)\frac{\partial^2 u}{\partial t^2} = \frac{\partial}{\partial x}\left(\left(\lambda(x) + 2\mu(x)\right)\frac{\partial u}{\partial x}\right), \tag{6.27}$$

and/or for a S wave as follows

$$\rho(x)\frac{\partial^2 u}{\partial t^2} = \frac{\partial}{\partial x}\left(\mu(x)\frac{\partial u}{\partial x}\right). \tag{6.28}$$

Obviously, the fact that the coefficients of the equation vary in space explains that the main difficulty comes form space discretization (Cohen and Joly, 1996). There are many different approximations respect to the choice of the elastic parameter. In this study we just show the most simple cases. The second order approximation in time and space is given by

$$\rho_x \frac{u_x^{t+\Delta t} - 2u_x^t + u_x^{t-\Delta t}}{\Delta t^2} = \frac{1}{\Delta x}\left[\mu_{x+\frac{\Delta x}{2}} \frac{u_{x+\Delta x}^t - u_x^t}{\Delta x} - \mu_{x-\frac{\Delta x}{2}} \frac{u_x^t - u_{x-\Delta x}^t}{\Delta x}\right] + \mathcal{O}\left(\Delta t^2, \Delta x^2\right), \tag{6.29}$$

where $\rho(x)$ and $\mu_{x+\frac{\Delta x}{2}}$ are defined by

$$\rho_x = \frac{1}{2\Delta x}\int_{x-\Delta x}^{x+\Delta x} \rho(x)\,\mathrm{d}x, \tag{6.30}$$

$$\mu_{x+\frac{\Delta x}{2}} = \frac{1}{\Delta x}\int_{x}^{x+\Delta x} \mu(x)\,\mathrm{d}x. \tag{6.31}$$

The fourth order accurate in space FD discretization given by

$$\rho_x \frac{u_x^{t+\Delta t} - 2u_x^t + u_x^{t-\Delta t}}{\Delta t^2} = \frac{4}{3}\frac{1}{\Delta x}\left[\mu_{x+\frac{\Delta x}{2}}\frac{u_{x+\Delta x}^t - u_x^t}{\Delta x} - \mu_{x-\frac{\Delta x}{2}}\frac{u_x^t - u_{x-\Delta x}^t}{\Delta x}\right] - \frac{1}{3}\frac{1}{2\Delta x}\left[\mu_{x+\Delta x}\frac{u_{x+2\Delta x}^t - u_x^t}{2\Delta x} - \mu_{x-\Delta x}\frac{u_x^t - u_{x-2\Delta x}^t}{2\Delta x}\right] + \mathcal{O}\left(\Delta t^2, \Delta x^4\right). \tag{6.32}$$

Note that the elastic coefficient μ is evaluated at point where the displacement is not defined ($x \pm \frac{\Delta x}{2}$).

In case of the first order wave equation the expression for heterogeneous media is given by

$$\frac{\partial u}{\partial t} = c(x)\nabla \cdot u. \tag{6.33}$$

Because the first order wave equation does not involves velocity derivatives, FD discretizations are the same for the homogeneous case avoiding evaluation of velocity parameters where displacements are not defined.

6.3 Complex Step Finite Differences approximations to the 1D elastic wave equation

The Complex Step (CS) method was introduced by Squire and Trapp (1998) and generalized by Abreu et al. (2013b). Based on this work Abreu et al. (2013a) introduced the called Complex Step Finite Differences Method (CSFDM) applied to he acoustic wave propagation problem in a 1D, 2D and 3D homogeneous medium. CSFDM can be seen as an extension to the complex numbers of the original FDM. An important difference outlined by Abreu et al. (2013a), is difference between the kind of wave equation that both method can be applied: CSFD can be used to propagate in two directions the one-way wave equation which can not be done by FDM without introducing parasitic modes.

The generalization made by Abreu et al. (2013b) consisted in taking complex steps in a strict sense, i.e., $h + \mathbf{i}v$, where h and v are differential steps ($h, v \in \mathbb{R}$ and $h, v \to 0$).

Follow, we list the CSFD approximations used in this study

$$f'(x) = \frac{\mathfrak{Im}(f(x + h + \mathbf{i}v))}{v} + \mathcal{O}\left(h, v^2\right), \tag{6.34}$$

$$f'(x) = \frac{\mathfrak{Im}(f(x + h + \mathbf{i}v)) + \mathfrak{Im}(f(x - h + \mathbf{i}v))}{2v} - \left(\frac{3h^2 - v^2}{3!}\right) f'''(x) - \left(\frac{5h^4 - 10h^2v^2 + v^4}{5!}\right) f^v(x) + \mathcal{O}\left(7h^6 - 35h^4v^2 + 21h^2v^4 - v^6\right). \tag{6.35}$$

Note that we can choose values of v in order to be able to control the approximation error in Eq. 6.35. For instance, if we set $v = \sqrt{3}h$, the approximation error becomes $\mathcal{O}\left(h^4\right)$.

Simple expressions for the second, third and fifth derivative are given by Eq. 4.35 and the following expressions

$$f''(x) = \frac{\mathfrak{Im}(f(x + h + \mathbf{i}v)) - \mathfrak{Im}(f(x + \mathbf{i}v))}{hv} + \mathcal{O}\left(h, v^2\right). \tag{6.36}$$

$$f'''(x) = \frac{\mathfrak{Im}(f(x+h+\mathbf{i}v)) - 2\,\mathfrak{Im}(f(x+\mathbf{i}v)) + \mathfrak{Im}(f(x-h+\mathbf{i}v))}{h^2 v} + \mathcal{O}\left(h^2 - 2v^2\right). \tag{6.37}$$

Note that the CSFD expression for the third order derivative (Eq. 6.37) is just a simple three levels scheme, also if we choose $h = \sqrt{2}v$ the error becomes $\mathcal{O}(h^4)$.

$$\begin{aligned} f'''(x) = & \frac{\mathfrak{Im}(f(x+h+\mathbf{i}v)) - 2\,\mathfrak{Im}(f(x+\mathbf{i}v)) + \mathfrak{Im}(f(x-h+\mathbf{i}v))}{5h^2 v} \\ & + \frac{\mathfrak{Im}(f(x+2h+\mathbf{i}v)) - 2\,\mathfrak{Im}(f(x+\mathbf{i}v)) + \mathfrak{Im}(f(x-2h+\mathbf{i}v))}{5h^2 v} + \mathcal{O}\left(34h^2 - 20v^2\right). \end{aligned} \tag{6.38}$$

We can obtain the fourth order version of Eq. 6.38 by using the appropriate weights

$$\begin{aligned} f'''(x) = & \left(16h^2 - 8v^2\right) \frac{\mathfrak{Im}(f(x+h+\mathbf{i}v)) - 2\,\mathfrak{Im}(f(x+\mathbf{i}v)) + \mathfrak{Im}(f(x-h+\mathbf{i}v))}{72h^4 v} \\ & + \left(2v^2 - h^2\right) \frac{\mathfrak{Im}(f(x+2h+\mathbf{i}v)) - 2\,\mathfrak{Im}(f(x+\mathbf{i}v)) + \mathfrak{Im}(f(x-2h+\mathbf{i}v))}{72h^4 v} \\ & + \mathcal{O}\left(4h^4 - 10h^2v^2 + 7v^4\right). \end{aligned} \tag{6.39}$$

$$\begin{aligned} f^v(x) = & \frac{\mathfrak{Im}(f(x+2h+\mathbf{i}v)) - 4\,\mathfrak{Im}(f(x+h+\mathbf{i}v)) + 6\,\mathfrak{Im}(f(x+\mathbf{i}v))}{h^4 v} \\ & + \frac{-4\,\mathfrak{Im}(f(x-h+\mathbf{i}v)) + \mathfrak{Im}(f(x-2h+\mathbf{i}v))}{h^4 v} + \mathcal{O}\left(h^2 - v^2\right). \end{aligned} \tag{6.40}$$

If we choose h and v to satisfy the equations $34h^2 = 20v^2$ and $h^2 = v^2$ in Eqs. 6.38 and 6.40 the error becomes $\mathcal{O}\left(h^4\right)$ respectively.

CSFD approximations can also be written in a general operator way by introducing the following operators

$$\rhd_x f(x) = f\left(x + \Delta x\right), \tag{6.41}$$

$$\lhd\rhd_x^n f(x) = f\left(x + n\Delta x\right) + f\left(x - n\Delta x\right). \tag{6.42}$$

We can write Eqs. 6.34-6.38 and Eq. 4.35, 6.40, respectively as follows

$$f'(x) = \frac{\rhd_x}{v}\mathfrak{Im}(f(x+\mathbf{i}v)) + \mathcal{O}\left(h, v^2\right), \tag{6.43}$$

$$\begin{aligned} f'(x) = & \frac{\lhd\rhd_x}{2v}\mathfrak{Im}(f(x+\mathbf{i}v)) - \left(\frac{3h^2 - v^2}{3!}\right) f'''(x) \\ & - \left(\frac{5h^4 - 10h^2v^2 + v^4}{5!}\right) f^v(x) + \mathcal{O}\left(7h^6 - 35h^4v^2 + 21h^2v^4 - v^6\right). \end{aligned} \tag{6.44}$$

$$f''(x) = \frac{\Delta_x^+}{hv}\mathfrak{Im}(f(x+\mathbf{i}v)) + \mathcal{O}\left(h, v^2\right). \tag{6.45}$$

$$f'''(x) = \frac{\Delta_x^+ \circ \Delta_x^-}{h^2 v} \Im\mathfrak{m}(f(x + \mathbf{i}v)) = \frac{\square_x^{1/2} \circ \square_x^{1/2}}{h^2 v} \Im\mathfrak{m}(f(x + \mathbf{i}v)) + \mathcal{O}\left(h^2 - 2v^2\right). \tag{6.46}$$

$$\begin{aligned} f'''(x) &= \frac{1}{5h^2 v}\left(\Delta_x^+ \circ \Delta_x^- + \square_x \circ \square_x\right) \Im\mathfrak{m}(f(x + \mathbf{i}v)) + \mathcal{O}\left(34h^2 - 20v^2\right) \\ &= \frac{1}{5h^2 v}\left(\square_x^{1/2} \circ \square_x^{1/2} + \square_x \circ \square_x\right) \Im\mathfrak{m}(f(x + \mathbf{i}v)) + \mathcal{O}\left(34h^2 - 20v^2\right), \end{aligned} \tag{6.47}$$

$$f''(x) = \frac{\square_x^{1/2}}{hv} \Im\mathfrak{m}(f(x + \mathbf{i}v)) + \mathcal{O}\left(h^2 - v^2\right), \tag{6.48}$$

$$f^v(x) = \frac{1}{h^4 v}\left(\square_x \circ \square_x - 4\,\Delta_x^+ \circ \Delta_x^-\right) \Im\mathfrak{m}(f(x + \mathbf{i}v)) + \mathcal{O}\left(h^2 - v^2\right) \tag{6.49}$$

$$= \frac{1}{h^4 v}\left(\square_x \circ \square_x - 4\,\square_x^{1/2} \circ \square_x^{1/2}\right) \Im\mathfrak{m}(f(x + \mathbf{i}v)) + \mathcal{O}\left(h^2 - v^2\right). \tag{6.50}$$

Based on the previous approximations we can construct discretizations to the first order wave equations in order to solve the wave propagation problem.

6.3.1 CSFD discretizations in homogeneous media (constant velocity)

Abreu et al. (2013a) showed the equivalence of propagating the second order wave equation by the FDM and the first order wave equation by the CSFDM in homogeneous media. Unlike the second order wave equation, the first order wave equation does not involves derivatives of the coefficients in homogeneous and/or heterogeneous media. In this study we construct a family of CSFD approximations considering the same procedure followed in the introduction for constructing FDM schemes. Following we name the schemes as CSFD (Complex Step Finite Difference) followed by two numbers referred as the error order in time and space. We use operator formulation in order be compact in our notation.

CSFD22

The second order accurate in time and space CSFD approximation fo the first order wave equation is given by the following expression

$$\lhd\rhd_t \Im\mathfrak{m}\left(u_{x+\mathbf{i}\Delta x}^{t+\mathbf{i}\Delta t}\right) = \frac{cv_t}{v_x} \lhd\rhd_x \Im\mathfrak{m}\left(u_{x+\mathbf{i}\Delta x}^{t+\mathbf{i}\Delta t}\right) + \mathcal{O}\left(\Delta t^2, \Delta x^2\right). \tag{6.51}$$

We can write Eq. 6.51 including the higher order derivatives terms to obtain

$$\begin{aligned} &\frac{\lhd\rhd_t}{2v_t} \Im\mathfrak{m}\left(u_{x+\mathbf{i}\Delta x}^{t+\mathbf{i}\Delta t}\right) - \left(\frac{3\Delta t^2 - v_t^2}{3!}\right)\frac{\partial^3 u}{\partial t^3} - \left(\frac{5\Delta t^4 - 10\Delta t^2 v_t^2 + v_t^4}{5!}\right)\frac{\partial^5 u}{\partial t^5} \\ &\quad = c\frac{\lhd\rhd_x}{2v_x} \Im\mathfrak{m}\left(u_{x+\mathbf{i}\Delta x}^{t+\mathbf{i}\Delta t}\right) - c^3\left(\frac{3\Delta x^2 - v_x^2}{3!}\right)\frac{\partial^3 u}{\partial x^3} \\ &\quad - c^5\left(\frac{5\Delta x^4 - 10\Delta x^2 v_x^2 + v_x^4}{5!}\right)\frac{\partial^5 u}{\partial x^5} + \mathcal{O}\left(\Delta t^6, \Delta x^6\right). \end{aligned} \tag{6.52}$$

Because the CSFD expression for the third derivative is a three levels discretization (Eq. 6.37) we can use it in time and space in order to gain more accuracy into the discretization without including more computational cost. We can also combine approximations 6.38 and 6.40 in order to find higher order CSFD schemes. Following this we can construct the next four CSFD approximations.

CSFD44A

$$\left(\lhd\rhd_t - \frac{3\Delta t^2 - v_t^2}{3!}\frac{\Delta_t^+ \circ \Delta_t^-}{\Delta t^2}\right)\mathfrak{Im}\left(u_{x+\mathbf{i}\Delta x}^{t+\mathbf{i}\Delta t}\right)$$
$$= \frac{cv_t}{v_x}\left[\lhd\rhd_x - c^2\frac{3\Delta x^2 - v_x^2}{3!}\frac{\Delta_x^+ \circ \Delta_x^-}{\Delta x^2}\right]\mathfrak{Im}\left(u_{x+\mathbf{i}\Delta x}^{t+\mathbf{i}\Delta t}\right) + \mathcal{O}\left(\Delta t^4, \Delta x^4\right). \tag{6.53}$$

CSFD44B

$$\left(\lhd\rhd_t - \frac{3\Delta t^2 - v_t^2}{3!}\frac{1}{5\Delta t^2}\left(\Delta_t^+ \circ \Delta_t^- + \square_t \circ \square_t\right)\right)\mathfrak{Im}\left(u_{x+\mathbf{i}\Delta x}^{t+\mathbf{i}\Delta t}\right)$$
$$= \frac{cv_t}{v_x}\left[\lhd\rhd_x - c^2\frac{3\Delta x^2 - v_x^2}{3!}\frac{1}{5\Delta x^2}\left(\Delta_x^+ \circ \Delta_x^- + \square_x \circ \square_x\right)\right]\mathfrak{Im}\left(u_{x+\mathbf{i}\Delta x}^{t+\mathbf{i}\Delta t}\right) + \mathcal{O}\left(\Delta t^4, \Delta x^4\right). \tag{6.54}$$

CSFD46A

$$\left(\lhd\rhd_t - \frac{3\Delta t^2 - v_t^2}{3!}\frac{\Delta_t^+ \circ \Delta_t^-}{\Delta t^2} - \frac{5\Delta t^4 - 10\Delta t^2 v_t^2 + v_t^4}{5!}\frac{1}{\Delta t^4}\left(\square_t \circ \square_t - 4\,\Delta_t^+ \circ \Delta_t^-\right)\right)\mathfrak{Im}\left(u_{x+\mathbf{i}\Delta x}^{t+\mathbf{i}\Delta t}\right)$$
$$= \frac{cv_t}{v_x}\left[\lhd\rhd_x - c^2\frac{3\Delta x^2 - v_x^2}{3!}\frac{\Delta_x^+ \circ \Delta_x^-}{\Delta x^2}\right.$$
$$\left. - c^4\frac{5\Delta x^4 - 10\Delta x^2 v_x^2 + v_x^4}{5!}\frac{1}{\Delta x^4}\left(\square_x \circ \square_x - 4\,\Delta_x^+ \circ \Delta_x^-\right)\right]\mathfrak{Im}\left(u_{x+\mathbf{i}\Delta x}^{t+\mathbf{i}\Delta t}\right) + \mathcal{O}\left(\Delta t^4, \Delta x^6\right). \tag{6.55}$$

CSFD46B

$$\left[\lhd\rhd_t - \frac{3\Delta t^2 - v_t^2}{3!}\frac{1}{5\Delta t^2}\left(\Delta_t^+ \circ \Delta_t^- + \square_t \circ \square_t\right) - \frac{5\Delta t^4 - 10\Delta t^2 v_t^2 + v_t^4}{5!}\frac{1}{\Delta t^4}\left(\square_t \circ \square_t - 4\,\Delta_t^+ \circ \Delta_t^-\right)\right]$$
$$\mathfrak{Im}\left(u_{x+\mathbf{i}\Delta x}^{t+\mathbf{i}\Delta t}\right) = \frac{cv_t}{v_x}\left[\lhd\rhd_x - c^2\frac{3\Delta x^2 - v_x^2}{3!}\frac{1}{5\Delta x^2}\left(\Delta_x^+ \circ \Delta_x^- + \square_x \circ \square_x\right)\right.$$
$$\left. - c^4\frac{5\Delta x^4 - 10\Delta x^2 v_x^2 + v_x^4}{5!}\frac{1}{\Delta x^4}\left(\square_x \circ \square_x - 4\,\Delta_x^+ \circ \Delta_x^-\right)\right]\mathfrak{Im}\left(u_{x+\mathbf{i}\Delta x}^{t+\mathbf{i}\Delta t}\right) + \mathcal{O}\left(\Delta t^4, \Delta x^6\right). \tag{6.56}$$

6.4 Stability and dispersion analysis

Unfortunately there is no a perfect numerical method when we are in presence of heterogeneous media. All of different numerical methods suffer from different problems which do not allow them to reproduce the real (analytical) solution of the problem. One of the most common basis to understand the nature of a numerical discretization, which will allow us later to be able to decide whether or not the method can be used under certain conditions, is the stability and dispersion analysis.

The basis of the stability and dispersion analysis is a plane wave of the form

$$u(x,t) = \mathrm{A}e^{\mathbf{i}(kx+\omega t)}, \tag{6.57}$$

where ω is the frequency of the wave and k is the wave number, $\mathbf{i}$ is the imaginary unit ($\mathbf{i}^2 = -1$) and A is the amplitude.

Usually k and ω are dependent variables. The relation between ω and k is commonly called the dispersion relation. If we substitute Eq. 6.57 into the two-way (Eq. 3.15) and/or the one-way (Eq. 6.5) wave equations we obtain the following expressions respectively

$$\omega^2 = c^2 k^2 \quad \text{and} \quad \omega = c\,k. \tag{6.58}$$

in the two directional case (two-way wave equation) we can express the velocity in terms of frequency ω and the wave number k as

$$c = \pm\frac{\omega}{k}. \tag{6.59}$$

Note that we have two velocities in the two directional case, one propagating in the positive direction $(c = +\omega/k)$ and the other propagating in the negative direction $(c = -\omega/k)$, hence its name "two-way wave equation". For the one-way wave propagation we have only the positive branch of the velocity.

In both cases, we can appreciate the relation between ω and k can be decomposed into linear functions. In other words, the true (theoretical) relation between ω and k is linear. As we will see in later sections, the basic problem with FDM and the introduced CSFDM is the relation between ω and k is not longer linear.

Note that is we substitute $\mathrm{A} = \hat{u}$ in Eq. 6.57 then the relation $\omega = \omega(k)$ is simply given by the finite Fourier transform, hence by considering $0 \leq kx \leq \pi$ we obtain information on all the modes present in the finite Fourier Transform representation of the solution, Thomas (1995).

In the next analysis we followed a similar methodology given by Moczo et al. (2014) and Thomas (1995) and generalize it. Moczo et al. (2014) only considered the analysis of the imaginary factors and Thomas (1995) only considered the true wave number.

To analyze dispersion properties of difference schemes, we first consider complex values of frequency $(\omega = \omega_{real} + \mathbf{i}\,\omega_{imag})$ and the wave number $(k = k_{real} + \mathbf{i}\,k_{imag})$. We can express a discrete plane wave (the discrete plane wave is given by substituting $x = n\Delta x$ and $t = m\Delta t$ into Eq. 6.57) as follows

$$\begin{aligned} u_x^t &= \mathrm{A}\, e^{\mathbf{i}((k_{real}+\mathbf{i}\,k_{imag})n\Delta x+(\omega_{real}+\mathbf{i}\,\omega_{imag})m\Delta t)} \\ &= \mathrm{A}\, e^{-k_{imag}n\Delta x-\omega_{imag}m\Delta t} e^{\mathbf{i}(\omega_{real}m\Delta t-k_{real}n\Delta x)}, \end{aligned} \tag{6.60}$$

where n and m are positive integers.

Based on expression 6.60 we can infer what will happen with a wave propagating with the numerical method of our choice. First we can assume the numerical method reproduces the real frequency ω but not the wave number and/or we can assume the numerical method reproduces the real wave number k but not the real frequency and/or finally we can assume the numerical method dos not reproduces the real frequency or real wave number but gives us a decent approximation of both. We separate the analysis in three cases:

Case 1: we assume the numerical method reproduces the real the wave number k but not the frequency. The approximated frequency can adopt complex values, the corresponding discrete plane wave will be given by

$$\begin{aligned} u_x^t &= \mathrm{A}\, e^{\mathbf{i}(kn\Delta x+(\omega_{real}+\mathbf{i}\,\omega_{imag})m\Delta t)} \\ &= \mathrm{A}\, e^{-\omega_{imag}m\Delta t} e^{\mathbf{i}k(n\Delta x+\frac{\omega_{real}}{k}m\Delta t)}. \end{aligned} \tag{6.61}$$

Analyzing expression 6.61 we can infer the following

Parameter ω_{real}:

- If $\omega_{real} = 0$ there will be no wave propagation.
- If $\omega_{real} \neq 0$ there will be wave propagation with speed $\frac{\omega_{real}}{k}$.
- If $\frac{\omega_{real}}{k}$ is a nonlinear function of $\omega(k)$ the scheme will be dispersive.

Parameter ω_{imag}:

- If $\omega_{imag} < 0$ the solution of the scheme will grow without bounds with time.
- If $\omega_{imag} > 0$ the solution of the scheme will decrease with time (dissipative).
- If $\omega_{imag} = 0$ the solution of the scheme will not decrease with time (non-dissipative).

Case 2: we assume the numerical method reproduces the real frequency ω but not the wave number. The approximated wave number can adopt complex values, the corresponding discrete plane wave will be given by

$$\begin{aligned} u_x^t &= \mathrm{A}\, e^{\mathbf{i}((k_{real}+\mathbf{i}\,k_{imag})n\Delta x+\omega\, m\Delta t)} \\ &= \mathrm{A}\, e^{-k_{imag}n\Delta x} e^{\mathbf{i}k_{real}(n\Delta x+\frac{\omega}{k_{real}}m\Delta t)}. \end{aligned} \tag{6.62}$$

Analyzing expression 6.62 we can infer the following
Parameter k_{real}:

- If $k_{real} = 0$ there will be no wave propagation over the space.
- If $k_{real} \neq 0$ there will be wave propagation with speed $\frac{\omega}{k_{real}}$.
- If $\frac{\omega}{k_{real}}$ is a nonlinear function of $k(\omega)$ the scheme will be dispersive.

Parameter k_{imag}:

- If $k_{imag} < 0$ the solution of the scheme will grow without bounds with spatial position.
- If $k_{imag} > 0$ the solution of the scheme will decrease with spatial position (attenuative).
- If $k_{imag} = 0$ the solution of the scheme will not decrease with spatial position (non-attenuative).

Case 3: we assume the numerical method does not reproduces the real frequency or wave number. In this case, both cases explained before are applied together in order to determine how reliable the numerical approximation is.

6.4.1 Analysis of the dispersion relations

All dispersion relation can be written in a general form as follows

$$\varphi = \frac{1}{\Delta}\left(\frac{\pi}{2} - \arcsin\chi\right), \tag{6.63}$$

where $\{\varphi, \Delta, \chi\}$ correspond to $\{\omega, \Delta t, \xi\}$ and/or $\{k, \Delta x, \zeta\}$, from which we can obtain explicit expressions for ω and k for all schemes.

Note all dispersion relation written in a general form (Eq. 6.63) are dependent on $\arcsin$ function, that is, the real and/or imaginary values that φ can adopt are strictly conditioned by values of the $\arcsin$ function, and this one conditioned by values of χ.

By simple definition of the $\arcsin$ function, we investigate the case when χ is in the interval $[-1, 1]$ or outside the interval $[-1, 1]$ and also when the imaginary part is different from zero.

We show in Appendix D if $-1 \leq \xi \leq 1$ then $\arcsin(\chi)$ is pure real. If $\chi < 1$ then $\arcsin(\chi)$ is positive real with negative imaginary part and if $\chi > 1$ then $\arcsin(\chi)$ is negative real with negative imaginary part. In case of a complex χ then $\arcsin(\chi)$ all the previous cases before apply. This gives us a general rule to analyze the dispersion relations of FD and CSFD schemes.

6.4.2 Dispersion relations

In order to avoid clutter in our analysis, we show in Appendix C how to compute dispersion relation for FD or CSFD approximations in a simple way. Following, we list by corresponding names the FD and the introduced CSFD schemes in order to be able to make comparisons of dispersion and stability properties.

Scheme FD22

The FD scheme second order in time and space is not commonly used in seismological research due to its limitations in heterogeneous media. A complete dispersion study of this scheme can be found in Moczo et al. (2014) and Taflove and Hagness (2005). In this study we start to illustrate dispersion and stability analysis of FD24 and FD44 schemes in the following Subsections.

Scheme FD24

The dispersion relation for the FD scheme second order accurate in time and fourth order accurate in space (discretization 6.20) is given by the following expression

$$2\cos\omega\Delta t - 2 = \mathrm{S}^2\left[\frac{4}{3}\left(2\cos k\Delta x - 2\right) - \frac{1}{12}\left(2\cos 2k\Delta x - 2\right)\right], \tag{6.64}$$

where $\mathrm{S} = c\frac{\Delta t}{\Delta x}$ is commonly refereed as the *stability factor* and/or the *Courant number*. By using Eq. 6.64 we can find explicit expressions for ω and/or k.

Case 1: we assume the numerical method reproduces the real the wave number k but not the frequency. The explicit expression for the frequency is given by the following expression

$$\omega = \frac{1}{\Delta t}\arccos\left\{\mathrm{S}^2\left[-\frac{1}{6}\cos^2 k\Delta x + \frac{4}{3}\cos k\Delta x - \frac{7}{6}\right] + 1\right\}. \tag{6.65}$$

Denoting by

$$\xi = \mathrm{S}^2\left[-\frac{1}{6}\cos^2 k\Delta x + \frac{4}{3}\cos k\Delta x - \frac{7}{6}\right] + 1, \tag{6.66}$$

note we can write Eq. 6.65 as the general expression (Eq. 6.63).

We are interested in finding values of S for which $-1 \leq \xi \leq 1$, that is, the interval for which the FD scheme is stable.

We study boundaries of $\cos k\Delta x$: when $\cos k\Delta x = -1$ we have

$$\xi = 1 - \frac{8}{3}\mathrm{S}^2, \tag{6.67}$$

when $\cos k\Delta x = 1$ we have $\xi = 1$.

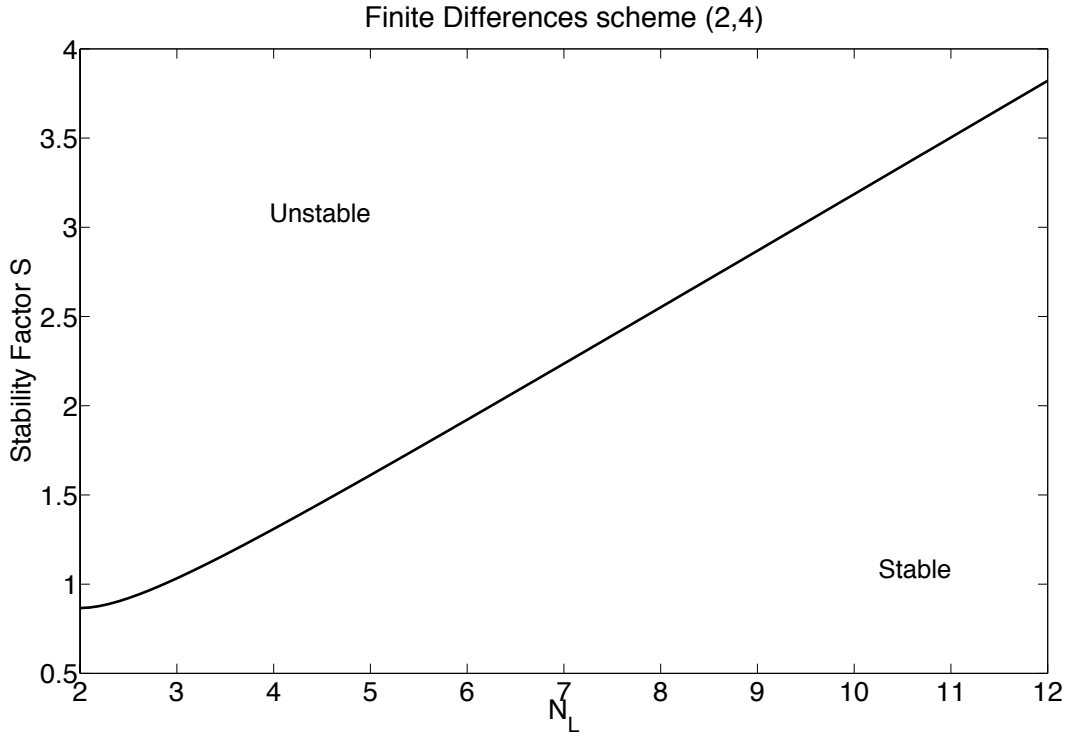

Figure 6.1: Courant number S as function of the spatial sampling N_λ, discriminating the stable and unstable regimes of a wave with real wavelength.

It is clear always $\xi \leq 1$, for the condition $\xi \geq -1$ we obtain

$$\mathrm{S}^2 \leq \frac{2}{\frac{1}{6}\cos^2 k\Delta x - \frac{4}{3}\cos k\Delta x + \frac{7}{6}}. \tag{6.68}$$

Stability condition is given by using expression $1 - \frac{8}{3}\mathrm{S}^2 \leq \xi \leq 1$, which leads to: the FD24 scheme is stable if $0 \leq \mathrm{S} \leq \sqrt{\frac{3}{4}}$, otherwise the scheme is unstable. This stability condition can also be found in Cohen (2001).

We can express the spatial sampling N_λ (Moczo et al., 2014) as $N_\lambda = \frac{\lambda}{\Delta x} = \frac{2\pi}{k\Delta x}$, where λ is the wavelength. We can express Eq. 6.68 as

$$\mathrm{S}^2 \leq \frac{2}{\frac{1}{6}\cos^2 \frac{2\pi}{N_\lambda} - \frac{4}{3}\cos \frac{2\pi}{N_\lambda} + \frac{7}{6}}. \tag{6.69}$$

Fig. 6.1 shows values of the Courant number S, discriminating the stable and unstable regimes of a wave with real (analytical) wavelength as function of the spatial sampling N_λ.

Case 2: we assume the numerical method reproduces the real frequency ω but not the wave number. The explicit expression for the wave number is given by rearranging Eq. 6.64 as follows

$$-\frac{\mathrm{S}^2}{6}\cos^2 k\Delta x + \frac{4}{3}\mathrm{S}^2 \cos k\Delta x - \frac{7}{6}\mathrm{S}^2 + 1 - \cos\omega\Delta t = 0. \tag{6.70}$$

If we set the indeterminate of the polynomial to be $\cos k\Delta x$, then we can write Eq. 6.70 as follows

$$-\frac{\mathrm{S}^2}{6}\mathrm{X}^2+\frac{4}{3}\mathrm{S}^2\mathrm{X}-\frac{7}{6}\mathrm{S}^2+1-\cos\omega\Delta t=0. \tag{6.71}$$

Values of k are easily obtained in the following way

$$k=\frac{1}{\Delta x}\arccos\Big\{\text{root of Eq. 6.71}\Big\}. \tag{6.72}$$

We can write $\omega\Delta t=\frac{2\pi}{T}\Delta t=\frac{2\pi}{N_T}$, where the time sampling is defined as $N_T=\frac{T}{\Delta t}$, we write Eq. 6.70 as

$$-\frac{\mathrm{S}^2}{6}\cos^2 k\Delta x+\frac{4}{3}\mathrm{S}^2\cos k\Delta x-\frac{7}{6}\mathrm{S}^2+1-\cos\frac{2\pi}{N_T}=0. \tag{6.73}$$

Denoting

$$\zeta=\text{root of Eq. 6.73.} \tag{6.74}$$

Following, we write the general case of the polynomial root as

$$a\cos^2 k\Delta x+b\cos k\Delta x+c-\cos\frac{2\pi}{N_T}=0, \tag{6.75}$$

where a,b,c are constants. ζ will be given by

$$\zeta=\frac{-b\pm\sqrt{b^2-4a(c-\cos\frac{2\pi}{N_T})}}{2a}, \tag{6.76}$$

for the case $-1\leq\zeta\leq 1$ we have

$$-1\leq\frac{-b\pm\sqrt{b^2-4a(c-\cos\frac{2\pi}{N_T})}}{2a}\leq 1, \tag{6.77}$$

after some algebra we find

$$a-b+c\leq\cos\frac{2\pi}{N_T}\leq a+b+c, \tag{6.78}$$

substituting

$$1-\frac{8}{3}\mathrm{S}^2\leq\cos\frac{2\pi}{N_T}\leq 1, \tag{6.79}$$

which implies

$$N_T\geq\frac{2\pi}{\arccos\left(1-\frac{8}{3}\mathrm{S}^2\right)}, \tag{6.80}$$

transformed into the frequency domain we have

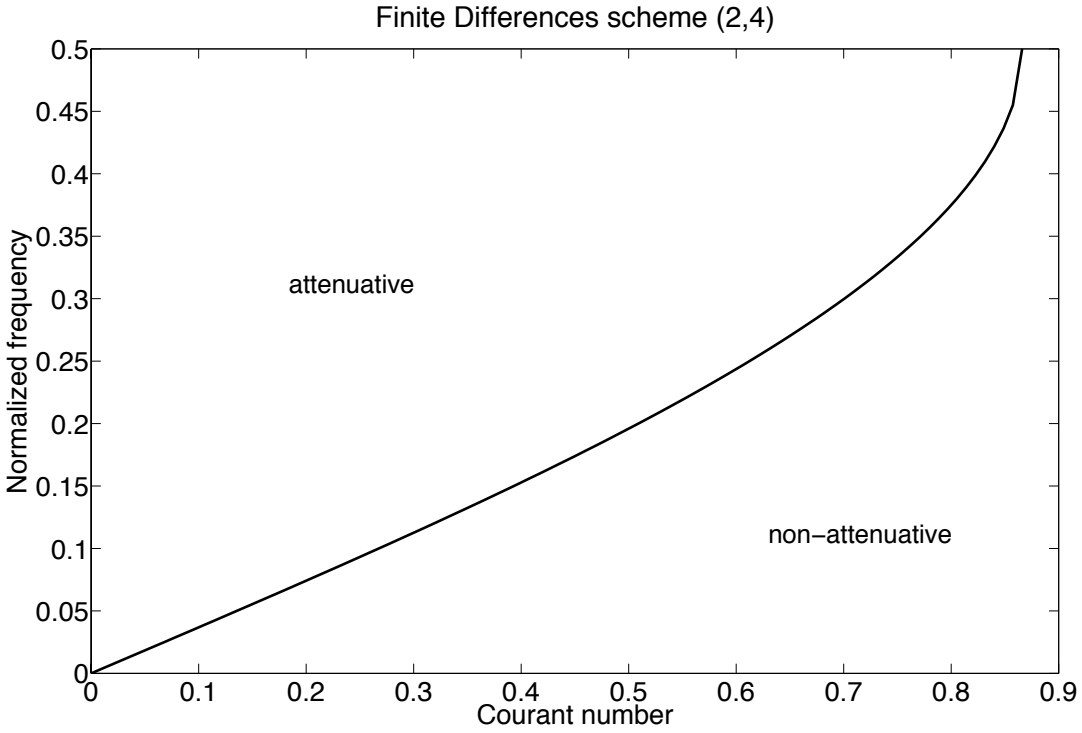

Figure 6.2: Normalized frequency as function of the Courant Number S, discriminating the attenuative and non-attenuative regimes of a single mode.

$$f = \frac{1}{T} = \frac{1}{\Delta t N_T} \leq \frac{\arccos\left(1 - \frac{8}{3}\mathrm{S}^2\right)}{\pi} \frac{1}{2\Delta t}. \tag{6.81}$$

Define the frequency f_{ATT} as

$$f_{ATT} = \frac{1}{T} = \frac{1}{\Delta t N_T} \leq \frac{\arccos\left(1 - \frac{8}{3}\mathrm{S}^2\right)}{\pi} f_N, \tag{6.82}$$

where f_N is the Nyquist frequency $f_N = \frac{1}{2\Delta t}$. The frequency domain of condition 6.80 can be written as $f \leq F_{ATT}$. It is clear from Eq. 6.82 that only for $\mathrm{S} = \sqrt{\frac{3}{4}}$ the FD scheme is non-attenuative up to the Nyquist frequency.

To illustrate the relation between frequency and the Courant number, consider the normalized frequency $f_{normalized} = f\Delta t$, we can define

$$f_{ATT,normalized} = \frac{\arccos\left(1 - \frac{8}{3}\mathrm{S}^2\right)}{2\pi}. \tag{6.83}$$

We have identified two regimes of the scheme behavior with spatial position. The non-attenuative regime is determined by condition 6.80 and the attenuative regime is determined by its complement. The value of f_{ATT} discriminating the two regimes depends on S. Fig. 6.2 illustrates $f_{ATT,normalized}$ as function of the Courant number.

In order to determine dispersion and dissipation properties of the FD24 scheme for different Courant numbers, we plot graphics in terms of the normalized velocity (ratio factor). The ratio factor (R) is the ratio of the numerical velocity c_{num} to the phase velocity c (true velocity), that is

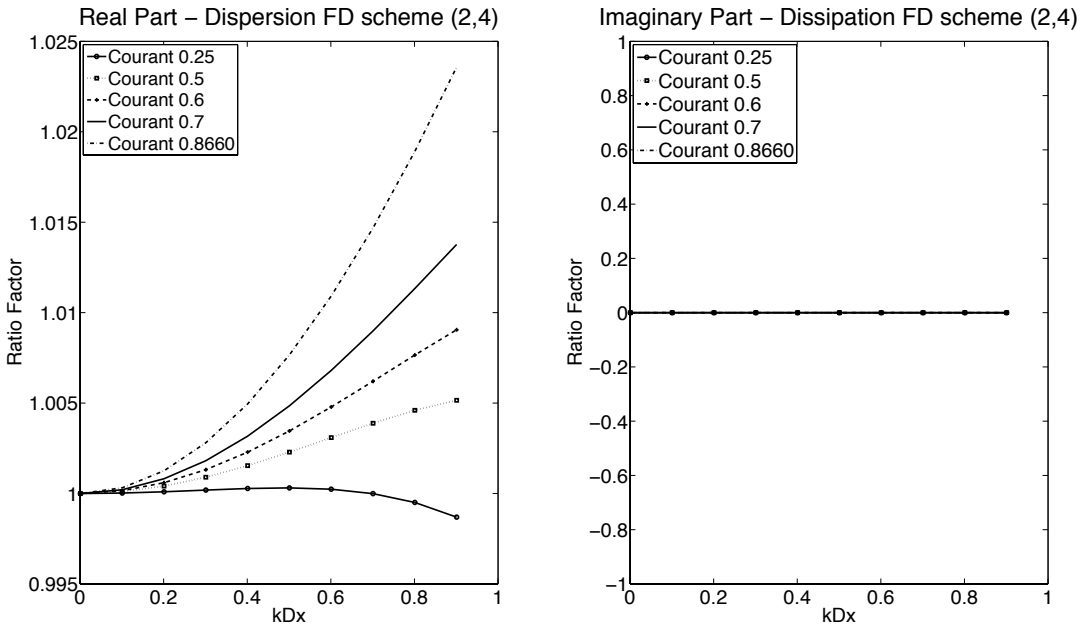

Figure 6.3: Dispersion and dissipation properties of the FD24 scheme.

$$R = \frac{c_{num}}{c} = \frac{\omega_{num}}{kc} = \frac{\omega \Delta t}{k \Delta x \mathrm{S}}. \tag{6.84}$$

Fig. 6.3 shows dispersion and dissipation properties of the FD24 scheme. For computing R values, we are only using real values of $k\Delta x$ and $\omega\Delta t$ values are computed by using Eq. 6.65, so the imaginary part of the ratio factor (R) only comes from the frequency ω values found using Eq. 6.65. This is the reason why the real part of the Plot of $k\Delta x$ vs R represents the *dispersion* of the FD scheme, while the imaginary part represents the *dissipation*.

The *ideal* ratio factor will be equal to one, which physically means the numerical velocity is equal to the real velocity. We can appreciate in the real part of the ratio factor plot (left graphic Fig. 6.3) closest values to one are given by smaller Courant numbers, and all are non-linear functions, which means the FD24 scheme is dispersive for all values of the Courant numbers. Also note lower dispersion values are given by low values of the Courant number (which is very convenient for heterogeneous media). The right-hand graphic shows a ratio factor equal to zero which is translated into non-dissipation of the scheme. This is due to frequency values found with expression 6.65 are all real (see analysis in beginning of Section 6.4).

FD44

The dispersion relation for the FD scheme fourth order accurate in time and fourth order accurate in space (discretization 6.23) is given by the following expression

$$\begin{aligned} 2\cos\omega\Delta t - 2 = \mathrm{S}^2 \left[\frac{4}{3}\left(2\cos k\Delta x - 2\right) - \frac{1}{12}\left(2\cos 2k\Delta x - 2\right) \right] \\ + \mathrm{S}^4 \frac{1}{12}\left[-4\left(2\cos k\Delta x - 2\right) + 2\cos 2k\Delta x - 2 \right], \end{aligned} \tag{6.85}$$

which can be written as

$$\cos\omega\Delta t = \mathrm{S}^2\frac{1}{6}\left[-\cos^2 k\Delta x + 8\cos k\Delta x - 7\right] + \mathrm{S}^4\frac{1}{6}\left[\cos^2 k\Delta x - 2\cos k\Delta x + 1\right] + 1. \tag{6.86}$$

Case 1: we assume the numerical method reproduces the real the wave number k but not the frequency. The explicit expression for the frequency is given by the following expression

$$\omega = \frac{1}{\Delta t}\arccos\left\{\mathrm{S}^2\frac{1}{6}\left[-\cos^2 k\Delta x + 8\cos k\Delta x - 7\right] + \mathrm{S}^4\frac{1}{6}\left[\cos^2 k\Delta x - 2\cos k\Delta x + 1\right] + 1\right\}. \tag{6.87}$$

Denoting by

$$\xi = \mathrm{S}^2\left[-\frac{1}{6}\cos^2 k\Delta x + \frac{4}{3}\cos k\Delta x - \frac{7}{6}\right] + \mathrm{S}^4\frac{1}{6}\left[\cos^2 k\Delta x - 2\cos k\Delta x + 1\right] + 1, \tag{6.88}$$

we can write Eq. 6.87 as the general expression (Eq. 6.63). By following analysis of the previous subsection, we are interested in finding values of S for which $-1 \leq \xi \leq 1$. We study boundaries of $\cos k\Delta x$: when $\cos k\Delta x = -1$ we have

$$\xi = \frac{2}{3}\mathrm{S}^4 - \frac{8}{3}\mathrm{S}^2 + 1, \tag{6.89}$$

when $\cos k\Delta x = 1$ we have $\xi = 1$.

The case $-1 \leq \xi \leq 1$, that is, the interval for which the FD scheme is stable. It is clear always $\xi \leq 1$, the condition $\xi \geq -1$ we obtain

$$\mathrm{S}^2\left[\frac{1}{6}\cos^2\frac{2\pi}{N_\lambda} - \frac{4}{3}\cos\frac{2\pi}{N_\lambda} + \frac{7}{6}\right] + \mathrm{S}^4\frac{1}{6}\left[-\cos^2\frac{2\pi}{N_\lambda} + 2\cos\frac{2\pi}{N_\lambda} - 1\right] \leq 2, \tag{6.90}$$

where we have replaced $k\Delta x = \frac{2\pi}{N_\lambda}$.

Stability condition is given by using the expression $\frac{2}{3}\mathrm{S}^4 - \frac{8}{3}\mathrm{S}^2 + 1 \leq \xi \leq 1$, which leads to: The FD44 scheme is stable if $0 \leq \mathrm{S} \leq 1$, otherwise the scheme is unstable. This condition can also be found by the work of Cohen and Joly (1996) found by a different method.

Fig. 6.4 shows values of the Courant number S, discriminating the stable and unstable regimes of a wave with real wavelength as function of the spatial sampling N_λ. Note N_λ values are given until a smaller range than FD24 scheme (Fig. 6.1) this is because after certain limit the Courant number only take complex values.

Case 2: we assume the numerical method reproduces the real frequency ω but not the wave number. The explicit expression for the wave number is given by the following expression

$$\cos^2 k\Delta x\left(\frac{\mathrm{S}^4 - \mathrm{S}^2}{6}\right) + \cos k\Delta x\left(\frac{4\mathrm{S}^2 - \mathrm{S}^4}{3}\right) + \frac{\mathrm{S}^4 - 7\mathrm{S}^2}{6} + 1 - \cos\frac{2\pi}{N_T} = 0. \tag{6.91}$$

Values of k are obtained in the following way

$$k = \frac{1}{\Delta x}\arccos\left\{\text{root of Eq. 6.91}\right\}. \tag{6.92}$$

Denoting

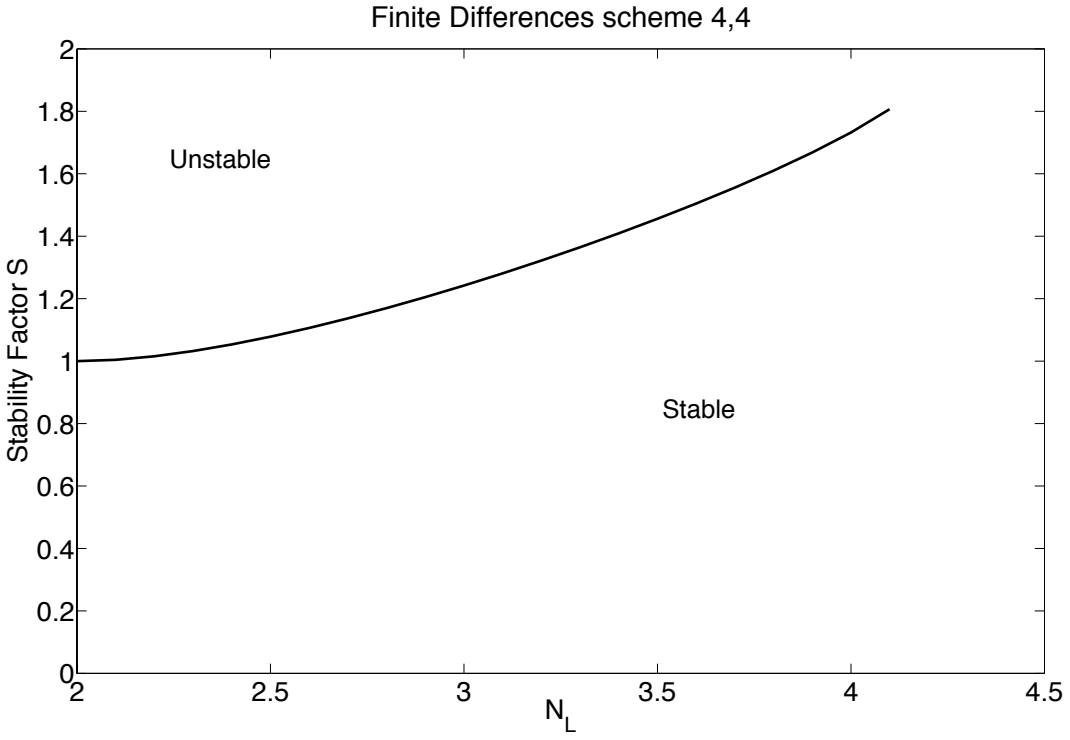

Figure 6.4: Courant number S as function of the spatial sampling N_λ, discriminating the stable and unstable regimes of a wave with real wavelength for FD44 scheme.

$$\zeta = \text{root of Eq. 6.91}, \tag{6.93}$$

for the case $-1 \leq \zeta \leq 1$ we obtain

$$\frac{2}{3}\mathrm{S}^4 - \frac{8}{3}\mathrm{S}^2 + 1 \leq \cos\frac{2\pi}{N_T} \leq 1, \tag{6.94}$$

which implies

$$N_T \geq \frac{2\pi}{\arccos\left(\frac{2}{3}\mathrm{S}^4 - \frac{8}{3}\mathrm{S}^2 + 1\right)}. \tag{6.95}$$

Defining the frequency f_{ATT} as

$$f_{ATT} = \frac{1}{T} = \frac{1}{\Delta t N_T} \leq \frac{\arccos\left(\frac{2}{3}\mathrm{S}^4 - \frac{8}{3}\mathrm{S}^2 + 1\right)}{\pi} f_N, \tag{6.96}$$

where f_N is the Nyquist frequency $f_N = \frac{1}{2\Delta t}$, the frequency domain of condition 6.95 can be written as $f \leq F_{ATT}$. It is clear from Eq. 6.96 that only for $\mathrm{S} = 1$, the FD scheme is non-attenuative up to the Nyquist frequency.

To illustrate the relation between frequency and the Courant number, considering the normalized frequency $f_{normalized} = f\Delta t$, we can define

$$f_{ATT,normalized} = \frac{\arccos\left(\frac{2}{3}\mathrm{S}^4 - \frac{8}{3}\mathrm{S}^2 + 1\right)}{2\pi}. \tag{6.97}$$

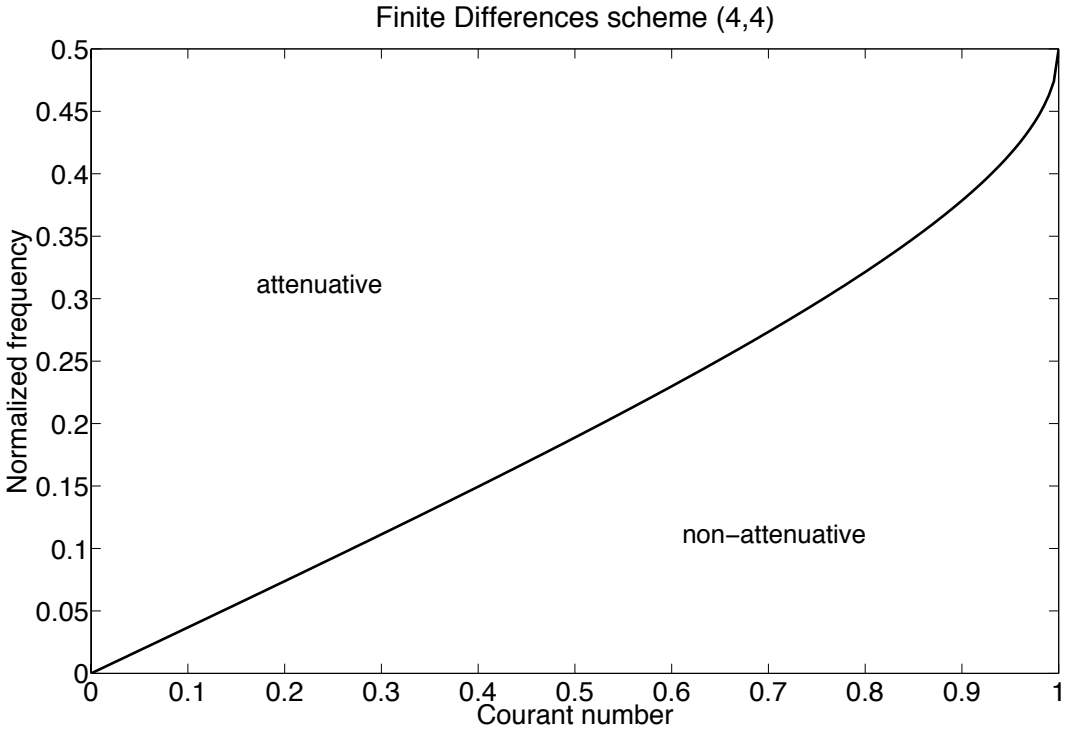

Figure 6.5: Normalized frequency as function of the Courant Number S, discriminating the attenuative and non-attenuative regimes of a single mode of FD44 scheme.

We have identified two different types of behavior of the scheme depending on spatial position. The non-attenuative regime is determined by condition 6.95 and the attenuative regime is determined by its complement. The value of f_{ATT}, discriminating the two regimes, depends on S. Fig. 6.5 illustrates $f_{ATT,normalized}$ as function of the Courant number.

Fig. 6.6 shows dispersion and dissipation properties of the FD44 scheme. Unlike the FD24 scheme, we can appreciate that in the real part of the ratio factor plot (left graphic Fig. 6.3) the closest values to one are given by bigger Courant numbers, and only the curve corresponding to $\mathrm{S} = 1$ is a linear function, which means the FD24 scheme is non-dispersive only for a Courant number equal to one. Also note that higher dispersion values correspond to small values of the Courant number, which is not convenient for heterogeneous media. The right-hand graphic shows a ratio factor equal to zero which means the scheme has no dissipation.

After analyzing several FD24 and FD44 schemes, we proceed to study CSFD schemes in order to make a comparison between the two methods.

CSFD22

The dispersion relation for the most simple CSFD scheme with second order accuracy in time and space (Eq. 6.51) is given by the following expression

$$\cos\omega\Delta t = \mathrm{S}\cos k\Delta x, \tag{6.98}$$

where the stability factor for the CSFD approximations is defined as $\mathrm{S} = c\frac{v_t}{v_x}$. We can write

$$\omega = \frac{1}{\Delta t}\arccos\left(\mathrm{S}\cos k\Delta x\right) \quad \text{and} \quad k = \frac{1}{\Delta x}\arccos\left(\frac{1}{\mathrm{S}}\cos\omega\Delta t\right). \tag{6.99}$$

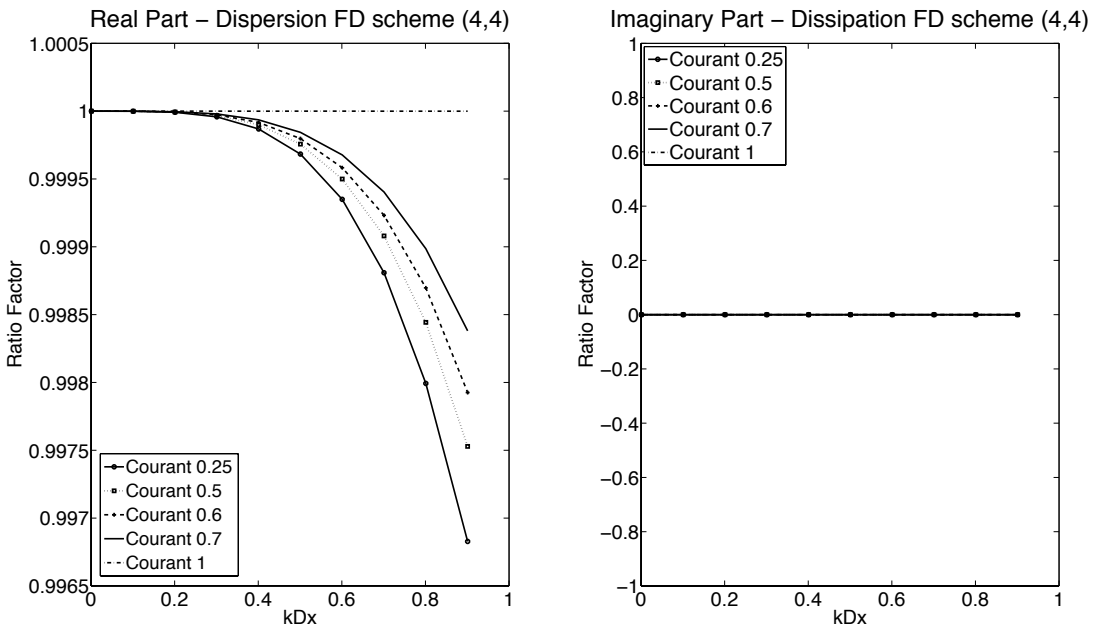

Figure 6.6: Dispersion and dissipation properties of the FD44 scheme.

Denoting

$$\xi = c\frac{v_t}{v_x}\cos k\Delta x \quad \text{and} \quad \zeta = \frac{v_x}{cv_t}\cos\omega\Delta t, \tag{6.100}$$

and using

$$\arccos x = \frac{\pi}{2} - \arcsin x, \tag{6.101}$$

we can write

$$\omega = \frac{1}{\Delta t}\left(\frac{\pi}{2} - \arcsin\xi\right) \quad \text{and} \quad k = \frac{1}{\Delta x}\left(\frac{\pi}{2} - \arcsin\zeta\right). \tag{6.102}$$

Case 1: we assume the numerical method reproduces the true wave number k but not the true frequency. By inspection of ξ (Eq. 6.100), using $-1 \leq \cos x \leq 1$, it is straightforward to see that $-\mathrm{S} \leq \xi \leq \mathrm{S}$, and the stability condition is $0 < \mathrm{S} \leq 1$.

Case 2: we assume the numerical method reproduces the true frequency ω but not the true wave number. For the case $-1 \leq \zeta \leq 1$ we obtain

$$-\mathrm{S} \leq \cos\frac{2\pi}{N_T} \leq \mathrm{S}, \tag{6.103}$$

which implies

$$N_T \geq \frac{2\pi}{\arccos\left(\mathrm{S}\right)}, \tag{6.104}$$

Define the frequency f_{ATT} as

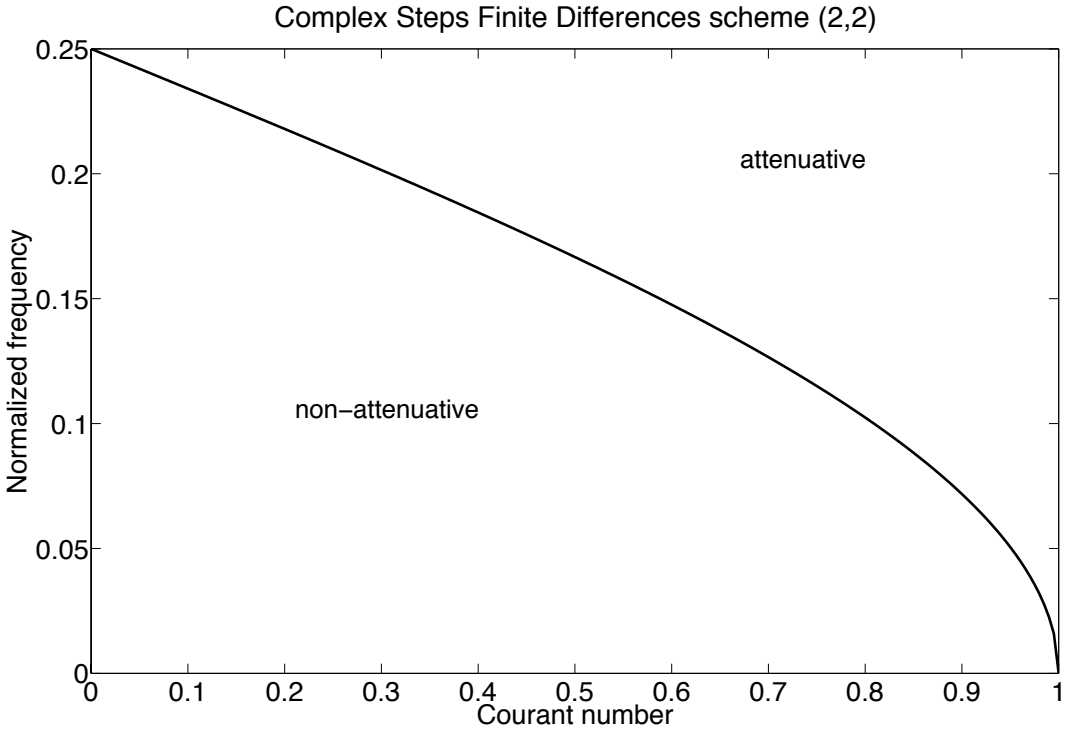

Figure 6.7: Normalized frequency as function of the Courant Number S, discriminating the attenuative and non-attenuative regimes of a single mode for the CSFD22 scheme.

$$f_{ATT} = \frac{1}{T} = \frac{1}{\Delta t N_T} \leq \frac{\arccos\left(\mathrm{S}\right)}{\pi} f_N, \tag{6.105}$$

where f_N is the Nyquist frequency $f_N = \frac{1}{2\Delta t}$. The frequency domain expression of condition 6.104 can be written as $f \leq F_{ATT}$. It is clear from Eq. 6.96 that only for $\mathrm{S} = 1$, the FD scheme is non-attenuative up to the Nyquist frequency.

To illustrate the relation between frequency and Courant number, considering the normalized frequency $f_{normalized} = f\Delta t$, we can define

$$f_{ATT,normalized} = \frac{\arccos\left(\mathrm{S}\right)}{2\pi}. \tag{6.106}$$

Again, we have distinguish two different type of behavior of the scheme with respect to the position in space. The non-attenuative regime is determined by condition 6.104 and the attenuative regime is determined by its complement. The value of f_{ATT}, discriminating the two regimes, depends on S. Fig. 6.7 illustrates $f_{ATT,normalized}$ as function of the Courant number.

In order to determine dispersion and dissipation properties of the CSFD22 scheme for different Courant numbers, we plot graphics in terms of the normalized velocity (ratio factor). Fig. 6.8 shows dispersion and dissipation properties of the CSFD22 scheme. We only obtain non dispersion properties for the Courant number equal to one, otherwise the scheme is highly dispersive. The right-hand graphic shows a ratio factor equal to zero which is translated into non-dissipation of the scheme.

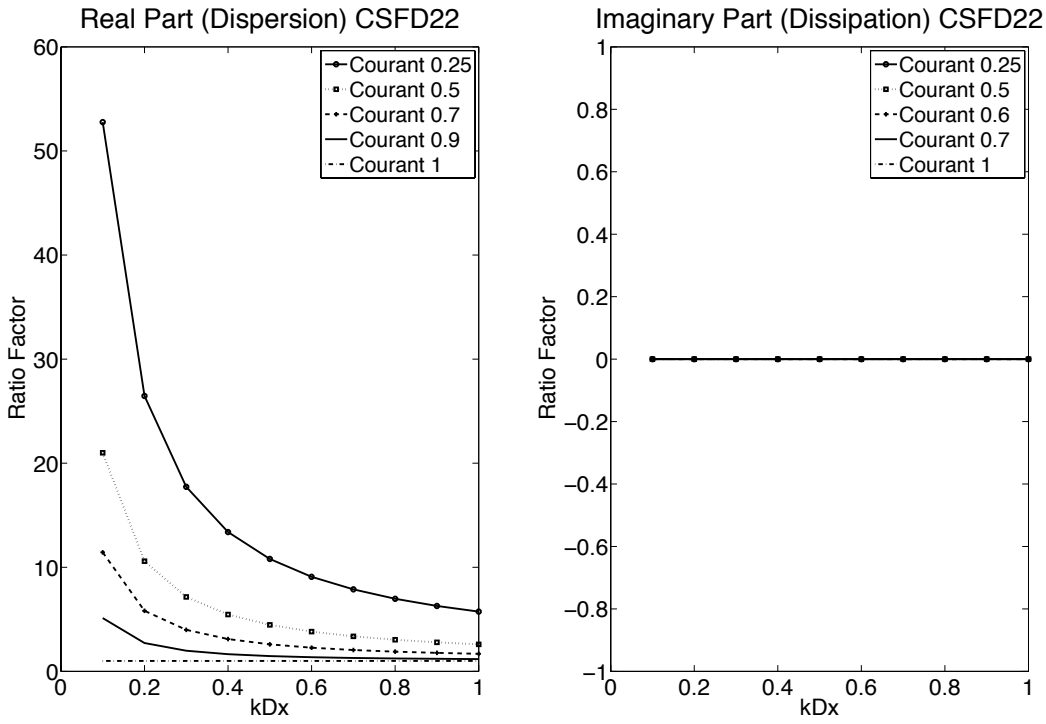

Figure 6.8: Dispersion and dissipation properties of the CSFD22 scheme.

CSFD44A

The dispersion relation for the CSFD scheme fourth order accurate in time and space (Eq. 6.53) is given by the following expression

$$\cos\omega\Delta t\left(1-\frac{3\Delta t^2-v_t^2}{3\Delta t^2}\right)+\left(\frac{3\Delta t^2-v_t^2}{3\Delta t^2}\right)=c\frac{v_t}{v_x}\left[\cos k\Delta x\left(1-\frac{3\Delta x^2-v_x^2}{3\Delta x^2}\right)+\left(\frac{3\Delta x^2-v_x^2}{3\Delta x^2}\right)\right], \tag{6.107}$$

Case 1: we assume the numerical method reproduces the real the wave number k but not the frequency. The explicit expression for the frequency is given by the following expression

$$\omega=\frac{1}{\Delta t}\arccos\left\{\frac{3\Delta t^2}{v_t^2}\left[\mathrm{S}\left(\cos k\Delta x\left(\frac{v_x^2}{3\Delta x^2}\right)+\left(\frac{3\Delta x^2-v_x^2}{3\Delta x^2}\right)\right)-\frac{3\Delta t^2-v_t^2}{3\Delta t^2}\right]\right\}, \tag{6.108}$$

Denoting by

$$\xi=\frac{3\Delta t^2}{v_t^2}\left[\mathrm{S}\left(\cos k\Delta x\left(\frac{v_x^2}{3\Delta x^2}\right)+\left(\frac{3\Delta x^2-v_x^2}{3\Delta x^2}\right)\right)-\frac{3\Delta t^2-v_t^2}{3\Delta t^2}\right], \tag{6.109}$$

we can write Eq. 6.108 as the general expression (Eq. 6.63). By following analysis of the previous section, we are interested in finding values of S for which $-1\leq\xi\leq 1$. We study boundaries of $\cos k\Delta x$: when $\cos k\Delta x=-1$

$$\xi=\frac{3\Delta t^2}{v_t^2}\left[\mathrm{S}\left(\frac{3\Delta x^2-2v_x^2}{3\Delta x^2}\right)-\frac{3\Delta t^2-v_t^2}{3\Delta t^2}\right], \tag{6.110}$$

when $\cos k\Delta x = 1$

$$\xi = \frac{3\Delta t^2}{v_t^2}\left[\mathrm{S} - \frac{3\Delta t^2 - v_t^2}{3\Delta t^2}\right], \tag{6.111}$$

we have

$$\frac{3\Delta t^2}{v_t^2}\left[\mathrm{S}\left(\frac{3\Delta x^2 - 2v_x^2}{3\Delta x^2}\right) - \frac{3\Delta t^2 - v_t^2}{3\Delta t^2}\right] \leq \xi \leq \frac{3\Delta t^2}{v_t^2}\left[\mathrm{S} - \frac{3\Delta t^2 - v_t^2}{3\Delta t^2}\right], \tag{6.112}$$

for $\xi = 1 \rightarrow \mathrm{S} = 1$,
for $\xi = -1 \rightarrow \mathrm{S} = \frac{\Delta x^2}{\Delta t^2}\frac{3\Delta t^2 - 2v_t^2}{3\Delta x^2 - 2v_x^2}$,

we can conclude the scheme is stable if $0 \leq \mathrm{S} \leq \frac{\Delta x^2}{\Delta t^2}\frac{(3\Delta t^2 - 2v_t^2)}{(3\Delta x^2 - 2v_x^2)} \leq 1$, otherwise the scheme is unstable.

Case 2: we assume the numerical method reproduces the real frequency ω but not the wave number. The explicit expression for the wave number is given by the following expression

$$k = \frac{1}{\Delta x}\arccos\left\{\frac{3\Delta x^2}{v_x^2}\left[\frac{1}{\mathrm{S}}\left(\cos\omega\Delta t\left(\frac{v_t^2}{3\Delta t^2}\right) + \left(\frac{3\Delta t^2 - v_t^2}{3\Delta t^2}\right)\right) - \frac{3\Delta x^2 - v_x^2}{3\Delta x^2}\right]\right\}. \tag{6.113}$$

Denoting

$$\zeta = \frac{3\Delta x^2}{v_x^2}\left[\frac{1}{\mathrm{S}}\left(\cos\omega\Delta t\left(\frac{v_t^2}{3\Delta t^2}\right) + \left(\frac{3\Delta t^2 - v_t^2}{3\Delta t^2}\right)\right) - \frac{3\Delta x^2 - v_x^2}{3\Delta x^2}\right], \tag{6.114}$$

we study boundaries of $\cos\omega\Delta t$: when $\cos\omega\Delta t = -1$

$$\zeta = \frac{3\Delta x^2}{v_x^2}\left[\frac{1}{\mathrm{S}}\left(\frac{3\Delta t^2 - 2v_t^2}{3\Delta t^2}\right) - \frac{3\Delta x^2 - v_x^2}{3\Delta x^2}\right], \tag{6.115}$$

when $\cos\omega\Delta t = 1$

$$\zeta = \frac{3\Delta x^2}{v_x^2}\left[\frac{1}{\mathrm{S}} - \frac{3\Delta x^2 - v_x^2}{3\Delta x^2}\right], \tag{6.116}$$

we have

$$\frac{3\Delta x^2}{v_x^2}\left[\frac{1}{\mathrm{S}}\left(\frac{3\Delta t^2 - 2v_t^2}{3\Delta t^2}\right) - \frac{3\Delta x^2 - v_x^2}{3\Delta x^2}\right] \leq \zeta \leq \frac{3\Delta x^2}{v_x^2}\left[\frac{1}{\mathrm{S}} - \frac{3\Delta x^2 - v_x^2}{3\Delta x^2}\right], \tag{6.117}$$

for $\xi = 1 \rightarrow \mathrm{S} = 1$,
for $\xi = -1 \rightarrow \mathrm{S} = \frac{\Delta x^2}{\Delta t^2}\frac{3\Delta t^2 - 2v_t^2}{3\Delta x^2 - 2v_x^2}$,

we can conclude that the scheme is non-attenuative if $0 \leq \mathrm{S} \leq \frac{\Delta x^2}{\Delta t^2}\frac{(3\Delta t^2 - 2v_t^2)}{(3\Delta x^2 - 2v_x^2)} \leq 1$, otherwise the scheme is attenuative.

In order to determine dispersion and dissipation properties of the CSFD44A scheme for different Courant numbers, we plot graphics in terms of the normalized velocity (ratio factor). Fig. 6.9 shows dispersion and dissipation properties of the CSFD44A scheme by choosing $\Delta = v$ in time and space. In fact, we can choose values between Δ and v for both space and time, and control stability and grid dispersion of the scheme, however, all results obtained in different test for different values are very dispersive, which makes also this scheme unsuitable for wave propagation in heterogeneous media.

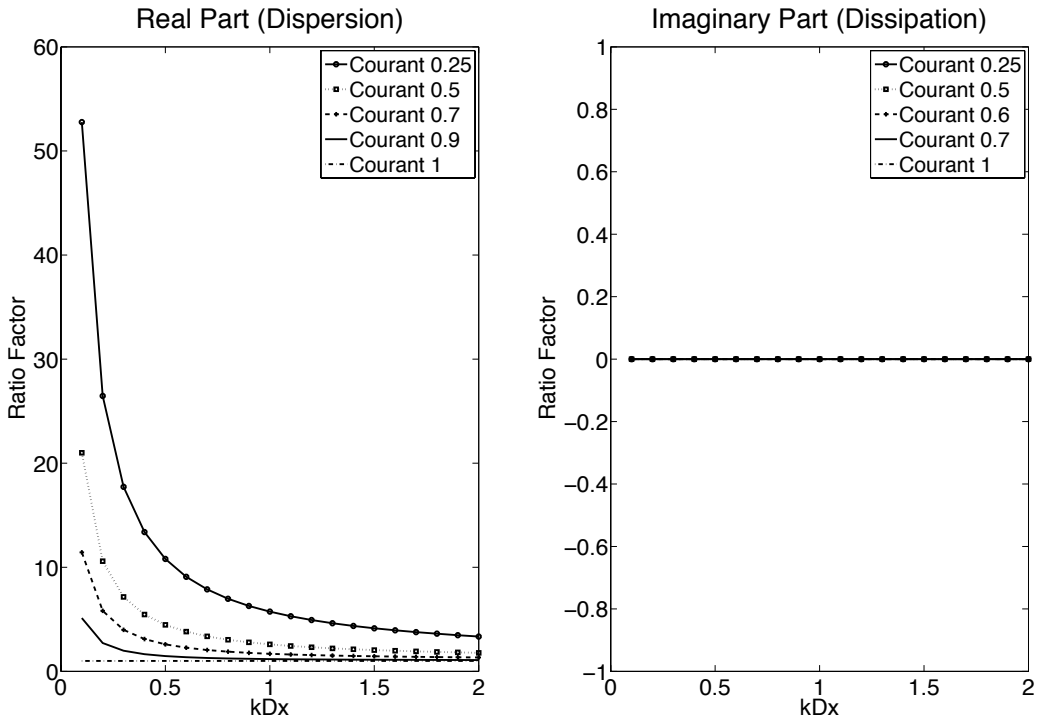

Figure 6.9: Dispersion and dissipation properties of the CSFD44A scheme.

6.4.3 CSFD44B, CSFD46A and CSFD46B

The dispersion relations for the schemes CSFD44B, CSFD46A and CSFD46B (Eqs. 6.54-6.56) are given by the following expressions

$$\cos\omega\Delta t\left(\frac{v_t^2}{3\Delta t^2}\right)+\left(\frac{3\Delta t^2-v_t^2}{3\Delta t^2}\right)=c\frac{v_t}{v_x}\Bigg\{\cos k\Delta x-\left(\frac{3\Delta x^2-v_x^2}{3\Delta x^2}\right)\left[\frac{1}{5}\left(\cos k\Delta x-1\right)+\frac{2}{5}\left(\cos^2 k\Delta x-1\right)\right]\Bigg\}, \tag{6.118}$$

$$\cos\omega\Delta t\left(\frac{v_t^2}{3\Delta t^2}\right)+\left(\frac{3\Delta t^2-v_t^2}{3\Delta t^2}\right)=c\frac{v_t}{v_x}\Bigg\{\cos k\Delta x\left(\frac{v_x^2}{3\Delta x^2}\right)+\left(\frac{3\Delta x^2-v_x^2}{3\Delta x^2}\right)-\left(\frac{5\Delta x^4-10\Delta x^2v_x^2+v_x^4}{5!}\right)\left[-\frac{8}{\Delta x^4}\left(\cos k\Delta x-1\right)+\frac{4}{\Delta x^4}\left(\cos^2 k\Delta x-1\right)\right]\Bigg\}, \tag{6.119}$$

$$\cos\omega\Delta t\left(\frac{v_t^2}{3\Delta t^2}\right)+\left(\frac{3\Delta t^2-v_t^2}{3\Delta t^2}\right)=c\frac{v_t}{v_x}\Bigg\{\cos k\Delta x-\left(\frac{3\Delta x^2-v_x^2}{3\Delta x^2}\right)\left[\frac{1}{5}\left(\cos k\Delta x-1\right)+\frac{2}{5}\left(\cos^2 k\Delta x-1\right)\right]-\left(\frac{5\Delta x^4-10\Delta x^2v_x^2+v_x^4}{5!}\right)\left[-\frac{8}{\Delta x^4}\left(\cos k\Delta x-1\right)+\frac{4}{\Delta x^4}\left(\cos^2 k\Delta x-1\right)\right]\Bigg\}. \tag{6.120}$$

Unfortunately, the discretizations CSFD44B, CSFD46A and CSFD46B are highly dispersive like 6.51 and 6.53, presenting very similar graphics. We only mention this results for the

Deriv. order	**Finite Differences**	**Complex Step Finite Differences**
$f'(x)$	$\frac{\Delta_x^+}{\Delta x}$ and/or $\frac{\square_x^{1/2}}{\Delta x}$	$\frac{\triangleright_x}{v}$ and/or $\frac{\triangleleft\triangleright_x^{1/2}}{v}$
$f''(x)$	$\frac{1}{\Delta x^2}\left(\Delta_x^+ \circ \Delta_x^-\right) = \frac{1}{\Delta x^2}\left(\square_x^{1/2} \circ \square_x^{1/2}\right)$	$\frac{\Delta_x^+}{hv}$ and/or $\frac{\square_x^{1/2}}{hv}$
$f'''(x)$	——	$\frac{1}{h^2 v}\left(\Delta_x^+ \circ \Delta_x^-\right) = \frac{1}{h^2 v}\left(\square_x^{1/2} \circ \square_x^{1/2}\right)$
$f^{iv}(x)$	$\frac{1}{\Delta x^4}\left(\square_x \circ \square_x - 4\Delta_x^+ \circ \Delta_x^-\right)$	——
$f^{v}(x)$	——	$\frac{1}{h^4 v}\left(\square_x \circ \square_x - 4\Delta_x^+ \circ \Delta_x^-\right)$

Table 6.1: General overview of Finite Differences and Complex Step Finite Differences operators used in this study. Note we have the same difference operator for both methods in different derivative orders.

schemes (Eqs. 6.54 - 6.56) but do not show the figure, for the sake of shortness. Their high dispersion does not bring any contribution for wave propagation in presence of heterogeneous media.

6.5 Equivalence of Finite Differences and Complex Step Finite Differences methods

After this analysis, we understand the analogy between CSFDM and traditional FDM schemes. While FD schemes involve difference operators applied over a displacement field (u_x^t), CSFDM schemes involve difference operators applied over the imaginary part of the imaginary perturbation of the displacement: $\mathfrak{Im}(u_{x+\mathbf{i}\Delta x}^{t+\mathbf{i}\Delta t})$ in case of of the double perturbation, $\mathfrak{Im}(u_x^{t+\mathbf{i}\Delta t})$ in case of a time perturbation (time-dependent source) and $\mathfrak{Im}(u_{x+\mathbf{i}\Delta x}^t)$ in case of a space perturbation (plane wave source). Depending on our needs, we can use any efficient difference operator over the imaginary perturbation or the displacement field in order to propagate a wave.

In Table 6.1 we give a final overview of difference operators for both methods used in this study. The main observation here is that we have the same difference operator (in the numerator) for both methods for a different derivative order.

Chapter 7

General conclusions and future research

This work extends the well known Complex Step method (CSM) by introducing the complex step in a strict sense. Simple and straightforward, this derivative concept allows developing many different approximations for the first and second order derivatives of any complex valued analytic function using its real and imaginary parts. We give a complete list of generalized complex step (CS) schemes on a compact stencil, including ten approximations for the first order derivative that avoid term cancellation inherent to classic FD approximations, as well as ways of computing second order derivatives in a single step. A superior accuracy and stability of the new CS approximations over traditional finite differences (FD) approximations have been demonstrated for an appropriate analytic test function that has been extensively used in previous studies on numerical differentiation. For an appropriate choice of step sizes in the real and imaginary directions, fourth accuracy can be reached in a simple two step scheme. On the other hand, the generalized CS method is essentially as computational efficient and easy to implement as the corresponding classic FD schemes. In conclusion, generalized CS may provide a valuable alternative for accurate numerical modeling in many science and engineering applications, especially for problems that string together many successive FD operations and are particularly susceptible to error propagation.

Based on the generalization of the CSM we have developed the Complex Step Finite Differences method (CSFDM) to efficiently solve in two directions the acoustic one-way wave equation in 1D, 2D and 3D homogeneous medium. Introducing the use of complex numbers in numerical modeling of wave propagation, this work extends the well known Finite Differences method (FDM) to a wide range of applications, allowing more accurate results under the same computational requirements. A theoretical analysis of stability dispersion-dissipation relations of the introduced schemes has been presented. Advantages of the introduced CSFDM is the separation between gradients and velocities as initial conditions of the wave propagation problem. The introduced numerical method is based on a generalization of the standard FDM and therefore its implementation is rather simple and straightforward. We have explicitly established the relation between both methods. The introduction of complex numbers in numerical modeling allow to translate dispersive discretizations in dissipative discretizations and the other way around.

We have computed stability and dispersion properties of the most common FD schemes for the second order wave equation in a standard and unified way. We have introduced several Complex Step Finite Differences (CSFD) operators for solving the wave equation and compared to general FD schemes. We have seen, the inclusion of more space/time information into the discretizations (FD44 scheme, four order accurate in time and space) is not translated into better discretizations for heterogeneous media, being the FD24 scheme (second order

accurate in time and four order accurate in space) more appropriate than the FD44 scheme in presence of non constant coefficients. From the methodological point of view, differences between gradients and velocities as initial conditions, related to the imaginary perturbation in space and/or time (related to plane waves or point sources) of the wave propagation problem, has never been taken into account in a FD discretization. The introduced method (CSFDM) offers a new way of translating dispersion to dissipation and the other way around in partial differential equations. Although, the proposed CSFD schemes do not bring any contribution, related to dispersion properties, in presence of heterogeneous media over the popular FD schemes, they can also be applied to solve the wave propagation problem in order to separate velocity and gradients as initial conditions of the problem.

This work has made advances in understanding the numerical solution of the wave propagation problem using complex numbers on the one hand, and contributes to the knowledge of numerical modeling of differential equations on the other hand. This study represent the search for an improved and simpler difference scheme for solving the wave propagation problem in seismology. The introduced CSFDM can be seen as numerical technique that complements the conventional FDM. The advantages of the CSFDM over the FDM are related to imposing different kinds of initial conditions and showing its higher order accuracy under the same computational cost and similar numerical dispersion.

In this study, the newly introduced CS approximations were developed and discussed in the conceptual framework of finite difference schemes (FDM). However, like many numerical techniques, CSM could be also applied to the integral form (weak or strong) of the PDE in study. An obvious possible application is the generalization of the Finite Volume Method (FVM) (e.g. LeVeque (2002)) by using complex steps. Further, we recall here that FD/CS approximations are not restricted to spatial discretizations. Many methods common in seismology, like SEM, FEM, DGM and others, use FD discretizations in time, meaning that a wide range of numerical techniques can be reformulated by the use of complex steps in time. In this context, the higher formal accuracy of CS schemes may be particularly useful for simulations of wave propagation that involve a large number of time-steps, like for example the analysis of free oscillations of the Earth.

Another obvious possible application is the development of implicit CSFD schemes, such as variants of FDM like the alternating direction implicit (ADI) methods (e.g. Douglas (1955)), where the main idea of ADI is to decompose the DE into simpler equations for which only tridiagonal systems of linear algebraic equations need to be solved in each time-step and leading to unconditionally stable discretizations. Also *compact FD schemes* with higher accuracy (e.g. Lele (1992)) and Multigrid methods (MGM) (e.g. Hackbusch (2010)) can be immediately generalized by the CSM developed in this work.

In the authors' opinion, the simple and intuitive structure of the CS approximations favors that a wide range of CS applications may yet be explored in the future. In this work, we have focused our attention on the acoustic/elastic wave equation, achieving significant results, but realizing that further studies are required to design a proper CSFD solver for the numerical simulation of wave propagation in realistic media. In a more general context, we would like to better understand the complete potential of the use of the complex numbers in numerical modeling. It is expected that the CSFD method can be naturally extended to find solutions for many different differential equations that are relevant in Geophysics, such as the Navier-Stokes equations, heat equation and shallow water equations among many others.

Chapter 8

Conclusiones generales y trabajos futuros

En este trabajo extiende el bien conocido Método del Paso Complejo (MPC) introduciendo un paso complejo en el sentido estricto. De forma simple y sencilla, este concepto de derivada permite desarrollar varios tipos diferentes de aproximaciones para la primera y segunda derivada de cualquier función analítica usando su parte real e imaginaria. Se muestra una lista completa de esquemas generalizados de paso complejo de forma compacta, incluyendo diez aproximaciones para la primera derivada que evitan el problema de cancelación de términos inherente a las aproximaciones clásicas de diferencias finitas (DF), como también formas de calcular segundas derivadas usando un solo paso. Mayor precisión y estabilidad de las nuevas aproximaciones de paso complejo (PC) sobre las tradicionales de DF clásicas se demostró usando una función analítica de prueba, la cual ha sido usada extensamente en estudios previos. De diferenciación numérica. Se pudo alcanzar precisión de cuarto orden en esquemas de dos pasos usando una elección apropiada en la dirección real e imaginaria. Por otro lado, el MPC es esencialmente tan eficiente computacionalmente y fácil de implementar como los correspondiente esquemas de DF. El PC generalizado puede proveer una alternativa valiosa para modelado numérico de alta precisión en varias aplicaciones de ciencia e ingeniería, especialmente en problemas que traigan consigo sucesivas operaciones de DF y las cuales sean particularmente susceptibles a errores de propagación.

Basado en la generalización del MPC se desarrollo el Método de Paso Complejos con Diferencias Finitas (MPCDF) para de forma eficiente resolver en dos direcciones la ecuación de onda acústica unidireccional en un medio homogéneo 1D, 2D y 3D. Introduciendo el uso de números complejos en modelado numérico de la ecuación de onda, este trabajo extiende el bien conocido Método de Diferencias Finitas (MDF) a un rango más amplio de aplicaciones, permitiendo resultados más precisos bajo los mismos costos computacionales. Un análisis teórico de estabilidad y propiedades de dispersión de los esquemas introducidos ha sido de igual forma presentado. Las ventajas relacionadas en el MPCDF introducido es la separación entre gradientes y velocidades como condiciones iniciales del problema de propagación de ondas. El método numérico introducido es basado en una generalización del MDF estándar, por lo tanto su implementación es simple y sencilla. En este trabajo hemos establecido la relación entre ambos métodos. La introducción de números complejos en modelado numérico permite el trasladar discretizaciones dispersivas en discretizaciones disipativas y de manera inversa.

Hemos calculado propiedades de estabilidad y dispersión para los más comunes esquemas de DF para la ecuación de onda de segundo orden de forma estándar y unificada. Hemos introducido varios operadores de Diferencias Finitas con Pasos Complejos (DFPC) para la solución de la ecuación de onda y los hemos comparado con esquemas generales de DF. Hemos visto como la inclusión de mas información espacio/tiempo dentro de la discretización (p.ej.

el esquema de diferencias finitas FD44, cuarto orden de precisión en tiempo y espacio) no es traducido en mejores discretizaciones cuando nos encontramos en presencia de medios heterogéneos, siendo el esquema FD24 (segundo orden de precisión en tiempo y cuarto orden en espacio) más apropiado que el FD44 en presencia de coeficientes no constantes. Desde el punto de vista metodológico, diferencias entre gradientes y velocidades como condiciones iniciales, relacionados con la perturbación imaginaria en espacio y/o tiempo (relacionados con ondas planas o fuentes puntuales) del problema de propagación de ondas, nunca ha sido tomado en cuenta en una discretización de DF. El método introducido (MPCDF) ofrece una nueva forma de intercambiar dispersión por disipación y de forma contraria en ecuaciones diferenciales parciales. Aunque, los esquemas propuestos de PCDF no traen ninguna contribución, en relación con las propiedades de dispersión, en presencia de medios heterogéneos sobre los esquemas populares de DF, ellos también pueden ser aplicados en la resolución del problema de propagación de onda para separar velocidades y gradientes como condiciones iniciales del problema.

Este trabajo ha hecho avances en el entendimiento de la solución numérica del problema de propagación de onda usando números complejos por un lado, y contribuye al conocimiento del modelado numérico de ecuaciones diferenciales por otro lado. Este estudio representa la búsqueda por un mejorado y más simple esquema numérico para la solución del problema de propagación de ondas en la sismología. El introducido MPCDF puede ser entendido como una técnica numérica que complementa el MDF convencional. Las ventajas del MPCDF sobre MDF esta relacionado con la imposición de diferentes tipos de condiciones iniciales y su mayor precisión bajo el mismo costo computacional y propiedades similares de dispersión.

En este estudio, las nuevas introducidas aproximaciones de PC fueron desarrolladas y discutidas en un esquema conceptual de esquemas de DF. Sin embargo, como muchas otras técnicas numéricas, el MPCDF puede ser aplicado a la ecuación integral (débil o fuerte) de la ecuación diferencial en estudio. Una posible aplicación es la generalización del método de los Volúmenes Finitos (ej. LeVeque (2002)) usando pasos complejos. Además, recalcamos que las aproximaciones de FD/PC no están restringidas a discretizaciones espaciales. Muchos métodos numéricos, comúnmente usados en sismología, usan dicretizaciones de diferencias finitas en el tiempo, significando que un amplio rango de técnicas numéricas puede ser reformulado por el uso de números complejos. En este contexto, la mayor precisión de esquemas de PC podría ser particularmente útil para simulaciones de propagación de ondas que involucren un gran número de pasos de tiempo, como por ejemplo el análisis de modos fundamentales de la Tierra. Otra aplicación obvia posible es el desarrollo de esquemas implícitos de PCDF, tal como variantes del MDF como Método de Direcciones Alternates (ej. Douglas (1955)), donde la idea principal es descomponer la ecuación diferencial en ecuaciones más sencillas por las cuales sólo sistemas tridiagonales de ecuaciones lineales algebraicas necesitas ser resueltas en cada paso de tiempo, conduciendo a discretizaciones incondicionalmente estables. También esquemas *compactos* de gran precisión (ej. Lele (1992)) y Métodos Multigrid (ej. Hackbusch (2010)) pueden ser inmediatamente generalizados por el MPC desarrollado en este trabajo.

En opinión de los autores, la estructura simple e intuitiva de las aproximaciones de PC favorece que un gran rango de aplicaciones de PC pueda ser explorado en el futuro. En este trabajo, nos hemos enfocado nuestra atención en la ecuación acústica/elástica, logrando resultados importantes, pero entendiendo que muchos más estudios son requeridos para diseñar un esquema de PCDF para la solución numérica del problema de propagación de ondas en medios realísticos. En un contexto más general, nos gustaría entender con mayor profundidad el completo potencial del uso de números complejos en modelado numérico. Se espera que el MPCDF pueda ser naturalmente extendido a la solución de muchas ecuaciones diferenciales relevantes en el campo de la Geofísica, tal como las ecuaciones de Navier-Stokes, la ecuación de calor y las ecuaciones de aguas someras dentro de muchas otras.

Bibliography

Abokhodair, A. (2007). Numerical tools for geoscience computations: Semiautomatic differentiation (SD) . *Computational Geosciences*, 11:283–296. 10.1007/s10596-007-9052-z.

Abokhodair, A. A. (2009). Complex differentiation tools for geophysical inversion. *Geophysics*, 74(2):H1–H11.

Abreu, R., Stich, D., and Morales, J. (2013a). The complex step finite differences method applied to the acoustic wave equation. submitted.

Abreu, R., Stich, D., and Morales, J. (2013b). On the generalization of the complex step method. *Journal of Computational and Applied Mathematics*, 241(0):84 – 102.

Abubakar, A., Pan, G., Li, M., Zhang, L., Habashy, T., and van den Berg, P. (2011). Three-dimensional seismic full-waveform inversion using the finite-difference contrast source inversion method. *Geophysical Prospecting*, 59(5):874–888.

Aki, K. and Richards, P. G. (2009). *Quantitative Seismology*. University Science Books, 2nd edition edition.

Al-Mohy, A. and Higham, N. (2010). The Complex Step Approximation to the Fréchet Derivative of a Matrix Function. *Numerical Algorithms*, 53:133–148.

Anderson, J. G. (2004). Quantitative measure of the goodness-of-fit of synthetic seismograms. In *Proceedings of the 13th World Conference on Earthquake Engineering*, page 243.

Anderson, W., Newman, J., Whitfield, D., and Nielsen, E. (2001). Sensitivity analysis for the Navier-Stokes equations on unstructured meshes using complex variables. *American Institute of Aeronautics and Astronautics Journal*, 39(1):56–63.

Angus, D., Thomson, C., and Pratt, R. (2004). A one-way wave equation for modelling seismic waveform variations due to elastic anisotropy. *Geophysical Journal International*, 156:595 – 614.

Aochi, H., Ducellier, A., Dupros, F., Delatre, M., Ulrich, T., Martin, F., and Yoshimi, M. (2013). Finite difference simulations of seismic wave propagation for the 2007 mw 6.6 niigata-ken chuetsu-oki earthquake: Validity of models and reliable input ground motion in the near-field. *Pure and Applied Geophysics*, 170(1-2):43–64.

Bagley, R. (2006). On Fourier Differentiation - A Numerical Tool for Implicit Functions. *International Journal of Applied Mathematics*, 19(3):255–282.

Belytschko, T., Lu, Y. Y., and Gu, L. (1994). Element-free galerkin methods. *International Journal for Numerical Methods in Engineering*, 37(2):229–256.

Bezada, M. J., Levander, A., and Schmandt, B. (2010). Subduction in the southern Caribbean: Images from finite-frequency P wave tomography. *Journal of Geophysical Research: Solid Earth*, 115(B12):B12333.

Bozdag, E., Zhu, H., Peter, D., and Tromp, J. (2013). Global adjoint tomography: Perspectives, initial results and future directions. In *EGU General Assembly Conference Abstracts*, volume 15 of *EGU General Assembly Conference Abstracts*, page 3555.

Burg, C. and Newman, J. (2003). Computationally efficient, numerically exact design space derivatives via the complex Taylor's series expansion method. *Computers and Fluids*, 32(3).

Cao, Y. (2008). HESSIANCSD: Complex Step Hessian. *http://www.mathworks.de/matlabcentral/fileexchange/18177-complex-step-hessian/content/hessiancsd.m*.

Capdeville, Y., Guillot, L., and Marigo, J.-J. (2010). 2-D non-periodic homogenization to upscale elastic media for P-SV waves. *Geophysical Journal International*, 182(2):903–922.

Cerveny, V. (2011). SEISMIC RAY THEORY. *Encyclopedia of Solid Earth Geophysics*, pages 1098–1107.

Cerviño, L. I. and Bewley, T. R. (2003). On the extension of the complex-step derivative technique to pseudospectral algorithms. *J. Comput. Phys.*, 187:544–549.

Chaillat, S., Bonnet, M., and Semblat, J.-F. (2008). A fast multipole accelerated BEM for 3-D elastic wave computation. *European Journal of Computational Mechanics Revue Européenne de Mécanique Numérique*, 17(5-7):701–712.

Chaljub, E., Moczo, P., Tsuno, S., Bard, P.-Y., Kristek, J., Käser, M., Stupazzini, M., and Kristekova, M. (2010). Quantitative Comparison of Four Numerical Predictions of 3D Ground Motion in the Grenoble Valley, France. *Bulletin of the Seismological Society of America*, 100(4):1427–1455.

Chin, R., Hedstrom, G., and Thigpen, L. (1984). Numerical methods in seismology. *Journal of Computational Physics*, 54(1):18 – 56.

Claerbout, J. F. (1986). Imaging the Earth's Interior. *Geophysical Journal of the Royal Astronomical Society*, 86(1):217–217.

Clarke, T. (1989). SEISMOGRAMS: SYNTHETIC. *Encyclopedia of Solid Earth Geophysics*, pages 1192–1017.

Clayton, R. W. and Engquist, B. (1980). Absorbing boundary conditions for wave-equation migration. *Geophysics*, 45(5):895–904.

Cohen, G. (2001). *Higher-Order Numerical Methods for Transient Wave Equations*. Springer Verlag New York.

Cohen, G. and Joly, P. (1996). Construction analysis of fourth-order finite difference schemes for the acoustic wave equation in nonhomogeneous media. *SIAM Journal on Numerical Analysis*, 33(4):1266–1302.

Cooke, M. (2011). NUMERICAL METHODS, BOUNDARY ELEMENT. *Encyclopedia of Solid Earth Geophysics*, pages 877–879.

Dablain, M. A. (1986). The application of high-order differencing to the scalar wave equation. *Geophysics*, 51(1):54–66.

de la Puente, J., Dumbser, M., Käser, M., and Igel, H. (2008). Discontinuous Galerkin Methods for Wave Propagation in Poroelastic Media. *Geophysics*, 73(5):T77–T97.

Dennis, B. H., Jin, W., Dulikravich, G. S., and Jaric, J. (2011). Application of the Finite Element Method to inverse problems in solid mechanics. *The International Journal of Structural Changes in Solids*, 3(2):11–21.

DePauw, D. and Vanrolleghem, P.-A. (2005). Using the complex-step derivative approximation method to calculate local sensitivity functions of highly nonlinear bioprocess models. In *Proceedings 17th IMACS World Congress on Scientific Computation, Applied Mathematics and Simulation (IMACS 2005)*.

Douglas, Jim, J. (1955). On the numerical integration $\frac{\partial^2 u}{\partial x^2} + \frac{\partial^2 u}{\partial y^2} = \frac{\partial u}{\partial t}$ by implicit methods. *Journal of the Society for Industrial and Applied Mathematics*, 3(1):42–65.

Dumbser, M. and Käser, M. (2007). Arbitrary high order non-oscillatory finite volume schemes on unstructured meshes for linear hyperbolic systems. *Journal of Computational Physics*, 221(2):693 – 723.

Dumbser, M., Käser, M., and de la Puente, J. (2007a). Arbitrary High Order Finite Volume Schemes for Seismic Wave Propagation on Unstructured Meshes in 2D and 3D. *Geophysical Journal International*, 171(2):665–694.

Dumbser, M., Käser, M., and Toro, E. F. (2007b). An arbitrary high-order Discontinuous Galerkin method for elastic waves on unstructured meshes - V. Local time stepping and p-adaptivity. *Geophysical Journal International*, 171(2):695–717.

Dziewonski, A. M. and Anderson, D. L. (1981). Preliminary reference earth model. *Physics of the Earth and Planetary Interiors*, 25(4):297–356.

Fichtner, A., Bunge, H.-P., and Igel, H. (2006). The adjoint method in seismology: II. Applications: traveltimes and sensitivity functionals . *Physics of the Earth and Planetary Interiors*, 157(1-2):105 – 123.

Fichtner, A., Kennett, B. L., Igel, H., and Bunge, H.-P. (2010). Full waveform tomography for radially anisotropic structure: New insights into present and past states of the australasian upper mantle. *Earth and Planetary Science Letters*, 290(3?4):270 – 280.

Fichtner, A., Trampert, J., Cupillard, P., Saygin, E., Taymaz, T., Capdeville, Y., and Villaseñor, A. (2013). Multiscale full waveform inversion. *Geophysical Journal International*.

Fornberg, B. (1981). Numerical differentiation of analytic functions. *ACM Transactions on Mathematical Software*, 7(4):512–526.

Frankel, A. and Clayton, R. W. (1986). Finite difference simulations of seismic scattering: Implications for the propagation of short-period seismic waves in the crust and models of crustal heterogeneity. *Journal of Geophysical Research: Solid Earth*, 91(B6):6465–6489.

Galis, M., Moczo, P., and Kristek, J. (2008). A 3-D hybrid finite-difference finite-element viscoelastic modelling of seismic wave motion. *Geophysical Journal International*, 175:153–184.

Gao, X.-W. and He, M.-C. (2005). A new inverse analysis approach for multi-region heat conduction BEM using complex-variable-differentiation method. *Engineering Analysis with Boundary Elements*, 29(8):788 – 795.

Gingold, R. and Monaghan, J. (1977). Smoothed particle hydrodynamics - Theory and application to non-spherical stars. *Monthly Notices of the Royal Astronomical Society*, 181:375–389.

Girard, P. R. (2007). *Quaternions, Clyfford Algebras and Relativistic Physics*. Birkhäuser Verlag.

Hackbusch, W. (2010). *Multi-Grid Methods and Applications*. Springer Series in Computational Mathematics.

Halldin, M. (2013). Earth layers model. `http://commons.wikimedia.org/wiki/File:Earth_layers_model.png`. Accessed October, 2013.

Hao, S., Park, H. S., and Liu, W. K. (2002). Moving particle finite element method. *International Journal for Numerical Methods in Engineering*, 53(8):1937–1958.

Hesthaven, J., Gottlieb, S., and Gottlieb, D. (2007). *Spectral Methods for Time-Dependent Problems*. Cambridge Monographs on Applied and Computational Mathematics.

Igel, H. (1999). Wave propagation in three-dimensional spherical sections by the Chebyshev spectral method. *Geophysical Journal International*, 136:559–566.

Inan, U. S. and Marshall, R. A. (2004). *Numerical Electromagnetics: The FDTD Method*. Cambridge University Press, first edition edition.

Jin, W., Dennis, B., and Wang, B. (2010). Improved sensitivity analysis using a complex variable semi-analytical method. *Structural and Multidisciplinary Optimization*, 41:433–439. 10.1007/s00158-009-0427-8.

Kang, T.-S. and Baag, C.-E. (2004). An Efficient Finite-Difference Method for Simulating 3D Seismic Response of Localized Basin Structures. *Bulletin of the Seismological Society of America*, 94(5):1690–1705.

Käser, M., Dumbser, M., de la Puente, J., and Igel, H. (2007). An Arbitrary High Order Discontinuous Galerkin Method for Elastic Waves on Unstructured Meshes III: Viscoelastic Attenuation. *Geophysical Journal International*, 168(1):224–242.

Käser, M., Hermann, V., and Puente, J. d. l. (2008). Quantitative accuracy analysis of the discontinuous Galerkin method for seismic wave propagation. *Geophysical Journal International*, 173(3):990–999.

Käser, M., Pelties, C., Castro, E. C., Djikpesse, H., and Prange, M. (2010). Wave Field Modeling in Exploration Seismology Using the Discontinuous Galerkin Finite Element Method on HPC-infrastructure. *The Leading Edge*, 29:76–85.

Kim, J., Bates, D., and Postlethwaite, I. (2005). Complex-Step Gradient Approximation For Robustness Analysis Of Nonlinear Systems. In *The 16th IFAC World Congress*.

Kim, J., Bates, D. G., and Postlethwaite, I. (2006). Nonlinear robust performance analysis using complex-step gradient approximation. *Automatica*, 42(1):177 – 182.

Koketsu, K., Fujiwara, H., and Ikegami, Y. (2004). Finite-element simulation of seismic ground motion with a voxel mesh. *Pure and Applied Geophysics*, 161(11-12):2183–2198.

Komatitsch, D., Erlebacher, G., Goddeke, D., and Michéa, D. (2010). High-order finite-element seismic wave propagation modeling with MPI on a large GPU cluster. *Journal of Computational Physics*, 229(20):7692 – 7714.

Komatitsch, D. and Tromp, J. (1999). Introduction to the spectral-element method for 3-D seismic wave propagation. *Geophys. J. Int.*, 139(3):806–822.

Komatitsch, D. and Tromp, J. (2002a). Spectral-element simulations of global seismic wave propagation-I. Validation. *Geophysical Journal International*, 149(2):390–412.

Komatitsch, D. and Tromp, J. (2002b). Spectral-element simulations of global seismic wave propagation-II. Three-dimensional models, oceans, rotation and self-gravitation. *Geophysical Journal International*, 150(1):303–318.

Komatitsch, D., Tromp, J., et al. (2013). *SPECFEM3D GLOBE: User Manual Version 5.1*.

Komatitsch, D. and Vilotte, J. P. (1998). The spectral-element method: an efficient tool to simulate the seismic response of 2D and 3D geological structures. *Bull. Seismol. Soc. Am.*, 88(2):368–392.

Kristek, J. and Moczo, P. (2003). Seismic-Wave Propagation in Viscoelastic Media with Material Discontinuities: A 3D Fourth-Order Staggered-Grid Finite-Difference Modeling. *Bulletin of the Seismological Society of America*, 93(5):587–603.

Käser, M. and Dumbser, M. (2006). An arbitrary high-order discontinuous Galerkin method for elastic waves on unstructured meshes - I. The two-dimensional isotropic case with external source terms. *Geophysical Journal International*, 166(2):855–877.

Lai, K.-L. and Crassidis, J. (2008). Extensions of the first and second complex step derivative approximations. *Journal of Computational and Applied Mathematics*, 219:276–293.

Lai, K.-L., Crassidis, J., Cheng, Y., and Kim, J. (2005). New Complex Step derivative approximations with application to second-order Kalman filtering. *American Institute of Aeronautics and Astronautics, Guidance, Navigation, and Control Conference, San Francisco, CA.*, (2005-5944):202–210.

Lamb, H. (1904). On the propagation of tremors over the surface of an elastic solid. *Philosophical Transactions of the Royal Society of London. Series A, Containing Papers of a Mathematical or Physical Character*, 203(359-371):1–42.

Lax, P. D. and Richtmyer, R. D. (1956). Survey of the stability of linear finite difference equations. *Communications on Pure and Applied Mathematics*, 9(2):267–293.

Lele, S. K. (1992). Compact finite difference schemes with spectral-like resolution. *Journal of Computational Physics*, 103(1):16 – 42.

LeVeque, R. J. (2002). *Finite Volume Methods for Hyperbolic Problems*. Cambridge Texts in Applied Mathematics.

Liszka, T. and Orkisz, J. (1980). The finite difference method at arbitrary irregular grids and its application in applied mechanics. *Computers and Structures*, 11(1-2):83 – 95.

Luo, Y. (2013). *SEISMIC IMAGING AND INVERSION BASED ON SPECTRAL-ELEMENT AND ADJOINT METHODS*. PhD thesis, Princeton University.

Luo, Y., Tromp, J., Denel, B., and Calandra, H. (2013). 3D coupled acoustic-elastic migration with topography and bathymetry based on spectral-element and adjoint methods. *GEOPHYSICS*, 78(4):S193–S202.

Lyness, J. (1968). Differentiation Formulas for Analytic Function. *Mathematics of Computation*, 22(102):352–362.

Lyness, J. and Moler, C. (1967). Numerical Differentiation of Analytic Functions. *Journal of Numerical Analysis*, 4(4):202–210.

Lyness, J. N. and Sande, G. (1971). Algorithm 413: ENTCAF and ENTCRE: evaluation of normalized Taylor coefficients of an analytic function. *Commun. ACM*, 14:669–675.

Madariaga, R. (1976). Dynamics of an expanding circular fault. *Bulletin of the Seismological Society of America*, 66(3):639–666.

Martins, J., Kroo, I., and Alonso, J. (2000). An Automated Method For Sensitivity Analysis Using Complex Variable. *American Institute of Aeronautics and Astronautics*, 38(1):1–12.

Martins, J., Sturdza, P., and Alonso, J. (2003). The Complex Step Derivative Approximation. *ACM Transactions on Mathematical Software*, 29(3):245–262.

Moczo, P., Kristek, J., and Galis, M. (2014). *The Finite-difference Modelling of Earthquake Motions: Waves and Ruptures*. Cambridge University Press.

Moczo, P., Kristek, J., and Gális, M. (2004a). Simulation of the planar free surface with near-surface lateral discontinuities in the finite-difference modeling of seismic motion. *Bulletin of the Seismological Society of America*, 94(2):760–768.

Moczo, P., Kristek, J., and Halada, L. (2004b). The Finite Difference Method for Seismologist: An Introduction. Technical report, Comenius University Bratislavia.

Moczo, P., Kristek, J., Vavryuk, V., Archuleta, R. J., and Halada, L. (2002). 3D Heterogeneous Staggered-Grid Finite-Difference Modeling of Seismic Motion with Volume Harmonic and Arithmetic Averaging of Elastic Moduli and Densities. *Bulletin of the Seismological Society of America*, 92(8):3042–3066.

Montagner, J.-P. (2011). EARTH'S STRUCTURE, GLOBAL. *Encyclopedia of Solid Earth Geophysics*, pages 144–153.

Nolet, G. (2011). SEISMIC TOMOGRAPHY. *Encyclopedia of Solid Earth Geophysics*, pages 1195–1198.

Nour, A., Slimani, A., Laouami, N., and Afra, H. (2003). Finite element model for the probabilistic seismic response of heterogeneous soil profile. *Soil Dynamics and Earthquake Engineering*, 23(5):331 – 348.

Patera, A. T. (1984). A spectral element method for fluid dynamics: Laminar flow in a channel expansion. *Journal of Computational Physics*, 54(3):468 – 488.

Pelties, C., de la Puente, J., Ampuero, J.-P., Brietzke, G. B., and Kaser, M. (2012). Three-dimensional dynamic rupture simulation with a high-order discontinuous galerkin method on unstructured tetrahedral meshes. *Journal of Geophysical Research: Solid Earth*, 117(B2):B02309.

Peter, D., Tape, C., Boschi, L., and Woodhouse, J. H. (2007). Surface wave tomography: global membrane waves and adjoint methods. *Geophysical Journal International*, 171(3):1098–1117.

Rand, O. and Rovenski, V. (2005). *Analytical Methods in Anisotropic Elasticity: with Symbolic Computational Tools*. Birkhäuser Boston.

Ritsema, J. and Van Heijst, H. (2000). Seismic imaging of structural heterogeneity in Earth's mantle: evidence for large-scale mantle flow. *Science progress*, 83 (Pt 3):243–59.

Rojas, O., Dunham, E. M., Day, S. M., Dalguer, L. A., and Castillo, J. E. (2009). Finite difference modelling of rupture propagation with strong velocity-weakening friction. *Geophysical Journal International*, 179(3):1831–1858.

Sadd, M. H. (2005). *Elasticity: Theory, Applications and Numerics*. Elsevier Inc.

Shaofan, L. and Wing-Kam, L. (2002). Meshfree and particle methods and their applications. *Applied Mechanics Reviews*, 55(1):1–34.

Sidler, R., Carcione, J. M., and Holliger, K. (2013). A pseudo-spectral method for the simulation of poro-elastic seismic wave propagation in 2d polar coordinates using domain decomposition. *Journal of Computational Physics*, 235(0):846 – 864.

Spakman, W., van der Lee, S., and van der Hilst, R. (1993). Travel-time tomography of the european-mediterranean mantle down to 1400 km. *Physics of the Earth and Planetary Interiors*, 79(12):3–74.

Squire, W. and Trapp, G. (1998). Using complex variables to estimate derivatives of real functions. *SIAM Journals Online*, 40(1):110–112.

Stadler, G., Gurnis, M., Burstedde, C., Wilcox, L. C., Alisic, L., and Ghattas, O. (2010). The dynamics of plate tectonics and mantle flow: From local to global scales. *Science*, 329(5995):1033–1038.

Stich, D., Mancilla, F. d. L., Pondrelli, S., and Morales, J. (2007). Source analysis of the february 12th 2007, mw 6.0 horseshoe earthquake: Implications for the 1755 lisbon earthquake. *Geophysical Research Letters*, 34(12):L12308.

Strang, G. (2007). *Computational Science and Engineering*. Wellesley-Cambridge Press.

Strikwerda, J. (2004). *Finite Differences Schemes and Partial Differential Equations*. Society for Industrial and Applied Mathematics, second edition edition.

Suzuki, Y. and Koshizuka, S. (2008). A hamiltonian particle method for non-linear elastodynamics. *International Journal for Numerical Methods in Engineering*, 74(8):1344–1373.

Tadi, M. (2004). Finite Volume Method for 2D Elastic Wave Propagation. *Bulletin of the Seismological Society of America*, 94(4):1500–1509.

Taflove, A. and Hagness, S. (2005). *Computational Electrodynamics: The Finite-Difference Time-Domain Method*. Artech House, third edition edition.

Takekawa, J., Madariaga, R., Mikada, H., and Goto, T.-N. (2012). Numerical simulation of seismic wave propagation produced by earthquake by using a particle method. *Geophysical Journal International*, 191(3):1305–1316.

Tape, C., Liu, Q., Maggi, A., and Tromp, J. (2010). Seismic tomography of the southern california crust based on spectral-element and adjoint methods. *Geophysical Journal International*, 180(1):433–462.

Tappert, F. D. (1977). The parabolic approximation method. In *Wave Propagation and Underwater Acoustics*, volume 70, pages 224–287. Springer Berlin Heidelberg.

Thomas, J. W. (1995). *Numerical Partial Differential Equations: Finite Difference Methods*. Springer Verlag New York.

Thorne, M. S., Crotwell, H. P., Jahnke, G., and Igel, H. (2013). Wave propagation animations. `http://web.utah.edu/thorne/animations.html`. Accessed October, 2013.

Tromp, J., Komatitsch, D., Hjörleifsdóttir, V., Liu, Q., Zhu, H., Peter, D., Bozdag, E., McRitchie, D., Friberg, P., Trabant, C., and Hutko, A. (2010). Near real-time simulations of global CMT earthquakes. *Geophysical Journal International*, 183(1):381–389.

van der Hilst, R. D. and Spakman, W. (1989). Importance of the reference model in linearized tomography and images of subduction below the Caribbean Plate. *Geophysical Research Letters*, 16(10):1093–1096.

Veer N., V. (1999). Computation of Sensitivity Derivatives of Navier-Stokes Equations Using Complex Variables. Technical report.

Virieux, J. (1984). SH-wave propagation in heterogeneous media; velocity-stress finite-difference method. *Geophysics*, 49(11):1933–1942.

Virieux, J. (1986). P-SV wave propagation in heterogeneous media: Velocity-stress finite-difference method. *Geophysics*, 51(4):889–901.

Virieux, J. and Madariaga, R. (1982). Dynamic faulting studied by a finite difference method. *Bulletin of the Seismological Society of America*, 72(2):345–369.

Voorhees, A., Bagley, R., Millwater, H., and Golden, P. (2009). Application of complex variable methods for fatigue sensitivity analysis. Technical report, Department of Mechanical Engineering - University of Texas at San Antonio.

Voorhees, A., Millwater, H., and Bagley, R. (2011). Complex variable methods for shape sensitivity of finite element models. *Finite Element in Analysis and Design*, 47:1146–1156.

Wang, B. P. and Apte, A. P. (2006). Complex Variable Method for Eigensolution Sensitivity Analysis. *American Institute of Aeronautics and Astronautics*, 44:2958–2961.

Wenk, S., Pelties, C., Igel, H., and Käser, M. (2013). Regional wave propagation using the discontinuous galerkin method. *Solid Earth*, 4(1):43–57.

Wu, R.-S. (1989). Seismic Wave Scattering. *Encyclopedia of Solid Earth Geophysics*, pages 1166–1187.

Yan, J.-p. and Wang, Y.-b. (2008). Modeling seismic wave propagation in heterogeneous medium using overlap domain pseudospectral method. *Acta Seismologica Sinica*, 21(1):46–57.

Yee, K. (1966). Numerical solution of initial boundary value problems involving Maxwell's equations in isotropic media. *IEEE Transactions on Antennas and Propagation*, 3(14):302–307.

Zhu, H., Bozdag, E., Peter, D., and Tromp, J. (2012). Structure of the european upper mantle revealed by adjoint tomography. *Nature Geosciences*, 5(7):493–498.

Appendix A

Further numerical simulations

A.1 The 1D second order wave equation and the Complex Step Finite Differences method

To illustrate how the introduced CSFDM can solve the hyperbolic PDE 3.15, we will apply an approximation based only in the imaginary of the function for the second derivative (Eq. 4.35) found by Abreu et al. (2013b) (Chapter 4) at both sides of the equation to get the following expression

$$\begin{aligned}\mathfrak{Im}\left(u_{x+\mathbf{i}\Delta x}^{t+\Delta t+\mathbf{i}\Delta t}\right) = \mathrm{S}^2 \left(\mathfrak{Im}\left(u_{x+\Delta x+\mathbf{i}\Delta x}^{t+\mathbf{i}\Delta t}\right) - \mathfrak{Im}\left(u_{x-\Delta x+\mathbf{i}\Delta x}^{t+\mathbf{i}\Delta t}\right)\right) \\ + \mathfrak{Im}\left(u_{x+\mathbf{i}\Delta x}^{t-\Delta t+\mathbf{i}\Delta t}\right) + \mathcal{O}\left(\Delta t^4, \Delta x^4\right).\end{aligned} \tag{A.1}$$

We can also use discretization 5.4 to get the following

$$\mathfrak{Im}\left(u_{x+\mathbf{i}\Delta x}^{t+\Delta t+\mathbf{i}\Delta t}\right) = \mathrm{S}^2\,\mathfrak{Im}\left(u_{x+\Delta x+\mathbf{i}\Delta x}^{t+\mathbf{i}\Delta t}\right) + \left(1-\mathrm{S}^2\right)\mathfrak{Im}\left(u_{x+\mathbf{i}\Delta x}^{t+\mathbf{i}\Delta t}\right) + \mathcal{O}\left(\Delta t, \Delta x\right). \tag{A.2}$$

A.1.1 Convergence, consistence and stability analysis

Applying Von-Neuman stability condition to discretization A.1 we obtain the following

$$\mathrm{G}^2 + \mathrm{S}^2 2\mathbf{i}\sin k\Delta x\,\mathrm{G} - 1 = 0, \tag{A.3}$$

with solutions

$$\mathrm{G}_1 = e^{\mathbf{i}\arcsin\left(\mathrm{S}^2\sin k\Delta x\right)},$$
$$\mathrm{G}_2 = -e^{-\mathbf{i}\arcsin\left(\mathrm{S}^2\sin k\Delta x\right)}.$$

G_1 and G_2 are exactly on the unit circle. With $\|\mathrm{G}\| = 1$ there is no room to move, (Strang, 2007). If we substitute S^2 by S in Eq. A.3, it can be appreciated how it represents the stability equation of the Leapfrog method for the one-wave wave equation, i.e., the centered approximation to the first derivative applied to the one-way wave equation, which is stable for $\mathrm{S} \leq 1$.

For discretization A.2 we obtain

$$\mathrm{G} = \mathrm{S}^2 e^{\mathbf{i}k\Delta x} + 1 - \mathrm{S}^2, \tag{A.4}$$

Eq. A.4 is the stability equation for the forward FD scheme with the distinction only in the power of the Courant number.

A.1.2 Dispersion and dissipation analysis

Introducing the plane wave solution into Eq. A.1 and A.2 we get respectively

$$\sin \omega \Delta t = \mathrm{S}^2 \, \sin k \Delta x. \tag{A.5}$$

$$e^{\omega \Delta t} - 1 = \mathrm{S}^2 \left(e^{k \Delta x} - 1 \right). \tag{A.6}$$

Clearly the schemes are non-dissipative and dispersive.

Note that if we substitute S^2 by S, Eq. A.5 is identical to the the dispersion-dissipation relation of the Leapfrog discretization for the one-way wave equation (see Inan and Marshall (2004)). In other words, the CSFDM solves the second order wave equation by a discretization that has equivalent dispersion properties of the Leapfrog discretization to the one-way wave equation.

Numerical simulations to the second order wave equation by using the CSFDM will show the parasitic root appreciated in Figure 5.9. The effects of the parasitic mode can be solved by introducing numerical dissipation. To this end and following same approach done by the Lax-Friedrich method (see Thomas (1995)) we construct the following approximation:

$$u_{x+\mathbf{i}\Delta x}^{t-\Delta t+\mathbf{i}\Delta t} \approx \frac{1}{2} \left(u_{x+\Delta x+\mathbf{i}\Delta x}^{t+\mathbf{i}\Delta t} + u_{x-\Delta x+\mathbf{i}\Delta x}^{t+\mathbf{i}\Delta t} \right), \tag{A.7}$$

which is in fact the space mean of $u_{x+\mathbf{i}\Delta x}^{t-\Delta t+\mathbf{i}\Delta t}$ at the next time level, so discretization A.1 can be written as

$$\begin{aligned} &\mathfrak{Im} \left(u_{x+\mathbf{i}\Delta x}^{t+\Delta t+\mathbf{i}\Delta t} \right) - \frac{1}{2} \mathfrak{Im} \left(\left(u_{x+\Delta x+\mathbf{i}\Delta x}^{t+\mathbf{i}\Delta t} + u_{x-\Delta x+\mathbf{i}\Delta x}^{t+\mathbf{i}\Delta t} \right) \right) \\ &\quad = \mathrm{S}^2 \, \left(\mathfrak{Im} \left(u_{x+\Delta x+\mathbf{i}\Delta x}^{t+\mathbf{i}\Delta t} \right) - \mathfrak{Im} \left(u_{x-\Delta x+\mathbf{i}\Delta x}^{t+\mathbf{i}\Delta t} \right) \right) + \mathcal{O} \left(\Delta t, \Delta x \right). \end{aligned} \tag{A.8}$$

Discretization A.8 is identical to the analogous CSFD discretization to the popular Lax-Friedrich method for the one-way wave equation. A clear advantage is that discretization A.8 propagates the wave in one direction only, i.e., by using this discretization to propagate the second order wave equation, there is no need of absorbing boundary conditions. Both directions are obtained by just interchanging signs in the velocity term (c). The first order CSFD approximation to the second order wave equation although the method is very robust and represent a new way of propagate the second order wave equation in one direction, its low accurate in space and time which make it unsuitable for most of realistic problems.

A.2 2D second order acoustic wave equation and the FD and CSFD methods

The second order acoustic wave equation in a homogeneous two dimensional space is given by the following mathematical expression:

$$\frac{\partial^2 \mathrm{P}}{\partial t^2} = \frac{\kappa}{\rho} \left(\frac{\partial^2 \mathrm{P}}{\partial x^2} + \frac{\partial^2 \mathrm{P}}{\partial z^2} \right) + f(x, z, t), \tag{A.9}$$

where $\mathrm{P} = \mathrm{P}(x, z, t)$.

The most common and simple discretization for Eq. A.9 is the well known Leapfrog discretization given by the centered approximation for the second order derivative (Eq. 3.6) at both sides of the equation A.9, which leads to the following expression

$$\mathrm{P}_{x,z}^{t+\Delta t} = \Delta t^2 \frac{\kappa}{\rho}\left(\frac{\mathrm{P}_{x+\Delta x,z}^{t} - 2\mathrm{P}_{x,z}^{t} + \mathrm{P}_{x-\Delta x,z}^{t}}{\Delta x^2} + \frac{\mathrm{P}_{x,z+\Delta z}^{t} - 2\mathrm{P}_{x,z}^{t} + \mathrm{P}_{x,z-\Delta z}^{t}}{\Delta z^2}\right) + 2\mathrm{P}_{x,z}^{t} - \mathrm{P}_{x,z}^{t-\Delta t}. \tag{A.10}$$

The FD discretization A.10 is a well known consistent, convergent, stable, dispersive and non-dissipative discretization which propagates a wave in a two dimensional medium without the presence of any parasitic wave. Its analogous CSFD discretization is given by

$$\begin{aligned}\mathfrak{Im}\left(\mathrm{P}_{x+\mathbf{i}\Delta x,z+\mathbf{i}\Delta z}^{t+\Delta t+\mathbf{i}\Delta t}\right) = {} & \Delta t^2 \frac{\kappa}{\rho}\left[\frac{\mathfrak{Im}\left(\mathrm{P}_{x+\Delta x+\mathbf{i}\Delta x,z+\mathbf{i}\Delta z}^{t+\mathbf{i}\Delta t}\right) - \mathfrak{Im}\left(\mathrm{P}_{x-\Delta x+\mathbf{i}\Delta x,z+\mathbf{i}\Delta z}^{t+\mathbf{i}\Delta t}\right)}{\Delta x^2}\right] \\ & + \Delta t^2 \frac{\kappa}{\rho}\left[\frac{\mathfrak{Im}\left(\mathrm{P}_{x+\mathbf{i}\Delta x,z+\Delta z+\mathbf{i}\Delta z}^{t+\mathbf{i}\Delta t}\right) - \mathfrak{Im}\left(\mathrm{P}_{x+\mathbf{i}\Delta x,z-\Delta z+\mathbf{i}\Delta z}^{t+\mathbf{i}\Delta t}\right)}{\Delta z^2}\right] \\ & + \mathfrak{Im}\left(\mathrm{P}_{x+\mathbf{i}\Delta x,z+\mathbf{i}\Delta z}^{t-\Delta t+\mathbf{i}\Delta t}\right).\end{aligned} \tag{A.11}$$

Note that discretization A.11 is the analogous FD discretization to the two dimensional one-way acoustic wave equation (2D version of Eq. 5.45).

A.2.1 Convergence, consistence and stability analysis

Substituting $\mathrm{P} = \mathrm{G}(\omega, t)e^{\mathbf{i}k(x+z)}$ into discretization A.11 and by setting $\Delta x = \Delta z$ and $\mathrm{S} = \frac{\Delta t}{\Delta x}\sqrt{\frac{\kappa}{\rho}}$ we get the following

$$\mathrm{G}^2 - \mathrm{S}^2 4\mathbf{i}\sin k\Delta x\,\mathrm{G} - 1 = 0, \tag{A.12}$$

$$\mathrm{G}_1 = e^{\mathbf{i}\arcsin\left(2\mathrm{S}^2\sin k\Delta x\right)},$$
$$\mathrm{G}_2 = -e^{-\mathbf{i}\arcsin\left(2\mathrm{S}^2\sin k\Delta x\right)}.$$

Equation A.12 is a two dimensional version of Eq. A.3, i.e., a two dimensional version of the stability condition for the Leapfrog discretization of the one-way wave equation in a one dimensional space. It is easy to appreciate that the grow factor does not grow in time. To determine the stability condition we make use of the dispersion relation in the following section.

A.2.2 Dispersion-dissipation analysis

Introducing the plane wave solution into discretization A.11 and assuming $\Delta x = \Delta z$ we get

$$\sin\omega\Delta t = 2\left(\frac{\Delta t}{\Delta x}\right)^2 \frac{\kappa}{\rho}\sin k\Delta x, \tag{A.13}$$

which leads to

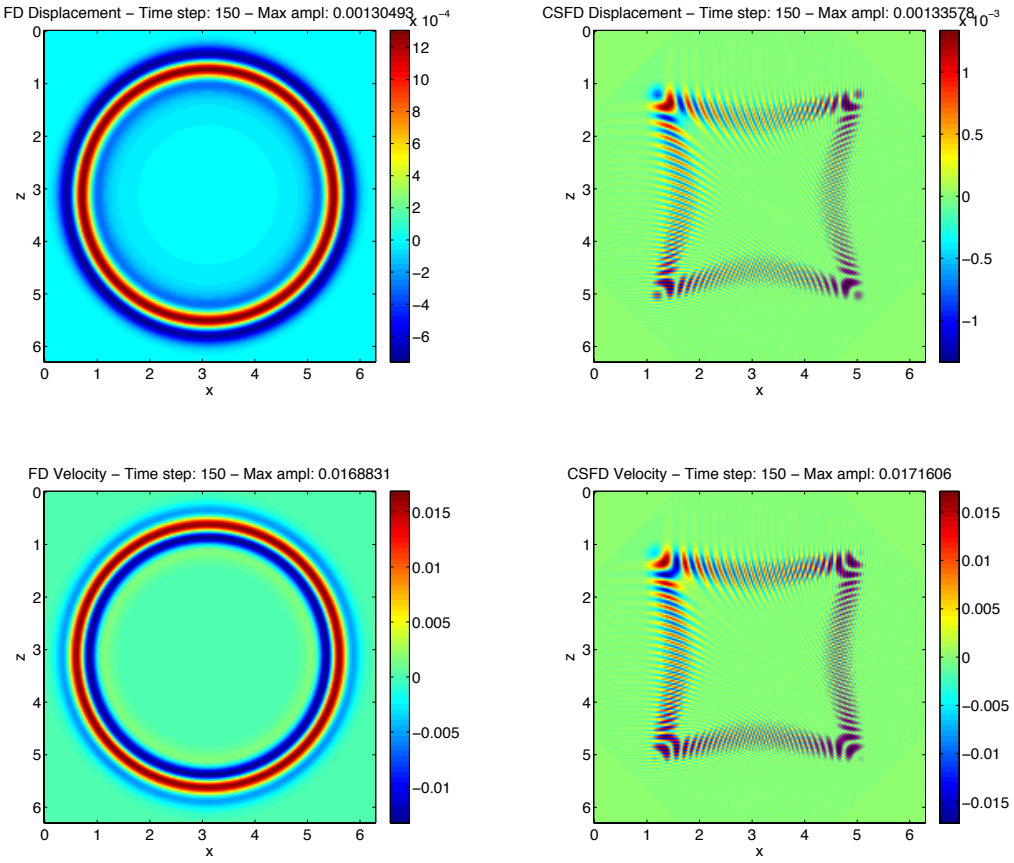

Figure A.1: Second order two dimensional acoustic wave equation simulation with Finite Differences and Complex Step Finite Differences.

$$2\left(\frac{\Delta t}{\Delta x}\right)^2 \frac{\kappa}{\rho} \leq 1, \tag{A.14}$$

or

$$\mathrm{S} \leq \frac{1}{\sqrt{2}} \tag{A.15}$$

Note that the scheme is dispersive and non-dissipative.

A.2.3 Numerical examples

The computational domain and values are the same that used the section for the two dimensional one-way wave equation with the difference in the maximum Courant number used that is 0.7071. Figure A.1 show displacement and velocity values for one snapshot of the medium with the FD and CSFD methods. We can appreciate that unlike the one dimensional medium, the parasitic wave intrinsic to the one-way Leapfrog scheme in a two dimensional space destroys the solution, making the scheme inappropriate for wave propagation simulations in a two dimensional media.

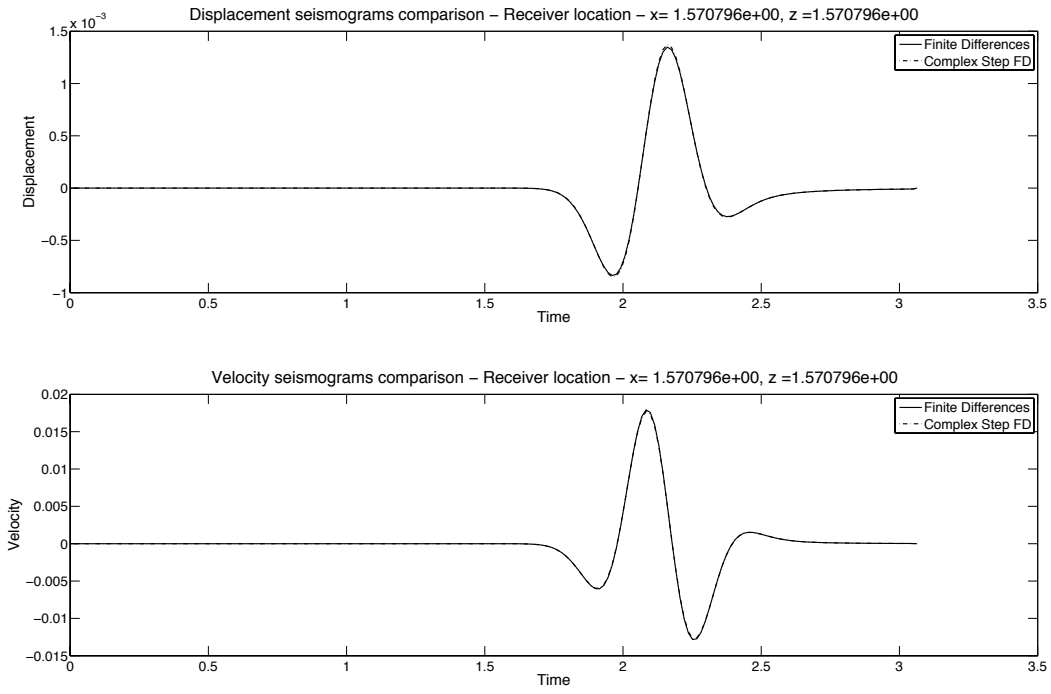

Figure A.2: Second order two dimensional acoustic wave equation simulation seismograms comparison with Finite Differences and Complex Step Finite Differences methods at a receiver located at 45 degrees.

Appendix B

Connection between CSFD and FD approximations

The one dimensional heat equation, also known as the diffusion equation, if given by the following mathematical expression (see Strikwerda (2004))

$$\frac{\partial u}{\partial t} = b\frac{\partial^2 u}{\partial x^2}, \tag{B.1}$$

where b is a positive number and $u(x,t)$ gives the temperature at time t and location x resulting from the initial temperature distribution.

The most common FD approximation to Eq. B.1 is given by the forward in time and centered in space finite differences scheme

$$u^x_{t+\Delta t} = u^t_x + \frac{b\Delta t}{2\Delta x}\left(u^t_{x+\Delta x} - 2u^t_x + u^t_{x-\Delta x}\right) + \mathcal{O}\left(\Delta t, \Delta x^2\right). \tag{B.2}$$

As we have shown, any CSFD discretization that keeps the algebraic structure of a FD approximation reproduces the same stability and dispersion-dissipation relations with the distinction only in the Courant number. Consider the following CSFD discretization analogous to FD discretization B.2 given by an approximation forward in time and centered in space:

$$\mathfrak{Im}\left(v^{t+\Delta t+\mathbf{i}\sqrt{3}\Delta t}_{x+\mathbf{i}\sqrt{3}\Delta x}\right) = \frac{b\Delta t}{2\Delta x}\left[\mathfrak{Im}\left(u^{t+\mathbf{i}\sqrt{3}\Delta t}_{x+\Delta x+\mathbf{i}\sqrt{3}\Delta x}\right) + \mathfrak{Im}\left(u^{t+\mathbf{i}\sqrt{3}\Delta t}_{x-\Delta x+\mathbf{i}\sqrt{3}\Delta x}\right)\right] + \mathcal{O}\left(\Delta t, \Delta x^4\right). \tag{B.3}$$

Equation B.3 is a CSFD discretization that correspond to the to the one-way wave equation made by using Eq. 4.9 in time and and Eq. 4.15 in space. Eq. B.3 has the same properties of dispersion-dissipation relations that the FD discretization to the heat equation B.2 for a Courant number equal to one. This example illustrates that the introduced CSFD numerical techniques offers a way of interchanging dispersion by dissipation and the other way around in the finite discretizations. Depending on our needs we can make use of this techniques, for instance, interchanging dispersion and dissipation in our discretizations in more complex PDE like Navier-Stokes equations.

Appendix C

How to compute dispersion relations

Dispersion relations are commonly found by substituting the plane wave solution (5.23) into the FD discretization. The problem arises when complex FD schemes are to be analyzed. To overcome this, we employ the Fourier transform perspective of the dispersion relation.

We illustrate this computing the dispersion relation of the Leapfrog scheme for the second order wave equation (Eq. 6.19). Lets lets recall with the forward, backward and centered difference operators we can construct higher order FD operator as a convolution of these first (see Section 6.2.1)

It is well known the convolution is equal to the multiplication in the Fourier domain, i.e.,

$$\widehat{D_x^2} = \widehat{\frac{\Delta_x^+}{\Delta x} \circ \frac{\Delta_x^-}{\Delta x}} = \widehat{\frac{\square_x}{\Delta x} \circ \frac{\square_x}{\Delta x}} = \frac{\widehat{\Delta_x^+}}{\Delta x}\frac{\widehat{\Delta_x^-}}{\Delta x} = \frac{\widehat{\square_x}}{\Delta x}\frac{\widehat{\square_x}}{\Delta x}. \tag{C.1}$$

Based on this property, we can obtain the dispersion relation for the FD discretization 6.19. For convenience, lets write Eq. 6.19 in a operator way as follows

$$D_t^2 u = c^2 D_x^2 u \quad \text{and/or} \quad \Delta_t^+ \circ \Delta_t^- u = \Delta_x^+ \circ \Delta_x^- u \quad \text{and/or} \quad \square_t^{1/2} \circ \square_t^{1/2} u = \square_x^{1/2} \circ \square_x^{1/2} u. \tag{C.2}$$

Now, the discrete Fourier transform is given by

$$\widehat{u} = \sum_{x,t} u_x^t e^{-\mathbf{i}(kx+\omega t)}. \tag{C.3}$$

Taking the discrete Fourier transform of Eq. 6.19, i.e.,

$$\sum_{x,t} u_x^t e^{-\mathbf{i}(kx+\omega t)} \left(e^{\mathbf{i}\omega\Delta t} - 2 + e^{-\mathbf{i}\omega\Delta t}\right) = \sum_{x,t} u_x^t e^{-\mathbf{i}(kx+\omega t)} \left(e^{\mathbf{i}\omega\Delta x} - 2 + e^{-\mathbf{i}\omega\Delta x}\right), \tag{C.4}$$

after simplification and by using the property: $2\cos x = e^{\mathbf{i}x} + e^{-\mathbf{i}x}$, we can write

$$\cos\omega\Delta t - 1 = c^2 \frac{\Delta t^2}{\Delta x^2}\left(\cos k\Delta x - 1\right), \tag{C.5}$$

finally by using: $2\sin^2\frac{x}{2} = 1 - \cos x$, we get

$$\sin^2\frac{\omega\Delta t}{2} = c^2\frac{\Delta t^2}{\Delta x^2}\sin^2\frac{k\Delta x}{2}. \tag{C.6}$$

Expression C.6 can also been found in a simplest way: we know $\widehat{D_x^2} = \frac{\widehat{\Delta^+}}{\Delta x}\frac{\widehat{\Delta^-}}{\Delta x}$, we can find expressions for the Fourier transform for the operators Δ^+ and Δ^- in terms of space and time derivatives, i.e., Δ_t^+, Δ_x^+, and Δ_t^-, Δ_x^-

$$\widehat{\Delta_t^+ u_x^t} = \sum_{x,t} u_x^t e^{-\mathbf{i}(kx+\omega t)} \left(e^{i\omega\Delta t} - 1\right), \tag{C.7}$$

$$\widehat{\Delta_t^- u_x^t} = \sum_{x,t} u_x^t e^{-\mathbf{i}(kx+\omega t)} \left(1 - e^{-i\omega\Delta t}\right), \tag{C.8}$$

$$\widehat{\Delta_x^+ u_x^t} = \sum_{x,t} u_x^t e^{-\mathbf{i}(kx+\omega t)} \left(e^{i\omega\Delta x} - 1\right), \tag{C.9}$$

$$\widehat{\Delta_x^- u_x^t} = \sum_{x,t} u_x^t e^{-\mathbf{i}(kx+\omega t)} \left(1 - e^{-i\omega\Delta x}\right). \tag{C.10}$$

The discrete Fourier transform using first order operators is given by

$$\widehat{\Delta_t^+}\widehat{\Delta_t^- u_x^t} = c^2\widehat{\Delta_x^+}\widehat{\Delta_x^- u_x^t}, \tag{C.11}$$

substituting and simplifying the sum we get

$$\left(e^{i\omega\Delta t} - 1\right)\left(1 - e^{-i\omega\Delta t}\right) = c^2\left(e^{i\omega\Delta x} - 1\right)\left(1 - e^{-i\omega\Delta x}\right), \tag{C.12}$$

which after little algebra can be written as Eq. C.6.

The Fourier transform operator approach is more convenient for computing dispersion relations when higher order FD approximations are involved into the discretization. For example, recall the operator from of the FD44 scheme (Eq. 6.26). It is straight forward to check the dispersion relation is given by

$$\begin{aligned} 2\cos\omega\Delta t - 2 = \mathrm{S}^2\left[\frac{4}{3}\left(2\cos k\Delta x - 2\right) - \frac{1}{12}\left(2\cos 2k\Delta x - 2\right)\right] \\ + \mathrm{S}^4\frac{1}{12}\left[-4\left(2\cos k\Delta x - 2\right) + 2\cos 2k\Delta x - 2\right]. \end{aligned} \tag{C.13}$$

Note

$$\mathrm{S}^4\frac{1}{12}\left[-4\left(2\cos k\Delta x - 2\right) + 2\cos 2k\Delta x - 2\right] = \mathrm{S}^4\frac{1}{12}\left(2\cos k\Delta x - 2\right)^2, \tag{C.14}$$

which corresponds to

$$D_x^2 \circ D_x^2 u = -4\left(\frac{\Delta_x^+}{\Delta x^2} \circ \frac{\Delta_x^-}{\Delta x^2}\right)u + \frac{\square_x}{\Delta x^2} \circ \frac{\square_x}{\Delta x^2}u = -4\left(\frac{\square_x^{1/2}}{\Delta x^2} \circ \frac{\square_x^{1/2}}{\Delta x^2}\right)u + \frac{\square_x}{\Delta x^2} \circ \frac{\square_x}{\Delta x^2}u. \tag{C.15}$$

Appendix D

General analysis of dispersion relations values

In this Section we show the values that χ can adopt in order to produce real or complex values of φ given by the following equation:

$$\varphi = \frac{1}{\Delta}\left(\frac{\pi}{2} - \arcsin\chi\right). \tag{D.1}$$

Assume that χ is a complex number, we write

$$\chi = \mathfrak{Re}(\chi) + \mathfrak{Im}(\chi)\mathbf{i}, \tag{D.2}$$

where $\mathfrak{Re}(\chi)$ refers to real part of χ and $\mathfrak{Im}(\chi)$ to its imaginary part.

Because we assume that our inverse sine function $\arcsin$ can take complex values, we can write

$$z = \arcsin\chi, \tag{D.3}$$

where $z = a + b\mathbf{i}$, with $a, b \in \mathbb{R}$.

Equivalently by definition of the sine function we write

$$\chi = \sin z = \frac{e^{\mathbf{i}z} - e^{-\mathbf{i}z}}{2\mathbf{i}}, \tag{D.4}$$

if we multiply by $e^{\mathbf{i}z}$ we get the following quadratic equation

$$e^{2\mathbf{i}z} - 2\mathbf{i}\chi e^{\mathbf{i}z} - 1 = 0, \tag{D.5}$$

with solutions

$$\arcsin\chi = z = -\mathbf{i}\ln\left(\mathbf{i}\left(\chi \pm \sqrt{\chi^2 - 1}\right)\right). \tag{D.6}$$

Now we analyze different values that χ can adopt.

D.1 Case when χ is real

It is straightforward to see in Eq. D.6 if χ is real and $\chi^2 - 1 > 0$ the argument of the logarithm is pure imaginary. By using the property of a complex valued logarithm

$$\log z = \ln |z| + \mathbf{i}\text{Arg}(z), \tag{D.7}$$

where Arg is the common argument function used in complex variable calculus. We can write for any pure imaginary number $x\mathbf{i}$

$$\log x\mathbf{i} = \ln x \pm \mathbf{i}\frac{\pi}{2}, \tag{D.8}$$

If χ is real and $\chi^2 - 1 > 0$ what is $\chi < -1$or $\chi > 1$ we have

$$\arcsin \pm\chi = \mp\frac{\pi}{2} - \mathbf{i}\ln\left(\chi \pm \sqrt{\chi^2 - 1}\right), \tag{D.9}$$

or written in a separate way:
If $\chi < -1$ then

$$\arcsin \chi = \frac{\pi}{2} - \mathbf{i}\ln\left(\chi \pm \sqrt{\chi^2 - 1}\right), \tag{D.10}$$

If $\chi > 1$ then

$$\arcsin \chi = -\frac{\pi}{2} - \mathbf{i}\ln\left(\chi \pm \sqrt{\chi^2 - 1}\right), \tag{D.11}$$

otherwise when χ is real and $-1 \leq \chi \leq 1$ then is straightforward to write

$$-\frac{\pi}{2} \leq \arcsin \chi \leq \frac{\pi}{2}. \tag{D.12}$$

D.2 Case when χ is complex

By using the algebraic formula for a square root of a complex number

$$\sqrt{z} = \sqrt{a + \mathbf{i}b} = \sqrt{\frac{r+a}{2}} + \mathbf{i}\,\text{sgn}(b)\sqrt{\frac{r-a}{2}}, \tag{D.13}$$

where $r = \sqrt{a^2 + b^2}$ with $a, b \in \mathbb{R}$ and sgn refers to the sign function.
Denoting $\chi = a + \mathbf{i}b$ we can write

$$\begin{aligned}
\arcsin \chi &= -\mathbf{i}\ln\left(\mathbf{i}\chi \pm \mathbf{i}\sqrt{\chi^2 - 1}\right) \\
&= -\mathbf{i}\ln\left(\mathbf{i}\left(a + \mathbf{i}b\right) \pm \mathbf{i}\sqrt{\left(a + \mathbf{i}b\right)^2 - 1}\right) \\
&= -\mathbf{i}\ln\left(-b \mp \text{sgn}\left(2ab\right)\sqrt{\frac{r_\chi - a_\chi}{2}} + \left(a \pm \sqrt{\frac{r_\chi - a_\chi}{2}}\right)\mathbf{i}\right),
\end{aligned} \tag{D.14}$$

where

$$r_\chi = \sqrt{(a^2 - b^2 - 1)^2 + (2ab)^2} \tag{D.15}$$
$$a_\chi = a^2 - b^2 - 1. \tag{D.16}$$

By using Eq. D.7 we can write

$$\arcsin \chi = \mathsf{Arg}(z_\chi) - \ln |z_\chi| \mathbf{i}, \tag{D.17}$$

where

$$z_\chi = -b \mp \mathsf{sgn}\left(2ab\right) \sqrt{\frac{r_\chi - a_\chi}{2}} + \left(a \pm \sqrt{\frac{r_\chi - a_\chi}{2}}\right) \mathbf{i}. \tag{D.18}$$

By simple inspection of Eq. D.17 we can see that whatever the value of z_χ is, the imaginary part of $\arcsin \chi$ is going to be negative (simply because $\ln |z_\chi| > 0$). So we can analyze all different cases of the imaginary part in only one: when the imaginary part is different from zero.

D.3 Case when $\mathfrak{Im}(\chi) \neq 0$

The imaginary value when $\mathfrak{Im}(\chi) \neq 0$ is simply given by the term

$$\mathfrak{Im}(\arcsin \chi) = -\ln |z_\chi|. \tag{D.19}$$

We can conclude that always when $\mathfrak{Im}(\chi) \neq 0$ implies $\mathfrak{Im}(\arcsin \chi) < 0$.

List of abbreviations

ADI	Alternating Directions Implicit
ART	Asymptotic Ray Theory
BEM	Boundary Element Method
CS	Complex Steps
CSFD	Complex Steps Finite Differences
CSFDM	Complex Steps Finite Differences Method
CSM	Complex Step Method
CV	Control Volume
DE	Differential Equation
DF	Diferencias Finitas
DGM	Discontinuous Galerking Method
EFGM	Element Free Galerkin Method
FD	Finite Differences
FDM	Finite Differences Method
FEM	Finite Element Method
FFT	Fast Fourier Transform
FV	Finite Volume
FVM	Finite Volume Method
GRT	Geometric Ray Theory
HPM	Hamiltonian Particle Method
MDF	Método de Diferencias Finitas
MFFDM	Mesh Free Finite Difference Method
MFGM	Mesh Free Galerkin Methods
MFM	Mesh Free Methods
MFPM	Mesh Free Particle Methods
MGM	MultiGrid Methods
MPC	Método del Paso Complejo
MPCDF	Método del Paso Complejo con Diferencias Finitas
MPFEM	Moving Particle Finite Element Method
MWR	Method of Weighted Residuals
ODE	Ordinary Differential Equation
PC	Pasos Complejos
PCDF	Pasos Complejos con Diferencias Finitas
PDE	Partial Differential Equation

PREM	Preliminary Reference Earth Model
PM	Particle Methods
PSM	Pseudo-Spectral Method
RSM	Ray Series Method
RT	Ray Theory
SPH	Smoothed Particle Hydrodynamics
SEM	Spectral Element Method
SRM	Seismic Ray Method
SRT	Seismic Ray Theory

List of symbols

A	Amplitude of the wave
α	Real part of the frequency
c	Wave velocity
Δt	Time step
Δx	Differential step and/or grid size
e	Euler constant
f_N	Nyquist frequency
$f_{normalized}$	Normalized frequency
f_0	Dominating frequency
G	Growth factor
γ	Imaginary part of the frequency
h, v	Differential steps
h_t, v_t	Differential steps in time
h_x, v_x	Differential steps in space
$\mathbb{H}$	Field of Quaternions
$\mathbf{i} = \sqrt{-1}$	Imaginary unit
$\mathfrak{Im}$	Imaginary part of the function
k	Wave number
k_{real}, k_{imag}	Real and imaginary parts of the wave number
$\kappa(x)$	Bulk modulus
$\mathbb{N}$	Field of Integers numbers
N, n, m	Positive integers
$\mathcal{O}$	Approximation error made by truncating the Taylor series
$\mathrm{P}(\mathbf{x}, t)$	Pressure
π	Pi constant
$\mathbb{R}$	Field of Real numbers
$\mathfrak{Re}$	Real part of the function
$\rho(x)$	Density
S	Courant umber and/or stability factor
$\boldsymbol{\sigma}$	Second order stress tensor
t	Time variable
t_0	Time delay
$u(x, t)$	Displacement field
$\dot{u}(x, t)$	Derivative of displacement field respect to time
$v(x, t)$	Velocity field
$\mathrm{val}(x, t)$	Numerical value to be propagated
ω	Frequency
$\omega_{real}, \omega_{imag}$	Real and imaginary parts of the frequency
x, y, z	Space variables

$\circ$	Convolution operator
$\Delta^+, \Delta^-, \Box, \rhd, \lhd\rhd$	Differential operators
λ, μ	Lame elastic parameters
∇	Gradient operator
$\nabla\cdot$	Divergence operator
$\varphi, \chi, \xi, \zeta$	Dummy symbols